

**THERMAL DECOMPOSITION OF STRUVITE: A NOVEL APPROACH TO
RECOVER AMMONIA FROM WASTEWATER USING STRUVITE
DECOMPOSITION PRODUCTS**

by

Sharmeen Farhana

B.Sc. Eng. (Civil), Bangladesh University of Engineering and Technology,
Dhaka, Bangladesh, 2009

A THESIS SUBMITTED IN PARTIAL FULFILLMENT OF
THE REQUIREMENTS FOR THE DEGREE OF

MASTER OF APPLIED SCIENCE

in

THE FACULTY OF GRADUATE AND POSTDOCTORAL STUDIES
(Civil Engineering)

THE UNIVERSITY OF BRITISH COLUMBIA
(Vancouver)

July, 2015

© Sharmeen Farhana, 2015

Abstract

Ammonia recovery technology, utilizing newberyite ($\text{MgHPO}_4 \cdot 3\text{H}_2\text{O}$) as a struvite ($\text{MgNH}_4\text{PO}_4 \cdot 6\text{H}_2\text{O}$) decomposition product, is gaining interest as usage of newberyite can significantly reduce the cost of commercial reagents, by providing readily available magnesium and phosphate for struvite reformation. In this study, the efficiency of ammonia removal from struvite, and a transformation process of struvite to newberyite, were investigated through performing oven dry, bench-scale and pilot-scale experiments. In the oven dry experiments, the structural and compositional changes of synthetic struvite, upon decomposition, were evaluated. Around 60-70% ammonia removal efficiency was achieved through struvite thermal decomposition above $60^\circ \pm 0.5^\circ\text{C}$, with up to 71.1°C with prolonged heating. The 2D amorphous layered structure, present in the decomposed solid phase, entrapped around 30-40% residual ammonia between the layers of magnesium and phosphate, inhibiting further ammonia removal.

Subsequently, bench-scale experiments were conducted based on the hypothesis that humid air can prevent the formation of a layered structure including dittmarite ($\text{MgNH}_4\text{PO}_4 \cdot \text{H}_2\text{O}$) and an amorphous 2D layered structure. Struvite pellets of different sources and sizes were heated in a fluidized bed reactor in the presence of hot air and steam. Introduction of steam resulted in complete transformation of struvite pellets ($<1\text{mm}$) into newberyite at 80°C , 95% relative humidity and 2 hours of heating.

Finally, pilot-scale experiments were carried out to further optimize the operating conditions for industrial application. The smaller and softer pellets (size $<1\text{mm}$, hardness 300-500 g) were the best suited for struvite-to-newberyite conversion. The process was optimized further by narrowing down the relative humidity from 95% to 85% and reducing the heating duration from 2 to 1.5 hours. The operating cost of the pilot-scale process was estimated, which can be reduced through recycling the heat and moist air over the cycle. The number of cycles for which the decomposed product can be effectively reused depends on the required overall N-recovery efficiency, as well as the performance of the struvite recrystallization stage. The greatest advantage of the proposed technology, over other recovery methods, is that the operating costs can be turned into revenue by utilizing the recovered product as fertilizer or energy source.

Preface

This thesis is original, unpublished, independent work by the author, Sharmeen Farhana.

Table of Contents

Abstract.....	ii
Preface.....	iii
Table of Contents	iv
List of Tables	ix
List of Figures.....	x
List of Symbols and Abbreviations	xv
Acknowledgements	xvii
Dedication	xviii
Chapter 1: Introduction	1
1.1 Nitrogen supply and demand	1
1.1.1 Demand for nitrogenous fertilizers	2
1.1.2 Ammonia as a fuel	4
1.2 Commercial methods for ammonia synthesis - Haber Bosch process	6
1.3 The potential driving force for ammonia removal and recovery	7
1.3.1 Eutrophication and more stringent ammonia discharge regulations	7
1.3.2 Economic considerations for ammonia recovery from municipal WWTPs	9
Chapter 2: Background and Literature Review	13
2.1 Conventional methods for ammonia recovery from wastewater	13
2.1.1 Air stripping method	13
2.1.2 Membrane method	14
2.1.3 Ion exchange method	14
2.1.4 Chemical precipitation method	15
2.2 Struvite formation and recovery background	16
2.2.1 Formation of struvite in wastewater treatment works.....	16
2.2.2 Solubility product of struvite and other magnesium phosphates	17
2.2.3 Recovery of struvite through precipitation method	18
2.2.4 Ammonia recovery through struvite precipitation using commercial reagents	20
2.3 Ammonia recovery using struvite thermal decomposition product	25
2.3.1 Decomposition of struvite: Wet process	27

2.3.1.1	Removal of ammonia following thermal alkali treatment	27
2.3.1.2	Removal of ammonia following acidolysis	31
2.3.1.3	Disadvantages of wet process	33
2.3.2	Decomposition of struvite: Dry process	34
2.3.2.1	Phase transition of struvite during thermal decomposition using dry method..	36
2.3.2.2	Possible structural changes during struvite thermal decomposition	41
2.3.2.2.1	Amorphous structure vs crystalline structure.....	41
2.3.2.2.2	Struvite crystalline structure vs newberyite crystalline structure.....	42
2.3.2.2.3	2D layered structure vs 3D layered structure	44
2.3.2.2.4	Layered structure synthesis	47
2.3.2.3	Ammonia recovery using decomposed struvite product.....	49
2.3.2.4	Ammonia gas recovery techniques	54
Chapter 3: Research Objectives		56
Chapter 4: Materials and Methods		57
4.1	Experimental conditions of performed oven dry experiments.....	57
4.1.1	Preparation of synthetic struvite	58
4.1.2	Synthesized struvite analysis	59
4.1.3	Mass loss measurements	59
4.2	Experimental conditions of performed bench-scale experiments.....	60
4.2.1	Bench-scale experimental setup.....	61
4.3	Experimental conditions of performed pilot-scale experiments	64
4.3.1	Fluidized bed reactor design	65
4.3.2	Pilot-scale experimental setup	68
4.4	Sample collection and preservation	71
4.5	Analytical methods	71
4.5.1	Sample preparation	71
4.5.1.1	Magnesium.....	72
4.5.1.2	Ammonia and orthophosphate	72
4.5.1.3	XRD identification of solid phases	72
4.5.1.4	Struvite morphology	73
4.6	Development of hardness tester	73

4.7	Terminology.....	75
4.7.1	Molar ratio	75
Chapter 5: Results and Discussion		76
5.1	Oven dry experiments	76
5.1.1	Hypotheses and specific goals	76
5.1.2	Results and discussion of oven dry experiments	77
5.1.2.1	Influence of temperature with varying heating duration on decomposed product	77
5.1.2.1.1	Mass loss curves.....	77
5.1.2.1.2	Chemical composition and interpretation	79
5.1.2.1.3	XRD Results.....	82
5.1.2.1.3.1	Formation of layered structure	82
5.1.2.1.3.2	Identification of layered structure at temperatures below 61.5°C	85
5.1.2.2	Influence of different temperatures on layered structure formation	87
5.1.2.2.1	Chemical composition.....	87
5.1.2.2.2	XRD results	89
5.1.2.3	Layered structure transformation over time.....	93
5.1.2.4	Ammonia entrapment in a layered structure	96
5.1.2.5	Subsequent heating and rehydration	97
5.2	Bench-scale experiments with humid air	100
5.2.1	Background	100
5.2.1.1	Influence of humidity on dehydration of magnesium phosphate compounds	100
5.2.1.2	Finding operating range for struvite decomposition	103
5.2.2	Hypotheses and specific objectives	107
5.2.3	Results and discussion of bench-scale experiments.....	108
5.2.3.1	Identifying optimum condition with respect to temperature and relative humidity	108
5.2.3.1.1	Effects of temperature on rate and efficiency of ammonia removal	109
5.2.3.1.2	Effects of relative humidity on rate and efficiency of ammonia removal	111
5.2.3.1.3	Effects of struvite heating duration on ammonia removal	113
5.2.3.1.4	XRD results	114

5.2.4	Effects of relative humidity on layered structure formation	117
5.2.5	Effects of size and sources of different pellets on ammonia removal efficiency ...	121
5.2.5.1	Chemical content for different sources and sizes of pellets.....	121
5.2.5.2	XRD results.....	124
5.3	Pilot-scale experiments with humid air.....	126
5.3.1	Hypothesis and specific goals	126
5.3.2	Results and discussion of pilot-scale experiments.....	127
5.3.2.1	Process efficiency for different sources and sizes of struvite pellets.....	127
5.3.2.1.1	Chemical results and interpretation	128
5.3.2.1.2	XRD results	132
5.3.2.2	Penticton B.C. struvite pellets for process optimization.....	134
5.3.2.2.1	Chemical results and interpretation.....	134
5.3.2.2.2	XRD results	137
5.4	Struvite morphology	140
5.4.1	Background	140
5.4.2	Specific objective and hypothesis	144
5.4.3	Results and discussion of struvite morphological studies.....	145
5.5	Crushing strength of different sources and sizes of pellets.....	149
5.5.1	Influence of parameters on crushing strength of struvite pellets	150
5.5.2	Influence of size, shape and structural composition on crushing strength	150
5.6	Cost estimation and economic benefits over other ammonia removal and recovery methods	152
5.7	Options for increasing ammonia recovery efficiency and the reduction of operational costs	156
Chapter 6: Conclusions and Recommendations		162
References		166
Appendices		178
Appendix A : Operational settings for instruments		178
Appendix B : Oven dry experiments		179
B.1	Formation of layered structure.....	179
B.2	Transformation of layered structure over time	180

B.3	Temperature influence on layered structure formation.....	188
Appendix C : Bench-scale experiments		190
C.1	XRD results of decomposed samples using different combination of temperature and relative humidity	190
C.2	Relative humidity effects on layered structure formation.....	198
C.3	Layered structure transformation	199
C.4	Different sources and sizes of struvite pellets.....	201
Appendix D : Pilot-scale experiments		204
D.1	Identifying operational parameters for FBR	204
D.2	XRD results of decomposed struvite pellets from different sources and sizes at optimum conditions	206
D.3	Process optimization	209
Appendix E : Log data for pilot-scale experiments		215
E.1	Log data for process optimization.....	215
E.2	Log data for different sources and sizes of pellets.....	219
Appendix F : Cost estimation		222

List of Tables

Table 1.1 The loading rate of ammonia across Canada in 1996 (Environment Canada, 2001)	7
Table 2.1 Reported pK_{sp} values for different magnesium and phosphate compounds at 25°C (Wilson, 2013)	18
Table 2.2 Summary of ammonia removal studies through struvite precipitation using commercial reagents	21
Table 2.3 Struvite decomposition studies using thermal-alkali treatment (Wilson, 2013).....	29
Table 2.4 Ammonia recovery using struvite decomposition product obtained from thermal-alkali treatment (Wilson, 2013)	30
Table 4.1 Experimental conditions of oven dry experiments	58
Table 4.2 Experimental conditions of bench-scale experiments	61
Table 4.3 Experimental conditions of pilot-scale experiments.....	65
Table 5.1 XRD results of the decomposed oven dry samples after three months	95
Table 5.2 XRD results of Lulu Island pellets after heating at various temperatures and relative humidity	115
Table 5.3 XRD results of different sources and sizes of struvite pellets after decomposing at 80°C and 95% RH.....	124
Table 5.4 XRD results of different sources and sizes of pellets after heating at 80°C and 95% RH for 1 hour.....	132
Table 5.5 XRD results of Penticton B.C. pellets after heating at various temperatures and relative humidity	138
Table 5.6 The operating cost involves in the 2 nd generation of proposed ammonia recovery technology.....	154
Table 5.7 Operating cost comparison among different ammonia removal and recovery methods	155
Table 5.8 Advantages and disadvantages associated with different options for combined ammonia recovery processes	156

List of Figures

Figure 1.1 Ammonia production and net imports in Canada and United States from 1999 to 2005 (Frigon, 2007)	2
Figure 1.2 Global nitrogen input from different sources in crop production from 1990 to 2020 (Mosier and Kroeze, 2000)	3
Figure 1.3 Percentage of applied fertilizer in Canadian agricultural sector in 2008 and 2012 (Agricultural and Agri-Food Canada, 2013).....	4
Figure 1.4 Conventional schematic of wastewater treatment process (WERF, 2009)	9
Figure 1.5 A comparison of prices among nitrogen fertilizers from 1960 to 2013 (USDA ERS, 2013)	11
Figure 2.1 Pilot-scale struvite crystallization system (Bhuiyan et al., 2008b)	19
Figure 2.2 Process flow diagram of ammonia recovery using struvite decomposition product...	26
Figure 2.3 Aqueous ammonia removal using struvite decomposition product produced from acidolysis method by Zhang et al. (2004)	32
Figure 2.4 Process flow diagram of the proposed ammonia recovery technology	34
Figure 2.5 The possible transformation of struvite into various solid phases based on the decomposition method (Sarkar, 1991; Babić-Ivančić et al., 2002; Bhuiyan et al., 2008b; Cervantes, 2009)	40
Figure 2.6 (a) 3D crystalline structure (b) Amorphous structure.....	42
Figure 2.7 Crystalline structure of (a) struvite (Abbona and Boistelle, 1979) (b) newberyite (Boistelle and Abbona, 1981)	43
Figure 2.8 2D crystalline layered structure	44
Figure 2.9 Crystal structure of dittmarite-type compounds $M'M''PO_4 \cdot H_2O$ (Koleva, 2007)	45
Figure 2.10 XRD results of dittmarite $MgNH_4PO_4 \cdot H_2O$ (Sugiyama et al., 2005)	46
Figure 2.11 X-ray powder diffraction patterns for $MgHPO_4 \cdot 1.2H_2O$ (a) at room temperature, (b) heated at 200°C followed by exposure to air, (c) at 100°C, (d) at 200°C, (e) at 300°C, (f) at 500°C (Chen et al., 1993).....	48
Figure 4.1 Bench-scale experimental setup (a) detailed design with connections (b) actual setup	62
Figure 4.2 Fluidization patterns (a) turbulent regime (b) slugging regime.....	67

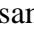
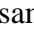
Figure 4.3 Pilot-scale experimental setup (a) detail design with connections (b) actual setup	69
Figure 4.4 Device used to determine crushing strength of struvite (a) actual device and (b) sketch (not to scale).....	74
Figure 4.5 Program window used to graphically illustrate force as a function of time and to determine peak load	74
Figure 5.1 Percent mass loss of struvite over time at different heating temperature.....	78
Figure 5.2 N-NH ₄ molar ratio with respect to Mg (PO ₄) over time at different heating temperatures.....	80
Figure 5.3 H ₂ O molar ratio with respect to Mg (PO ₄) over time at different heating temperatures	80
Figure 5.4 X-ray diffraction patterns of synthetic struvite decomposed at 61.5°C (a) scanning angle 0.8 to 50 degree (b) enlarged view of sample peaks formed between 0.8 and 12 degree...	83
Figure 5.5 X-ray diffraction patterns of synthetic struvite decomposed at 60.5°C for 24 hours; .	86
Figure 5.6 N-NH ₄ molar ratio with respect to Mg (PO ₄) after 7 hours duration of heating at different temperatures	88
Figure 5.7 H ₂ O molar ratio with respect to Mg (PO ₄) after 7 hours duration of heating at different temperatures.....	88
Figure 5.8 X-ray diffraction patterns of synthetic struvite decomposed for 7 hours at (a) 65.3°C (b) 85.5°C;  XRD performed on the samples without any delay,  XRD performed on the samples after 30 minutes exposure to the atmosphere.....	90
Figure 5.9 X-ray diffraction patterns of synthetic struvite decomposed for 7 hours at different temperatures (a) scanning angle 0.8 to 50 degree (b) enlarged view of scanning angle 0.8 to 12 degree	92
Figure 5.10 X-ray diffraction patterns of synthetic struvite decomposed at 61.5°C (a) after one day of heat treatment (b) after one year of heat treatment.....	94
Figure 5.11 N:P molar ratio of synthetic struvite that undergone subsequent heating at 60.5°C followed by rehydration.....	99
Figure 5.12 H ₂ O:P molar ratio of synthetic struvite that undergone subsequent heating at 60.5°C followed by rehydration.....	99


Figure 5.13 The kinetic curves of $\text{Mg}(\text{H}_2\text{PO}_4)_2 \cdot 4\text{H}_2\text{O}$ upon dehydration (1) in air at relative humidity $\text{RH} = 25\%$ (Samuskevich and Lukyanchenko, 1998), (2) in air at relative humidity $\text{RH} = 0\%$ and (3) in water vapour atmosphere at $p_{\text{H}_2\text{O}} = 5 \text{ hPa}$	103
Figure 5.14 Dissociation pressure of struvite-dittmarite-newberyite- H_2O - NH_3 and the equation model at different temperatures (Kiehl and Hardt, 1933).....	104
Figure 5.15 Operating temperature and relative humidity for struvite thermal decomposition .	106
Figure 5.16 N-NH_4 molar ratio with respect to $\text{Mg}(\text{PO}_4)$ of Lulu Island pellets ($<1\text{mm}$) heated at three different relative humidity with increasing temperatures for different heating durations .	110
Figure 5.17 H_2O molar ratio with respect to $\text{Mg}(\text{PO}_4)$ of Lulu Island pellets ($<1\text{mm}$) heated at three different relative humidity with increasing temperatures for different heating durations .	110
Figure 5.18 N-NH_4 molar ratio with respect to $\text{Mg}(\text{PO}_4)$ of Lulu Island pellets ($<1\text{mm}$) heated at three different temperatures with increasing relative humidity for different heating durations .	112
Figure 5.19 H_2O molar ratio with respect to $\text{Mg}(\text{PO}_4)$ of Lulu Island pellets ($<1\text{mm}$) heated at three different temperatures with increasing relative humidity for different heating durations .	112
Figure 5.20 X-ray diffraction patterns of Lulu Island pellets ($<1\text{mm}$) heated at 85°C with 65%, 80% and 95% relative humidity for 2 hours (a) scanning angle 0.8 to 50 degree;  standard newberyite,.....	118
Figure 5.21 X-ray diffraction patterns of Lulu Island pellets after one year ($<1\text{mm}$), decomposed at 85°C with 80% RH for 2hours (a) right after thermal decomposition (b) after four months..	120
Figure 5.22 N-NH_4 molar ratio with respect to $\text{Mg}(\text{PO}_4)$ of different sources and sizes of pellets heated at optimum conditions for different heating durations	122
Figure 5.23 H_2O molar ratio with respect to $\text{Mg}(\text{PO}_4)$ of different sources and sizes of pellets heated at optimum conditions for different heating durations	122
Figure 5.24 Temperature, relative humidity and air flow through reactor and jacket during thermal decomposition of Penticton B.C. pellets ($<1\text{mm}$) at optimum conditions in the pilot-scale setup.	128
Figure 5.25 N-NH_4 molar ratio with respect to $\text{Mg}(\text{PO}_4)$ of different sources and sizes of struvite pellets heated at optimum conditions for different heating durations.....	129
Figure 5.26 H_2O molar ratio with respect to $\text{Mg}(\text{PO}_4)$ of different sources and sizes of struvite pellets heated at optimum conditions for different heating durations.....	129

Figure 5.27 N-NH ₄ molar ratio with respect to Mg (PO ₄) of Penticton B.C. pellets (<1mm) heated at various combinations of temperature and relative humidity for different heating durations.....	135
Figure 5.28 H ₂ O molar ratio with respect to Mg (PO ₄) of Penticton B.C. pellets (<1mm) heated at various combinations of temperature and relative humidity for different heating durations..	135
Figure 5.29 SEM images of the interior and exterior of Lulu Island pellets harvested in LIWWTP (Fattah, 2010).....	141
Figure 5.30 SEM images of the Lulu Island pellets (a) exterior surface magnified at 18X (b) exterior smooth surface magnified at 300X (c) exterior coarse surface magnified at 300X (d) exterior coarse surface magnified at 3000X (e) interior surface magnified at 50X and (f) interior surface magnified at 300X (Huang, 2003).....	142
Figure 5.31 SEM images of raw Edmonton Gold Bar struvite interior (a) 35X, (b) 70X and (c) 500X (Novotny, 2011)	143
Figure 5.32 SEM images of interior surface of heated Edmonton Gold Bar pellets (a) 70X and (b) 500X (Novotny, 2011)	144
Figure 5.33 Morphology of the struvite pellets from different sources (a) Edmonton Gold Bar pellets (<1mm) (b) recrystallized pellets (>1mm)	145
Figure 5.34 Struvite morphology of the raw pellets (a) Lulu Island Pellets (<1mm) (b) Lulu Island pellets (>1mm) (c) Penticton B.C. pellets (<1mm) (d) Penticton B.C. pellets (>1mm) ..	147
Figure 5.35 Struvite morphology of the pellets after heating at 80°C, 95% RH (a) Penticton B.C. pellets (<1mm)-pilot-scale, 2hr at 3X magnification (b) Lulu Island Pellets-bench-scale (<1mm), 2hr at 3X magnification (c) Edmonton Gold Bar pellets (<1mm), 4hr at 3X magnification (d) Penticton B.C. pellets (>1mm), 4hr at 3X magnification	148
Figure 5.36 Influence of pellet size and sources on crushing strength. Error bars: 95% confidence interval	151
Figure 5.37 Process flow diagram of proposed ammonia recovery technology.....	153
Figure 5.38 Combined nitrogen recovery efficiency over number of cycles at different ammonia removal efficiencies from struvite (without addition of excess decomposed product)	157
Figure 5.39 Mole balance of the combined ammonia recovery process with addition of stoichiometric amount of decomposed product	160

Figure 5.40 Mole balance of combined ammonia recovery process with addition of excess decomposed product	161
-------------------------------------------------------------------------------------------------------------------	-----

List of Symbols and Abbreviations

AAS	Atomic Absorption Spectrophotometer
ANAMMOX	Anaerobic Ammonium Oxidation
ARP	Ammonia Recovery Process
AWWTP	Advanced Wastewater Treatment Plant
B.C.	British Columbia
BNR	Biological Nutrient Removal
°C	Degrees Celsius
CAD	Canadian Dollar
CO ₂	Carbon Dioxide Gas
COP	City of Penticton
CCME	Canadian Council of Ministers of the Environment
cm	Centimeter
EUR	Euro
FBR	fluidized bed reactor
g	gram
lb	Pound
kg	Kilogram
K _{sp}	Solubility Product
Kt	Kiloton
LIWWTP	Lulu Island Wastewater Treatment Plant
MAP	Magnesium Ammonium Phosphate
Mg	Magnesium
MGD	million gallons per day
m	meter
mm	millimeter
N	Nitrogen
N ₂	Nitrogen Gas
NH ₃	Ammonia
NH ₄ ⁺	Ammonium ion

List of Symbols and Abbreviations

NH ₄ -N	Ammonium Nitrogen
P	Phosphorus
PO ₄ -P	Phosphate Phosphorus
pH	Power of Hydrogen
QTG	quasi-isothermal thermogravimetry
RH	Relative Humidity
SEM	Scanning Electron Microscope
S _{newberyite}	supersaturation ratio with respect to newberyite
S _{struvite}	supersaturation ratio with respect to struvite
Tg	Teragram
UBC	University of British Columbia
USD	United States Dollar
USDA ERS	United States Department of Agriculture Economic Research Service
USEPA	United States Environmental Protection Agency
WEF	Water Environment Federation
WERF	Water Environment Research Foundation
WWTP	wastewater treatment plant
WWTF	wastewater treatment flow
XRD	X-ray diffraction
USDA ERS	US Department of Agriculture Economic Research Center

Acknowledgements

- Firstly, I would like to convey my deepest gratitude to my supervisor, Dr. Donald S. Mavinic for his firm support, understanding, encouragement and guidance throughout the course of this work. His optimism in research is refreshing and his ability to make his students feel at home has been very welcoming.
- In addition to my supervisors, I would like to thank my on-site mentor Dr. Sergey Lobanov for his unparalleled patience, inspirations, invaluable knowledge, guidance and experience.
- My special thanks go to Frederic Koch for his valuable assistance, suggestions and useful discussions during this study.
- I would like to thank Paula Parkinson and Tim Ma for their continuous assistance in the lab from sample analysis to fixing instruments.
- I would like to thank Henrique Falck Grimm for assisting me in the pilot plant and lab for sample preparations.
- Thanks to Natural Sciences and Engineering Research Council of Canada for their generous funding of this research project.
- Finally, my gratitude goes fellow graduate colleagues for fruitful discussions and making my time so enjoyable at UBC.

Dedication

To my parents and my husband who gave me their unparalleled support and guidance.

Chapter 1: Introduction

1.1 Nitrogen supply and demand

Nitrogen is one of the most essential nutrients for all forms of life including plants and organisms. Over 78% of the earth's atmosphere consists of nitrogen that is not fixed. In order to meet the nutritional needs for plants and organisms, nitrogen has to be fixed which can be accomplished through the production of synthetic ammonia using the Haber-Bosch process. The major consumption of ammonia in the agricultural industry is the direct application of anhydrous ammonia as a source of nitrogenous fertilizer for sufficient crop production (Smil, 2001). In contrast, the sector of animal husbandry inserts ammonia directly to the feed in order to increase its nutrient value; this eventually promotes the growth of animals (Smil, 2001). Apart from food production, ammonia application is required in other sectors that include mining, pulp and paper industry, animal husbandry, food processing, and refining, thereby increasing global ammonia consumption (CCME, 2010).

According to the CCME (2010), around 3,508 kt and 3,535 kt ammonia were required in order to satisfy the domestic demand in 1996 and 1997, respectively. The following Figure 1.1 represents the percent of ammonia produced and imported in Canada and the United States with respect to the percentage of consumption from the year of 1999 to 2005 (Frigon, 2007). From Figure 1.1, it is evident that the percentage of ammonia imported to Canada and United States, with respect to consumption, increased from 11% to 29% from 1999 to 2005. The production of ammonia in Canada and worldwide depends on the Haber-Bosch process. The majority of ammonia produced this way meets the demand for nitrogen fertilizer, estimated at around 80% of total ammonia (Erisman et al., 2008). In 2005, only 17 Tg out of 100 Tg nitrogen produced for global agricultural demand (utilizing Haber-Bosch process) was consumed by humans (Erisman et al., 2008; Aiking, 2011). A significant portion of applied nitrogenous fertilizer is not consumed by crops, due to loss to the environment.

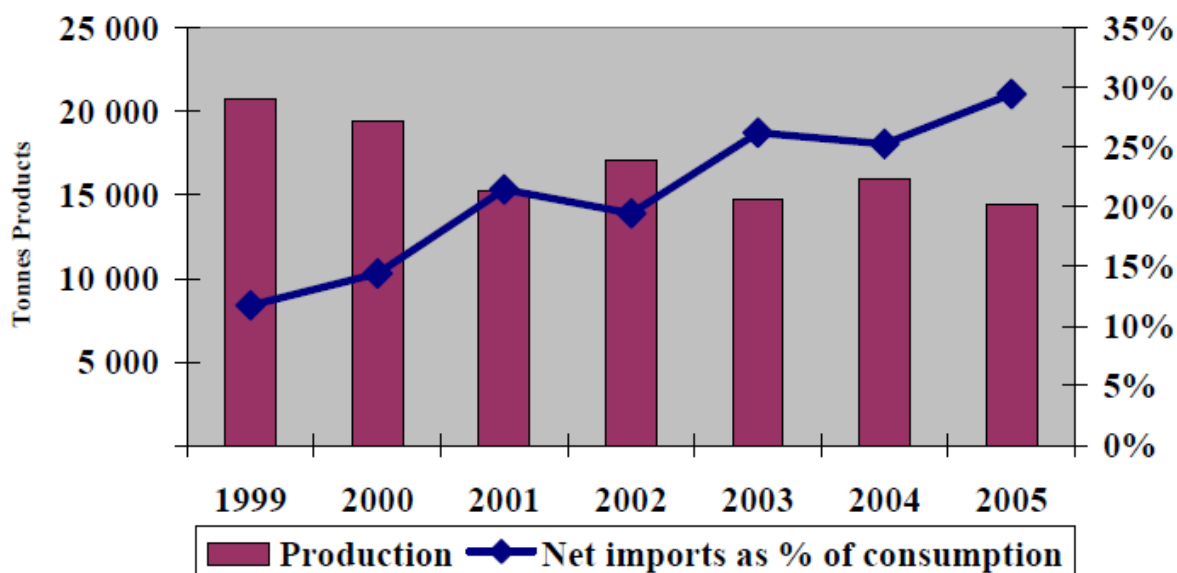


Figure 1.1 Ammonia production and net imports in Canada and United States from 1999 to 2005 (Frigon, 2007)

1.1.1 Demand for nitrogenous fertilizers

The application of nitrogen fertilizer is increasing worldwide, in order to enhance food production to serve a growing population. Figure 1.2 represents the estimation of global nitrogen input in agricultural sector across different sources from 1990 to 2020. During this period, the world population is predicted to increase from 5.3 billion to about 7.8 billion from 1990 to 2020 (Mosier and Kroeze, 2000). Therefore, the production and input of synthetic fertilizer must be increased proportionately in order to meet increasing food demand (Smil, 1999). It is evident from Figure 1.2 that the application of nitrogen for crop production as synthetic fertilizer increased from 8 Tg to around 56 Tg from 1900 to 1950 and reached 190 Tg in 1996; this demonstrates a continuing upward trend according to the prediction (Mosier and Kroeze, 2000; Bumb and Baanante, 1996). Approximately a 40% global increase in nitrogen consumption, as synthetic fertilizer between the years of 2000 to 2020, has been estimated and reported by Bumb and Baanante (1996).

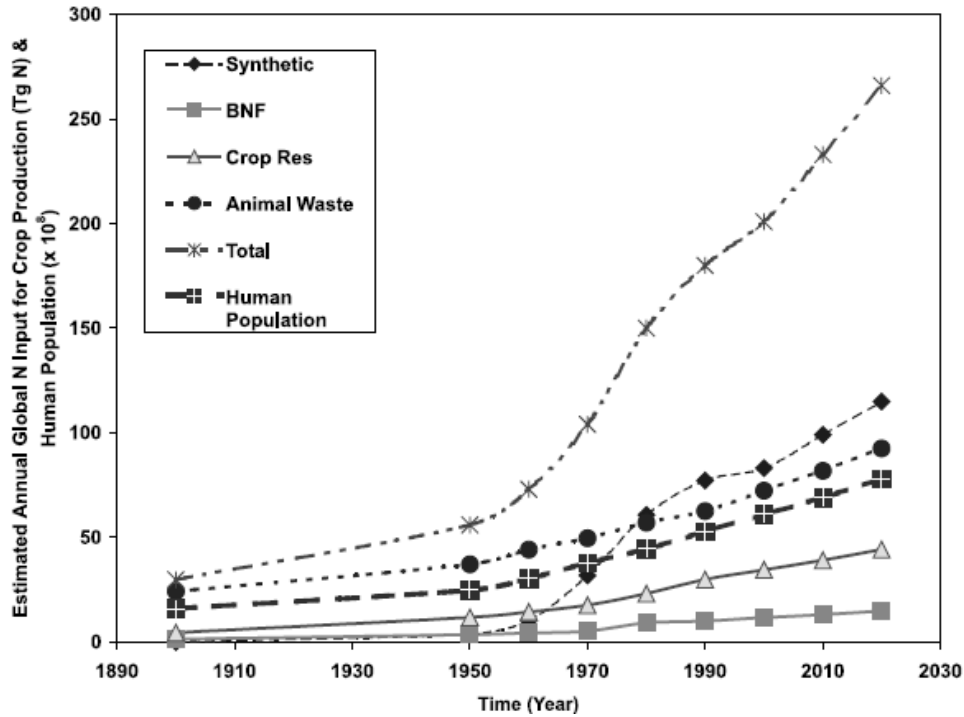


Figure 1.2 Global nitrogen input from different sources in crop production from 1990 to 2020 (Mosier and Kroeze, 2000)

Nitrogen is one of the major limiting nutrients for plant growth. It is provided as synthetic nitrogen fertilizer in the form of anhydrous ammonia, urea, nitrogen solution, ammonium nitrate and ammonium sulphate. Figure 1.3 represents the application of synthetic nitrogen, potash and phosphate fertilizer to the Canadian agricultural sector, during 2008 and 2012. In Canada, the contribution of nitrogen fertilizer to the agricultural sector was reported to be 75% (5.2 million tonnes) of total applied fertilizer in 2012 (Agricultural and Agri-Food Canada, 2013). The application of nitrogen fertilizer, increased by 7.7% between 2008 and 2012, which includes major contributions from urea, anhydrous ammonia and ammonium sulfate.

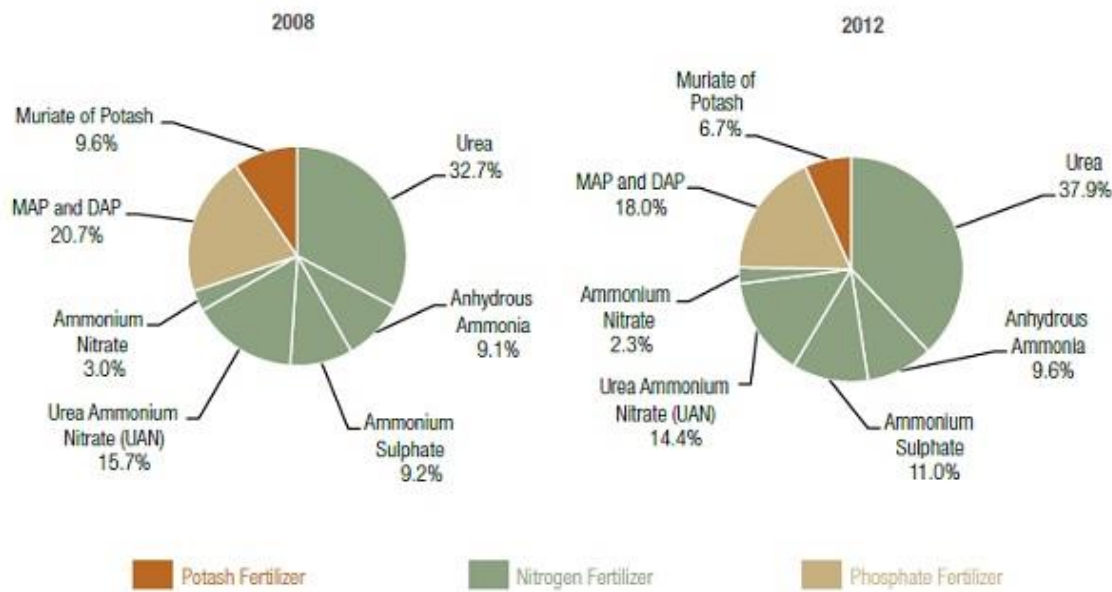


Figure 1.3 Percentage of applied fertilizer in Canadian agricultural sector in 2008 and 2012 (Agricultural and Agri-Food Canada, 2013).

1.1.2 Ammonia as a fuel

The global economy will shift towards the production and usage of sustainable fuels instead of non-renewable fossil fuels in the near future to minimize environmental impact. In several studies, synthesized hydrogen has been recommended as a sustainable fuel option, but this cannot be implemented without overcoming the risks associated with storage and distribution (Christensen et al., 2006; Lan et al., 2012). As far as storage is concerned, ammonia can be safely stored at room temperature with 8 bar vapour pressure (similar to propane) and can be delivered in large quantities (100 million tons/year). The energy per unit volume for ammonia is significantly higher than hydrogen and comparable to gasoline, supporting the applicability of ammonia in transportation sectors (Zamfirescu and Dincer, 2008; Zamfirescu and Dincer, 2009). In terms of safety, ammonia is considered non-flammable and is easily dissipated after releasing to the atmosphere, due to its lower density compared to air. Furthermore, ammonia can be easily detected when the leakage concentration is as low as 5 ppm, due to its typical odour (Zamfirescu and Dincer, 2008; Zamfirescu and Dincer, 2009).

The advantage of ammonia is the refrigeration effect which can be beneficial onboard in terms of reducing the size of cooling system and providing air conditioning, thereby increasing the engine efficiency by 10% (Zamfirescu and Dincer, 2009). In conventional internal combustion engines, ammonia cannot be used directly due to its low flame speed. The recent ‘ammonia truck’ with minor modification can run on a mixture of 80% ammonia and 20% gasoline. The compression ratio (40:1 to 100:1) 4 times higher than conventional internal combustion engines is incorporated in the special design of ammonia engines (Zamfirescu and Dincer, 2009). Considering the 100 km driving range, ammonia is an inexpensive fuel compared to gasoline, liquid petroleum gas, compressed natural gas, methanol and hydrogen. The driving cost of a vehicle run on ammonia is \$3.2/100 km, whereas a vehicle run on hydrogen with an internal combustion engine costs \$8.4/100 km (Zamfirescu and Dincer, 2008; Zamfirescu and Dincer, 2009). Continuous ammonia production in filling stations is under development and is currently being investigated by researchers at the Texas Tech University (Knight, 2013). These researchers have utilized the Haber-Bosch process, in order to produce ammonia, where hydrogen is produced from water electrolysis and nitrogen is added from the air. The researchers estimate that ammonia production, using this approach, could be between 4,000 and 40,000 litres per day. Further, the researchers note that the entire design could be easily scaled up and the cost of producing ammonia could be about 20 cents/l.

Ammonia is an environmentally-friendly fuel compared to other conventional fossil fuels. No greenhouse gases are emitted as a result of ammonia combustion. Wide application of ammonia as a sustainable fuel can be hindered due to its toxicity, but this can be overcome with improved storage technology (Zamfirescu and Dincer, 2008; Zamfirescu and Dincer, 2009). The problems associated with ammonia toxicity can be resolved through the formation of $\text{Mg}(\text{NH}_3)_6\text{Cl}_2$ (hexa-amine-magnesium chloride), a safer and longer lasting storage state for ammonia. This amine can be compacted and transformed into any desirable shape that can safely store hydrogen. Furthermore, the release of ammonia from the amine salt will allow onsite hydrogen production through thermal decomposition or catalyst incorporation (Yin et al., 2004; Christensen et al., 2006; Elmqvist et al., 2006; Zamfirescu and Dincer, 2008). The benefits of using ammonia as the hydrogen carrier are its cost-effectiveness, wide availability, limited hydrogen purification requirements, established infrastructure and green energy production. Considering all the benefits associated

with ammonia, it has been proposed as an appealing sustainable fuel option, as well as a sustainable solution for the advancement of a hydrogen-based economy.

1.2 Commercial methods for ammonia synthesis - Haber Bosch process

The surrounding atmosphere is comprised of 78% nitrogen, which is not fixed, and thus must be converted to synthetic ammonia through the Haber-Bosch process using nitrogen and hydrogen gas at a high temperature and pressure, as shown in Equation (1.1). The global production of synthetic ammonia increased from 3.5 Mt N to 85 Mt N from 1950 to 2000 and reached 133 Mt in 2010 (Smil, 2001; Smil, 2011). During the late 1990s, synthesized ammonia supplied more than 99% of fixed inorganic nitrogen (Smil, 2001; Smil, 2011).



Ammonia is synthesized from nitrogen and hydrogen at temperatures of 400 - 450°C and pressures of 10-30 MPa in the presence of an iron catalyst. The gasses are passed through four beds of catalyst and cooled after each pass to maintain equilibrium constant. After each pass, only about 15% ammonia conversion occurs. The unreacted gasses are recycled further and overall, 97% final conversion is achieved (Smil, 2001; Wood and Cowie, 2004). This process requires a 3:1 volume ratio of hydrogen and nitrogen. The main source of nitrogen is atmospheric air, whereas the main source of hydrogen gas is natural gas or light hydrocarbons. Steam reforming of light hydrocarbons, achieved through utilizing natural gas, is used to produce around 85% of the ammonia throughout the world.

Maxwell (2004) reported that worldwide ammonia synthesis is responsible for around 5% of natural gas consumption and the utilization of 1.3% of the energy derived from global fossil fuels. The consumption of natural gas or other hydrocarbons as feedstock causes emission of CO₂, which is the major component of greenhouse gases (Wood and Cowie, 2004). The consumption of fossil fuel for the production of 100 Mt ammonia through the Haber-Bosch process is responsible for introducing about four times as much reactive nitrogen into the environment (Smil, 2001).

1.3 The potential driving force for ammonia removal and recovery

1.3.1 Eutrophication and more stringent ammonia discharge regulations

The major quantifiable sources of ammonia release to aquatic ecosystems across Canada are municipal wastewater treatment plants (WWTPs). According to the most recently published data from Environment Canada (2001), Canadian aquatic systems receive around 62,000 tonnes of ammonia from municipal WWTPs per year. It is believed that this ammonia release from WWTPs has increased significantly in recent years. In domestic sewage, the estimated average total ammonia concentration was found to be about 14 mg/l (Environment Canada, 2001). The following Table 1.1 represents the ammonia discharge rate in 1996 in different urban centres across Canada. Negative environmental impacts on some aquatic ecosystems occur due to the enhanced discharge of ammonia. The eutrophication caused by discharge of excess nitrogen and phosphorus in a water body from WWTPs, can lead to the death of aquatic organisms (Schindler, 1974; Randall and Tsui, 2002).

Table 1.1 The loading rate of ammonia across Canada in 1996 (Environment Canada, 2001)

City	Province	Facility type	Average yearly effluent flow rate (million m ³ /year)	Yearly average NH ₃ concentration (mg/l)	NH ₃ discharge rate (tonnes/year)
Montreal urban Community	QC	Primary	930	6.59	6128
Metro Toronto	ON	Tertiary	463	12.0	5938
Greater Vancouver	BC	Primary/Secondary	432	14.0	5741
Winnipeg	MB	Secondary	83	26.02	2152
Metro Edmonton	AB	Secondary	91	21.42	1946
Hamilton	ON	Tertiary/Secondary	115	13.00	1499
Longueuil	QC	Primary	114	9.79	1121
Calgary	AB	Tertiary/Secondary	146	5.02	996
Metro Quebec City	QC	Secondary	57	11.63	667
Victoria Region	BC	Primary	26	13.89	377
Burlington	ON	Tertiary	27	13.89	370
Saskatoon	SK	Enhanced Primary	30	11.78	352

Eutrophication in water bodies (rivers, lakes and seas) results from enhanced algal blooms, which eventually decrease light penetration and available oxygen in the aquatic system. This eutrophication can cause oxygen-deficient zones in water bodies (i.e. “dead zones”) as the formation of extreme algal growth leads to the death of aquatic aerobic organisms (Khan and Ansari, 2005; Lee et al., 2003). Eutrophication in fresh water and salt water (lakes and oceans) increases un-ionized ammonia, which is known to be more toxic than the ammonium ion, due to its rapid diffusion through biological membranes of aquatic organisms (Environment Canada, 2001, USEPA, 1999). The relative percentage of un-ionized and ionized ammonia in aquatic environments are governed by the pH and temperature. Concentrations of 0.1 to 10 mg/l of un-ionized ammonia can cause acute toxicity for fish species, including salmonid and nonsalmonid species (USEPA, 1993; WEF, 2005). The maximum permissible one-hour average ammonia concentration in a three-year period is required to be below 1.0 mg/l for the protection of aquatic species (USEPA, 1993; WEF, 2005). For marine invertebrate species, the LC_{50} (24 and 48 hours) values of ammonia ranges from 0.77 to 19.1 mg/l, whereas they range from 0.49 to 2.9 mg/l for marine fish species (USEPA, 1999; Fisheries and Oceans Canada, 2007).

Most municipal WWTPs have been using biological nutrient removal (BNR) processes to satisfy the strict nitrogen discharge guidelines in aquatic systems. However, ammonia is destroyed during this process, while the same nitrogen is synthesized through Haber Bosch process at high temperature and pressure. Moreover, ammonia fertilizer production and BNR processes are both very energy-intensive. Alternatively, if ammonia could be recovered from wastewater, it would not only support the WWTPs to control effluent ammonia concentration, but also the recovered ammonia could be used as a commercial resource. The proper design of an ammonia recovery process both reduces the impact on the environment as well as presents a potential source of revenue.

1.3.2 Economic considerations for ammonia recovery from municipal WWTPs

Sludge production in wastewater treatment plants is very common and generally handled through the anaerobic digestion process especially at large facilities. A schematic of the conventional wastewater treatment process has been shown in Figure 1.4.

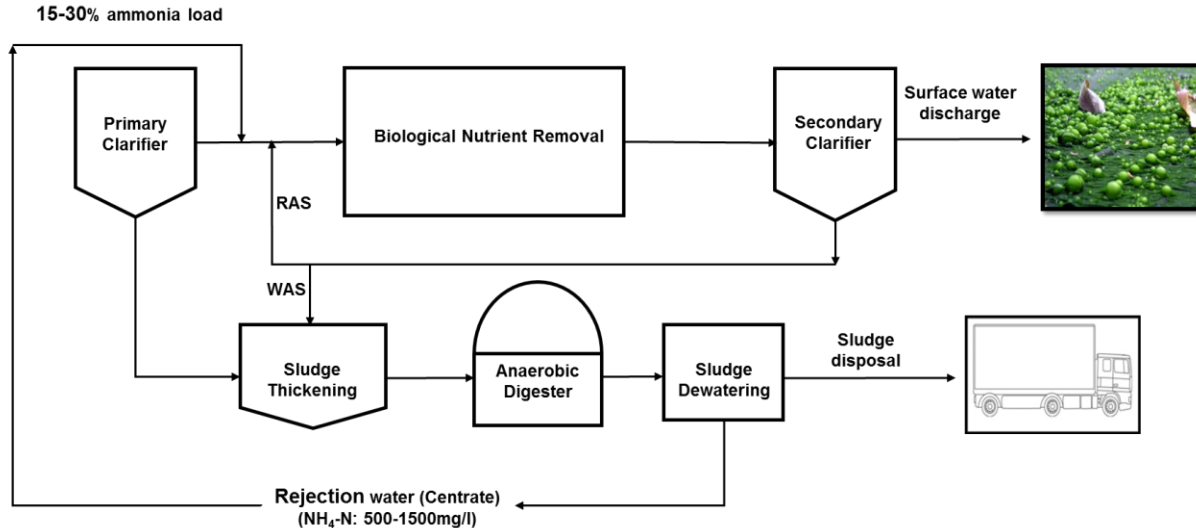


Figure 1.4 Conventional schematic of wastewater treatment process (WERF, 2009)

The centrate produced from the anaerobic digestion process contains high concentrations of ammonium-nitrogen, at around 500-1500 mg/l (Hassan, 2013); thus, it cannot be discharged directly to natural water bodies due to adverse effects on aquatic environments. Therefore, this high ammonium concentrated digester supernatant is recycled back to the main stream treatment process where it contributes only 1% of the influent flow, but 15-30% additional nitrogen loading (Fux and Siegrist, 2004; Constantine, 2006). This addition of nitrogen loading to the main stream treatment process can have a significant impact on process efficiencies. To handle this additional nitrogen loading, the main stream treatment process requires further modification, eventually increasing operating costs. The overall capital and operating cost of the mainstream treatment process also depends on the allowable permit of ammonia discharge, which has been evaluated for 18 secondary treatment plants containing average effluent concentration of 18 mg/l (Kessler, 2010). The capital cost has been reported at between \$45M to \$60M, in order to upgrade the plants

to meet the 8 mg/l ammonia discharge regulation; whereas the cost increased from \$58M to \$67M, to meet the discharge regulation of 3 mg/l. Similarly, the operating cost for total nitrogen removal also increased from 13-15 USD/kg to 70-86 USD/kg, in order to meet the discharge limit from 8 mg/l to 3 mg/l (Kessler, 2010).

Therefore, digester supernatant containing high ammonium needs to be treated separately, through a side-stream process, that is more economical than treating the centrate through a main stream process (Bilyk et al., 2012). The usual convention of treating high ammonium rich wastewater, through a side-stream process, involves the nutrient removal method. In Canada, the City of Winnipeg needed to implement a side-stream ammonia removal process in three WWTPs, to treat the centrate separately and help to resolve high eutrophication problems in Lake Winnipeg (Manitoba). Bilyk et al. (2012) estimated the cost comparison of ammonia removal methods among side-stream and mainstream treatment processes, using a process model representing the actual side-stream characteristics. The implemented side stream treatment process reduced the nitrogen load to the mainstream process, delaying the modification of BNR tanks by 10 years and saving around \$6.6 M USD of capital cost. The side-stream treatment process was found to be more economically feasible with respect to capital and operating costs than the mainstream treatment process, irrespective of methods used.

The ThermoEnergy Corporation (Fassbender, 2001; ThermoEnergy Corporation, 2007) has performed extensive studies regarding the efficiency of an ammonia recovery process (ARP) for centrate treatment, as well as the economic benefits for the implementation of an ARP process in side-stream treatment. A significant energy and cost reduction could be achieved from the WWTPs with incorporation of a separate ammonia recovery process for centrate treatment. The cost estimation for a plant size of 85 MGD with 90% centrate ammonia removal, following ARP processes, indicated that the ammonia reduction obtained from separate centrate treatment with a \$15 million capital investment would be similar to that of the main stream BNR treatment process, with a capital cost of \$115 million (ThermoEnergy Corporation, 2007).

The presence of ammonia in wastewater streams can be considered a resource, rather than a problem. Ammonia recovery from wastewater is not the only benefit but the revenue earned from

recovered nutrients can also counterbalance the overall treatment cost. Therefore, new approaches have been taken towards the development of ammonia recovery technology, which will offset the cost of meeting ammonia discharge regulations through a mainstream process. In addition, the revenue generated from recovered ammonia will offset the cost of a side-stream process. It has been estimated that around \$10,000 to \$75,000 per year can be generated through nitrogen recovery from the treatment facility containing wastewater flows of 10 MGD (WERF, 2010).

The major incentive for ammonia recovery is the potential for internal revenue generation through utilizing recovered ammonia as commercially available product, such as fertilizer. Figure 1.5 indicates the increasing trend of market price for commercially available nitrogen fertilizer over time, provided by the US Department of Agriculture Economic Research Center (2013). With the increase in world population, the demand for nitrogen fertilizer has also increased to meet the increasing food demand. Therefore, the market price for synthesized nitrogen fertilizer increased from \$50-\$150 USD to approximately \$400-\$750 USD between 1960 and 2013.

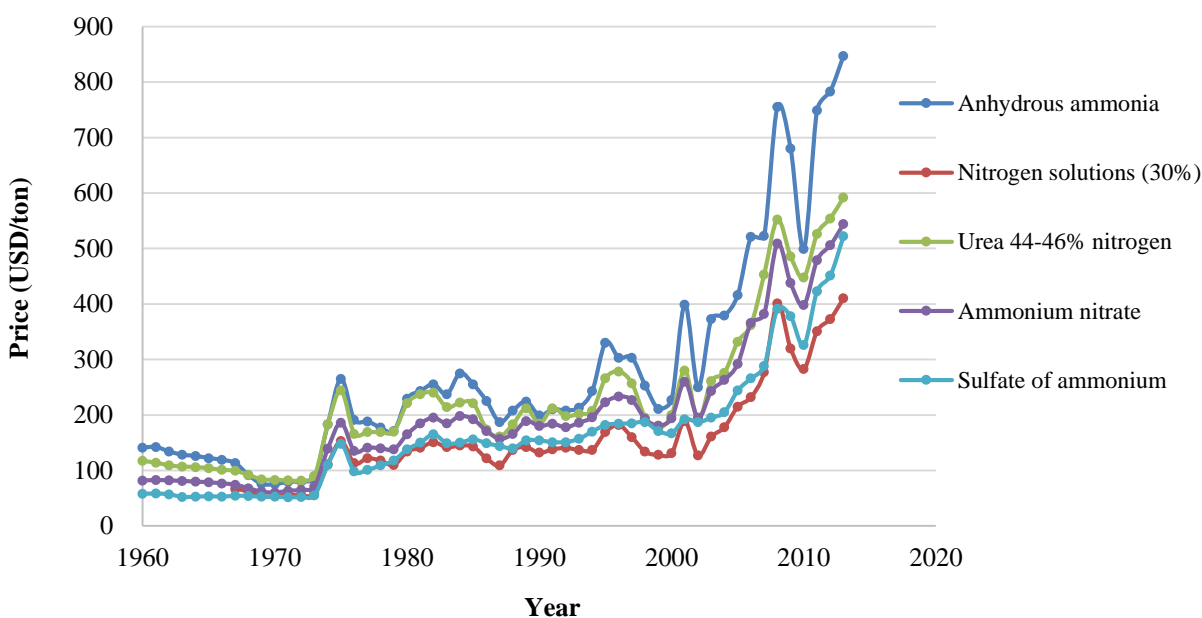


Figure 1.5 A comparison of prices among nitrogen fertilizers from 1960 to 2013 (USDA ERS, 2013)

Over 99% of the ammonia is synthesized from the Haber-Bosch process (Smil, 2001). This process is mainly dependent on the world's natural gases and holds responsibility for greenhouse gas

emissions. Further, the incorporation of high temperature and pressure in the Haber-Bosch process is energy-intensive and expensive. Therefore, sustainable ammonia production needs to be employed in order to meet agricultural demand. Equally important, wastewater effluent, containing high ammonia, can cause eutrophication and fish kills. Therefore, considering the abundance of ammonia in wastewater and further requirements for its removal, wastewater can be considered as a sustainable source for ammonia production, thereby turning a problem into an opportunity. The present work aimed to develop the technology for ammonia recovery from wastewater and explore its reuse as a fertilizer, or a source of energy.

Chapter 2: Background and Literature Review

2.1 Conventional methods for ammonia recovery from wastewater

The conventional ammonia recovery methods that are frequently applied include the air stripping method for ammonia gas evolution, membrane method for ammonia absorption, and ion exchange method for ammonia adsorption. These methods, briefly described in the following sections, require extensive resource and energy consumption.

2.1.1 Air stripping method

In wastewater, almost all nitrogen remains dissolved in the form of ammonium ions (NH_4^+) at around neutral pH and 25°C (Evans and Thompson, 2009). As temperature and pH increase, the solubility of ammonia decreases, (Saracco and Genon, 1994) and eventually the ammonium ion transforms into ammonia gas; this gas can be captured and transformed into synthetic fertilizer. In order to obtain ammonia removal through stripping, the pH of the water is maintained at 10.5 using lime or NaOH, and the temperature is increased from over 60°C to between 90-100°C by preheating. Compressed air is then forced through the wastewater in a stripping column to increase the mass transfer of ammonia into the atmosphere. Different wastewater streams including pig slurry (Bonmati and Flotats, 2003), landfill leachate, (Cheung et al., 1997) and wastewater produced from mineral fertilizer production (Minocha and Prabhakar, 1988) have been effectively treated for ammonia, using the air stripping method. In all these cases, the process was performed at high pH values using significant caustic addition. However, the addition of caustic can cause scaling of stripping towers and packing media, requiring biweekly descaling. Conversely, the addition of steam and air, conveyance and heating of huge amounts of wastewater, induce substantial operational and maintenance costs. Wastewater, with particulates, can clog the plant due to flocculation and precipitation of chemical sludge, requiring pre-treatment. The operating costs were estimated around 6 EUR/kg $\text{NH}_4\text{-N}$ removal which is \$13.50 per hour of operation (Cilona et al., 2009). This process requires high capital costs of 230,000 to 300,000 EUR for infrastructure establishment, such as a stripping tower (Evans and Thompson, 2009; Cilona et al., 2009). The expelled ammonia gas can be absorbed either in strong acid (i.e. sulphuric acid) or in

a biofilter in order to prevent air pollution and to recover an ammonium-rich fertilizer (Swartz et al., 1998; Lei et al., 2007; Elston and Karmarkar, 2003; Cilona et al., 2009).

2.1.2 Membrane method

In the membrane method, a hydrophobic hollow fiber membrane is used to separate the waste solution phase from the acid absorption phase, to provide an ammonia concentration gradient between the two phases. At high pH, dissolved ammonium ion (NH_4^+) converts into free ammonia gas which transfers through the hollow fiber membrane from the waste solution to the acid solution; this is due to a lower concentration of ammonia gas in the acid solution, compared to the waste solution. Ammonia gas then reacts with acid to form an ammonium salt which maintains the concentration gradient for continuous transfer of ammonia gas through the membrane. Cilona and colleagues (2009) demonstrated that about 85% ammonia recovery can be achieved through application of membrane gas transfer. The authors also estimated the capital cost at approximately 150,000 EUR, that included membrane contractors, pumps, and sensors. The operating costs due to membrane replacement and chemical and electrical consumption was around 1.21 EUR/kg of recovered nitrogen (Cilona et al., 2009; Ulbricht et al., 2013). Ulbricht et al. (2013) achieved up to 95% ammonia recovery from industrial wastewater using a similar membrane method and claimed that larger systems can cost more than conventional stripping or scrubbing systems.

2.1.3 Ion exchange method

Several researchers have performed studies on ammonium removal efficiency from wastewater using the ion exchange method. Ammonia removal from wastewater has been achieved successfully using the ion exchange method with zeolite resin, especially clinoptilolite (Komarowski and Yu, 1997; Nguyen and Tanner, 1998; McVeigh and Weatherley, 1999; Beler-Baykal et al., 2011). Clinoptilolite (alumina silicate) is a naturally occurring mineral that has a strong ion exchange affinity for ammonium (NH_4^+). When clinoptilolite is placed in a solution containing ammonium, such as human urine, more than 97% ammonia removal and an overall ammonium recovery of 86% can be achieved from exhausted clinoptilolite (Beler-Baykal et al., 2011; Allar and Beler-Baykal, 2013).

ThermoEnergy Corporation (Fassbender, 2001; ThermoEnergy Corporation, 2007) patented the Ammonia Recovery Process (ARP) using a complex ion exchange method to recover ammonia from wastewater. The ion exchange resin is used to adsorb aqueous ammonia from wastewater, which is then regenerated further using a solution containing zinc and sulfuric acid. The external addition of acid to the solution causes crystallization of ammonium zinc sulfate hexahydrate $((\text{NH}_4)_2\text{SO}_4\text{ZnSO}_4 \cdot 6\text{H}_2\text{O})$. Subsequently, the thermal decomposition of ammonium zinc sulfate hexahydrate is performed to release ammonia and sulfur trioxide. Finally, the decomposed product contains zinc sulfate. The evolved ammonia gas is captured in the sulfuric acid to produce commercial ammonium sulfate fertilizer. This ARP technology successfully recovered almost 100% ammonia, when it was implemented in a pilot study in the Oakwood Beach WWTP in New York. However, design complexity, as well as heavy chemical and heating requirements, led to a high capital cost associated with this technology (Fassbender, 2001).

The ion exchange method can successfully remove aqueous ammonia, if there are no other cations present in the solution (Stefanowicz et al., 1992b). The typical ammonia concentration for the ion exchange method was reported as 100 to 500 mg/l in a previous study (Palmer et al., 1988; Stefanowicz et al., 1992b). The ion exchange resin exhausts rapidly when the ammonium concentration increases beyond 2500 mg/l, ultimately increasing the operating cost for resin regeneration (Palmer et al., 1988; Stefanowicz et al., 1992b). Therefore, the ion exchange method cannot be a suitable economic option for ammonia removal from wastewater containing 1000 mg/l of NH_4^+ (Stefanowicz et al., 1992b).

2.1.4 Chemical precipitation method

The struvite precipitation method involves the addition of magnesium, orthophosphate, and caustic to ammonia-rich wastewater to provide Mg:N:P at a stoichiometric ratio of 1:1:1, to remove ammonia through struvite formation. Struvite crystals can be easily precipitated out from the solution and applied as a fertilizer (Le Corre et al., 2009; Liu et al., 2013). This method has been widely implemented for phosphorus recovery from wastewater, rather than ammonia recovery, due to high operational costs associated with the supplemental addition of magnesium and phosphate, with costs around 6 EUR/kg nitrogen recovered (Cilona et al., 2009). Therefore, several

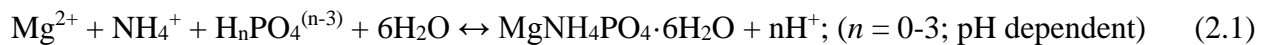
studies have been conducted on struvite thermal decomposition to reuse the decomposed struvite product as a source of magnesium and phosphate for further aqueous ammonium removal through struvite recrystallization (Stefanowicz et al., 1992b; Zhang et al., 2004; Sugiyama et al., 2005; Sugiyama et al., 2007; Türker and Çelen, 2007; He et al., 2007; Zhang et al., 2009b; Huang et al., 2009; Novotny, 2011). This process will be discussed in further detail.

2.2 Struvite formation and recovery background

2.2.1 Formation of struvite in wastewater treatment works

A major problem in many wastewater treatment plants is the accumulation of struvite in wastewater treatment works, causing operational problems and maintenance issues. A number of wastewater treatment plants have reported the occurrence of struvite deposition in pipe fittings and apparatus with increased turbulence (Borgerding, 1972; Mohajit et al. 1989). Struvite deposits are difficult to remove from equipment surfaces and pipe walls, thus requiring replacement of the damaged parts and increasing the operating cost of the treatment process. Importantly, struvite can be easily formed and precipitated out from wastewater solution. Thus, struvite recovery (Mavinic et al., 2007; Le Corre et al., 2009) from wastewater not only solves the aforementioned problem, but also recovers nutrients (nitrogen and phosphorus) from wastewater, and the struvite pellets can be utilized as a slow release fertilizer.

Struvite ($\text{MgNH}_4\text{PO}_4 \cdot 6\text{H}_2\text{O}$), also known as magnesium ammonium phosphate (MAP), is a white crystalline substance comprised of magnesium, ammonium and phosphorus at equimolar concentrations. Struvite forms according to the following Equation (2.1) (Abbona and Boistele, 1979):



2.2.2 Solubility product of struvite and other magnesium phosphates

The rate of struvite formation and dissolution can be described with regard to the struvite solubility product (K_{sp}). The solubility product K_{sp} is defined as the equilibrium constant of a reaction where a precipitate and its constituent ions are involved (Tchobanoglous, 1985). Struvite will precipitate in solution if the product of the concentrations of magnesium, phosphate and ammonium exceed the equilibrium solubility of struvite. On the other hand, struvite will dissolve in solution if the product is lower than equilibrium solubility. The precipitation of struvite can be controlled in solution through changing pH, temperature, supersaturation ratio and ionic activity of the ions present in the solution. Struvite starts forming in ammonia rich waste solution at a pH between 6 and 9, in the presence of sufficient phosphorus and magnesium. The solubility of struvite decreases with an increase in pH with minimum solubility occurring at pH 10.3 (Ohlinger et al., 1998; Ohlinger et al; 1999; Bhuiyan et al., 2007; Wilson, 2013). A further increase in pH above 10.3 actually causes an increase in the solubility of struvite. Table 2.1 represents the solubility product (K_{sp}) values for different magnesium phosphate compounds (Wilson, 2013).

During precipitation or dissolution of struvite, formation of other magnesium phosphate compounds such as $MgHPO_4 \cdot 3H_2O$ (newberyite), $Mg_3(PO_4)_2 \cdot 8H_2O$ (bobierrite) and magnesite ($MgCO_3$), along with struvite, have been reported by several researchers (Taylor et al., 1963a; Boistelle and Abbona, 1983; Kontrec et al., 2005; Babić-Ivančić et al., 2006; Königsberger and Königsberger, 2006; Shand, 2006). The formation of different precipitation products, other than struvite, causes a decrease in ammonium removal efficiency through consumption of magnesium and phosphate where the nitrogen component of struvite is not present in the newly-formed phases. Newberyite forms in ammonia rich solution at a lower pH 5-6, whereas bobierrite forms at a slightly higher pH, around 8. Crystallization of newberyite and bobierrite occurs due to a decrease in solubility of these compounds, as well as an increase in struvite solubility when the solution temperature is increased above 25°C (Boistelle and Abbona, 1983; Kontrec et al., 2005; Babić-Ivančić et al., 2006; Königsberger and Königsberger, 2006).

Table 2.1 Reported pK_{sp} values for different magnesium and phosphate compounds at 25°C (Wilson, 2013)

Solid Phase	$pK_{sp} = -\log_{10} K_{sp}$	Reference
Struvite $MgNH_4PO_4 \cdot 6H_2O$	13.15	Taylor et al., 1963a
	13.26	Ohlinger et al., 1998
	13.36	Babić-Ivančić et al., 2002
	13.36	Bhuiyan et al., 2007
	13.68	Koutsoukos et al., 2007
	13.47	Lobanov et al., 2013
Dittmarite $MgNH_4PO_4 \cdot H_2O$	12.77	Lobanov et al., 2013
Newberyite $MgHPO_4 \cdot 3H_2O$	5.82	Taylor et al., 1963b
	5.78	Verbeeck et al., 1984
	5.88	Lobanov et al., 2013
Bobierite $Mg_3(PO_4)_2 \cdot 8H_2O$	25.20	Taylor et al., 1963b
	25.47	Lobanov et al., 2013
Cattiite $Mg_3(PO_4)_2 \cdot 22H_2O$	23.10	Taylor et al., 1963b
	23.22	Lobanov et al., 2013

2.2.3 Recovery of struvite through precipitation method

The solution pH, degree of supersaturation, temperature, and the presence of other ions have significant influences on struvite precipitation in aqueous system (Ohlinger et al., 1999; Bouropoulos and Koutsoukos, 2000). Struvite contains magnesium, ammonium and orthophosphate at a molar ratio of 1:1:1. In order to precipitate struvite from a solution, the combined activity of Mg^{2+} , NH_4^+ and PO_4^{3-} must be higher than the solubility product of struvite. In municipal wastewater streams, the molar concentration of ammonium ions is higher than those of phosphorus and magnesium. Magnesium is usually the limiting factor for struvite formation and crystallization. Supplemental magnesium addition is required in many cases, for continuous operation and struvite recovery. Therefore, in various struvite recovery processes, MgO, $MgCl_2$ or $MgCl_2 \cdot 6H_2O$, seawater, and brucite ($Mg(OH)_2$) have been introduced as magnesium feed stock.

Jaffer et al. (2002) also showed that an increase in Mg:P molar ratio from 1.05:1 to 1.3:1 causes a substantial increase in orthophosphate removal efficiency, in the form of struvite.

Nutrient recovery through struvite crystallization using fluidized bed reactors has been well-studied at UBC since 1999 and was patented in 2009 (Koch et al., 2011). The typical process flow diagram of the patented system is presented in Figure 2.1 (Bhuiyan et al., 2008b; Koch et al., 2011). In most WWTPs the struvite crystallizers are comprised of a fluidized bed reactor (FBR), an injector, an external clarifier, and storage compartments for magnesium, caustic and feed (Fattah, 2004). The fluidized bed reactor (FBR) is the main part of the struvite crystallization process and consists of four cylindrical sections of different diameters. From top to bottom, the FBR includes a seeding zone, reaction zone, active zone and harvest zone. Nitrogen-and phosphorus-rich wastewater and a recycle stream are fed at the bottom of the reactor. In order to maintain optimum Mg:N:P molar ratio and pH value for struvite crystallization, magnesium-containing solution and caustic are added through the injector.

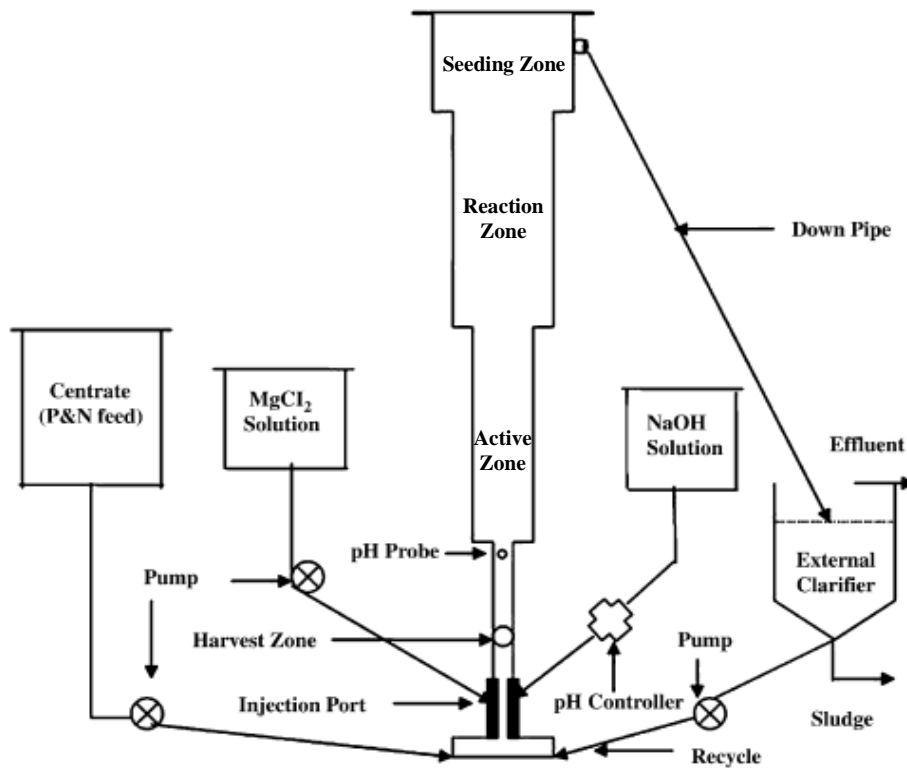


Figure 2.1 Pilot-scale struvite crystallization system (Bhuiyan et al., 2008b)

Struvite crystal growth results from a high supersaturation level in the reactor, whereas crystal agglomeration along with struvite pellet formation, result from proper hydrodynamics of the FBR. The struvite pellets become larger in size as they remain in the reactor for a longer duration and eventually this causes settling of struvite pellets. When the struvite pellets grow to a suitable size, they can be removed from the harvesting zone. The portion of clarified stream is then withdrawn as a treated effluent and the remaining part of the stream is returned to the lower part of the reactor. This struvite precipitation method has been widely accepted in practice as a phosphorus removal and recovery process from nutrient rich wastewater.

2.2.4 Ammonia recovery through struvite precipitation using commercial reagents

Wastewater streams contain high concentrations of nutrients (nitrogen and phosphorus) that are essential to all living organisms. Nutrient recovery from wastewater streams not only solves the problem of struvite deposition in wastewater treatment works, but helps to solve the eutrophication problem in natural waterbodies. In addition, struvite precipitation has gained commercial interest due to its value as fertilizer. Struvite formation occurs when Mg^{2+} , NH_4^+ and PO_4^{3-} react at equimolar ratios. Since most wastewater streams contain high N:P ratios, external addition of magnesium equivalent to phosphorus is required to provide the stoichiometric ratio for struvite formation. During this process, only 15~20% ammonia removal can be achieved from centrate, while phosphorus removal is over 90% (Adnan et al., 2003; Fattah et al., 2008a; Fattah et al., 2008b). Therefore, the effluent contains a high residual ammonium concentration; in order to remove excess ammonia, both magnesium and phosphate need to be added externally to maintain the stoichiometric ratio Mg:N:P of 1:1:1. Previous researchers conducted several studies on different wastewater streams such as landfill leachate, rare-earth wastewater, piggery effluents, calf manure, coking wastewater, anaerobic digester supernatant, leather tanning wastewater and swine wastewater, in order to observe the controlling factors and mechanisms for an ammonia removal process through precipitating struvite. The effects of different parameters such as pH, Mg:N:P molar ratio and source of magnesium and phosphate on ammonia removal efficiency of different wastewater streams, via struvite formation, are presented in Table 2.2.

Table 2.2 Summary of ammonia removal studies through struvite precipitation using commercial reagents

Type of Wastewater	pH	Initial NH ₄ -N Concentration (mg/l)	Removal % of NH ₄ -N	Sources of Mg ²⁺ and PO ₄ ³⁻ and Mg ²⁺ :NH ₄ ⁺ -N:PO ₄ ³⁻ -P	References
Industrial waste solutions	9.16-9.85	1000	100%	MgO and H ₃ PO ₄	Stefanowicz et al. (1992a)
Combined wastewater from bovine and leather tanning factories	9	200	82%	MgCl ₂ .2H ₂ O and Na ₂ HPO ₄ Mg:N:P = 1:1:1	Tünay et al. (1997)
Anaerobic digester effluents (Molasses Industry)	8.5-9	1400	> 90	MgCl ₂ and H ₃ PO ₄ Mg: N: P = 1.2:1:1.2	Çelen and Türker (2001)
Landfill leachate	9	2750	92%	MgCl ₂ .6H ₂ O and Na ₂ HPO ₄ .12H ₂ O Mg:N:P = 1:1:1	Li and Zhao (2002)
Landfill leachate	9	2750	36%	MgO and 85% H ₃ PO ₄ Mg:N:P = 1:1:1	Li and Zhao (2002)
Landfill leachate	9	2750	70%	MgSO ₄ .7H ₂ O and Ca(H ₂ PO ₄)H ₂ O	Li and Zhao (2002)
Leather tanning wastewater	9.5	6785	94%	MgCl ₂ .6H ₂ O and NaH ₂ PO ₄ .2H ₂ O Mg:N:P = 1:1:1.2	Zengin et al.(2002)
Synthetic wastewater	9.6	—	39%	Bittern as Mg ²⁺ Mg: N: P = 1.3:1.1:1.0	Lee et al.(2003)
Synthetic wastewater	10	—	54%	Seawater as Mg ²⁺ Mg: N: P = 1.3:1.1:1.0	Lee et al.(2003)
Synthetic wastewater	9.1	—	53%	MgCl ₂ as Mg ²⁺ Mg: N: P = 1.3:1.1:1.0	Lee et al.(2003)

Table 2.2 Continued

Type of Wastewater	pH	Initial NH ₄ -N Concentration (mg/l)	Removal % of NH ₄ -N	Sources of Mg ²⁺ and PO ₄ ³⁻ and Mg ²⁺ :NH ₄ ⁺ -N:PO ₄ ³⁻ -P	References
Slurry-type swine wastewater	8-10	2125	98%	MgO and H ₃ PO ₄ Mg: N: P = 3.0:1.0:1.5	Kim et al. (2004)
Anaerobically digested dairy manure	8.5	255	90%	MgCl ₂ ·6H ₂ O and Na ₂ HPO ₄ Mg: N: P = 1.3:1:4.8	Uludag Demiret et al.(2005)
Anaerobically digested dairy manure	8.5	480-520	90%	Mg(OH) ₂ and Na ₂ HPO ₄ Mg: N: P = 2.2:1:4.8	Uludag Demiret et al.(2005)
Simulated wastewater	8.5-10	2000	>95%	MgCl ₂ and Na ₂ HPO ₄	Lobanov and Poilov (2006)
Landfill leachate	8-11	1795	>98%	MgCl ₂ ·6H ₂ O, KH ₂ PO ₄ and struvite seed Mg: N: P = 1.2:1.0:1.2	Kim et al. (2007)
Landfill leachate	9	2132	98.3%	MgO (87%) and Na ₂ HPO ₄ ·12H ₂ O Mg:N:P = 1:1:1.2	Barnes et al. (2007)
Rare-earth smelting company wastewaters	11	1540	95%	MgSO ₄ and Na ₂ HPO ₄ Mg:N:P = 1.2:1:1.3	Li et al. (2007)
Landfill leachate	8.6-9	2700	91%	MgCO ₃ and H ₃ PO ₄ Mg: N: P = 1:1:1	Gunay et al. (2008)
Semiconductor wastewater	9.2	155	>89%	MgCl ₂ ·6H ₂ O and KH ₂ PO ₄ Mg: N: P = 1:1:1	Ryu et al. (2008)
Pre-treatment of Landfill leachate	9.5	2520	85%	MgCl ₂ ·6H ₂ O and Na ₂ HPO ₄ ·12H ₂ O Mg: N: P = 1.5:1:1	Zhang et al. (2009a)
Up-flow anaerobic sludge blanket (UASB) pretreated poultry manure wastewater effluent	9	1318	89.3%	MgCl ₂ ·6H ₂ O and KH ₂ PO ₄ Mg: N: P = 1.5:1:1	Yetilmezsoy and Sapci-Zengin (2009)

Previous researchers used different sources of magnesium and phosphate, in order to identify the optimal combination of reagents that maximizes the ammonia recovery efficiency. Çelen and Türker (2001) investigated the ammonia recovery efficiency from anaerobic digester effluents through struvite precipitation, using MgO or MgCl₂ and phosphoric acid as external sources of magnesium and phosphate. About 95% ammonia removal was achieved from anaerobic digester effluents after using MgCl₂ and phosphoric acid, at temperatures between 25°C-40°C and at pH 8.5-9. In order to obtain higher ammonia recovery efficiency, there was a requirement for a slight excess of Mg and P at a ratio of Mg:N:P=1.2:1:1.2; this is not economically feasible for widespread application. Further, to retrieve the struvite crystals from impurities, the precipitates had to be dissolved by acidification. Around 85% recovery of pure struvite crystals was obtained through centrifugation and pH adjustment. The estimated cost of ammonia recovery in the aforementioned study, without considering the commercial value of retrieved struvite, was around 7.5-8\$/kg NH₄-N.

Another study was conducted by Li and Zhao (2002), using three different combinations of magnesium and phosphate: MgCl₂·6H₂O with Na₂HPO₄·12H₂O, MgO with H₃PO₄ and MgSO₄·7H₂O with Ca(H₂PO₄)₂·H₂O to investigate the efficiency of ammonia recovery from landfill leachate through struvite precipitation. The maximum ammonia removal efficiency was obtained using MgCl₂·6H₂O with Na₂HPO₄·12H₂O followed by MgSO₄·7H₂O with Ca(H₂PO₄)₂·H₂O and MgO with H₃PO₄. The solubility of these compounds was found to vary with pH. The obtained ammonia removal efficiency from the experiment demonstrated that MgCl₂·6H₂O, along with Na₂HPO₄·12H₂O, has a high solubility, which can rapidly dissociate Mg²⁺ and HPO₄³⁻ for struvite precipitation. However, due to the low solubility of MgO together with Ca(H₂PO₄)₂·H₂O, the release rate of Mg²⁺ and HPO₄³⁻ was very slow, leading to a decreased rate of struvite formation. The different dissolution rates of magnesium and phosphate reagents might be responsible for the difference in the observed removal efficiencies of ammonium nitrogen from different wastewater streams.

A number of previous studies have mentioned that the proper sequence of feeding reagents can also enhance ammonia removal efficiency from wastewater, by preventing any undesirable

reactions that may hinder the ammonia removal efficiency. Kim et al. (2007) performed a study on landfill leachate in order to enhance ammonia recovery efficiency through the addition of reagents in a particular sequence. To form struvite, magnesium chloride ($\text{MgCl}_2 \cdot 6\text{H}_2\text{O}$) and potassium phosphate (KH_2PO_4) were used as the alternate sources of magnesium and orthophosphate ions, respectively. In all experiments, magnesium and orthophosphate were fed to reach a molar ratio of $\text{Mg} : \text{NH}_4 : \text{PO}_4$ of 1.2:1:1.2. Around 90% ammonia removal efficiency from landfill leachate was achieved by the addition of excess magnesium and phosphate, followed by addition of the buffering reagent, thus providing the optimum conditions for struvite precipitation. Further addition of 40 g/L struvite seed, increased the ammonia removal efficiency to 98%, at pH value of 8-11. However, the added struvite seed increased the residual level of $\text{PO}_4\text{-P}$ in the final effluent.

Lobanov and Poilov (2006) also studied the ammonia recovery process through crystallization of struvite, using commercial reagents where the sequence of adding reagents was different compared to Kim et al. (2007). Lobanov and Poilov (2006) used MgCl_2 as Mg^{2+} and Na_2HPO_4 as PO_4^{3-} for precipitating struvite from the simulated wastewater. A high degree of wastewater purification was achieved by adding Na_2HPO_4 as a source of PO_4^{3-} and NaOH to the wastewater, followed by addition of MgCl_2 as a source of Mg^{2+} . More than 95% ammonia removal was achieved at pH 8.5-10 with a minor excess of reagents (5%) in the described process. The solid precipitated phase, identified by XRD, was mainly struvite along with minor impurities of $\text{Mg}_3(\text{PO}_4)_2 \cdot 8\text{H}_2\text{O}$ and $\text{MgHPO}_4 \cdot 3\text{H}_2\text{O}$. The authors also noted that the presence of other impurities, such as potassium and calcium, during the treatment process, can reduce ammonia removal efficiency.

According to the results of previous studies, it is evident that different combinations of magnesium and phosphate salts have an influence on ammonium nitrogen removal efficiency. Sources of magnesium and phosphate that can dissociate easily and rapidly provide higher ammonia recovery efficiency through struvite precipitation. In addition, the feeding sequence of added reagents has a substantial effect on ammonia removal efficiency.

This section reviewed the research efforts carried out on ammonia removal from different wastewater streams through struvite precipitation. The economic feasibility of ammonia recovery

from different wastewater streams has also been evaluated by many researchers. To achieve maximum ammonia removal, significant amounts of magnesium and phosphate are required to provide a stoichiometric ratio of 1:1:1 for struvite precipitation. The required dose of added phosphate was found to be higher than the dose of magnesium (Huang et al., 2011a). The excess addition of phosphate not only increases the treatment cost but also increases the residual phosphate concentration in the solution, thereby requiring additional treatment. The high operating cost, resulting from the enhanced consumption of chemically available reagents, lessens the applicability of struvite process for effective ammonia recovery. Therefore, the utilization of struvite decomposition products as a source of magnesium and phosphate, could provide a sustainable solution for the ammonia recovery process.

2.3 Ammonia recovery using struvite thermal decomposition product

In the previous section the operating problems and economic constraints associated with external addition of magnesium and phosphate for excess ammonia removal were discussed. Due to high N:P ratio in wastewater streams, the external addition of magnesium and phosphate is required to maintain an equimolar ratio for struvite formation. However, it appears that external addition of magnesium and phosphate is not the most cost effective option for ammonia recovery. If struvite, itself, can be used as a source of magnesium and phosphate, the operational cost could be significantly reduced. This can be achieved only if ammonia from the struvite ($\text{MgNH}_4\text{PO}_4 \cdot 6\text{H}_2\text{O}$) structure can be released. The ammonia recovery process from wastewater, using a struvite decomposition product, is presented in Figure 2.2.

Ammonia removal from struvite can be accomplished through the thermal decomposition of struvite either in air (i.e. dry process) or in alkali media (i.e. wet process). During thermal decomposition, ammonia release from the struvite structure to solution has been referred to as the “Wet Process”, whereas the release of ammonia gas to the atmosphere upon decomposition is the “Dry Process”. Once decomposed, struvite or the saturated supernatant that is devoid of ammonia can be added to the ammonia-rich effluent as a source of magnesium and phosphorus, thus removing residual ammonia through struvite reformation (according to Figure 2.2).

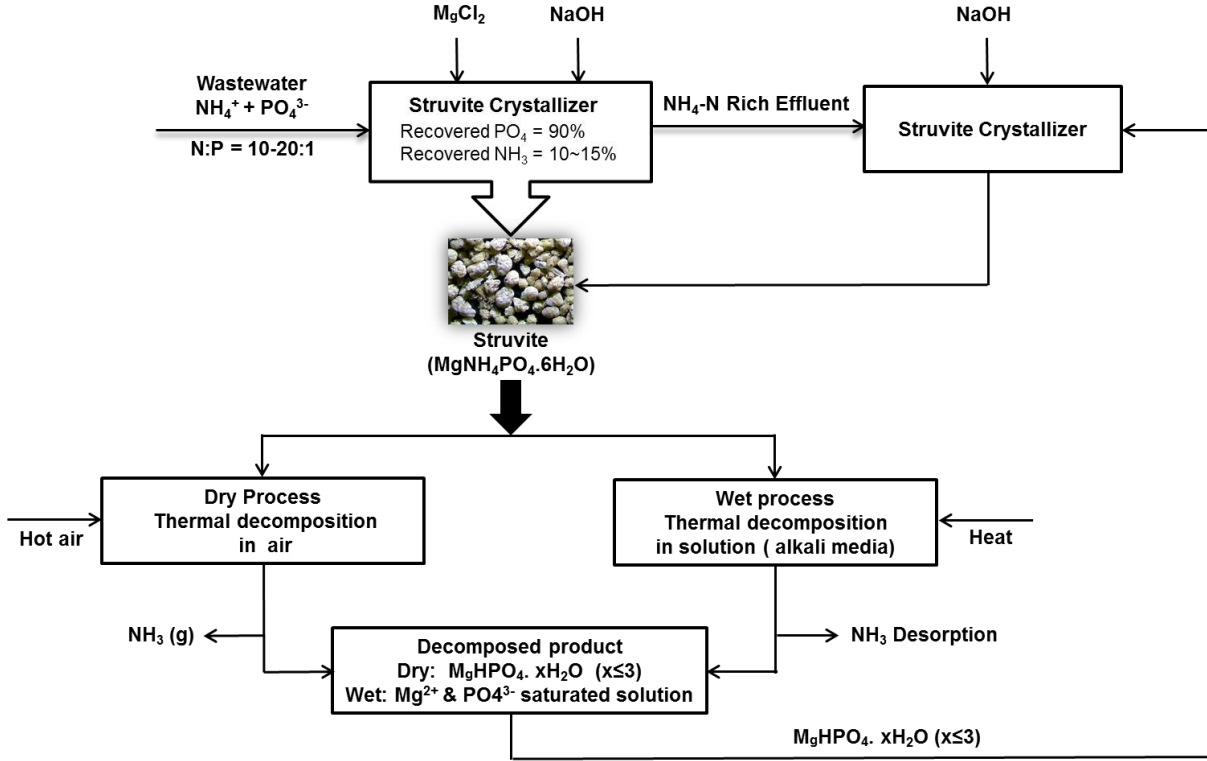
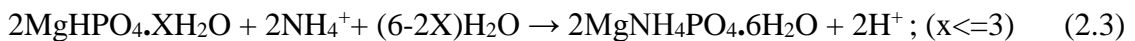
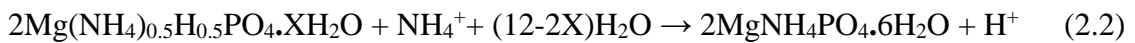


Figure 2.2 Process flow diagram of ammonia recovery using struvite decomposition product

It should be noted that maximum ammonia removal efficiency, using decomposed struvite, can be achieved, provided that the decomposed struvite is completely devoid of ammonia. The decomposed struvite product, devoid of ammonia, possesses a greater potential for maximum ammonia removal. For example, Equation 2.2 and 2.3 show that the decomposition product containing 50% ammonia can reduce aqueous ammonium removal efficiency by 50%, compared to the decomposed product containing no ammonia. Thermal decomposition of struvite performed by previous researchers and subsequent removal of ammonia using the wet and dry processes, are discussed in the following sections.

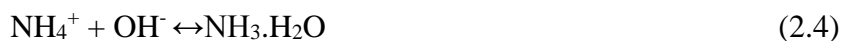


2.3.1 Decomposition of struvite: Wet process

Struvite thermal decomposition, using the wet process, is comprised of two main stages. In the first stage, ammonia is removed from the wastewater through struvite precipitation, using commercial reagents. In the second stage, the precipitated struvite is collected and then undergoes decomposition either in alkali or acid solution, resulting in a different magnesium phosphate solid phase formation, depending on experimental variables such as pH and temperature. Afterward, the decomposed product can be used as a source of magnesium and phosphate, instead of commercial reagents, to remove further ammonia from wastewater through struvite reformation.

2.3.1.1 Removal of ammonia following thermal alkali treatment

This section will review some previous studies performed on thermal decomposition of struvite in alkali solution. According to Zhang et al. (2009b), struvite dissolution in aqueous alkaline environment results in a solution system of $\text{NH}_4^+ - \text{OH}^- - \text{Mg}^{2+} - \text{Na}^+ - \text{PO}_4^{3-}$. Ammonia can easily escape from the solution due to instability of $\text{NH}_4^+ - \text{OH}^-$ represented in Equation 2.4.



The transformation of ammonium ions into $\text{NH}_3 \cdot \text{H}_2\text{O}$ increases with the increase in NaOH concentration. Afterwards, ammonia gas evolution increases with an increase in temperature (accomplished through heating the solution system).

Türker and Çelen (2007) investigated the ammonia removal efficiency from anaerobically pretreated industrial wastewater containing molasses, using a struvite decomposition product obtained through thermal-alkali treatment. Struvite was formed at pH 8.5 by providing excess $\text{MgCl}_2 \cdot 6\text{H}_2\text{O}$ and H_3PO_4 as a source of Mg^{2+} and PO_4^{3-} , at a molar ratio of $\text{Mg}^{2+} : \text{NH}_4^+ : \text{PO}_4^{3-} = 1:1:1$. The addition of NaOH to the precipitated struvite caused release of ammonia from struvite into the liquid phase. Further addition of NaOH, at a ratio of $\text{OH}^- : \text{NH}_4^+ = 1:1$, increased the pH and caused conversion of NH_4^+ into NH_3 . The provision of heat for 3 hours at a temperature of 110°C caused subsequent ammonia vapourization, resulting in about 81% ammonia removal from

the alkali solution. With the same heating temperature and duration, a higher ammonia removal efficiency (>90%) was reported by Zhang et al. (2009b), with the incorporation of a higher $\text{OH}^-:\text{NH}_4^+$ molar ratio (2:1). The decomposed product produced from the first stage was then reused to remove excess ammonia from the wastewater; this process was continued for another four cycles. The initial decomposed product was not reported by Türker and Çelen (2007), while Zhang et al. (2009b) declared the major solid phase as an amorphous MgNaPO_4 . Both authors claimed that the subsequent decomposed product may have contained a significant portion of $\text{Mg}_3(\text{PO}_4)_2$ and/or $\text{Mg}_2\text{P}_2\text{O}_7$, which are least soluble. The authors reported that the ammonia recovery efficiency decreased by 16% from the first cycle to the end of the fifth cycle (Table 2.4). Reduced efficiency in the subsequent recycle stages can be explained by the presence of $\text{Mg}_3(\text{PO}_4)_2$ or $\text{Mg}_2\text{P}_2\text{O}_7$ compounds in the decomposed product.

The efficiency of the ammonia recovery process using a struvite decomposition product depends on the complete dissociation of decomposed product. A study on saponification wastewater performed by Huang et al. (2009) reported that the addition of HCl into the reused struvite decomposition product, at a molar ratio of $\text{H}^+:\text{OH}^- = 0.8$, can increase the aqueous ammonium removal efficiency from 96.4% to 99.6%. The added HCl dissolved these amorphous compounds into Mg^{2+} and PO_4^{3-} , to enhance struvite precipitation and crystallization. Another study performed by He et al. (2007) investigated ammonia removal efficiency from landfill leachate, using a struvite decomposition product as a source of magnesium and phosphate obtained from heating struvite in alkali conditions. The addition of NaOH at a molar ratio of $\text{NH}_4^+:\text{OH}^- = 1:1$, maintaining a pH of 9 and a temperature of 90°C for 2 hours, caused over 96% ammonia release from the precipitated struvite and subsequent transformation of struvite into amorphous magnesium sodium phosphate (MgNaPO_4). The formation of MgNaPO_4 , as a major struvite decomposition product under thermal alkali treatment, has been mentioned by other previous researchers (Zhang et al., 2009b; Huang et al., 2011b). Similar to Türker and Çelen (2007), He et al. (2007) also repeatedly used the decomposed struvite product for excess ammonia removal. The author reported that an increase in the number of struvite recycles caused a decrease in ammonia removal efficiency from 96% to 62% by the end of 6th cycle of treating landfill leachate.

Huang et al. (2011b) also provided similar outcomes from a study performed on piggery wastewater, through struvite recycling for effective ammonia removal. Around 80% ammonia removal from piggery wastewater was achieved in the first cycle; this was reduced to around 65% by the end of fifth cycle. The author mentioned that the residual phosphate concentration was measured at around 4 mg/l at the first cycle and increased to between 70-80 mg/l by the end of fifth cycle. Huang and colleagues (2011b) posited that the formation of inactive substances, such as $\text{Mg}_3(\text{PO}_4)_2$ or $\text{Mg}_2\text{P}_2\text{O}_7$, in the reused decomposed product and subsequent loss of Mg^{2+} and PO_4^{3-} in the supernatant at each cycle, were responsible for the lower ammonia removal efficiency. Therefore, further addition of $\text{MgCl}_2 \cdot 6\text{H}_2\text{O}$ plus $\text{Na}_2\text{HPO}_4 \cdot 12\text{H}_2\text{O}$, along with a decomposed struvite product, was required to increase the ammonium removal efficiency up to 90% which remained constant during the five cycles. A summary of ammonia removal from struvite during struvite decomposition through thermal alkali treatments and the subsequent utilization of these decomposed products for ammonia recovery from different wastewater streams, is presented in Table 2.3 and Table 2.4.

Table 2.3 Struvite decomposition studies using thermal-alkali treatment (Wilson, 2013)

Wastewater	OH:NH ₄ Molar Ratio	Heating Temp. (°C)	Heating Time (hours)	% Release of NH ₄ -N	Solid Phases; Possible Impurities	Reference
Molasses industry	1:1	≥110	<3	^a 81-100	Not identified; $\text{Mg}_3(\text{PO}_4)_2$, $\text{Mg}_2\text{P}_2\text{O}_7$	Türker and Çelen, 2007
Landfill leachate	1:1	90	2	>96%	^b Amorphous MgNaPO_4 ; Ca, K, Al	He et al., 2007
Saponification	1:1:1	100	3	Not reported	Not identified; $\text{Mg}_3(\text{PO}_4)_2$, $\text{Mg}_2\text{P}_2\text{O}_7$	Huang et al., 2009
Coking	2:1	110	3	90	^b Amorphous MgNaPO_4 ; $\text{Mg}_3(\text{PO}_4)_2$, $\text{Mg}_2\text{P}_2\text{O}_7$	Zhang et al., 2009b
Piggery	1:1	110	3	Not reported	^b Amorphous MgNaPO_4 ; Ca, K,	Huang et al., 2011b

a. Percent removal of solubilized NH_3 from liquid phase by volatilization; Percent elimination of NH_4^+ from struvite was not reported

b. XRD identified amorphous phase; MgNaPO_4 was suggested as dominant material by authors

Table 2.4 Ammonia recovery using struvite decomposition product obtained from thermal-alkali treatment (Wilson, 2013)

Wastewater	pH	Reaction Time (h)	% Removal of NH ₄ -N	Cycle No.	PO ₄ Residual (mg/L)	Reference
Molasses industry	8.5	Not reported	92 77	1st 5th	Not reported	Türker and Çelen, 2007
Landfill leachate	9.0	2.0	96 62	1st 6th	2-10	He et al., 2007
Saponification	9.0	0.5	99 ^a 99	1st 6th	<1	Huang et al., 2009
Coking	9.5	1.5	85 70	1st 5th	Not reported	Zhang et al., 2009b
Piggery	^b 9.4-8.5	1.0	80 65	1st 5th	<5-70	Huang et al., 2011b

a. Initially Mg and PO₄ are in excess and separate stages were employed for dissolution of decomposition products and residual PO₄ recovery

b. Required no adjustment of pH; pH varied as struvite formed; Initially Mg was in excess as magnesite

From an economic perspective, He et al. (2007) reported that the reuse of a struvite decomposition product, as a source of magnesium and phosphate for three cycles, could save up to 44% in chemical costs, compared to using commercial sources for the treatment of landfill leachate. The findings of Huang et al. (2011b) were in agreement with He et al (2007), where the author reported that the cost of precipitating struvite from piggery wastewater could be reduced by around 59% of the average cost, through reusing decomposed struvite for three cycles compared to using commercial reagents. Furthermore, Türker and Çelen (2007) state that the cost of ammonia removal using commercial reagents was found to be 20% higher relative to recycled nutrients. The cost of NH₃ recovery, using recycled precipitate, was reported at \$0.36/kg NH₄⁺-N in a multi-step process, whereas the cost of using commercial reagents was estimated at \$3.2/kg NH₄⁺-N recovery in a single-step process (Türker and Çelen, 2007). Therefore, ammonia removal efficiency from wastewater, using recycled nutrients (i.e. magnesium and phosphate), appears to be more promising and economically feasible, than from commercial reagents.

2.3.1.2 Removal of ammonia following acidolysis

In aqueous systems, transformation of struvite into a decomposed product devoid of ammonia through the addition of acid, is referred to as acidolysis. Similar to struvite ammonia removal through the thermal alkali treatment, various studies have been conducted on ammonia removal through acidolysis. Newberyite as a decomposed struvite product has been reported as a potential candidate for ammonia removal through acidolysis. Importantly, newberyite is completely devoid of ammonia and highly soluble in ammonium solution. Boistelle et al. (1983) investigated the transformation mechanism of struvite to newberyite in aqueous solution where the optimum pH, temperature and supersaturation ratio required for struvite to newberyite formation were reported. The authors found that, in aqueous solution at 25°C, struvite always crystallizes first at a supersaturation ratio of $S_{\text{newberyite}}/S_{\text{struvite}} < 2$ whereas at a ratio $S_{\text{newberyite}}/S_{\text{struvite}} > 4$, newberyite crystallizes first. In the ratio of $2 < S_{\text{newberyite}}/S_{\text{struvite}} < 4$, the solid phase that first precipitates depends on the initial pH. The precipitation of struvite causes a sharp decrease in pH and favours newberyite formation. The supersaturation ratio of struvite decreased to unity with the decrease in pH of the solution, causing the dissolution of precipitated struvite and formation of newberyite. Struvite completely transforms into newberyite when the solution becomes completely supersaturated, with respect to newberyite ($S_{\text{newberyite}} > 1$) at pH between 4 and 5.5. Apart from solution pH, temperature and supersaturation ratio, the transformation of struvite to newberyite can be enhanced by adequate mixing. Babić-Ivančić and colleagues (2006) carried out a similar study on the transformation mechanism of struvite to newberyite based on reaction kinetics, mixing times, varying initial pH and supersaturation ratios. According to the study, struvite was completely transformed into newberyite within 30 minutes at 25°C, pH 6.1 and $S_{\text{newberyite}}/S_{\text{struvite}}$ ratio of 1.48. An initial solution with a low pH of around 4-6 and high supersaturation ratio of newberyite to struvite, caused the rapid conversion of struvite to newberyite in aqueous solution.

Ammonia recovery from wastewater, using acidolyzed struvite residues, was proposed by Zhang et al. (2004). The ammonia recovery process was performed in two stages, as shown in Figure 2.3. The first stage involved the removal of ammonia from wastewater through struvite crystallization and in the second stage, the crystallized or precipitated struvite was transformed into newberyite (through acidification); this was then repeatedly used as a source of magnesium and phosphate for

removing excess ammonia as in the previous stage. The main purpose was to lower the use of commercially available magnesium and phosphate for excess ammonia removal and overcome the limitations of widespread application of the process. Zhang et al. (2004) reported that an increase in temperature up to 60°C and a decrease in pH to 5 caused maximum release of ammonium from struvite into the acid solution after 1.5 hours, leading to the formation of a solid phase containing struvite along with newberyite. According to the authors, XRD results confirmed the major portion of the solid phase to be newberyite. The authors also deduced that the supernatant contained a high concentration of ammonia along with hydrochloric acid, which can be useful as ammonium chloride fertilizer.

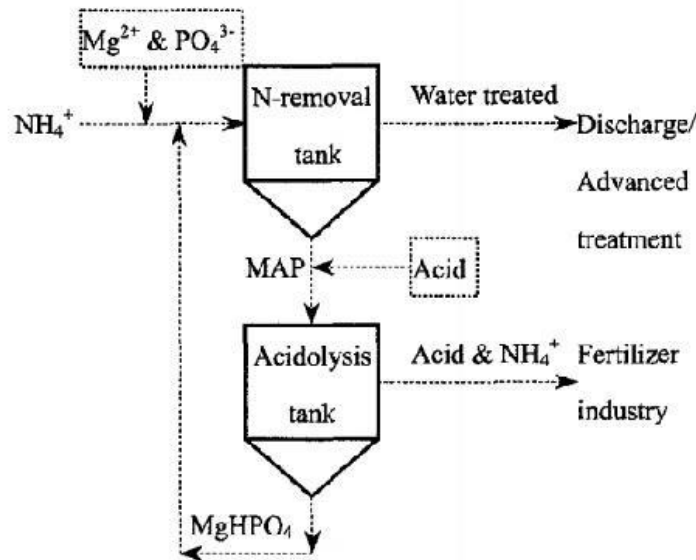


Figure 2.3 Aqueous ammonia removal using struvite decomposition product produced from acidolysis method by Zhang et al. (2004)

The struvite residue believed to be newberyite was further used as a source of magnesium and phosphate at a molar ratio of $\text{Mg} : \text{N} : \text{P} = 2 : 1 : 2$ at pH 8.5 and temperature 25°C for 4 hours, to remove maximum aqueous ammonium from the wastewater through struvite recrystallization. The precipitated struvite was converted back to newberyite through acid dipping and then the residue was recycled for further ammonium removal. The residues formed from struvite acidolysis were reused 6 times in order to observe ammonia removal efficiency from wastewater. The authors

reported that more than 98% aqueous ammonium removal efficiency was achieved through reusing of acidolyzed struvite residues in the first 5 cycles, confirming the effectiveness of the residues as a precipitating agent in ammonium removal. However, between 2-4% of phosphate and magnesium was lost both in struvite precipitation and acidolysis stages. The substantial loss of phosphate and magnesium, by the end of the fifth cycle, may have been responsible for the significant reduction in ammonium removal efficiency to 88% by the end of the 6th cycle.

Moerman (2013) expanded on the results shown by Zhang et al. (2004) and reported that while transforming struvite into newberyite through acidification, an impure NH_4Cl may form due to the presence of impurities in the struvite. As a result, this process requires high energy, as well as HCl consumption, for removal of impure NH_4Cl . To avoid the formation of NH_4Cl and lower the cost of external acid addition, Moerman (2013) proposed that CO_2 produced from the anaerobic digestion process can be injected as the acidifying agent instead of HCl acid. The addition of CO_2 can reduce the pH to below 4.8 through formation of carbonates and/or carbonic acid in the acidolysis tank. An increase in temperature up to 60°C and a decrease in pH to 4.8 favours the formation of newberyite through the maximum release of ammonium from struvite into solution as a pure form of $(\text{NH}_4)_2\text{CO}_3$ and/or NH_4HCO_3 . Further, the retrieved ammonia as $(\text{NH}_4)_2\text{CO}_3$ and/or NH_4HCO_3 can be used as smelling salts or fertilizer. Afterwards, the decomposed product ($\text{MgHPO}_4 \cdot 3\text{H}_2\text{O}$) would be repeatedly used as a precipitating agent, ultimately reducing the need for the external addition of magnesium and phosphate reagents.

2.3.1.3 Disadvantages of wet process

The wet process, which includes the thermal alkali and acidolysis methods, involves complex solid-liquid equilibria. The reported operating conditions corresponding to maximum ammonia release from struvite and subsequent solid phase formation are controversial. For instance, previous researchers (Huang et al., 2011b; Zhang et al., 2009b; He et al., 2007) presumed the formation of MgNaPO_4 (Equation, 2.5) in alkali solution which is very unlikely to form (Lobanov, 2014).



The major challenges of the wet process include solids-liquid separation, ammonia gas stripping, excess chemical consumption (acid and/or alkali) and increased loss of magnesium and phosphate in the solution. In thermal alkali treatments, the ammonia removal efficiency from struvite depends on high solution pH and high temperature. The operating cost would be significantly higher if additional NaOH is required to improve the process efficiency. The implementation of high temperatures to remove maximum NH_4^+ from the solution is also energy intensive. In the acidolysis method, the requirement of chemical reagents is also cost intensive. For instance, a considerable amount of HCl is added in the acidolysis process to dissociate struvite and release ammonia into the solution. Apart from acid consumption, a number of researchers reported only partial conversion of struvite to newberyite which, in turn, reduces the ammonia removal efficiency over the cycle. Further, external additions of magnesium and phosphate, along with decomposed products, increases the operational cost and further underlines the limitations of the process.

2.3.2 Decomposition of struvite: Dry process

The dry process involves thermal decomposition of struvite in air, resulting in the expulsion of ammonia gas along with water of crystallization to the atmosphere; this leads to the formation of an ammonia-free solid phase (Stefanowicz et al., 1992b; Sugiyama et al., 2005; 2007; 2009). This decomposed solid phase can be used as a source of magnesium and phosphate for effective ammonia removal from wastewater. Figure 2.4 represents the ammonia recovery technology proposed by previous researchers utilizing the dry process of struvite thermal decomposition (Stefanowicz et al., 1992b; Sugiyama et al., 2005; 2007; 2009).

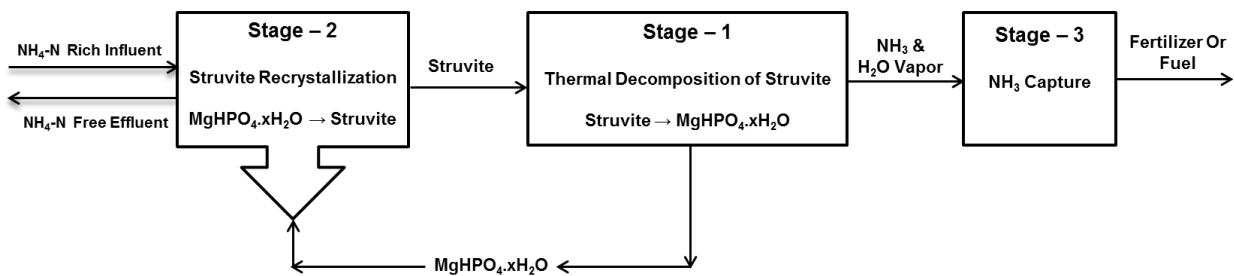


Figure 2.4 Process flow diagram of the proposed ammonia recovery technology

The first stage of the ammonia recovery technology utilizes optimum conditions for the transformation of struvite to $\text{MgHPO}_4 \cdot x\text{H}_2\text{O}$. The efficiency of the technology depends on effective and continuous recycling of the decomposed product that will maximize reformation of struvite over the cycle. The proper optimization of this first stage will not only provide a cost-effective solution for the overall technology but will also maximize ammonia recovery efficiency.

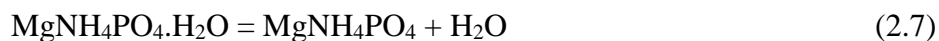
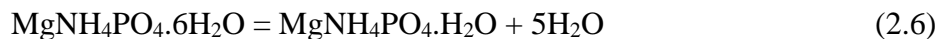
The decomposed product obtained in the 1st stage is then incorporated in the 2nd stage for removal of aqueous ammonia through struvite recrystallization (Stefanowicz et al., 1992b; Sugiyama et al., 2005; 2007; Huang et al., 2011c; Novotny, 2011; Wilson, 2013). The struvite decomposition product $\text{MgHPO}_4 \cdot x\text{H}_2\text{O}$ (where $x \leq 3$) is thermodynamically unstable and dissociates easily to release magnesium and orthophosphate in the presence of ammonium ions in solution, resulting in removal of ammonia through rapid struvite formation. This process will be continued until complete aqueous ammonia removal is achieved from wastewater streams. The third stage of ammonia recovery technology involves “ammonia capture” that evolves from the first stage of struvite thermal decomposition. The evolved ammonia gas can be absorbed or adsorbed in the 3rd stage, using standard methods, and subsequently transformed into commercially available product such as fertilizer or fuel.

One of the biggest challenges in the aforementioned ammonia recovery technology is identifying the proper struvite decomposed product in the 1st stage, which can be utilized in the 2nd stage as the precipitating agent. By thermal decomposition, struvite can transform into different solid phases depending on temperature, method and duration of heating. There are some discrepancies in the literature about the exact temperatures corresponding to different solid phase formations, as well as the sequence of solid phase transition upon decomposition (Kiehl and Hardt, 1933; Paulik and Paulik, 1975a; 1975b; Abdelrazig and Sharp, 1988). To produce a struvite decomposition product devoid of ammonia, a better understanding of struvite transformation into different solid phases, thermal stability, and transitional temperature of each solid phase is necessary to avoid the formation of undesired solid phases.

2.3.2.1 Phase transition of struvite during thermal decomposition using dry method

Several studies have been performed in the fields of kidney stone decomposition (Boistelle et al., 1983; Frost et al., 2004), mineral struvite decomposition (Cohen and Ribbe, 1966; Whitaker, 1968; Ribbe, 1969), and thermal stability of struvite in magnesium ammonium phosphate cement systems (Abdelrazig and Sharp, 1988; Sarkar, 1991). Before the 1900's, the concentration determination technique of magnesium or orthophosphate relied upon struvite precipitation and ignition to magnesium pyrophosphate. However, due to discrepancies associated with transformation conditions from orthophosphate to pyrophosphate upon ignition, contributing to errors in the results, subsequent research focused on thermal decomposition of struvite to improve the measurement technique of magnesium or orthophosphate. In response, Kiehl and Hardt (1933) performed a study on different magnesium phosphates to identify the dissociation pressure during transition of orthophosphate to pyrophosphate through ignition. The results of the dissociation pressure revealed that struvite can easily lose five moles of water in an open atmosphere and transform into dittmarite, at temperatures between 50°C and 60°C, without any loss of ammonia. Both ammonia and water evolution from struvite were noticed at temperatures above 60°C. Magnesium pyrophosphate was identified during dittmarite heating as soon as ammonia and water evolved from the structure. Based on the dissociation pressure, struvite transformed into magnesium pyrophosphate by losing both water of crystallization, constitution and ammonia at 250°C.

According to thermo-analysts, the transitional phase of struvite to magnesium pyrophosphate, during decomposition, can be separated and controlled by providing favourable conditions for specific reactions. Paulik and Paulik (1975a) performed a study to separate and identify the transitional phases and the corresponding partial reactions under quasi-isothermal and quasi-isobaric conditions. The authors used thermogravimetric methods that determined more precise temperatures corresponding to transitional solid phase formation. Equations 2.6-2.9 represent the possible partial reactions that can occur during thermal decomposition of struvite.



The authors hypothesized that the thermal decomposition of struvite would follow the sequence of the aforementioned equations. At the first stage of thermal decomposition, dittmarite- $\text{MgNH}_4\text{PO}_4 \cdot \text{H}_2\text{O}$ (2.6) was expected to form followed by MgNH_4PO_4 salt (2.7), amorphous MgHPO_4 (2.8), and finally, magnesium phosphate- $\text{Mg}_2\text{P}_2\text{O}_7$ (2.9) with the evolution of the last water of constitution. The authors found that struvite nearly decomposed under quasi-isothermal conditions between 60°C and 90°C and transformed into dittmarite, without forming any intermediate substances (Equation 2.6). Above 90°C, only 5% loss of ammonia from dittmarite solid phase was noticed during the thermal treatment, inferring that dittmarite was thermally stable between the 90°C and 230°C (Paulik and Paulik, 1975b). Further heating of transitionally formed dittmarite caused evolution of its water of crystallization, ammonia and water of constitution in a single step, where Equations (2.7), (2.8) and (2.9) occurred simultaneously and finally transformed to magnesium pyrophosphate at 500° C. Notably, no XRD was performed on the decomposed solid phase after every stage of thermal decomposition.

The formation of transitional solid phases was also examined by Abdelrazig and Sharp (1988), using semi-isothermal method. Struvite samples were heated at 10°C/min up to 1000°C as well as heated isothermally at temperatures 100°C and 235°C, until no significant weight loss was observed. XRD was performed to identify the solid phases after conducting thermal decomposition on struvite solid phase. Based on the XRD results of the decomposed product and corresponding weight loss, Abdelrazig and Sharp (1988) reported that struvite started losing significant mass above 60°C and completely transformed into dittmarite around 100°C (4.6). Further increases in heating temperature caused the decomposition of dittmarite at temperatures between 200°C and 300°C. The formation of an amorphous solid phase, along with dittmarite, was observed at 235°C and the structure completely transformed into an amorphous solid phase, when the temperature was increased to 300°C. Afterwards, the presence of $\text{Mg}_2\text{P}_2\text{O}_7$ was first observed in the decomposed sample at around 575°C (4.9) and reached its highest intensity at a temperature

850°C. Further increases in temperature above 850°C caused the formation of $\text{Mg}_3(\text{PO}_4)_2$, which continued to increase as temperature increased to 1000°C. Abdelrazig and Sharp (1988) identified the amorphous phase as a transitional solid phase, while transforming struvite into $\text{Mg}_2\text{P}_2\text{O}_7$; this was not reported by Paulik and Paulik (1975a). Based on the weight loss measurement, Abdelrazig and Sharp (1988) speculated that this amorphous solid phase could be either MgNH_4PO_4 and/or MgHPO_4 . However, the performed XRD only confirmed the amorphous characteristics of the decomposed solid phase, but did not verify it as MgNH_4PO_4 or MgHPO_4 as suspected by the authors. Abdelrazig and Sharp (1988) also contradict Paulik and Paulik (1975a) on the point of ammonia and water evolution. A preliminary study done by Abdelrazig and Sharp (1988), using evolved gas analysis by means of mass spectrometry, confirmed that water vapour and ammonia evolve simultaneously between 200°C and 300°C; whereas, Paulik and Paulik (1975a) found that ammonia and water of crystallization evolve simultaneously from the beginning of the thermal decomposition process. However, Frost et al. (2004) found that at a faster heating rate of 2°C/min, ammonia and water molecules are lost simultaneously, whereas at a very low heating rate of 1°C/min, ammonia was lost before the water of crystallization. Other researchers found only one peak in the differential thermogravimetric analysis (TGA) curve, suggesting that water and ammonia are simultaneously released from the struvite structure (Paulik and Paulik (1975a); Sarkar (1991); Bhuiyan et al., 2008b).

Struvite decomposition using the dry process has been further investigated under isothermal and non-isothermal heating conditions. The isothermal heat treatment performed by Novotny (2011), on commercial struvite pellets, showed no mass loss or ammonia release at heating temperatures of 40°C and 60°C. Maximum mass loss and ammonium removal from commercial struvite pellets occurred between 60°C and 80°C, which is the recorded temperature range for struvite thermal decomposition (Novotny, 2011). Novotny (2011) reported the formation of a $\text{MgH}(\text{NH}_3)_x\text{PO}_4 \cdot \text{H}_2\text{O}$ -type compound, with low N- NH_4 (16%~30%) and water content (0.18~1 mole), as a stable solid phase during thermal decomposition of struvite pellets at temperatures higher than 80°C up to 200°C. No XRD analysis was performed on decomposed struvite samples. According to Sarkar (1991), isothermal heat treatment, between 50°C and 98°C, showed that the decomposed solid phase could be amorphous after heating either at lower temperatures for a longer

duration, such as 55°C for 4 days, or at higher temperature within a short duration, such as 70°C for 1 hour.

In studies performed by Bhuiyan et al. (2008b) and Sarkar (1991), the TGA and DTGA curves obtained from decomposition of struvite under non-isothermal heating conditions indicated that the struvite completely transformed into an amorphous solid phase, when the temperature reached over 250°C. The slower heating rate at 0.5°C/min caused the formation of amorphous structure at lower temperatures around 110°C. Approximately 50-51% weight loss was observed at this decomposition temperature, corresponding to the formation of MgHPO_4 . Therefore, Sarkar (1991) and Bhuiyan et al. (2008b) posited that the decomposed amorphous solid phase contained MgHPO_4 without performing any XRD. Abdelrazig and Sharp (1988) observed a similar outcome, where the amorphous phase MgNH_4PO_4 or MgHPO_4 was suspected from the shape of the quasi-isothermal thermogravimetry (QTG) curve and corresponding weight loss.

The possible transformations of struvite into different solid phases reported in previous studies, are presented in Figure 2.5 (Cervantes, 2009; Sarkar, 1991; Babić-Ivančić et al., 2002; Bhuiyan et al., 2008b). Thermal decomposition of struvite is dependent on the temperature and rate of heating. Struvite can decompose rapidly at temperatures ranging from 85°C to 160°C (Frost et al., 2004; Sarkar, 1991; Bhuiyan et al., 2008b) depending on the heating rate. Dittmarite, which is more thermally stable than struvite, decomposes at temperatures between 60°C to 230°C (Kiehl and Hardt, 1933; Paulik and Paulik, 1975b; Abdelrazig and Sharp 1988; Sarkar, 1991; Sugiyama et al., 2005). The process of dittmarite decomposition appears to be very similar to that of struvite, as both decompose through simultaneous expulsion of NH_3 and H_2O molecules. In spite of this similarity, struvite and dittmarite decompose at two extensively different temperatures. The decomposition of dittmarite results in an amorphous solid phase that is obtained at temperatures extending from 70°C to 500°C. Previous researchers reported this solid phase as MgHPO_4 , based on the weight loss measurements (Sarkar, 1991; Sugiyama et al., 2005; Bhuiyan et al., 2008b; Kurtulus and Tas, 2011). Further increases of temperature from 230°C to 850°C cause decomposition of the amorphous structure and subsequent formation of magnesium pyrophosphate, the least soluble compound (Kiehl and Hardt, 1933; Paulik and Paulik, 1975a; 1975b; Abdelrazig and Sharp 1988; Sugiyama et al., 2005).

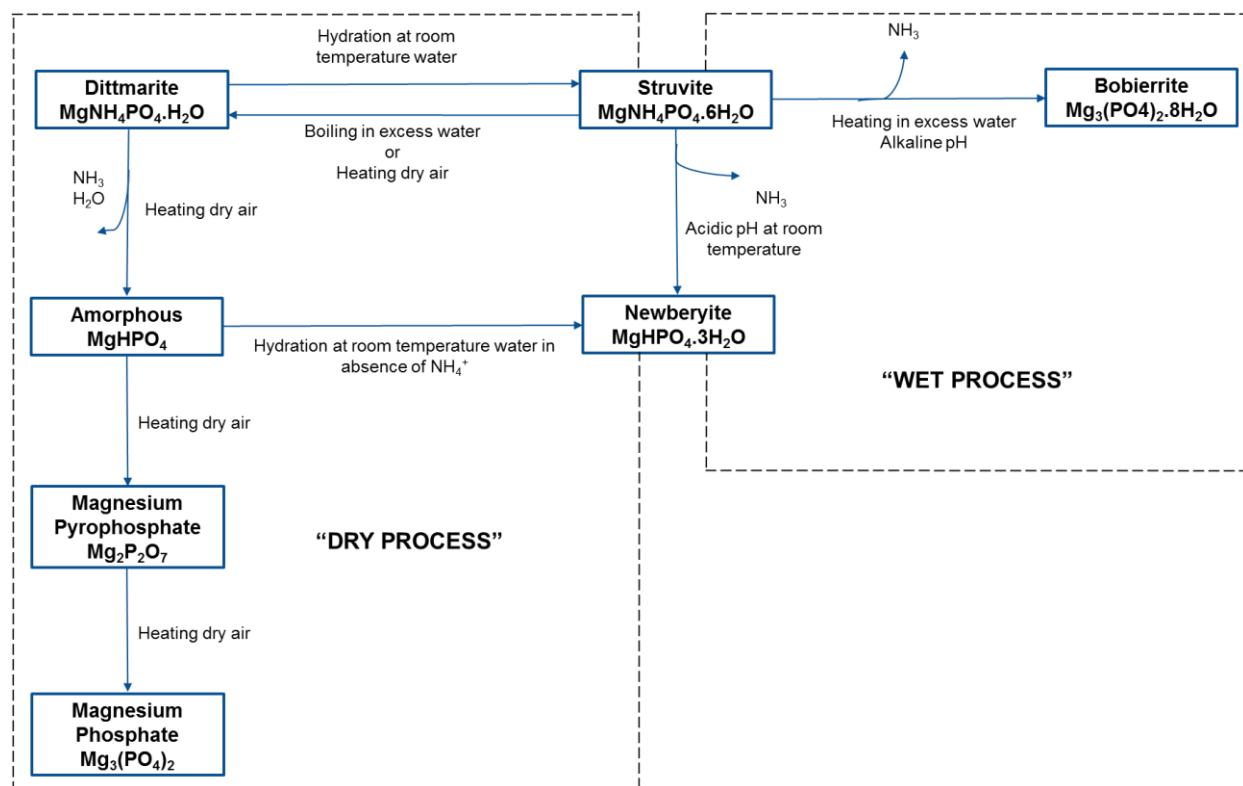


Figure 2.5 The possible transformation of struvite into various solid phases based on the decomposition method (Sarkar, 1991; Babić-Ivančić et al., 2002; Bhuiyan et al., 2008b; Cervantes, 2009)

After reviewing the possible phase formations, it can be speculated that the amorphous phase may contain some dittmarite and/or magnesium pyrophosphate in the structure, depending on the decomposition temperature. The formation of newberyite, through thermal decomposition of struvite in the dry process, was not reported in any study. However, the formation of newberyite was mentioned by previous researchers, when the amorphous phase obtained from thermal decomposition was rehydrated in excess water (Sarkar, 1991; Kurtulus and Tas, 2011). Kurtulus and Tas (2011) kept the amorphous powder obtained from heating at 200°C in pure water at 37°C for 48 hours and observed almost complete transformation into newberyite ($\text{MgHPO}_4 \cdot 3\text{H}_2\text{O}$). In contrast, amorphous powder was transformed back into struvite, along with some unknown compound, upon rehydration for 4 hours at room temperature in ammonium ($(\text{NH}_4)_2\text{HPO}_4$)-containing solution (Kurtulus and Tas, 2011). According to Sarkar (1991), upon rehydration at room temperature in excess water, the decomposed amorphous product was found to be reformed

back into either struvite with unknown hydrates, newberyite alone, or combination of all phases, depending on the amount of ammonia left in the decomposed structure. However, the presence of dittmarite was not found in any of the rehydrated samples by the XRD technique (Sarkar, 1991). On the other hand, the boiling of struvite in excess water can cause formation of dittmarite (Sarkar, 1991), depending on the duration of boiling. Struvite was transformed into dittmarite when struvite was boiled for 24 hours (Sarkar 1991, Bhuiyan et al., 2008b) and confirmed by the XRD results. However, if dittmarite is slowly hydrated at room temperature for 24 hours, it can transform into the more stable struvite, along with less dittmarite over time (Sarkar, 1991; Cervantes, 2009). In a study performed by Bhuiyan et al. (2008b), the formation of bobierrite, upon boiling struvite in excess water was reported and confirmed by XRD. The gradual loss of ammonia, while boiling struvite at temperatures below 100°C for 24 hours, was posited to be responsible for partial transformation of struvite to bobierrite. The formation of bobierrite and newberyite was also reported in the wet process using thermal alkali treatment and acidolysis, discussed in detail in Section 2.3.1.

2.3.2.2 Possible structural changes during struvite thermal decomposition

Based on the published data, it seems that some uncertainty and discrepancies exist regarding the processes underlying struvite thermal decomposition. The following section will discuss in detail struvite crystalline structure and some phenomena that might take place during thermal decomposition of struvite and its transformation into various solid phases.

2.3.2.2.1 Amorphous structure vs crystalline structure

The structural dimension of a solid phase can be defined depending on how many dimensions (X, Y, Z axis) the covalently bonded molecular units can be extended into. The molecular units are referred to as three dimensional (3D) structures (Figure 2.6, a) if found to be infinite in three dimensions, whereas they can be defined as zero dimensions if the molecular units cannot be extended in any dimension (Figure 2.6, b). The zero dimensional crystals consist of simply individual neutral atoms such as orthorhombic sulfur (S₈) (Zallen, 1998), which does not possess any extended covalently bonded molecular units in any dimensions.

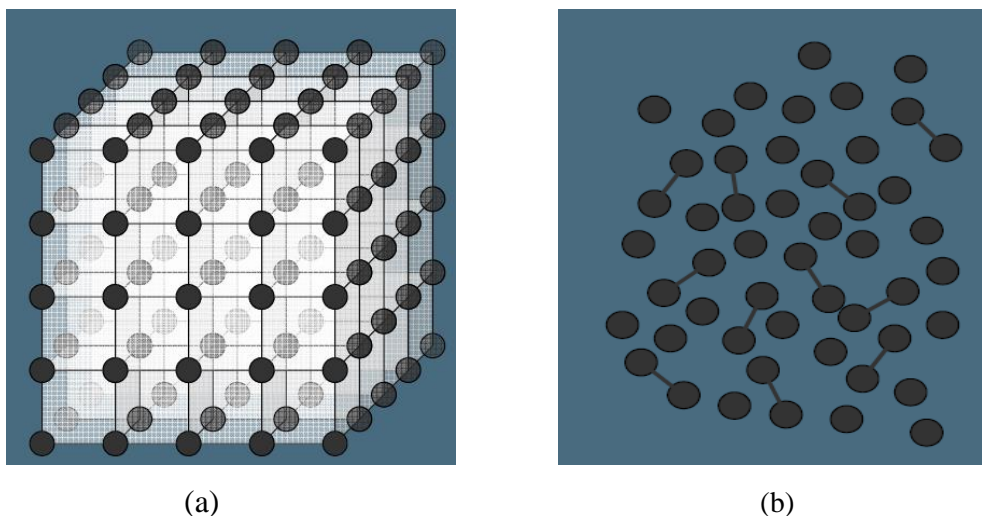


Figure 2.6 (a) 3D crystalline structure (b) Amorphous structure

The 3D crystalline structure forms by arranging atoms or molecules in a 3D network, in a particular geometric pattern, which repeats periodically in three dimensions. Therefore, the 3D crystalline lattice has long range order and symmetric structure in all dimensions due to particular geometric arrangements. On the other hand, amorphous structures can be referred to as zero dimensional, as they lack the long-range order in any dimension and crystalline lattice structure. The atoms or molecules in amorphous non-crystalline structures, such as glass, plastic, and gel, are arranged irregularly.

2.3.2.2.2 Struvite crystalline structure vs newberyite crystalline structure

Struvite and newberyite are naturally occurring minerals that have been found in decomposed organic material such as guano deposits (Cohen and Ribbe, 1966; Frost et al., 2012). The struvite crystals preserved in coated monetite (CaHPO_4) found on Paoha Island, Mono Lake, California, were subsequently replaced by newberyite, thereby indicating the occurrence of struvite to newberyite decomposition (Cohen and Ribbe, 1966). The formation of struvite and newberyite has been identified in both human and animal urinary tracts and kidneys (Boistelle and Abbona, 1985; 1981; Suzuki et al., 1997; Frost et al., 2012). Many researchers suspect that the presence of

newberyite in human calculi is related to thermal decomposition struvite (Sutor, 1967; Frost et al., 2012).

Struvite and newberyite are white crystalline substances and both have distinctive orthorhombic structures. The struvite structure consists of regular PO_4^{3-} tetrahedral, distorted $\text{Mg}(\text{H}_2\text{O})_6^{2+}$ octahedral and NH_4^+ groups that are all held together by hydrogen bonding, as shown in Figure 2.7 (a) (Abbona and Boistelle, 1979). The newberyite structure also consists of PO_4 tetrahedra and magnesium octahedra where an acidic H atom is attached to the PO_4 tetrahedra; the magnesium ions are surrounded by three H_2O molecules along with three O atoms, that belong to the three other PO_4 as shown in Figure 2.7 (b) (Boistelle and Abbona, 1981).

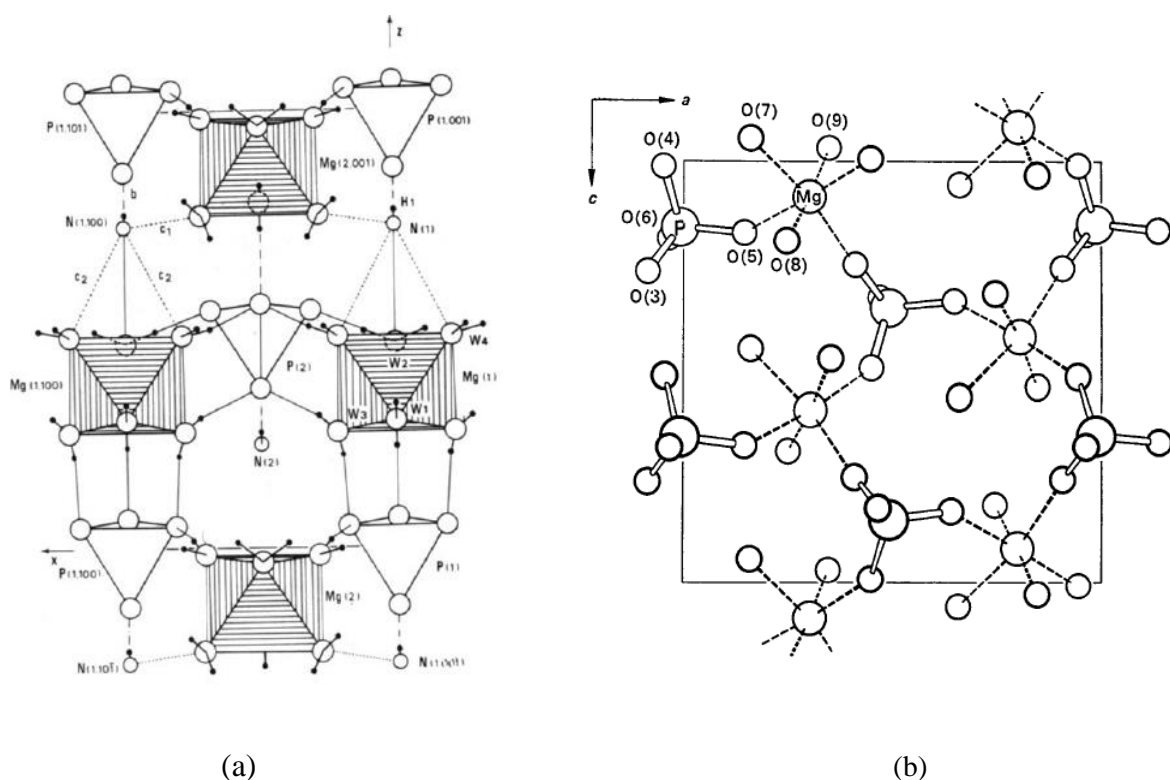


Figure 2.7 Crystalline structure of (a) struvite (Abbona and Boistelle, 1979) (b) newberyite (Boistelle and Abbona, 1981)

The thermal stability of magnesium phosphate compounds increases with the decrease in water molecules upon decomposition. In struvite, magnesium ions are surrounded by six oxygen, which

are provided by six water molecules (Abbona and Boistelle, 1979). However, in newberyite structures, magnesium atoms are also surrounded by 6 oxygen atoms, 3 of which come from three water molecules and the other three from phosphate (Boistelle and Abbona, 1981). Therefore, newberyite is more thermally stable than struvite. Frost et al. (2012) performed thermal treatment on newberyite, in order to identify the thermal stability of newberyite upon decomposition. The author stated that newberyite starts decomposing at temperatures around 72°C and maximum decomposition occurs at 145°C, where it transforms into MgHPO_4 with the loss of water of crystallization based on mass loss measurement. However, no XRD results have been presented in the literature. A further increase in temperature from 256°C to 1000°C caused the formation and complete transformation into $\text{Mg}_2\text{P}_2\text{O}_7$ through evolving of the water of crystallization, as well as water of constitution.

2.3.2.2.3 2D layered structure vs 3D layered structure

A 2D layered structure exhibits strong chemical, typically covalent, bonding in a two dimensional horizontal plane. These 2D planes are stacked one above the other (Figure 2.8) and possess weaker bonds between the layers such as Van der Waals forces, electrostatic interactions and hydrogen bonding. Graphite is an example of a 2D layered structure that possess Van der Waals forces between the layers of carbon sheets. The layers of graphite can easily slide across each other, due to the presence of high lubricity in between the layers (Chang and Hellring, 1989).

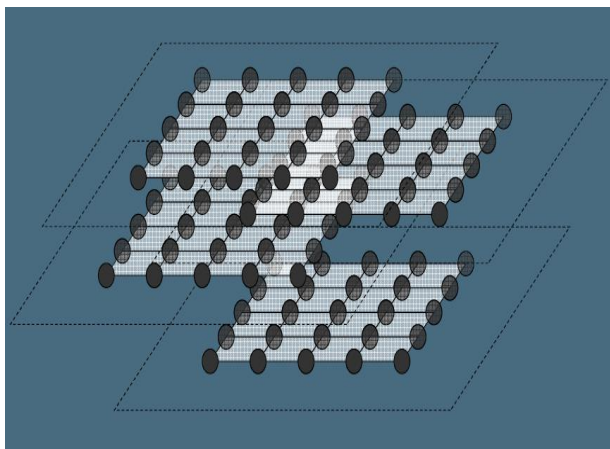


Figure 2.8 2D crystalline layered structure

Dittmarite-type compounds have a 3D crystalline layered structure of $M^{2+}O_6$ octahedra with PO_4 tetrahedron, which are separated by NH_4^+ ions as shown in the following Figure 2.9 (Koleva, 2007).

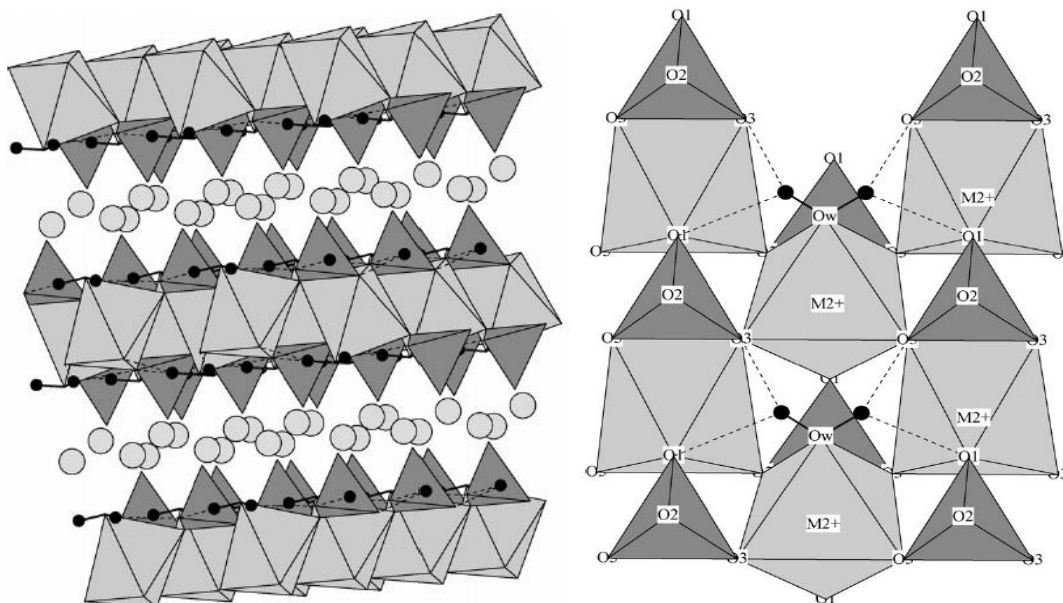


Figure 2.9 Crystal structure of dittmarite-type compounds $M'M''PO_4 \cdot H_2O$ (Koleva, 2007)

Figure 2.9 represents the crystal structure of a dittmarite-type compound where M' and M'' indicate NH_4^+ and Mg^{2+} ions, respectively. The magnesium atoms in the struvite structure are surrounded by six water molecules that form hydrogen bonds with NH_4 and PO_4 . The struvite structure is based on hydrogen bonding that is provided by water molecules. In addition, magnesium is known to have strong affinity towards oxygen. The thermal decomposition of struvite causes simultaneous release of ammonia and water molecules from the struvite structure (Paulik and Paulik, 1975b; Sarkar, 1991; Bhuiyan et al., 2008b). After releasing five water molecules from the struvite, the structure reorganises such that magnesium atoms are still surrounded by six oxygen atoms, 5 of which are provided by PO_4 , instead of water molecules. Therefore, excessive dehydration and release of water molecules from the struvite structure, upon decomposition, eventually leads to the formation of very packed layered structures such as dittmarite. In previous research, Sugiyama and colleagues (2005) were the only researchers to detect dittmarite in heated struvite samples after

isothermal heat treatment of struvite at temperatures from 100°C to 150°C. The XRD analysis is presented in Figure 2.10.

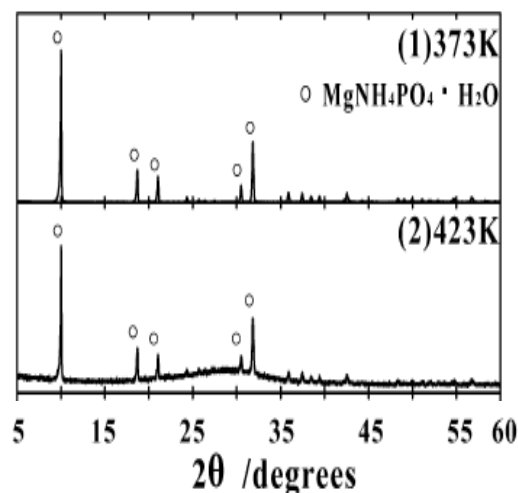


Figure 2.10 XRD results of dittmarite $\text{MgNH}_4\text{PO}_4 \cdot \text{H}_2\text{O}$ (Sugiyama et al., 2005)

A strong peak at 10° angle can be seen in dittmarite structure from Figure 2.10. Several groups (Šoptrajanov et al., 2002, Kongshaug et al., 2000 and Koleva, 2007) have performed studies on dittmarite-type compounds and have found that dittmarite is a 3D crystalline layered structure that has water molecules and NH_4 groups between layers of magnesium and phosphate. Moreover, in the case of dittmarite, ammonium ions are involved in strong hydrogen bonds. Collectively, these factors are believed to be the main reason for the thermal stability of dittmarite, compared to struvite. The trapped ammonia and water molecules between the layers can be completely removed at temperatures greater than 200°C when the structure completely collapses and transforms into magnesium pyrophosphate, through the release of both water of crystallization and water of constitution (Kiehl and Hardt, 1933; Paulik and Paulik 1975a; 1975b; Abdelrazig and Sharp, 1988; Sarkar 1991).

2.3.2.2.4 Layered structure synthesis

During thermal decomposition of different magnesium phosphates, the formation of MgHPO_4 , with low crystalline water content, has been shown in a few studies. The formation of $\text{MgHPO}_4 \cdot \text{H}_2\text{O}$ as an intermediate solid phase during thermal decomposition of dittmarite has been suggested by previous researchers without support of any XRD evidence (Abdelrazig and Sharp, 1988). Finch and Sharp (1989) have performed research on magnesia-phosphate cements and first noticed the formation of a magnesium hydrogen phosphate phase, with a water content lower than that of newberyite. The composition of the newly found substance was $\text{MgHPO}_4 \cdot \text{H}_2\text{O}$, or $\text{MgHPO}_4 \cdot 2\text{H}_2\text{O}$ referred to as “hayesite”. This substance was partially crystalline, stable at high temperatures and formed under the presence of low-water conditions. The water of crystallization is released from hayesite, when heated at temperatures between 190°C and 200°C. The thermal stability of hayesite was found to be higher than that of newberyite, which is around 145°C. This infers that water molecules are more strongly bonded to surrounding magnesium ions in hayesite, in comparison to newberyite. Furthermore, the direct synthesis of $\text{MgHPO}_4 \cdot x\text{H}_2\text{O}$ (where $x = 0.78$ -1.29) has been reported previously (Chen et al., 1993 and Bensalem et al., 1995). Chang and Hellring (1989) and Chen et al. (1993), reported the preparation of $\text{MgHPO}_4 \cdot 1.2\text{H}_2\text{O}$ under hydrothermal conditions whereas Bensalem et al. (1995), reported the preparation of a new layered structure $\text{MgHPO}_4 \cdot 0.78\text{H}_2\text{O}$, under ambient temperature and pressure.

Chen et al. (1993) prepared a new layered structure, $\text{MgHPO}_4 \cdot 1.2\text{H}_2\text{O}$ at 180°C under hydrothermal conditions. This newly formed $\text{MgHPO}_4 \cdot 1.2\text{H}_2\text{O}$ compound possesses a new structure that has been confirmed by XRD results (Figure 2.11) and chemical analysis. The sample was heated from room temperature to 500°C, to observe the change of composition to identify the characteristics of the layered structure upon thermal treatment. The sample showed unidentified XRD results when heated at 100°C and 200°C for 1 hr. A further increase in temperature to 300°C caused formation of an unknown solid phase and transformed into $\text{Mg}_2\text{P}_2\text{O}_7$, when the temperature reached 500°C. The sample heated at 200°C reformed to the initial layered structure composition upon rehydration at moist air for 3-5 hours. Chen et al. (1993) and Bensalem et al. (1995), reported that the layered structure is thermally stable and undergoes reversible dehydration-rehydration, provided it is not heated beyond 200°C. At temperatures below 200°C, the intercalated water only

evolved from the structure which can be retrieved through rehydration in moist air. The authors reported that $\text{MgHPO}_4 \cdot 1.2\text{H}_2\text{O}$ retains a layered structure with water molecules in between the layers and shows a high intensity peak at low angles, between 5 and 10 degrees, under XRD.

A strong peak at 10 degree angle has also been observed in 3D crystalline layered structure as shown in Figure 2.10 which is similar to the peak formed at low angles in between 5 and 10 degrees in the structure of MgHPO_4 , with 1.2 water molecules (Figure 2.11).

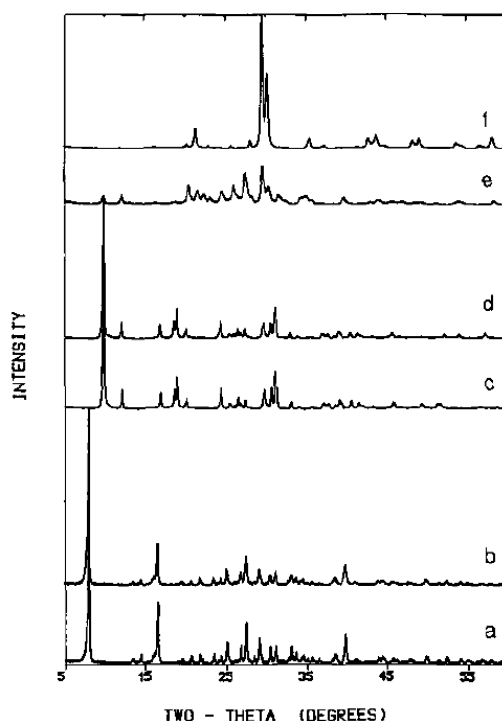


Figure 2.11 X-ray powder diffraction patterns for $\text{MgHPO}_4 \cdot 1.2\text{H}_2\text{O}$ (a) at room temperature, (b) heated at 200°C followed by exposure to air, (c) at 100°C, (d) at 200°C, (e) at 300°C, (f) at 500°C (Chen et al., 1993)

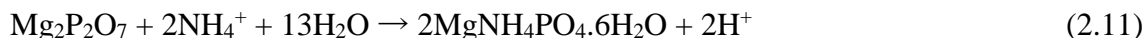
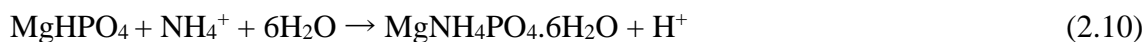
The presence of a strong peak at low angles indicates the similarities between $\text{MgNH}_4\text{PO}_4 \cdot \text{H}_2\text{O}$ (dittmarite) and MgHPO_4 with low water of crystallization. Both structures are orthorhombic and exhibit layered structure properties. In a dittmarite structure, NH_4 and H_2O molecules are entrapped between the layers of magnesium and phosphate, whereas the layers of MgHPO_4 , with

low water of crystallization, contain H₂O molecules between the layers. Therefore, both structures exhibit similar thermal stability upon decomposition.

Based on the literature review, dehydration of some magnesium phosphates may lead to the formation of a layered structure, either as 3D crystalline (like dittmarite), or some kind of 2D amorphous structure. In both cases, ammonium ions might be trapped between strongly-bonded, packed layers of Mg-PO₄, preventing ammonia gas from escaping the structure. The literature review suggests that there might be a way of detecting this layered structure through XRD analysis – a strong X-ray diffraction peak should be expected at low scattering angles.

2.3.2.3 Ammonia recovery using decomposed struvite product

The removal of aqueous ammonia from wastewater streams follows a dissolution–precipitation mechanism (Sugiyama et al., 2005). The ammonia removal efficiency is primarily dependent on the solubility of the decomposed magnesium phosphate compounds and the extent of ammonia present in the decomposed solid phase. The compounds with higher solubility rapidly dissociate in solution and readily release Mg²⁺ and PO₄³⁻ ions for struvite formation. Afterwards, readily available Mg²⁺ and PO₄³⁻ react with the NH₄⁺ present in wastewater at a stoichiometric ratio of 1:1:1 and, subsequently, remove aqueous ammonia from the solution through struvite precipitation. It can be expected that the decomposed product, with higher solubility, has higher potential to remove more aqueous ammonia within a shorter period of time, with less chemical consumption. Previous researchers have suggested different magnesium phosphate compounds as precipitating agents and evaluated the ammonia removal efficiency using different struvite decomposition products. Stefanowicz et al. (1992b) proposed Mg₃(PO₄)₂ as a suitable precipitating agent, whereas Sugiyama et al. (2005) suggested MgHPO₄, Mg₂P₂O₇ and Mg₃(PO₄)₂ as possible candidates for the removal and recovery of aqueous ammonium through struvite reformation, following Equations 2.10, 2.11 and 2.12.



With respect to the solubility of different struvite decomposition products, the maximum solubility has been found for MgHPO_4 (Dean, 1985) followed by $\text{Mg}_3(\text{PO}_4)_2$ (0.02 g/100 ml) and MgNH_4PO_4 (0.0023 g/100 ml), whereas $\text{Mg}_2\text{P}_2\text{O}_7$ is slightly soluble in hot water. Based on solubility order, aqueous ammonia removal efficiency is expected to be higher using decomposed products with similar composition to MgHPO_4 , rather than $\text{Mg}_3(\text{PO}_4)_2$ and $\text{Mg}_2\text{P}_2\text{O}_7$. Previous researchers performed a few studies on the formation of struvite decomposition products and investigated aqueous ammonia removal capacity utilizing the decomposed product as a renewable source of magnesium and phosphate for struvite recrystallization. For example, Stefanowicz et al. (1992b) first introduced the decomposed struvite product- $\text{Mg}_3(\text{PO}_4)_2$ as a source of Mg^{2+} and PO_4^{3-} to replace commercial reagents for ammonia removal. Precipitated struvite powder, that transformed into a decomposed product after heating at 250°C for 24 hours, was claimed to be $\text{Mg}_3(\text{PO}_4)_2$, but no XRD results were performed to confirm the decomposed product as $\text{Mg}_3(\text{PO}_4)_2$.

The ammonium removal capacity, using a decomposed struvite product, depends on the solution composition, solution volume, rate of agitation, pH and temperature. The decomposed struvite product, which was suspected to be $\text{Mg}_3(\text{PO}_4)_2$ in the above discussed study, was added to the aqueous ammonium solution containing 1000 mg NH_4^+/l , at a stoichiometric ratio of 1:1:1 required for struvite crystallization. The pH of the solution was reduced to 1-2 units using HCl, in order to dissolve the residues in the solution. The pH was then raised to 9.3 using NaOH for struvite formation and approximately 100% ammonium removal was achieved after 24 hours of agitation. Although 100 % ammonia removal was claimed using $\text{Mg}_3(\text{PO}_4)_2$, no XRD was presented to confirm the solid phase of decomposed product. Notably, $\text{Mg}_3(\text{PO}_4)_2$ is not the most soluble compound (Sugiyama et al., 2005). Hence, significant amounts of chemical reagents and extended mixing duration (24 hours) were required in the aforementioned study, reducing economic feasibility. As well, supernatant phosphate concentration at the end of the process was not reported, which is important due to the fact that 100% ammonia removal requires significant addition of $\text{Mg}_3(\text{PO}_4)_2$ in the solution and may contribute to high aqueous phosphate concentration.

The ammonia removal capacity of different magnesium phosphate compounds, including $\text{Mg}_3(\text{PO}_4)_2$, was investigated by Sugiyama et al. (2005). In their study, synthetic $\text{MgHPO}_4 \cdot 3\text{H}_2\text{O}$ (newberyite), $\text{Mg}_3(\text{PO}_4)_2 \cdot 8\text{H}_2\text{O}$ (bobierite) and $\text{Mg}_2\text{P}_2\text{O}_7$ (magnesium pyrophosphate) were used

to identify a potential decomposed product for aqueous ammonia removal through struvite precipitation. The order of aqueous ammonium removal efficiency reported by the authors was $\text{MgHPO}_4 > \text{Mg}_3(\text{PO}_4)_2 > \text{Mg}_2\text{P}_2\text{O}_7$, which was identical to the solubility of those magnesium phosphates. The incorporation of newberyite ($\text{MgHPO}_4 \cdot 3\text{H}_2\text{O}$) in the ammonium solution at a molar ratio of $\text{Mg:N:P} = 1:1:1$, with initially adjusted pH 8, caused 77% ammonia removal after 3 hours. On the other hand, $\text{Mg}_3(\text{PO}_4)_2 \cdot 8\text{H}_2\text{O}$, as a precipitating agent, provided 44% ammonium removal efficiency. However, no ammonia removal was observed using $\text{Mg}_2\text{P}_2\text{O}_7$ as a precipitating agent after one hour at pH 8. After identifying the potential decomposed compound $\text{MgHPO}_4 \cdot 3\text{H}_2\text{O}$ (newberyite), the authors further expanded the study by investigating the recyclability of the decomposed commercial struvite compound. Commercial struvite was heated at 200°C for 3 hours, resulting in an amorphous decomposed solid phase. The authors reported the phase as MgHPO_4 (which was recycled twice) to identify the ammonia removal efficiency. Around 41.2% aqueous ammonium removal was achieved in the first cycle using the decomposed product. The resulting precipitate obtained from the solution was decomposed again to reuse the residue for further ammonium removal in the second cycle, resulting in 33.2% further ammonium removal. The authors did not state the final solid phase or residual phosphate concentration after recycling decomposed residues. The low ammonia removal efficiency was also not clearly explained by the authors.

Sugiyama et al. (2007) further performed a study to demonstrate the potential of MgHPO_4 as a decomposed recycling agent by preparing a thin-layer of $\text{MgHPO}_4 \cdot 1.2\text{H}_2\text{O}$ on a glass plate, using sol-gel technique and immersing it in ammonia-rich solution, at room temperature for 3 hours. The obtained XRD results confirmed that dittmarite was formed, along with $\text{MgHPO}_4 \cdot 1.2\text{H}_2\text{O}$. The precipitated residues were recovered from the solution and further decomposed at 200°C for 3 hours, to release maximum ammonia for the decomposed product for aqueous ammonia removal in the following cycle. No XRD analysis was performed on the decomposed material. The recycling process was continued three times and the aqueous ammonium removal efficiency, using heated sheets decreased as the number of recycle times increased. Around 30% ammonia removal efficiency was achieved on the 1st run and eventually decreased to less than 10%, by the third recycle. Sugiyama et al. (2007) posited that the calcination temperature (200°C) was insufficient

for complete removal of ammonia from the dominant dittmarite solid phase that formed, believed to be responsible for lower ammonium removal efficiency after the 2nd and 3rd recycle times.

The previous study conducted by Stefanowicz et al. (1992b) and Sugiyama and colleagues (2005) involved decomposition of struvite at temperatures higher than 150°C, which is energy intensive. Therefore, a similar study was performed by Huang et al. (2011c) to evaluate the ammonia removal efficiency with a decomposed struvite compound formed at different temperatures and heating durations. The struvite decomposed products were formed from struvite heating at 150°C with 1 to 4 hours heating and added to aqueous ammonia solution at pH 9. The addition of decomposed struvite product, obtained from 1 hour of heating, resulted in a maximum of 53% ammonia removal efficiency, whereas the ammonia removal efficiency was 47% from 4 hours of heating. The authors suspected that the formation of inactive $\text{Mg}_2\text{P}_2\text{O}_7$ and $\text{Mg}_3(\text{PO}_4)_2$, in the decomposed solid residues from prolonged heating, might have reduced the aqueous ammonia removal capacity. Hence, the authors re-evaluated the aforementioned process with a decomposed struvite product produced at temperatures ranging from 180°C to 250°C and concluded that the optimum condition for decomposed struvite formation is 150°C, with 1h heating duration. The authors further investigated the recycling potential of the struvite decomposition product obtained at optimum condition for aqueous ammonia removal. The decomposed product was added to the aqueous ammonia solution with initial pH 9, reaction time 1 hour and reused the precipitating agent for four cycles. The ammonia removal efficiency decreased from 97.8% to 46% by the end of the 4th cycle and the residual phosphate concentration by the end of the 4th cycle was 5.2 mg/l.

The enhanced formation of $\text{Mg}_2\text{P}_2\text{O}_7$ and $\text{Mg}_3(\text{PO}_4)_2$ in the struvite decomposition product, as well as increased loss of magnesium and phosphate in the supernatant at each cycle, were believed to be responsible for the reduction of aqueous ammonia removal efficiency with an increasing number of cycles. It should be noted that the author did not report the final solid phase obtained from the struvite thermal decomposition.

Sugiyama et al. (2005) reported the formation of dittmarite around 100°C-150°C, with 3 hours of heating. The formation of dittmarite, a layered structure, could significantly reduce aqueous ammonia removal capacity due to entrapment of ammonia within layers of dittmarite (Novotny,

2011; Wilson, 2013). Thus, the decomposed compound loses its potential for ammonia removal when repeatedly used over the cycle (Novotny, 2011). Furthermore, the formation of $\text{MgHPO}_4(\text{NH}_3)_x(\text{H}_2\text{O})_y$ with 19% residual ammonia and 0.31 mole residual water, was reported by Novotny (2011), after heating commercial struvite pellets at 160°C for 24 hours. The increase in temperature up to 200°C for 24 hours caused the formation of $\text{MgHPO}_4(\text{NH}_3)_x(\text{H}_2\text{O})_y$ with 13% ammonia remaining in the structure. The decomposed product obtained at 160°C for 24 hours was added to the ammonium solution at pH 8 for 2 hours. The addition of 80 g/L doses provided 93% ammonia removal efficiency, with residual phosphate concentration of 190 mg/L. It appears that the excess addition of decomposed compound was required, due to incomplete ammonia removal efficiency from struvite. After reviewing the previous studies, it is likely that the decomposed compound might have contained $\text{MgHPO}_4(\text{NH}_3)_x(\text{H}_2\text{O})_y$ along with $\text{Mg}_2\text{P}_2\text{O}_7$, at that temperature range, reducing the solubility of the decomposed compound.

Ammonia removal capacity, using newberyite as a decomposed product, was first demonstrated by Sugiyama et al. (2005). Newberyite was found to be the most effective in aqueous ammonia removal, compared to other decomposed products reported in previous studies (Stefanowicz et al., 1992b; Sugiyama et al., 2005; Huang et al., 2011c; Novotny, 2011). The potential of newberyite as a surrogate for the struvite decomposition product was further explored by Wilson (2013), who identified the optimum operating conditions corresponding to maximum aqueous ammonia removal efficiency. To achieve this, synthetic newberyite was added to the ammonia solution, synthetic centrate and synthetic struvite crystallizer effluent. The addition of newberyite at a molar ratio Mg:N:P of 1:1:1, caused a maximum of 87% ammonia removal efficiency when the pH, temperature and reaction time varied from 7-8, 10°C - 25°C and 1-3 hours, respectively. The minimum residual orthophosphate concentration was found to be 10 mg/L, corresponding to 87% ammonia removal efficiency. According to the author, the ammonia recovery technology relies on the complete conversion of newberyite to struvite. A maximum 92% conversion of newberyite to struvite was achieved during the experiment. The precipitated solid phase was further identified, using XRD, as a mixture of struvite along with newberyite. It is probable that the incomplete conversion of newberyite to struvite reduced the aqueous ammonia removal efficiency.

Lower temperatures favour the formation of a decomposed product containing ammonia, reducing ammonia removal efficiency from wastewater (Novotny, 2011; Wilson, 2013). At high temperatures ($>250^{\circ}\text{C}$), struvite thermal decomposition may form magnesium pyrophosphate ($\text{Mg}_2\text{P}_2\text{O}_7$), the least suitable decomposed product due to its low solubility (Kiehl and Hardt, 1933; Paulik and Paulik, 1975a; 1975b; Abdelrazig and Sharp, 1988; Sugiyama et al., 2005). Newberyite ($\text{MgHPO}_4 \cdot 3\text{H}_2\text{O}$) as a struvite decomposition product, devoid of ammonia, has a greater potential for maximum aqueous ammonia removal from wastewater. It is more soluble than other magnesium phosphate compounds, dissolves rapidly, and releases magnesium and orthophosphate readily which ultimately enhance the struvite recrystallization process. The formation of newberyite, while decomposing struvite in acid solution, has been discussed in several studies (Boistelle and Abbona, 1983; Kontrec et al., 2005; Babić-Ivančić et al., 2006). However, the decomposition of struvite, using the wet process, involves complex chemical equilibrium studies and extensive chemical consumption. In addition, the operating conditions reported in previous studies for transformation of struvite to newberyite are rather controversial. Importantly, none of the previous researchers reported the formation of newberyite during thermal decomposition of struvite, following the dry process. If newberyite could be formed through the dry process, then it would be more economically feasible and industrially applicable, compared to the wet process, due to lower operational complexity.

2.3.2.4 Ammonia gas recovery techniques

Researchers have proposed that evolved ammonia from the thermal decomposition of struvite can be recovered and utilized as a valuable commercial product. The conventional methods of ammonia (gas) recovery include distillation and acid absorption. The ammonia captured in acid solution (i.e. sulfuric acid, nitric acid, and phosphoric acid) can be effectively used as commercial ammonium sulfate, ammonium nitrate and diammonium phosphate fertilizer (Lei et al., 2007; Swartz et al., 1998; Orentlicher, 2012). The compressed ammonia produced through cryogenic or condensation techniques can be marketed as a fuel or as a hydrogen precursor (Türker and Çelen, 2007; Orentlicher, 2012). Alternatively, the absorption of ammonia over anhydrous magnesium chloride (MgCl_2) at room temperature causes formation of $\text{Mg}(\text{NH}_3)_6\text{Cl}_2$ (Christensen et al., 2006; Zamfirescu and Dincer, 2009), the thermal decomposition of which would allow desorption of

ammonia from MgCl_2 . In this way, ammonia can be stored safely in the form of ammine, to prevent ammonia toxicity in the event of an accident. The main obstacle for the adoption of hydrogen as a sustainable fuel is its safe storage and transportation, which can be bypassed by storing ammonia, instead of hydrogen, in the form of $\text{Mg}(\text{NH}_3)_6\text{Cl}_2$.

Chapter 3: Research Objectives

Conventional ammonia removal and recovery technologies are subject to certain limitations, including high operating cost, as well as the technical challenges associated with the treatment of high ammonia-containing wastewater. Ammonia recovery using struvite precipitation can minimize these limitations. It was hypothesized that struvite pellets can be heated and transformed into a thermally decomposed product, through the removal of ammonia and water from the crystal structure. The decomposed pellets can then be used as a source of magnesium and orthophosphate for removing aqueous ammonia through struvite recrystallization. This recycling process can be theoretically continued until the excess aqueous ammonia is completely removed from wastewater streams. The success of this process mainly depends on the conversion of struvite to a thermally decomposed product, which can be used effectively as a precipitating agent to remove aqueous ammonia from wastewater. A proper understanding of the composition and characteristics of this thermally decomposed product is crucial for the overall process.

The overall purpose of this study was to transform struvite into newberyite, through thermal decomposition. The struvite decomposition process is dependent on the temperature, water and ammonia vapour pressure, duration of heating, sample size, shape and hardness. Proper selection of these conditions is necessary for an energetically efficient and economically feasible method, facilitating ammonia evolution from struvite without forming any other intermediate solid phases (other than newberyite). In order to achieve these objectives, the following questions needed to be answered.

- What solid phase formation does this process include?
- How can struvite be fully transformed into newberyite?
- In what way(s) does the solid phase formation change with the change of experimental conditions?
- What are the optimum operating parameters for struvite to newberyite transformation during thermal decomposition?

Chapter 4: Materials and Methods

4.1 Experimental conditions of performed oven dry experiments

In the study performed by Novotny (2011), commercial struvite pellets were isothermally heated from 40°C to 200°C for 24 hours at the UBC Environmental Engineering Laboratory. Maximum mass loss and ammonia removal from commercial struvite pellets occurred between 60°C and 80°C, which has been referred to as the struvite thermal decomposition temperature (Novotny, 2011). However, no experiments were conducted at that temperature range to observe the formation and composition of solid phases. In addition, complete ammonia removal from the commercial struvite pellets was not achieved even after heating at temperatures up to 200°C for 24 hours. Therefore, the present study was conducted on synthetic struvite samples at temperatures between 55°C and 70°C for different time intervals, in order to observe the ammonia removal efficiency, as well as the transformation of struvite to magnesium hydrogen phosphate.

Synthetic struvite was used in the oven dry experiments to observe changes in the structural composition of struvite upon heat treatment. Preparation and chemical analysis of the synthetic struvite are discussed in Section 4.1.1 and 4.1.2. In order to be consistent, one oven was used throughout the duration of the experiments. Synthetic struvite samples were prepared in the lab and heated isothermally at temperatures ranging from 56.6°C to 71.1°C, for a duration ranging from 1 to 24 hours. Experiments for two particular temperature values (60.5 and 61.5°C), the reported starting point of struvite thermal decomposition (Novotny, 2011), were also performed on a different synthetic struvite samples, obtained from the UBC Staging Environmental Research Centre (SERC, aka UBC Pilot Plant) to verify the effects of these two temperatures on the composition and structure of the decomposed solid phase. Individual samples, in triplicates, were used for every temperature and time period. An aluminum dish was weighed on a balance and the weight of the dish was recorded. The appropriate mass of synthetic struvite (0.1-0.2g) was placed into the aluminum dish and the weight of the dish, with struvite sample, was recorded. The aluminum dish with struvite samples was placed in the oven at a specified temperature and the starting time of the experiments as noted. After the desired time interval, the aluminum dish was taken out from the oven and the mass change of the samples was measured. The samples were then

stored in air-tight bags and placed in the vacuum desiccator until they were analyzed. The experimental condition of struvite drying, with respect to temperature and heating duration, is presented in Table 4.1.

Table 4.1 Experimental conditions of oven dry experiments

Struvite	Temperature, (°C)	Duration of Heating, (hours)
Synthetic struvite prepared in the lab Mg:NH ₄ :PO ₄ :H ₂ O = 0.92:1.02:1:6.34	56.6, 59.6, 62.5	3, 6, 9, 16, 24
	61.5, 66.2, 71.1	1, 3, 5, 7, 9, 16, 24
Synthetic struvite prepared in the pilot plant Mg:NH ₄ :PO ₄ :H ₂ O = 0.82:0.87:1:6.46	60.5, 61.5	1, 3, 5, 7, 9, 16, 24

4.1.1 Preparation of synthetic struvite

Synthetic struvite used for thermal decomposition was prepared in the laboratory by mixing equimolar quantities of magnesium chloride (MgCl₂·6H₂O) and ammonium di-hydrogen phosphate (ADP). Reagent grade 165.76 g MgCl₂·6H₂O and 93.73 g NH₄H₂PO₄ solutions were prepared in a 1L stirred reactor using distilled water at 25°C. The pH of the solution was adjusted to a value of 8-9, using the slow addition of concentrated ammonium hydroxide (NH₄OH) (Johnson, 1959; Ohlinger, 1999; Babić-Ivančić et al., 2002; Bhuiyan et al., 2008b). The solution was agitated for 15 minutes, until the pH stabilized and then was retained in the reactor without any agitation, to precipitate struvite at a stoichiometric ratio of Mg: NH₄:PO₄ equal to 1:1:1. The reaction is depicted Equation 4.1:



The resulting suspension was filtered using Whatman 5 qualitative 12.5 cm diameter filters and a vacuum apparatus. The retained precipitates were washed thoroughly with distilled water and reagent alcohol. The synthetic struvite was then allowed to dry in open air at room temperature overnight, to evaporate any residual water and alcohol. This procedure yielded about 200 g of struvite that was further stored in a sealed plastic jar. Following a similar approach, the synthetic

struvite was prepared in the pilot plant in a 30-gallon tank in which the technical chemicals were added proportionally.

4.1.2 Synthesized struvite analysis

The purity of synthesized struvite was evaluated by chemical analysis and X-ray diffraction (XRD) analysis. A known amount of synthetic struvite (~ 0.1 g) was dissolved in distilled water with the addition of concentrated hydrochloric acid (HCl). The solution was further diluted and analyzed for orthophosphate, ammonia and magnesium. The detailed description of performed magnesium, ammonia and orthophosphate tests are outlined in Section 4.5.1.1 and Section 4.5.1.2, respectively. Chemical analysis of the synthetic struvite prepared in the lab and in the pilot-scale showed that the actual molar ratios of $\text{Mg}:\text{NH}_4:\text{PO}_4:\text{H}_2\text{O}$ corresponded to 0.92:1.02:1.0:6.34 and 0.82:0.87:1:6.46, respectively. This difference in composition is believed to be due to possible analytical errors as well as small differences in the method of synthesis, such as crystallization temperature and pH, as well as drying and storage time. During synthetic struvite preparation, some moisture might have remained in the struvite bulk powder, therefore causing the water content to be higher than 6 moles in the prepared synthetic struvite samples. XRD analysis was also performed on the samples of struvite prepared in the lab and pilot-scale, confirming that no other crystalline phase was formed while forming synthetic struvite. XRD output graphs for this struvite product are provided in the Appendix B.1.

4.1.3 Mass loss measurements

The mass loss was calculated for each temperature and time period to observe struvite thermal stability and composition after oven dry heating. The percent of mass loss will change with the change of ammonia and water content in the decomposed struvite structure. The exact temperature and time interval at which both ammonia and water start to evolve from the struvite structure can be identified from the mass loss measurement. On the contrary, mass loss can be predicted based on the composition of decomposed solid. However, composition cannot be exactly predicted based only on mass loss; it can only be roughly estimated. Equation (4.2) demonstrates this relationship between initial mass and that at sample time, x .

$$\text{Mass loss} = \frac{\text{Final Mass}_{(t=x)} - \text{Initial Mass}_{(t=0)}}{\text{Initial Mass}_{(t=0)}} \times 100\% \quad (4.2)$$

4.2 Experimental conditions of performed bench-scale experiments

In the bench-scale experiments, heat treatment was performed on real struvite pellets such as Lulu Island Wastewater Treatment Plant (LIWWTP) pellets, pellets from the Gold Bar WWTP in Edmonton, AB, Penticton B.C. pellets from the COP AWWTP and recrystallized pellets from the UBC Pilot Plant. The struvite pellets that passed through a 1 mm sieve, but which were retained on a 0.5 mm sieve, were categorized as the less than 1 mm sample, whereas the pellets that passed through 2 mm sieve and were retained on a 1 mm sieve were referred to as the greater than 1 mm sample. Multiple tests were employed on various sizes and sources of struvite pellets, to identify the optimum temperature and relative humidity (RH) for struvite to newberyite conversion in the presence of hot air and steam. The relative humidity was maintained above 65%, to prevent dehydration and below 100%, to avoid condensation, (discussed in detail in Section 5.2.1.2).

In order to suppress dehydration during thermal decomposition of struvite, 65% to 95% relative humidity was used in the bench-scale setup. Discussion on the selection and importance of relative humidity control is discussed in Section 5.2.1.2. Therefore, the temperature and relative humidity were varied from 65°C-85°C and 65%-95%, respectively, in order to identify the optimum conditions. These conditions were first applied to the struvite pellets from Lulu Island Wastewater Treatment Plant (LIWWTP), to observe the process mechanism, as well as to identify the optimum conditional parameters corresponding to maximum ammonia removal efficiency. After identifying the optimum experimental condition from the smaller Lulu Island (<1mm sample) pellets, different sources and sizes of struvite pellets (<1mm and >1mm) from the Gold Bar WWTP, COP AWWTP, UBC Pilot Plant and LIWWTP were decomposed in the “optimal” range, in order to compare the ammonia removal efficiency among different sources, sizes and shapes of pellets. The outcome of these experiments provided information on the suitable pellets, in terms of size, source and hardness corresponding to maximum ammonia removal. Each combination of parameters was represented by single batch tests. The various parameters that were involved in the bench-scale experiments have been presented in Table 4.2.

Table 4.2 Experimental conditions of bench-scale experiments

Types of Struvite	Sources of Struvite Pellets	Initial Mg:N:P:H ₂ O Molar Ratio	Size	Duration of Heating, (hours)	Relative Humidity, (%)	Temperature, (°C)
Lulu Island	LIWWTP	0.97:0.95:1:6.1	<1mm	2 , 4	65% ± 5%	65°C, 75°C, 85°C
					80% ± 5%	
					95% ± 5%	
			<1mm	2 , 4	95% ± 5%	80°C
			>1mm			
Penticton B.C.	COP AWWTP	0.97:0.89:1:6.36	<1mm	2		
Edmonton Gold Bar	Gold Bar WWTP	0.97:0.88:1:6.58	<1mm	3		
Recrystallized	UBC Pilot Plant	1.04:1:1:6.25	>1mm	3		

4.2.1 Bench-scale experimental setup

The bench-scale experimental setup is presented in Figure 4.1. The bench-scale reactor consisted of a fluidized-bed reactor (FBR) with jacket, heated water bath, diffuser, steamer, heater, heat tape with thermostat, flow meter, pressure gage, temperature, and humidity probe. The bench-scale, fluidized-bed reactor was cylindrical with an inside diameter of 1.5 cm (0.6 inch), as shown in Figure 4.1. The FBR reactor was surrounded by a jacket of 1.3 cm (0.5 inch) diameter. To prevent condensation inside the reactor, the jacket temperature was always maintained a few degrees higher than that inside the reactor. Temperature control was accomplished using a heated water bath (VWR Scientific-1130A) that provided continuous flow of water through the jacket. This reactor was connected to the heated water bath by (Fisher brand) 0.8 cm (5/16 inch) tubing both at the top and bottom, to maintain continuous hot water circulation. The reactor was connected at one corner atop the diffuser, a circular object 22.9 cm (9 inches) in diameter. The purpose of the diffuser is to mix the hot air and steam uniformly, prior to entering the reactor, and also to store inevitable condensed water. The condensed water was further collected from the bottom of the diffuser, by opening the lid (which remained closed during the experiment).

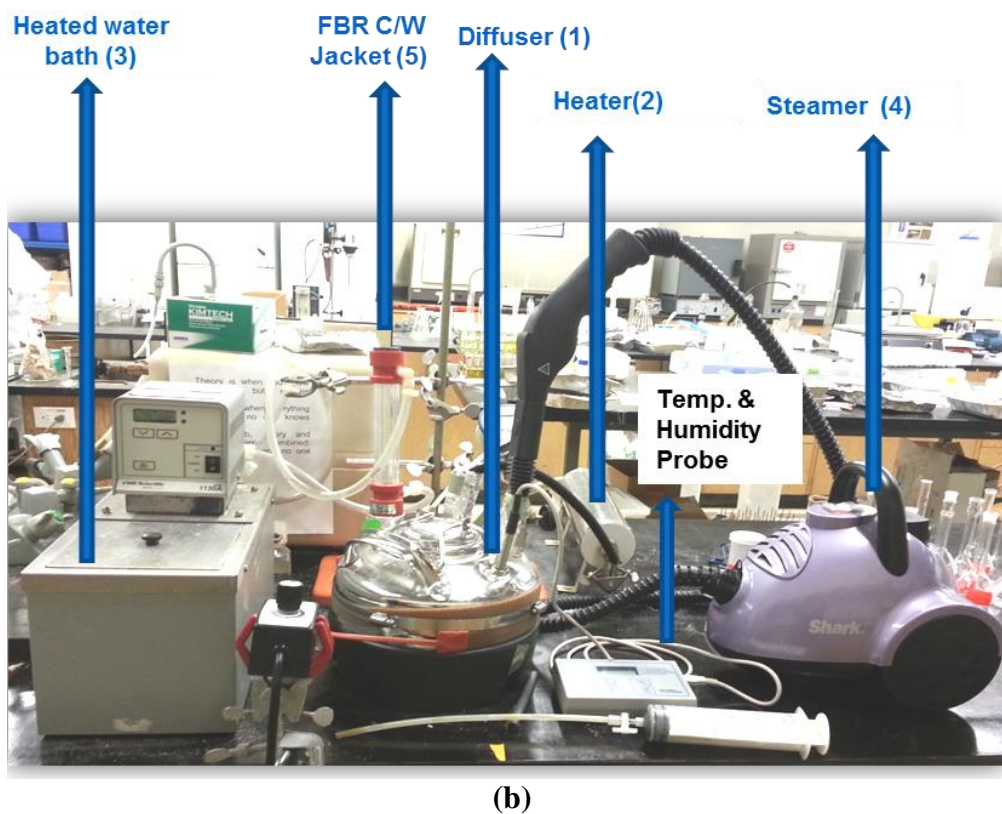
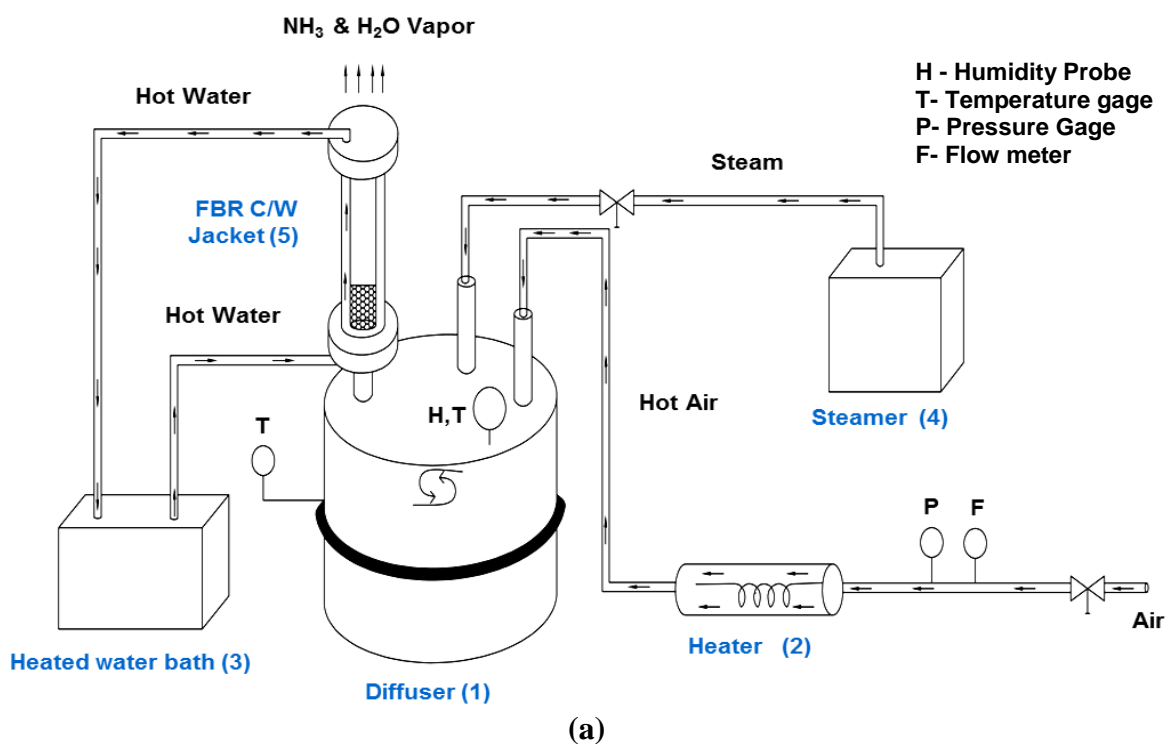


Figure 4.1 Bench-scale experimental setup (a) detailed design with connections (b) actual setup

The diffuser had two separate injection ports for the hot air and steam. One injection port was connected to the heater through a heat tube, to supply continuous hot air, and another injection port was connected to the steamer. The floor steamer (Shark) used to supply steam had limited capacity and could only produce steam continuously for 1-1.5 hours; after that, it had to be refilled with 300-400 mL water during the experiment. To prevent heat loss, the diffuser was surrounded by heat tape with thermostat (OMEGALUXTM HTWC101-004). In order to monitor the pressure inside the diffuser, a pressure gage (Cole Parmer-model) was employed between the air valve and the heater. A flow meter was placed between the air inlet and the heater, to maintain proper fluidization of struvite pellets.

The reactor needed to be stabilized at the desired temperature and relative humidity, before decomposition of each batch of struvite pellets. The maximum temperature achieved from the heated water bath was 79°C. Once the temperature of the water bath, as well as the jacket, reached 79°C, the heater was turned on to increase the temperature inside the reactor. The heat tape thermostat was adjusted to maintain the desired temperature inside the diffuser and the reactor. Steam was introduced into the diffuser after reaching the desired temperature inside the reactor, and a steam valve used to control the flow of steam. A humidity and temperature probe (Fisher ScientificTM Certified TraceableTM Digital Hygrometer/Thermometers: 11-661-7B) was mounted inside the diffuser, in order to monitor the relative humidity and temperature continuously during the process. Once the reactor was stabilized with respect to temperature and relative humidity, a suitable amount of struvite (3~4 g) was added to the reactor from the top. The struvite was positioned over the mesh attached to the bottom of the reactor. The air flow was then adjusted by the air valve, to avoid slugging of the struvite bed. While refilling the steamer, condensed water was collected from the bottom of the diffuser and disposed of by a 5 cc syringe. After every experiment, the reactor was disassembled and the heated struvite pellets were collected from the reactor and stored in individually sealed sample bags. After each set of experiments, the reactor was cleaned using distilled water and 5% hydrochloric acid solution, to dissolve any residual heated struvite that had adhered to the surface during the experiments.

4.3 Experimental conditions of performed pilot-scale experiments

The pilot-scale experiments were performed to observe ammonia removal efficiency from different sources and sizes of struvite under optimum conditions. The main objective was to transform struvite into a single phase of pure newberyite, without forming any other additional solid phases (such as dittmarite), as well as to identify the influencing factors corresponding to 100% ammonia removal (such as source, size and duration of struvite heating). The optimum temperature (80°C) and relative humidity (95%±5%) found from the bench-scale experiments were believed to remove 100% ammonia from the struvite pellets in the pilot-scale experiments. Therefore, struvite from different sources and sizes (<1mm and >1mm) were heated for different time intervals, ranging from 1 to 6 hours at optimum operating conditions, in order to identify the exact size, source and duration of struvite heating for maximum ammonia removal.

The limitations from the bench-scale experiments were eliminated in the pilot-scale set up. The continuous heating process was achieved throughout the pilot-scale experiments due to uninterrupted supply of air and steam. The entire heating process was performed in the FBR, similar to the bench-scale experiments, in order to increase the mass transfer and heat transfer which eventually provided the uniform decomposed products throughout the batches. Further modifications to the pilot-scale setup were made to improve ammonia removal efficiency based on the operating experience, energy consumption and outputs obtained from these experiments. The pilot-scale experiments were performed on the same sourced pellets. The pellets were sieved through a 1 mm sieve and retained on a 0.5 mm sieve. Thus, all struvite pellets for thermal decomposition were categorized as less than 1 mm sample and greater than 1 mm sample. The various parameters that were involved in the pilot-scale experiments have been presented in Table 4.3.

Table 4.3 Experimental conditions of pilot-scale experiments

Type of Struvite	Size of Struvite, (mm)	Duration of Heating, (hours)	Relative Humidity, (%)	Temperature, (°C)
Penticton B.C.	<1mm	0.5 - 3	70% \pm 5%	80°C
		1 - 6	80% \pm 5%	65°C
		1 - 6		75°C
		0.5 - 3		80°C
		1 - 6	95% \pm 5%	65°C
		0.5 - 4		75°C
		0.5 - 2		80°C
		0.5 - 2		85°C
Penticton B.C.	>1mm	1 - 4	95% \pm 5%	80°C
Recrystallized	>1mm	0.5 - 3		
Edmonton Gold Bar	<1mm	1 - 4		
Lulu Island	>1mm	1 - 4		
Lulu Island Crushed	0.5-1mm	1 - 4		

The performance of the pilot-scale reactor depended on the operational conditions with respect to temperature, RH and air flow throughout the process. Therefore, the temperature, relative humidity, and air flow were monitored continuously and logged throughout the experiment, using temperature and humidity probes.

4.3.1 Fluidized bed reactor design

In the pilot-scale experiments, a continuous supply of hot air and steam as provided in order to transform all of the struvite pellets into newberyite, by maintaining high vapour pressure surrounding the struvite. The intensive mixing of struvite pellets with hot air and steam will provide uniform temperature and relative humidity throughout the decomposition process and thus, the final product would be uniform. In order to achieve this operating condition, the thermal decomposition of struvite needed to be performed in a fluidized bed reactor (FBR). In an FBR, the struvite pellets were brought from the static state to the dynamic, fluid-like state, through the incorporation of a hot air and steam mixture from the bottom of the bed. The fluidization occurred when the volume flow rate of the fluidizing medium (steam or gas) exceeded a certain limiting value. The major advantage of the fluidized bed reactor was the continuous removal of ammonia from the struvite pellets due to increased heat and mass transfer, also providing temperature

uniformity in the fluidized bed reactors. In addition, in industrial operations, fluidized bed reactors are preferable due to their simple geometric configuration.

The major challenge of operating a fluidized bed reactor is the disintegration of solid particles due to turbulence, resulting from the high upward velocities. The fluidization of the solid particles depends on the gas flow velocity. The upward gas flow velocity was measured considering the gas flow through the empty reactor and expressed as superficial velocity. The typical superficial velocity usually varies from 0.15 m/s (0.5 ft/s) to 6 m/s (20 ft/s) (Perry et al., 1997). The solids remain motionless in the fluidized bed reactor when the upward gas velocity is low and can be considered in the fixed-bed state. A further increase in gas velocity causes an increase in pressure drop, until the weight of particles along with the interparticle forces, are exceeded by the drag force, together with the buoyancy force on the particles. At this condition, the bed is expanded slightly and particles exhibit minimum motion in the fluidized bed reactor. This is referred to as minimum fluidization (Avidan, 2000). The gas velocity at this minimum fluidization state has been referred to as minimum fluidization velocity (w_{\min}). The length of time the solid particles will remain in the upward fluidizing medium is dependent on the terminal velocity or maximum velocity (w_{\max}). The gas velocity at which a single solid particle remains suspended in the flowing fluidizing medium is referred to as the terminal velocity. The particles will be removed quickly from the FBR if the operating superficial velocity is significantly higher than the terminal velocity of the particles.

During fluidization, different solid particles exhibit different properties in different fluidizing media. A satisfactory understanding of particle properties is required while designing the fluidized bed reactor. In a fluidization system, the particle size, particle density, porosity, medium density, viscosity and other factors influence the minimum and maximum fluidization velocity, eventually controlling the proper fluidization of particles in the fluidized bed reactor. Volumetric flow rate and the allowable fluidizing velocity of the gas governs the cross sectional area of the fluidized bed.

An increase in superficial velocity, beyond the minimum velocity, causes formation of gas bubbles in the reactor. The increase in bubble size compared to the diameter of the bed causes slugging in

the fluidized bed reactor, as shown in Figure 4.2 (b). When large heavy particles are fluidized in the smaller diameter bed with large bed heights, slugging occurs.

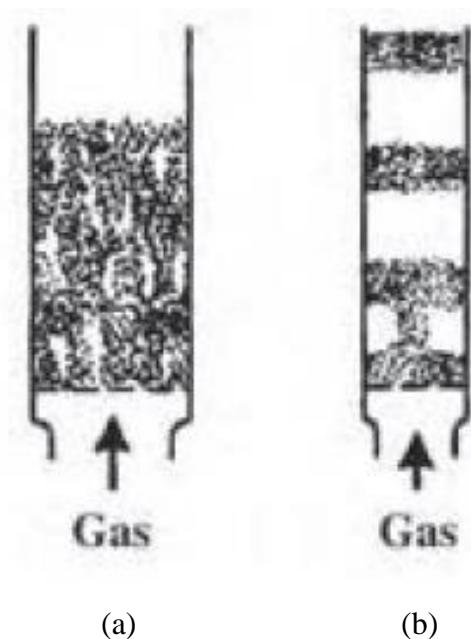
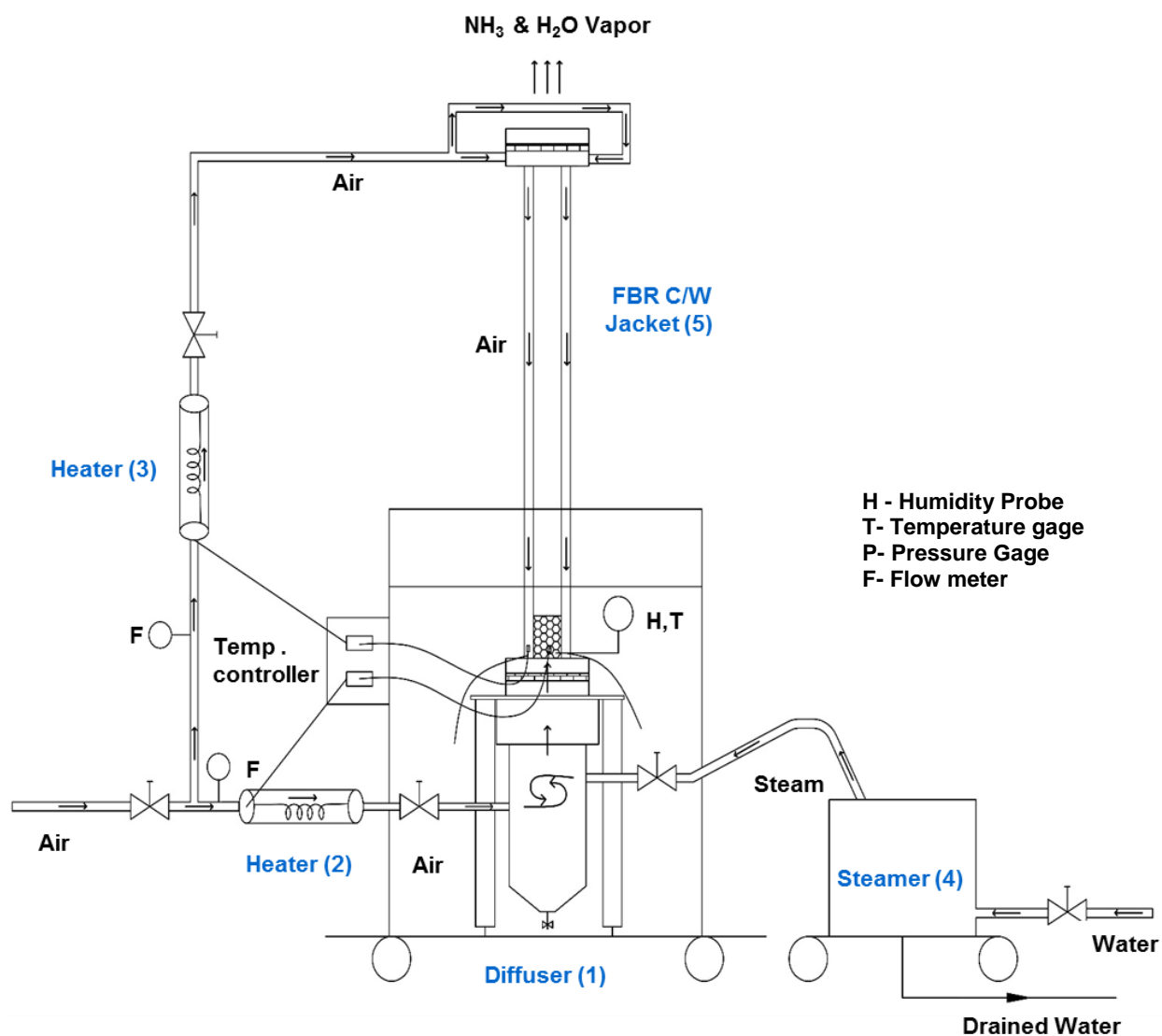


Figure 4.2 Fluidization patterns (a) turbulent regime (b) slugging regime

In this study, the fluidization of the struvite pellets was maintained in the turbulent regime (Figure 4.2, a) where the gas velocities are maintained high enough such that the gas and solids occupy similar volumes. In this way, the voids will be the gas voids, rather than distinct bubbles. The occurrence of slugging was avoided through maintaining proper gas velocity through the struvite pellets. Design of the fluidized bed reactor used in the pilot-scale experiments is given in the Appendix D.1.

4.3.2 Pilot-scale experimental setup

The pilot-scale experimental setup is presented in Figure 4.3. The pilot-scale reactor consisted of a fluidized bed reactor with jacket, diffuser, steam generator, heater for both jacket and reactor, temperature and process controller, flow meter both for jacket and reactor, temperature and humidity probe.



(a)

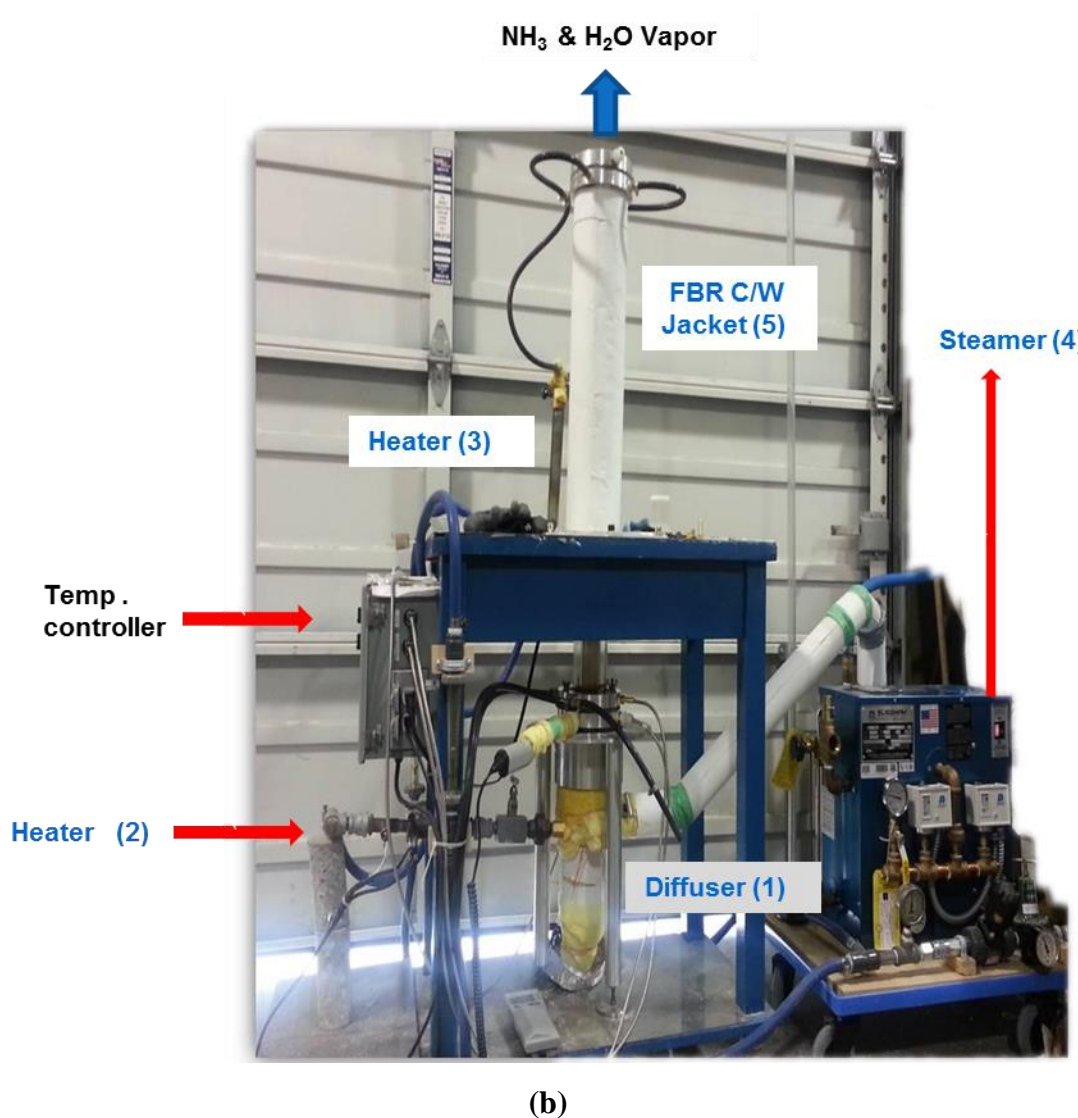


Figure 4.3 Pilot-scale experimental setup (a) detail design with connections (b) actual setup

The pilot-scale fluidized bed reactor (FBR) was cylindrical glass with an inner diameter of 41.275 mm (1.625) inch and a height of 91.44 cm (3ft) as shown in Figure 4.3. The FBR is surrounded by a jacket of 76.2 mm (3 inch) diameter. In order to prevent condensation inside the reactor, the jacket temperature was always maintained higher than that inside the reactor. To minimize cost, the temperature was raised inside the jacket using hot air, instead of the hot water that was used in the bench-scale experiments. The temperature in the jacket always needed to be maintained 7°C-10°C higher, compared to the reactor. Therefore, two separate heaters were used to provide continuous, hot air supply through the jacket and the reactor; these heaters were connected to the

temperature and process controller, which was used to maintain the desired temperatures. Hot air entered into the jacket from the top of the reactor and exited from the bottom of the reactor. This prevented condensation from happening at the top of the reactor by maintaining a higher temperature throughout the jacket, compared to that inside the reactor. The reactor was sitting at the top of the aluminum diffuser, which was cylindrical and had a 4 inch diameter. The purpose of the diffuser was to supply the mixture of hot air and steam, prior to entering the reactor and also to store inevitable condensed water, which was drained from the bottom of the diffuser. The diffuser had two separate injection ports for the hot air and steam. The ports were installed on the opposite sides, with tangential injection of the gases. A steam generator (SUSSMAN MBA9 electric steam generator), with 0.0034 kg/s (27 lb/hr) steam capacity, was employed for continuous supply of steam inside the reactor. To prevent heat loss, the diffuser and the reactor were thermally insulated by glass cotton.

The reactor needed to reach the desired temperature and relative humidity prior to the start of struvite heating. In the temperature controller, the jacket temperature was set at 7-10°C higher than the desired reactor temperature. The heaters and the air valve were turned on simultaneously. A humidity and temperature probe (Vaisala HUMICAP® HMI41 humidity indicator with HMP46 humidity and temperature probe) was inserted between the diffuser and the reactor, in order to monitor the relative humidity and temperature continuously during the process. The steam was introduced into the diffuser, after reaching the desired temperature inside the reactor and the flow was controlled using a steam valve. Once the reactor was stabilized with respect to temperature and relative humidity, a suitable amount (20-25 g) of struvite was added to the reactor from the top. The struvite sat over the mesh, which was attached between the bottom of the reactor and the top of the diffuser. The air flow was then adjusted with an air valve, to avoid slugging of the struvite bed. The air and steam valves needed to be adjusted precisely, to achieve the desired temperature and relative humidity throughout the process. The steam generator was refilled with the water automatically after a specified pressure drop (set at 40 psi in the pressure gage). The air/steam ratio was almost 1:1 throughout the experiment. After every desired time interval, the decomposed struvite samples were collected from the top of the reactor, by using a long handled scoop.

At the end of every experiment, the reactor was detached from the diffuser and the heated struvite pellets were collected and stored in individual sealed sample bags. The reactor was then cleaned with a brush to remove any residual heated struvite that had adhered to the glass. At the very end of the experiment, the steamer water valve was opened to drain all remaining water and steam vapour. The air flow remained open for 30 minutes, to bring the heaters to normal temperature.

4.4 Sample collection and preservation

Struvite samples were collected immediately after thermal decomposition and preserved in individual sealed sample bags. In order to prevent moisture absorption, the samples were stored in the vacuum vacuum desiccator in the environmental lab prior to chemical analysis and XRD.

4.5 Analytical methods

4.5.1 Sample preparation

All initial and heated struvite samples were analyzed for magnesium, ammonia and orthophosphate, after completion of each experiment. All solid samples from the batch experiments were finely crushed, using a ceramic mortar and pestle to form a powder, before analysis. In order to determine the composition of the pellets, approximately 0.1 g of struvite powder was dissolved in 100 mL volumetric flask, using distilled water and several drops of concentrated hydrochloric acid. The flask was shaken by hand until all solid material was dissolved and no longer visible. Ammonia, magnesium and orthophosphate measurements were also involved in determining Mg: N: P: H₂O molar ratios of solid phase samples, dissolved in a weak HCl solution. Each sample was prepared in triplicate and all chemical analyses were undertaken at the UBC Environmental Engineering Laboratory.

4.5.1.1 Magnesium

The magnesium testing was performed using the Varian Inc. SpectrAA220 Fast Sequential Atomic Absorption Spectrophotometer. The dissolved samples were diluted at 1:10 volumetric ratio using distilled water. In order to do the magnesium test, the diluted liquid samples and calibration standard solutions were again diluted in 25 mL glass tubes at a 1:10 volumetric ratio with a 20 g/L lanthanum solution which was used in order to overcome interferences due to the presence of other ionic species. The 20 g/L lanthanum solution was prepared by dissolving 63.34 g reagent grade lanthanum nitrate ($\text{La}(\text{NO}_3)_3 \cdot 6\text{H}_2\text{O}$) and adding deionized water up to the 1L mark. One drop of concentrated nitric acid (HNO_3) was added to each tube and agitated using a vortex mixer for uniform mixing. Before analyzing each set of samples, continuous auto sampler rinsing was conducted with deionized water; magnesium lamp optimization was carried out by adjusting instrumental settings. Details can be found in Appendix A.

4.5.1.2 Ammonia and orthophosphate

To measure the ammonia and orthophosphate, the glass tubes were rinsed with the diluted liquid samples prepared at volumetric ratio of 1:10 and were filled with the same diluted samples. Ammonia and orthophosphate of the raw and decomposed samples were measured using the Lachat QuikChem 8000 through flow injection. The samples were analyzed for ammonia and orthophosphate using the method 4500-NH₃ H and 4500-P G obtained from Standard Methods for the Examination of Water and Wastewater (APHA, 2005). During analysis, reagent grade potassium phosphate monobasic (KH_2PO_4) and ammonium chloride in distilled water were used as calibration standard solutions. Details can be found in Appendix A.

4.5.1.3 XRD identification of solid phases

Crystalline phases of initial struvite samples, and residual solid samples after performing thermal decomposition, were identified using a Bruker D8 Advance X-ray diffractometer, with $\text{CuK}\alpha$ radiation. The test was performed in the UBC Department of Chemistry. The XRD output peaks of individual solid samples were matched with the standard peak of crystalline solid samples, using

the powder diffraction database file, PDF-2, provided by the International Center for Diffraction Data. Details of instrument settings can be found in Appendix A.

4.5.1.4 Struvite morphology

Struvite morphology was observed using a Motic B₃ Professional Series microscope and images were captured using Motic Images Plus software. Small quantities of the solid samples were placed on glass slides. Struvite pellets were viewed at 1x, 2x and 3x magnifications.

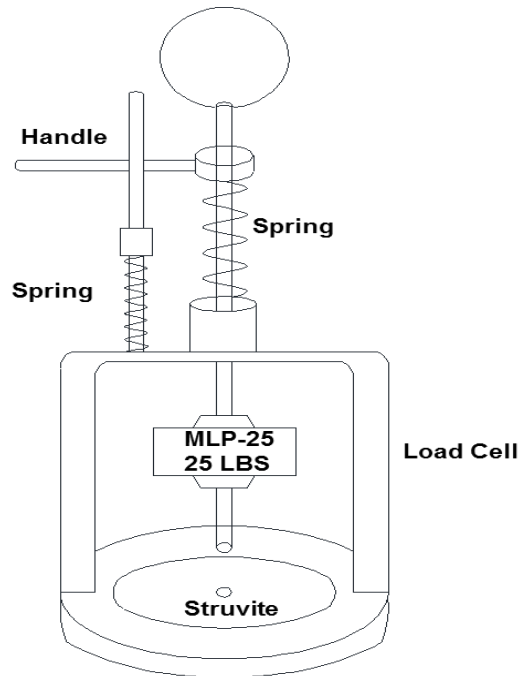
4.6 Development of hardness tester

Fattah (2010) developed a hardness tester to measure the crushing strength of the larger (≥ 1 mm) and harder (≥ 1800 g) struvite pellets. This instrument was modified further for the current study, in the Civil Engineering workshop at UBC, in order to quantify the crushing strength of softer and smaller struvite pellets ranging between 0.5-2 mm, as shown in Figure 4.4. The device consisted of a load cell which was attached close to the bottom of the handle. In this device, the load cell was connected to a computer and passed a signal to a data acquisition box (PMD-1208 LS, Measurement ComputingTM). A spring was attached at the top section of the handle to prevent shock load.

In order to record the continuous crushing strength measurement as force during each test, a program was developed in DASyLab[®]9.0, which is shown in Figure 4.5 (Measurement ComputingTM). During crushing, the maximum load (g) required to crush each pellet was recorded automatically in the program, which was also saved as an ASC file. Further, the ASC file was extracted to Microsoft Excel for data analysis and data comparison. The measurement of crushing strength involved the connection of the device, placement of each pellets and uniform load from the top of the handle. On average, over 100 pellets were randomly picked and crushed for each source and size of struvite pellets, that had been heated in the pilot and bench-scale experiments.



(a)



(b)

Figure 4.4 Device used to determine crushing strength of struvite (a) actual device and (b) sketch (not to scale)

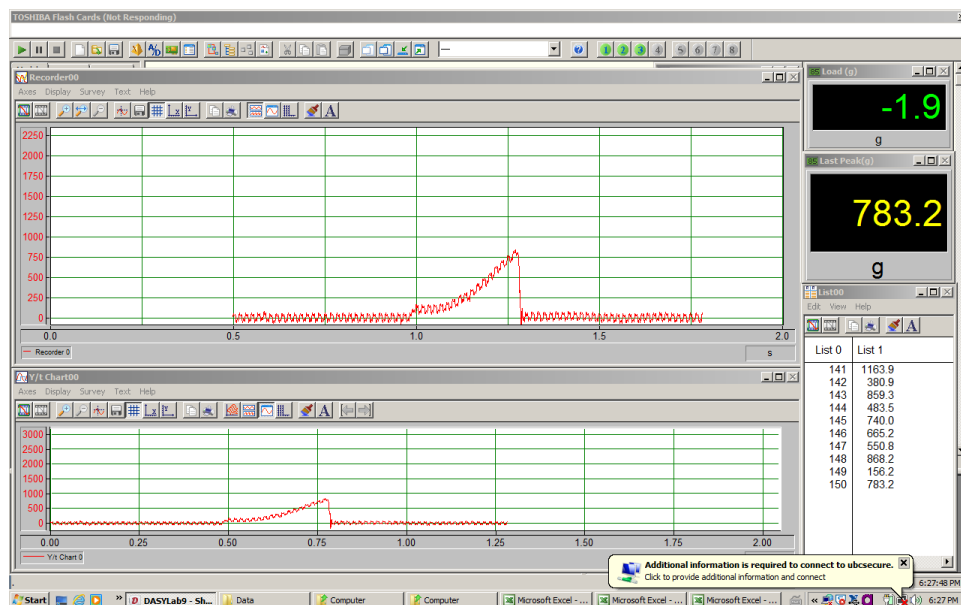


Figure 4.5 Program window used to graphically illustrate force as a function of time and to determine peak load

4.7 Terminology

4.7.1 Molar ratio

The molar ratios for the initial struvite samples and the decomposed samples were calculated using chemical results from aqueous ammonia-N, aqueous orthophosphate, and magnesium data, for each experiment. This molar ratio was calculated in order to determine the extent of ammonia and water after each batch test of thermal decomposition. The term molar ratio is used with respect to N:P, $\text{H}_2\text{O}:\text{P}$ and $\text{Mg}:\text{N}:\text{P}:\text{H}_2\text{O}$. In the context of raw struvite samples, these molar ratios consider the total of each element in the initial struvite sample, before commencing the heating process. In the context of struvite thermal decomposition product, N:P and $\text{H}_2\text{O}:\text{P}$ refer to the molar ratio of residual ammonia and the water content in struvite decomposition product, with respect to the orthophosphate content after completion of each batch test. Since newberyite contains no ammonia, the ratios of N:P were expected to be almost negligible with $\text{H}_2\text{O}:\text{P}$ ratios around 3. The decomposition product may contain a combination of newberyite and dittmarite when the $\text{H}_2\text{O}:\text{P}$ ratio is found to be less than 3, whereas the $\text{H}_2\text{O}:\text{P}$ ratio greater than 3 indicates the presence of newberyite, along with struvite, in the struvite decomposition product.

Chapter 5: Results and Discussion

The main purpose of this study was the complete transformation of struvite to newberyite by removing 100% of the ammonia through the thermal decomposition process. The thermal decomposition of struvite could result in various solid phases including dittmarite, newberyite, and amorphous structure, depending on the operating conditions. In order to achieve a decomposed struvite completely devoid of ammonia, such as newberyite, it is necessary to understand the solid phase transition with the change of various operating parameters. Once a successful transformation method of struvite to newberyite is identified, operating conditions could be optimized for maximum ammonia removal, to provide energy and a cost effective system.

5.1 Oven dry experiments

The first phase of the experiment was conducted using the oven dry method, to observe the solid phase transition and ammonia removal rate during the decomposition of struvite at different heating temperatures and durations of time. A better understanding of the changes in structure and composition is important to interpret the structural transition taking place in the residual solid phase, upon struvite decomposition. The hypotheses and specific purposes associated with these experiments are discussed in the following section.

5.1.1 Hypotheses and specific goals

The mechanism of ammonia and water loss during struvite decomposition was important to understand, prior to establishing the ammonia recovery technology. The oven dry experiments were performed to answer the following questions.

- How does the chemical, physical and structural composition of struvite solid phase change when heated isothermally, at different temperatures for different durations?
- Is it possible to remove all the ammonia from struvite through the oven dry method?
- What are the effects of temperature and the duration of heating on dehydration, which can cause layered structure formation?
- Does the structural composition of the decomposed solid remain the same over time?

- What is the ammonia removal efficiency through subsequent heating and rehydration of synthetic struvite, and if ammonia removal is incomplete, what are the reasons?
- What are the limitations of the oven dry method?

In order to understand the mechanism and to answer the aforementioned questions, three approaches were adopted: mass loss curves, wet-chemical analysis (orthophosphate, ammonium-N, and total magnesium), and solid sample analysis (XRD).

Hypotheses

- Ammonia gas evolution ceases when the struvite structure collapses, due to excessive dehydration and formation of some solid phase that entraps ammonia in between the structure.
- The structural composition of the decomposed solid phase would change with an increase in temperature and duration of heating.
- The decomposed solid phase (unstable layered structure) may reorganize itself and can transform into more organized structure over time.
- Subsequent heating and rehydration may increase ammonia gas evolution, since rehydration might increase the water content that would keep the structure loose; as a result, ammonia might escape easily from the structure.

5.1.2 Results and discussion of oven dry experiments

5.1.2.1 Influence of temperature with varying heating duration on decomposed product

5.1.2.1.1 Mass loss curves

The mass losses of heated synthetic struvite samples were calculated after a certain duration of heating, at a specific temperature, and are presented in Figure 5.1, in the form of kinetic curves.

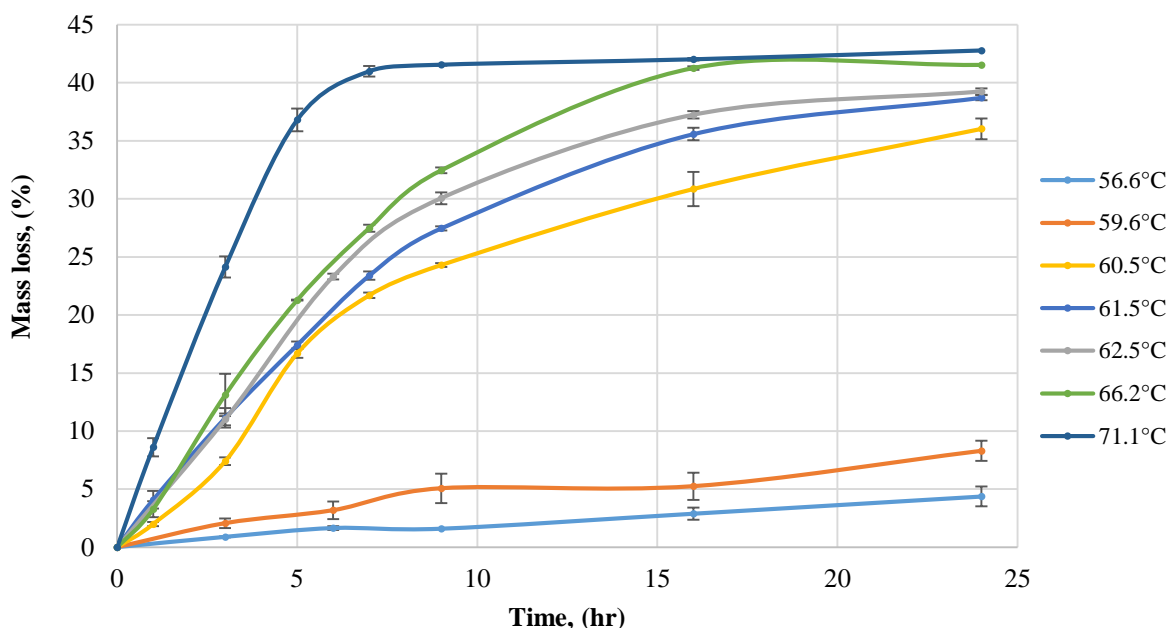


Figure 5.1 Percent mass loss of struvite over time at different heating temperature

In general, it was found that with an increase in temperature, the percent mass loss also increased. For any given temperature, the mass loss percentage was expected to increase with the increase in duration of the heating period. The mass loss percentage was not significant at temperatures below 60.5°C. Conversely, when the temperature was increased from 60.5°C to 66.2°C, the mass loss percentage continued to increase with an increase in heating duration. However, the mass loss percentage became almost constant after heating for 7 hours in the oven at a temperature of 71.1°C. A substantial mass loss occurred between the temperatures of 59.6°C and 60.5°C and the corresponding mass losses at these two temperatures, after 24 hours, were around 9% and 36%, respectively. This indicates that, within the range of $60^{\circ}\text{C} \pm 0.5^{\circ}\text{C}$, water vapour and gaseous ammonia evolution started and continued to increase further as the temperature increased. The maximum mass loss (42%) occurred at a temperature of 71.1°C after 7 hours of oven dry heating, and remained constant for up to 24 hours; this infers that higher temperatures lead to more rapid decomposition of struvite, due to enhanced loss of higher mass within a short period of time. According to Novotny (2011), around 42% mass loss occurred at temperature of 80°C after 24 hours of heating, similar to the mass loss percentage at the temperature of 71.1°C observed in this study. Novotny (2011) found that the mass loss percentage only increased about 10%, when the

temperature was increased further from 80°C to 200°C. Thus, in the present study, the increase in mass loss percentage was expected to be negligible at temperatures above 71.1°C.

5.1.2.1.2 Chemical composition and interpretation

The extent of ammonia gas evolution depends on the duration of struvite heating and the temperature. A relationship between Mg and PO_4 is not shown in this study since, according to the mass balance, the stoichiometric ratio always remained close to 1:1. Both magnesium and orthophosphate are non-volatile and cannot escape from the struvite upon heating. Therefore, the Mg:P ratio was expected to remain as unity across all temperatures, throughout the experiment. Also, according to the study performed by Novotny (2011), the samples heated at temperatures between 40°C to 105°C had a Mg:P ratio of unity. Figures 5.2 and 5.3 illustrate average measured ammonia and water content remaining in the synthetic struvite when decomposed over time, at different temperatures. The results from the mass loss percentage measurements are consistent with the results of chemical analysis.

In Figures 5.2 and 5.3, the difference in ammonia and water content between initial struvite samples and the struvite samples decomposed at temperatures below 60.5°C, were not significant. The result from the chemical analysis is in agreement with the mass loss analysis (Figure 5.1), where the percent mass loss is also insignificant, when struvite samples were heated below 60.5°C for 24 h duration. This confirms the thermal stability of struvite upon decomposition at temperatures below 60.5°C. At temperatures above 59.6°C, a sudden increase in ammonia and water evolution rate was observed with an increase in temperature and heating duration (Figure 5.2 and 5.3). Therefore, a significant increase in the mass loss percentage was observed at temperatures above 59.6°C. Kiehl and Hardt (1933) also reported simultaneous evolution of ammonia and water from a struvite structure at temperatures above 60°C. At each individual heating period, the ammonia removal rate increased with an increase in temperature. Similarly, at each individual heating temperature, the ammonia evolution rate increased with an increase in heating duration. In Figure 5.2, at a temperature of 56.6°C, NH_4 -kinetic curves showed little “humps” at the beginning of the drying process. This could be attributed to experimental and/or analytical inaccuracy.

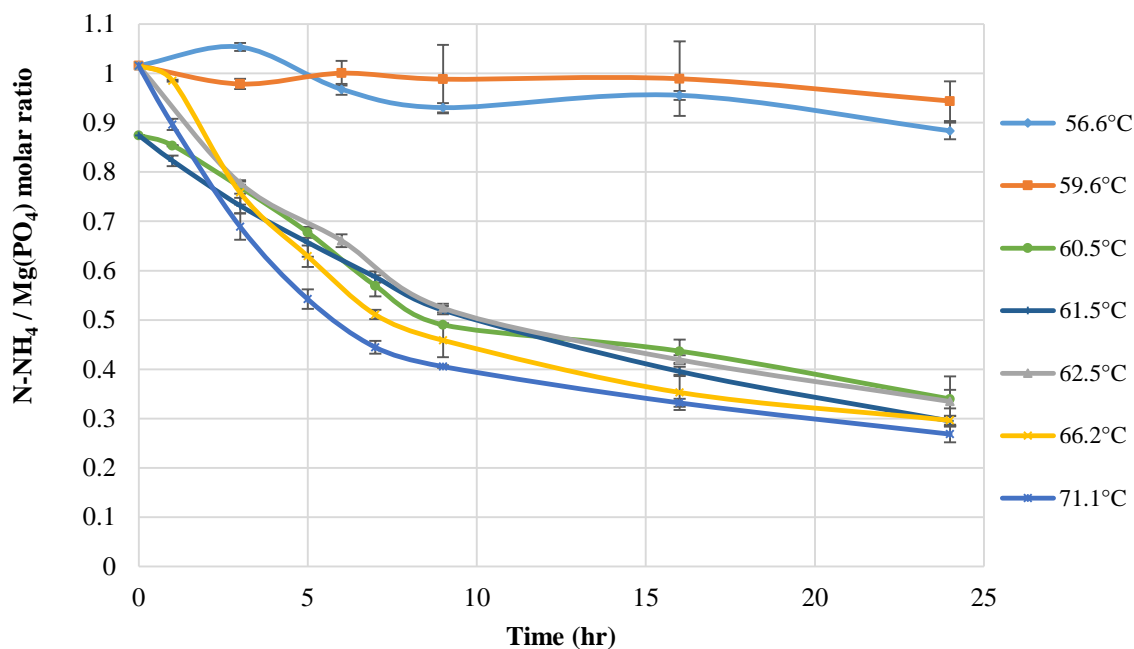


Figure 5.2 N-NH_4 molar ratio with respect to $\text{Mg (PO}_4\text{)}$ over time at different heating temperatures

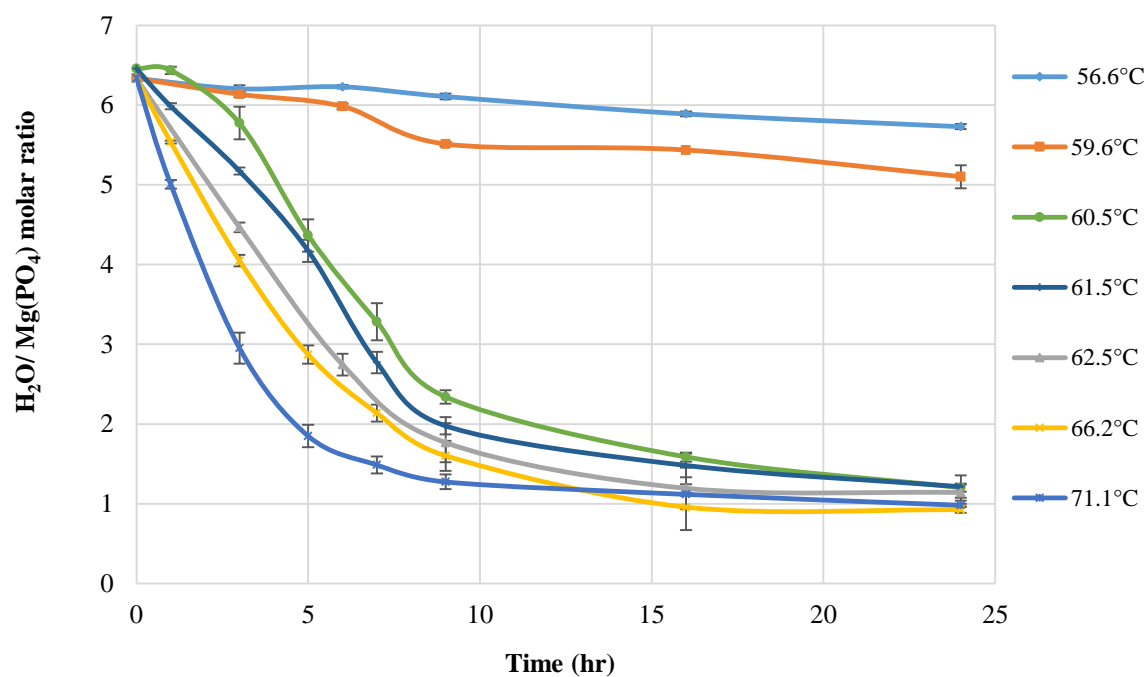


Figure 5.3 H_2O molar ratio with respect to $\text{Mg (PO}_4\text{)}$ over time at different heating temperatures

From Figure 5.2 and 5.3, it can be seen that the water molecules in struvite decreased from approximately 6 mole to approximately 1 mole, when decomposed at temperatures higher than 59.6°C after 24 hours of oven dry heating, where the residual ammonium nitrogen in the decomposed solid phase was around 25-35% of struvite molar ratio. This infers that complete ammonia removal was not possible to achieve through the oven dry method, even at temperatures as high as 71.1°C over 24 hours. These experimental results are in strong agreement with several previous studies performed of struvite thermal decomposition. In the study performed by Novotny (2011), residual ammonia appeared to decrease to around 30%, whereas residual water content was around 1 mole between 80°C and 105°C, with 24 hours of heating. The residual ammonia and water content in the decomposed struvite at temperatures higher than 80°C, found by Novotny, was similar to the findings of the present study, where struvite thermal decomposition was performed at temperatures between 60.5°C and 71.1°C for 24 hours. Novotny (2011) also reported that thermal decomposition of struvite at temperatures of 160°C and 200°C, for 24 hours, caused a further decrease in residual ammonia content to 22% and 16%, respectively. The residual ammonia and water content found in the study of Novotny did not change significantly at temperatures higher than 100°C, with prolonged heating durations. Therefore, it can be concluded that complete ammonia removal from struvite cannot be achieved with the isothermal oven dry method, even at higher temperatures with longer heating duration. However, the reason behind this incomplete ammonia removal was not addressed by this previous researcher.

Under certain heating conditions, the formation of a layered structure, such as magnesium hydrogen phosphate monohydrate, in decomposed solid samples has been reported by many previous researchers (Kiehl and Hardt, 1933; Finch and Sharp 1989; Sales et al., 1993). However, almost none of the previous studies, except Novotny (2011), reported the formation of a $\text{MgH}(\text{NH}_3)_x\text{PO}_4\cdot\text{H}_2\text{O}$ -type compound, with low N-NH_4 and water content, as a stable solid phase during thermal decomposition of struvite. The thermal stability of this layered structure was mentioned in several studies; it was found that total ammonia removal can be achieved only at temperatures higher than 200°C, when all the water of crystallization, as well as water of constitution, evolve from the structure and eventually cause formation of magnesium pyrophosphate ($\text{Mg}_2\text{P}_2\text{O}_7$) (Kiehl and Hardt, 1933; Paulik and Paulik 1975a; 1975b; Abdelrazig and Sharp, 1988; Sarkar 1991).

Based on the chemical analysis in this study, the composition of the residual solid phase was $\text{MgH}(\text{NH}_3)_x\text{PO}_4.y(\text{H}_2\text{O})$, with 25-35% ammonia content and 1-1.3 water molecules. This solid phase was believed to start forming at $60\pm0.5^\circ\text{C}$ and remained stable up to 71.1°C . Higher temperatures caused further dehydration, with ammonia remaining in the solid phase. Therefore, it can be postulated that, at the beginning of struvite decomposition, some solid phase (similar to a layered structure) might have formed, entrapping the ammonia in between the structure and inhibiting ammonia removal from the struvite, even at higher temperatures and with prolonged heating.

5.1.2.1.3 XRD Results

5.1.2.1.3.1 Formation of layered structure

A low scattering angle XRD analysis (with 2θ angle starting at 0.8°) was performed on the fresh heated struvite samples decomposed at 60.5°C and 61.5°C , in order to observe the presence of solid phases; this is where significant amounts of ammonia and water evolved (Figure 5.2 and 5.3) from the struvite structure, during the thermal decomposition process. The XRD results at 61.5°C , for different time intervals, are shown in Figure 5.4 (a) and Figure 5.4 (b). Figure 5.4 (a) shows the intensity of the peaks from the lowest to the highest scanning angles obtained from XRD whereas Figure 5.4 (b) indicates the enlarged view of the peaks that formed at low angles. The initial solid phase was crystalline struvite ($\text{MgH}_{0.15}(\text{NH}_4)_{0.85}\text{PO}_4.6.3\text{H}_2\text{O}$), before thermal decomposition, which had struvite peaks with high intensities that corresponded to the powder diffraction file (PDF) for struvite (PDF 00-015-0762). After performing thermal decomposition of struvite at 61.5°C , a strong peak was observed at $2\theta\ 1.8^\circ$ (scanning angle for XRD, $2\theta = 0.8^\circ\sim 50^\circ$) on the decomposed struvite samples (Figure 5.4 b).

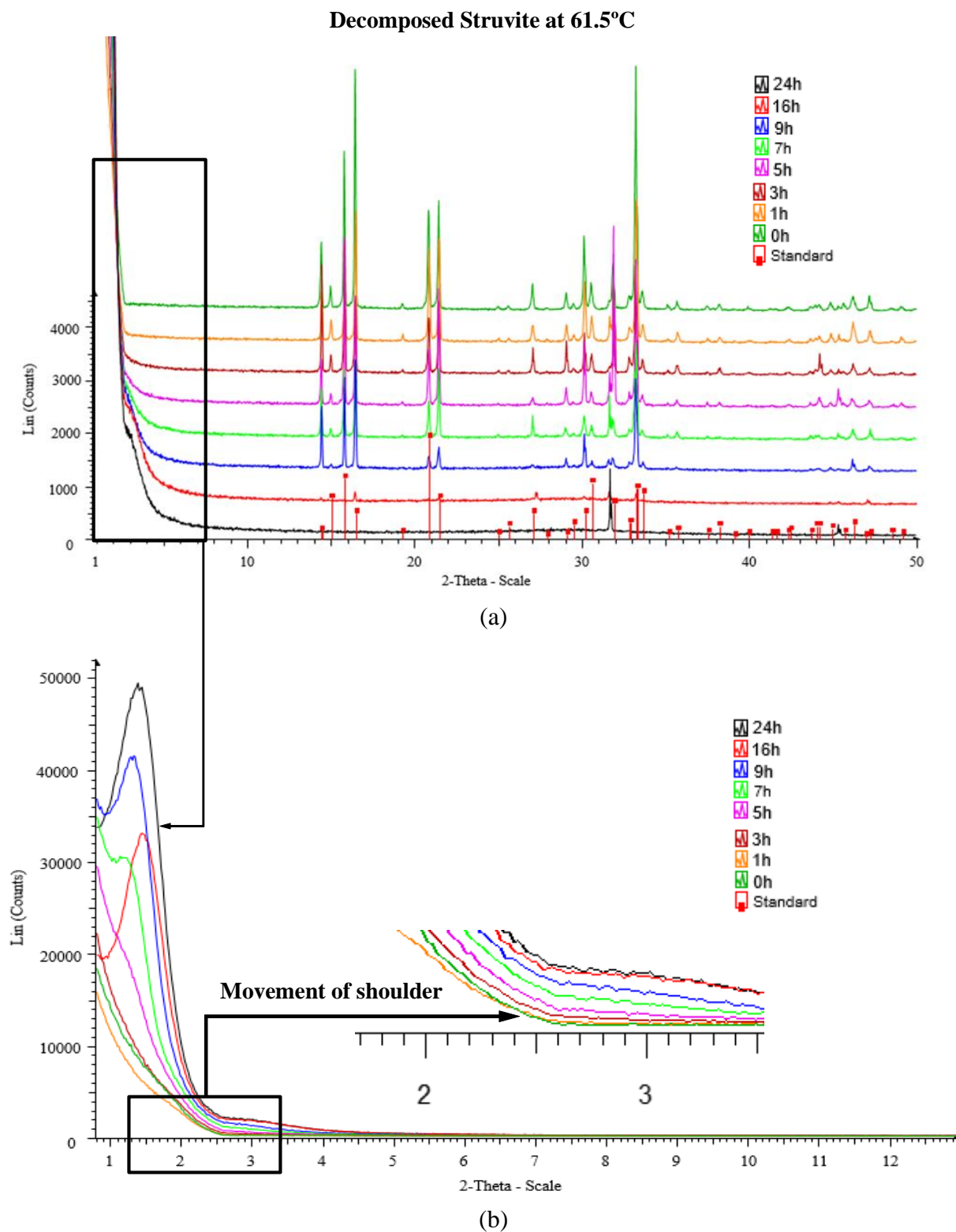


Figure 5.4 X-ray diffraction patterns of synthetic struvite decomposed at 61.5°C (a) scanning angle 0.8 to 50 degree (b) enlarged view of sample peaks formed between 0.8 and 12 degree

The peak at low angle became pronounced after 7 hours of heating. The presence of a peak at low angles indicates the presence of another solid phase, along with struvite. However, none of the existing files from the powder diffraction database PDF-2 could be matched to this peak. The XRD performed on the two different batches of samples heated at 61.5°C showed the highest intensity of this peak at low angles for 24 hours, followed by 9, 16, 7, and 5 hours, with the exception of one data point in triplicate samples. The reason for the higher intensity peak formed at 9 hours, compared to the peak formed at 16 hours, cannot be explained at this time. The similar high intensity peak at low angles also can be observed in the X-ray patterns of $\text{MgHPO}_4 \cdot x\text{H}_2\text{O}$ (where $x=0.78-1.29$) (Bensalem et al., 1995; Chen et al., 1993), as well as in that of dittmarite $\text{MgNH}_4\text{PO}_4 \cdot \text{H}_2\text{O}$ (PDF 00-036-1491). From previous studies, it has been found that both $\text{MgNH}_4\text{PO}_4 \cdot \text{H}_2\text{O}$ and $\text{MgHPO}_4 \cdot 1.2\text{H}_2\text{O}$ are thermally stable up to 200°C (Chen et al., 1993 and Bensalem et al., 1995) and both structures consist of similar molecular units. Both of these solid phases exhibit characteristics of layered structures, with H_2O molecules between the layers.

In addition, in a dittmarite structure, ammonia is also entrapped along with H_2O molecules between the layers of Mg and PO_4 . The XRD results and chemical composition ($\text{MgH}(\text{NH}_3)_{0.3}\text{PO}_4 \cdot 1.3\text{H}_2\text{O}$) of the decomposed solid phase obtained from the present study clearly indicate that the struvite decomposition products formed possess an intermediate structural composition, somewhere between dittmarite and $\text{MgHPO}_4 \cdot 1.2\text{H}_2\text{O}$, compounds with both ammonia and water molecules between the layers. The distinct characteristic of every layered structure is to pose a strong peak at low angles (also observed in the present study). Therefore, the XRD analysis provides strong support for the hypothesis of the formation of a layered structure during thermal decomposition of struvite.

The layered structure found in this study had similar characteristics to a 2D layered structure. It can be observed in Figure 5.4 (b) that the peak belonging to the layered structure is much broader and less sharp than the peak belonging to the struvite structure. In cases of an amorphous 2D layered structure, the layers may not be precisely situated upon one another, resulting in the inability to obtain a diffraction pattern in all 3 dimensions, but only in one. Only those X-rays reflected from the layers in parallel can interfere and create a greater amplitude (which, in turn, would be registered as a peak). Due to weak forces between the layers (and, possibly, a different

amount of ammonia between each pair of layers), the distance between the layers may vary slightly. Therefore, the peaks formed from a 2D layered structure, at low angles, are much broader than the peaks formed from any other 3D crystalline structure, such as struvite and dittmarite. Evidently, the solid phase obtained after struvite thermal decomposition had a low crystalline structure, which was a combination of a layered structure and struvite structure.

As the duration of heating was increased, the intensity of the layered structure peak increased and simultaneously the intensity of the struvite peak decreased at temperature of 61.5°C. The decrease in struvite peak, with an increase in heating duration, indicates a decrease in crystallinity of the bulk sample, as well as for the portion of struvite compound. Depending on the heating duration, a decomposed solid phase could be semi-crystalline and semi-amorphous. At a temperature of 61.5°C, with 9 hours heating duration, the decomposed structure was semi-crystalline and semi-amorphous. The crystalline portion of the decomposed structure belongs to a struvite compound, whereas the amorphous portion belongs to the 2D layered structure. Furthermore, the structure can be referred to as an amorphous structure when the struvite peaks completely disappears under XRD. Therefore, this shows that the crystalline struvite structure completely transformed into an amorphous structure, after heating at 61.5°C beyond 9 hours. Moreover, with the increase in the amorphous portion of the bulk sample, the 2D layered structure became pronounced and reached its highest intensity when the crystalline struvite structure completely transformed into an amorphous structure. The layered structure peak in the decomposed samples can only be detected in one dimension when the XRD wavelength permeates through the layers. While there is a long-range order within each plane in two dimensions (which consists of strongly-bound Mg and PO₄ units), there are only weak forces and lack of a long range order in the third dimension (which is perpendicular to the planes). Therefore, the layered structure obtained in this study has been referred to as a “2D amorphous layered structure”.

5.1.2.1.3.2 Identification of layered structure at temperatures below 61.5°C

The layered structure mentioned in previous studies (MgNH₄PO₄·H₂O and MgHPO₄·1.2H₂O) contained fewer molecules of water of crystallization, compared to the initial struvite sample which contained 6 moles of water. The excessive dehydration induced from evolution of water

from the struvite structure upon heating for longer duration, is believed to be the reason for the formation of a layered structure. Similarly, the decomposed samples containing a significant amount of water of crystallization are less likely to retain any layered structure. In this study, no significant difference in ammonia and water content was observed between the initial struvite samples and the struvite sample decomposed at temperatures lower than 60.5°C for 24 hours (Figure 5.2 and Figure 5.3). The water of crystallization at temperatures below 60.5°C ranged between 5-6 moles; therefore, the possibility of a layered structure formation at temperatures below 60.5°C is almost negligible. On the other hand, the 2D amorphous layered structure was more pronounced in the struvite samples decomposed at 61.5°C. In order to identify the presence of a layered structure at the exact decomposition temperature 60.5°C, XRD was carried out on the struvite sample decomposed for 24 hours (Figure 5.5).

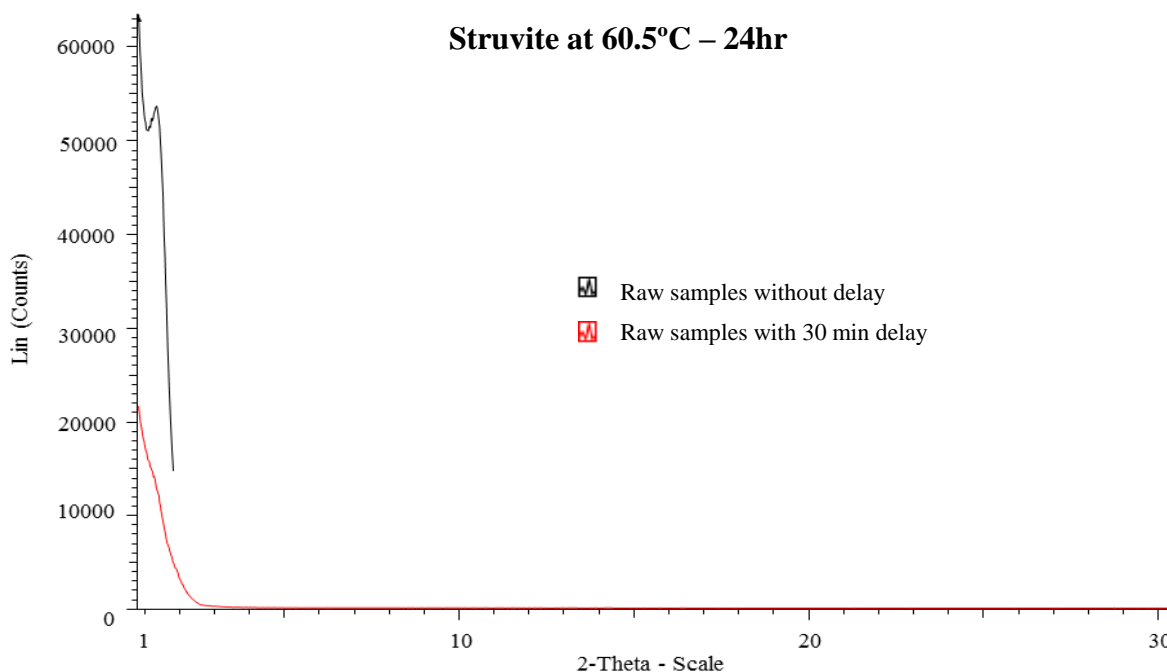


Figure 5.5 X-ray diffraction patterns of synthetic struvite decomposed at 60.5°C for 24 hours;

■ XRD performed on the samples without any delay, ■ XRD performed on the samples after 30 minutes exposure to the atmosphere

At the beginning of the experiment, a test run for XRD was performed on the struvite sample heated at 60.5°C, immediately after preparing the samples without any delay. During XRD, a

prominent peak at low angles appeared for the samples that had been prepared immediately after removal from the sealed bags. Afterwards, the sample for XRD analysis was prepared using the same heated struvite sample and exposed to the atmosphere for 30 minutes, prior to initializing the instrument.

The peak at low angles disappeared as the heated struvite samples absorbed moisture from the atmosphere during that period. Therefore, it can be inferred that the layered structure was found to be formed right on the edge of the temperature 60.5°C, which was unstable due to the availability of moisture in the exposed atmosphere. The absorption of moisture from the atmosphere by the heated struvite samples was also mentioned by Novotny (2011). The author reported that struvite pellets heated at 80-200°C absorbed around 1.2-1.5 moles of water, after being exposed to the atmosphere for two weeks. The water absorption by the heated samples was inevitable, despite storage in the desiccator. The author also mentioned that immediate exposure of struvite pellets after drying at high temperature, exhibits greater affinity towards atmospheric moisture. Therefore, the affinity of the layered structure towards atmospheric moisture content and possible transformation into a more organized and stable layered structure, is almost inevitable.

5.1.2.2 Influence of different temperatures on layered structure formation

The synthetic struvite with initial composition of $\text{Mg:N:P:H}_2\text{O} = 0.82:0.87:1:6.46$ was thermally decomposed under the oven dry method, at various temperatures (59.6°C, 65.3°C, 70.1°C and 85.5°C) for 7 hours, to observe the influence of temperature on layered structure formation. Chemical analysis was performed to determine the residual ammonia and water content and XRD was performed to assess the residual solid phase upon heat treatment.

5.1.2.2.1 Chemical composition

Figures 5.6 and Figure 5.7 represent the residual ammonia and water content in the synthetic struvite, when heated at different temperatures for 7 hours. According to the chemical analysis, the residual ammonia and water corresponding to the decomposed synthetic struvite, after 7 hours of heating at 59.6°C, were similar to those of the initial struvite composition.

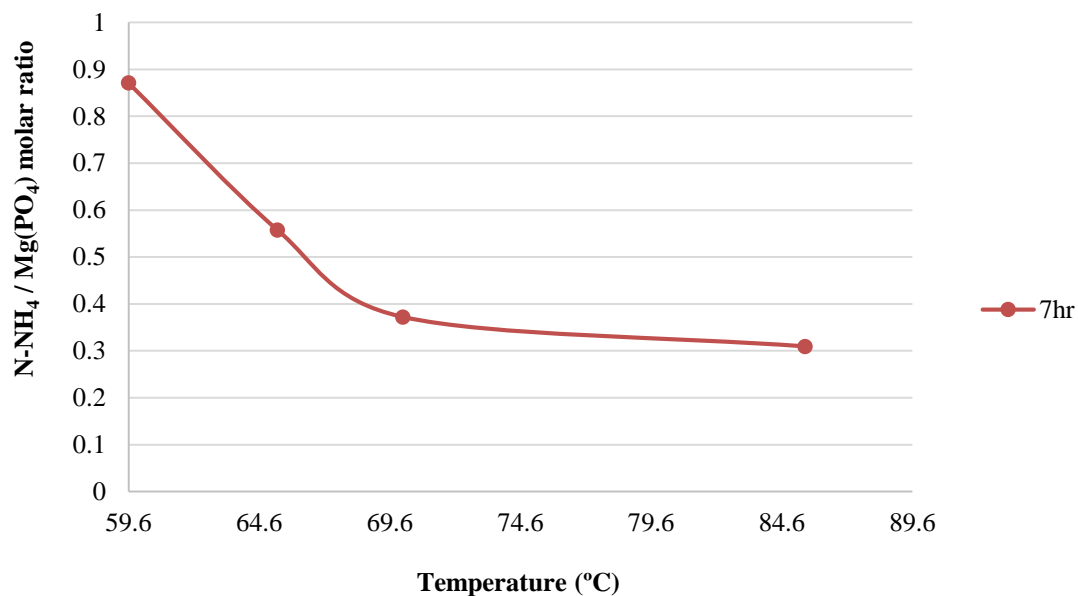


Figure 5.6 N-NH₄ molar ratio with respect to Mg (PO₄) after 7 hours duration of heating at different temperatures

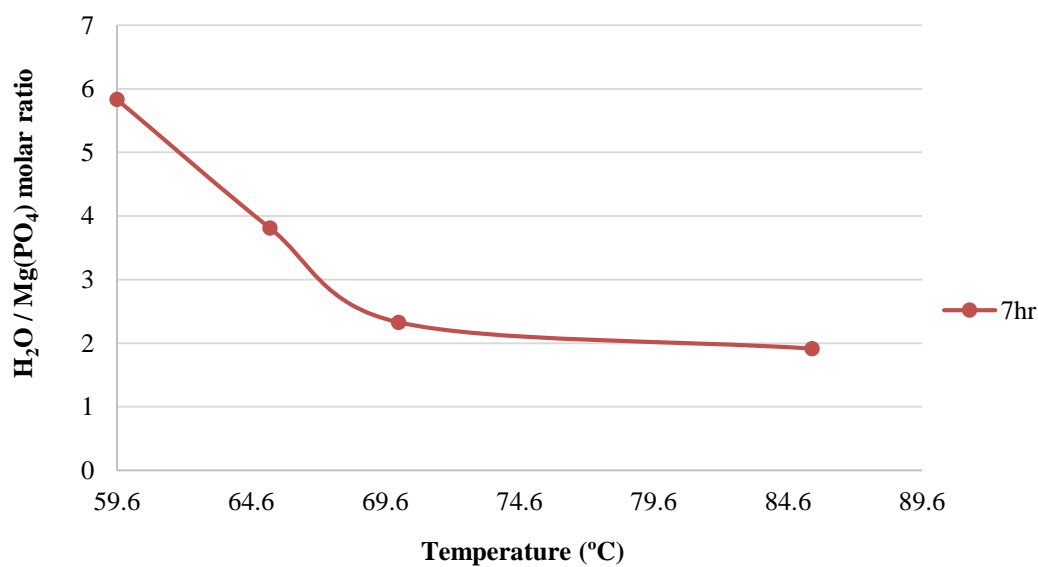


Figure 5.7 H₂O molar ratio with respect to Mg (PO₄) after 7 hours duration of heating at different temperatures

The higher temperatures caused rapid thermal decomposition of struvite, accompanied by a greater release of ammonia and water from the struvite solid phase. The ammonia and water removal rates

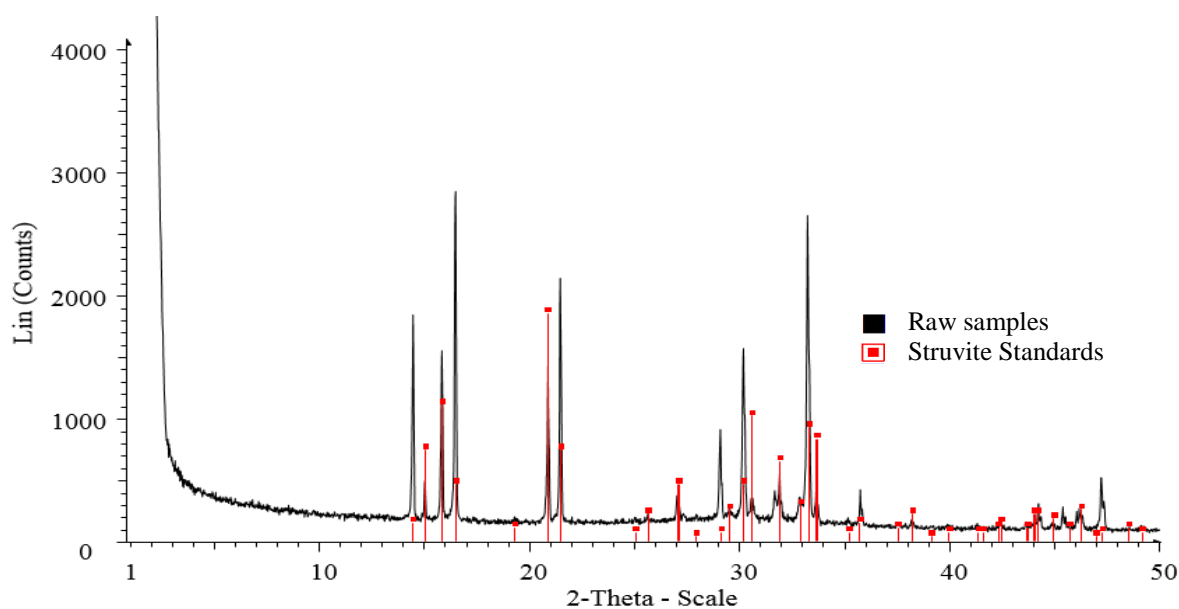
were found to be initially high and subsequently followed a decreasing trend up to 70.1°C within 7 hours of heat treatment, whereas the removal rate was slower at temperatures above 70.1°C. There was no significant difference in ammonia and water removal rates at temperatures between 70.1°C and 85.5°C and the decomposed solid phase contained 30-40% ammonia. Considering the residual ammonia and lower crystalline water content, it can be concluded that the layered structure might have formed during thermal decomposition of struvite.

5.1.2.2.2 XRD results

Figure 5.8 represents XRD results obtained from synthetic struvite, when oven dried at temperatures of 65.3°C and 85.5°C for 7 hours. The XRD was performed on all of the freshly heated struvite samples, in order to observe the formation of a layered structure with the increasing temperature, at that particular time (Appendix B.3).

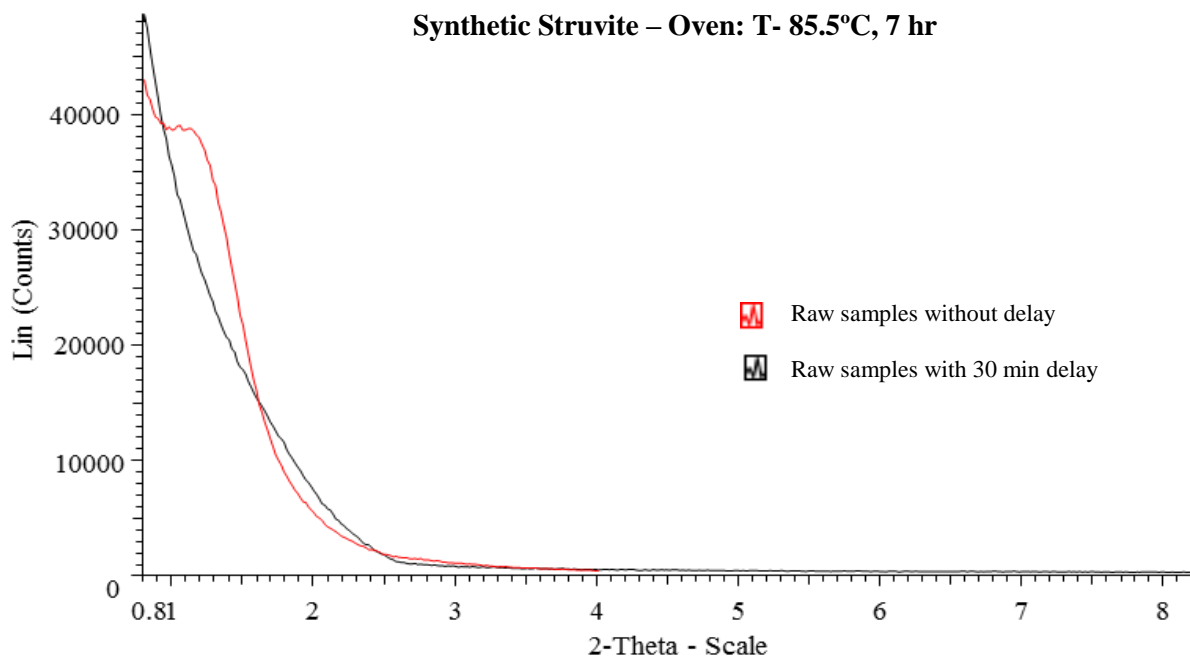
Figure 5.8 (a) shows that the struvite solid phase decomposed at 65.3°C for 7 hours contained only struvite peaks; no peaks of layered structure were observed along with struvite. Moreover, other struvite samples decomposed at temperatures below 85.5°C also showed no peaks of layered structure, while performing low angle XRD (Appendix B.3). Conversely, in Figure 5.8 (b), the layered structure peak was observed at low angles in the struvite samples decomposed at 85.5°C for 7 hours, when the XRD was performed on the instantly prepared samples without delay. However, the layered structure peak disappeared when the same sample was exposed to the atmosphere for 30 minutes prior to initializing the instrument (similar to the struvite sample decomposed at temperature 60.5°C for 24 hours (Figure 5.5)). The disappearance of the layered structure peak, after exposure to the atmosphere, indicates the instability of a layered structure exposed to the atmosphere. Therefore, it can be speculated that a layered structure might have formed at temperatures other than 85.5°C during 7 hours of heating (which was very unstable under atmospheric exposure). The instability of the layered structure under atmospheric exposure caused the rapid disappearance of layered structure peak, due to moisture absorption. Hence, only struvite peaks were detected in the decomposed samples under the XRD, instead of a layered structure peak along with struvite.

Synthetic Struvite – Oven: T- 65.3°C, 7 hr

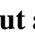



(a)

Synthetic Struvite – Oven: T- 85.5°C, 7 hr



(b)

Figure 5.8 X-ray diffraction patterns of synthetic struvite decomposed for 7 hours at (a) 65.3°C (b) 85.5°C;  XRD performed on the samples without any delay,  XRD performed on the samples after 30 minutes exposure to the atmosphere

The XRD results for the struvite sample decomposed at 65.3°C for 7 hours showed a struvite structure despite losing around 27% ammonia upon decomposition. It is well-known that the crystalline lattice of struvite compounds, $\text{MgNH}_4\text{PO}_4 \cdot 6\text{H}_2\text{O}$ consists of PO_4 tetrahedral and $\text{Mg}(\text{H}_2\text{O})_6$ octahedral, connected together by hydrogen bonds, with NH_4^+ inside the lattice (Whitaker and Jeffery, 1970; Banks et al., 1975; Abbona and Boistelle, 1979; Ferraris, 1986). The integrity of the struvite structure is based on magnesium, phosphate and water, instead of ammonia. The ammonium ion in the struvite structure remains loose and thus, can easily release upon heating at lower temperatures without causing any damage to the struvite structure.

Figure 5.9 indicates the combined XRD results obtained from the struvite samples decomposed at 59.6°C, 65.3°C, 70.1°C and 85.5°C for 7 hours. Figure 5.9 (a) shows the peaks present in the decomposed solid sample, after running XRD from the lowest to the highest angles, whereas Figure 5.9 (b) represents the enlarged view of the peaks formed at low scanning angles.

An increase in struvite drying temperature caused decreases in struvite peak intensity in the decomposed product and caused the transformation of crystalline struvite structure into an amorphous structure. The struvite peak was prominent in the decomposed struvite sample heated at 59.6°C for 7 hours, as shown in Figure 5.9 (a). The intensities of the struvite peaks in the residual solid phase, decomposed at 59.6°C for 7 hours, were similar to those of the initial samples, since the ammonia and water removal rates were insignificant (Figure 5.6 and 5.7). However, the struvite structure transformed into an amorphous structure after heating at temperature 85.5°C for 7 hours, whereas between 59.6°C and 85.5°C, the residual solid phase was a mixture of a crystalline and an amorphous structure. Figure 5.9 (b), shows that, during XRD, the shoulder of the sample decomposed at 59.6°C coincided with the shoulder of initial raw struvite samples. The increase in temperature above 59.6°C caused an increase in water removal rate from the struvite structure and also an increase in shoulder movement away from initial position.

The movement of the shoulder was maximal at 85.5°C, followed by 70.1°C and 65.3°C after 7 hours of heating. The shoulder movement has also been observed in the struvite samples decomposed at 61.5°C (Figure 5.4, b), where the formation of a layered structure was confirmed.

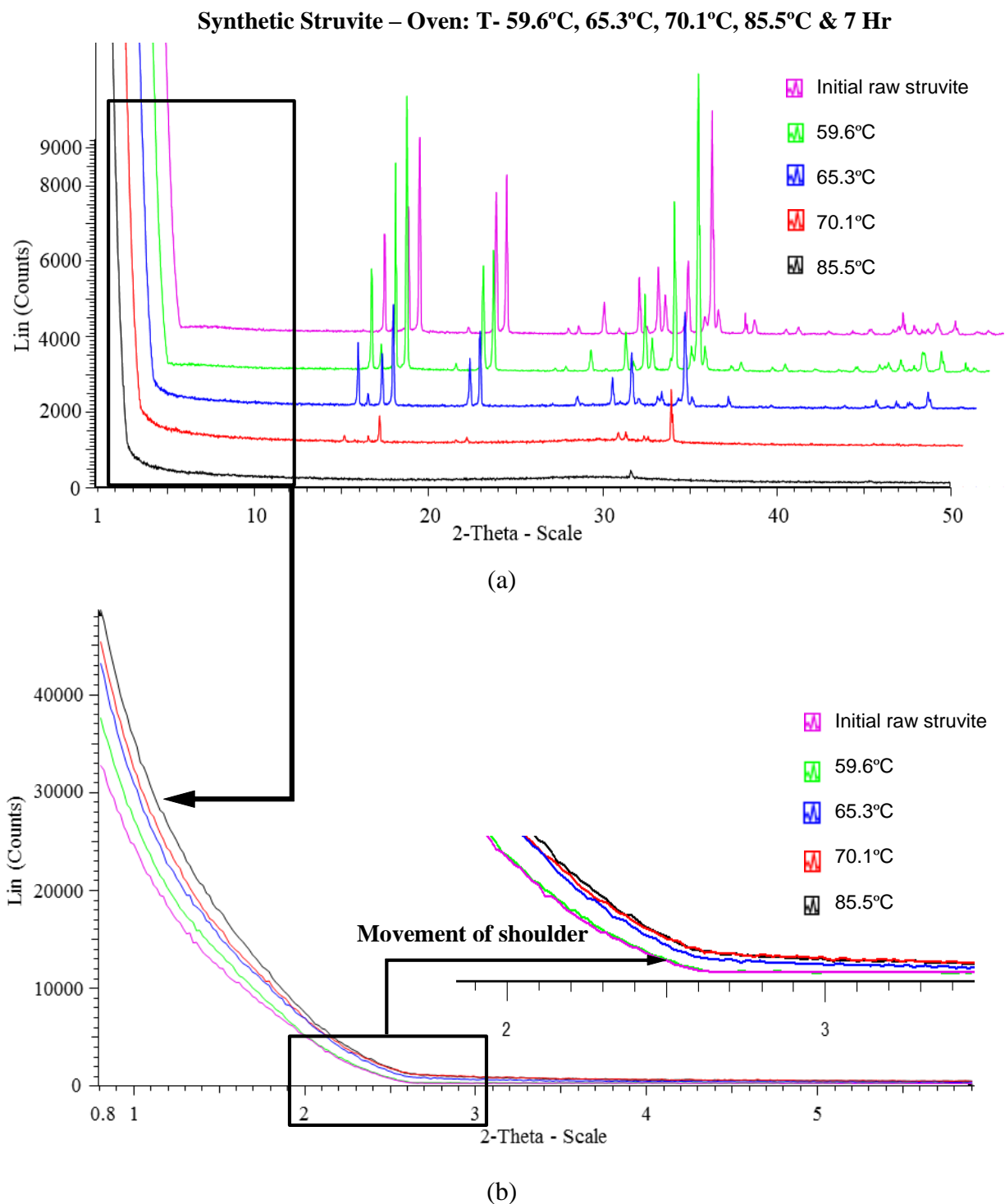


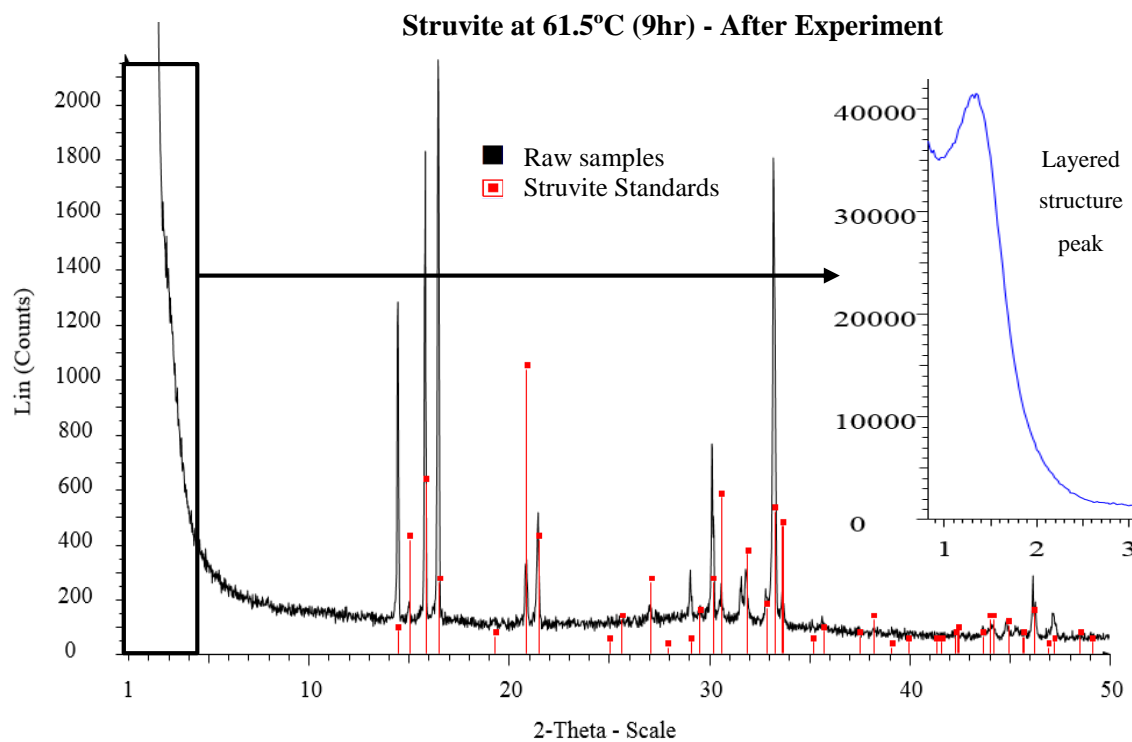
Figure 5.9 X-ray diffraction patterns of synthetic struvite decomposed for 7 hours at different temperatures (a) scanning angle 0.8 to 50 degree (b) enlarged view of scanning angle 0.8 to 12 degree

The XRD results obtained from samples decomposed at 61.5°C for 1 to 24 hours, show that the shoulder movement was not significant up to 5 hours, where no layered structure peak was observed. The movement of the shoulder increased with the increase in intensity of layered structure peak and reached the farthest point at 24 hours, when the layered structure peak reached its highest intensity. It is evident that the movement of the shoulder of the decomposed samples is associated with formation of a dominant layered structure. Therefore, the formation of a peak at low angles, along with movement of the shoulder from its initial position, can confirm the presence of a layered structure in the decomposed struvite samples. In this experiment, considering the movement of the shoulder from XRD results, and the presence of high residual ammonia and low crystalline water content from chemical analysis, it can be confidently speculated that the layered structure might have started forming at temperatures above 59.6°C, which was finally visible at a temperature 85.5°C (Figure 5.8, b).

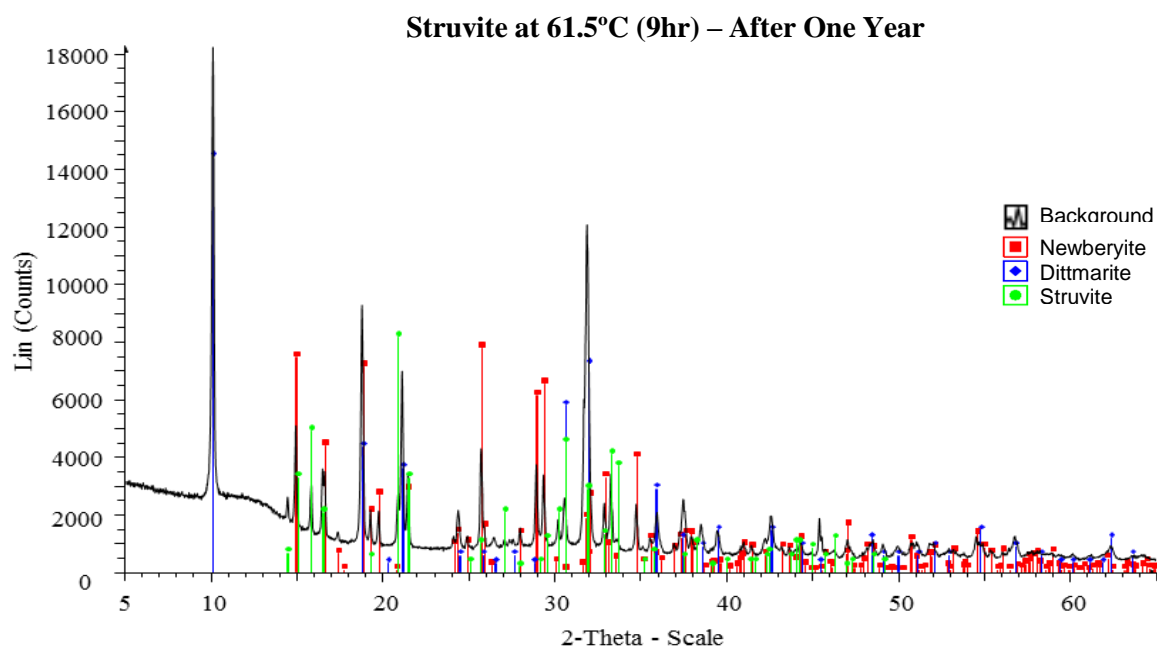
5.1.2.3 Layered structure transformation over time

The layered structure peak was more pronounced and stable in the struvite samples heated at 61.5°C, than at 60.5°C, even after exposure to the atmosphere. Therefore, it is speculated that the layered structure might have started forming at temperatures around $60.5 \pm 0.5^\circ\text{C}$ and became unstable, as the layered structure peak disappeared when exposed to the atmosphere.

Based on the instability of the layered structure, it is speculated that the layered structure may transform into a more organized structure over time through moisture absorption and structural reorganization. In order to investigate this possibility, XRD was performed after one year on the same struvite samples, which were decomposed at 61.5°C for 9, 16 and 24 hours under the oven dry method (Appendix B.2), where pronounced layered structure peaks were observed. Figure 5.10 (a, b) shows a comparison of the XRD patterns of the decomposed sample at 61.5°C right after the experiment and after one year. In Figure 5.10 (b), the XRD results confirmed the presence of dittmarite and newberyite, along with struvite, in the samples which were decomposed one year before, at a temperature of 61.5°C for 9 hours. The same samples had contained only a layered structure, along with struvite when XRD was performed on the decomposed samples one year earlier, without any delay (as shown in Figure 5.10, a).



(a)



(b)

Figure 5.10 X-ray diffraction patterns of synthetic struvite decomposed at 61.5°C (a) after one day of heat treatment (b) after one year of heat treatment

No presence of dittmarite and newberyite substances were found when the XRD was performed on the struvite samples freshly heated at 61.5°C (Figure 5.4). It might be concluded that freshly heated struvite samples absorb moisture over time and reorganize in such a way that the portion of layered structure containing ammonia transforms into dittmarite; whereas, the position of the layered structure, devoid of ammonia, transforms into newberyite. The portion of struvite substance remained unchanged.

It was clear from the previous discussion that, when decomposed samples were stored over time, a structural transformation may have occurred within the decomposed product. To further investigate this concept, a number of synthetic struvite samples were heated above 61.5°C and stored in a desiccator. Table 5.1 shows the XRD results performed after 3 months, to observe what, if any, structural transformations took place.

Table 5.1 XRD results of the decomposed oven dry samples after three months

Synthetic Struvite		Struvite	Newberyite	Dittmarite
Temperature, (°C)	Duration of Heating, (hours)			
62.5°C	3	+	+	+
	6			
	9			
	16	-	+	+
	24			
66.2°C	5	+	+	+
71.1°C	1	+	-	+
	3	-	+	+
	9			

+ refers to detected compound, - refers to non-detected compound

When struvite was heated at temperatures above 61.5°C to 71.1 for 3 hours or more, the decomposed sample contained dittmarite, along with newberyite. On the other hand, the decomposed sample heated at 71.1°C for 1 hour contained dittmarite, along with struvite. The heating period of one hour was insufficient for ammonia removal and hence, no newberyite was observed. However, no peak for a 2D amorphous layered structure was found in any of the decomposed samples, similar to the XRD results obtained from the one-year old decomposed

sample heated at 61.5°C (5.10, b). This indicates that a layered structure may have formed initially when the struvite samples were heated at temperatures above 61.5°C, but over time, the layered structure reorganized and transformed into dittmarite.

Sugiyama et al. (2005) mentioned the formation of dittmarite upon heating of struvite at 100-150°C. The amorphous 2D layered structure might have formed in the dried struvite samples heated at that temperature range and transformed into dittmarite over time. In order to observe the formation of a layered structure, the low angle XRD needed to be performed on the freshly heated, decomposed sample. Otherwise, the unorganized and chaotic 2D amorphous layered structure will absorb moisture and eventually transform into more organized 3D crystalline layered structure, which is dittmarite. Thus, it appears that the previous researchers have found the dittmarite compound in the decomposed struvite samples, instead of any 2D amorphous layered structure.

5.1.2.4 Ammonia entrapment in a layered structure

The reason behind a lack of ammonia removal from the struvite structure obtained from chemical results can be explained from the XRD results, where a layered structure formation was confirmed. Based on chemical analysis and XRD results, the intensity of the layered structure peak increased with the decrease in ammonia and water content from the struvite structure, which also occurred in turn with the increase in heating duration. The residual solid phase obtained from struvite thermal decomposition at 61.5°C contained a 2D amorphous layered structure along with a struvite structure (Figure 5.4), depending on heating duration. In the XRD results, it was observed that the intensity of a layered structure peak became pronounced, while the majority of the crystalline struvite structure was transforming into an amorphous 2D layered structure. The layered structure peak appeared at low angles, after performing struvite thermal decomposition at 61.5°C for 7 hours, after which the residual ammonia was around 67%. The ammonia gas evolution continued at a slower rate, as long as the struvite compound was present along with a layered structure. Any further increase in heating duration up to 24 hours at 61.5°C, caused a further decrease in 34% ammonia content in the decomposed samples. The enhanced formation of a layered structure lowered the ammonia and water evolution rate from the struvite structure, when thermal decomposition of struvite continued beyond 7 hours heating duration. A comparison of chemical

analysis (Figure 5.2 and Figure 5.3) with the XRD results (Figure 5.4) indicate that the struvite structure completely transformed into a 2D amorphous structure layered structure, when the water content declined to 1.3 molecules after 24 hours of heating at 61.5°C. The complete transformation of struvite into an amorphous 2D layered structure inhibited the residual 33% ammonia evolution from the struvite structure. Therefore, it can be said that the ammonia gas evolution ceased when the structure completely transformed into a layered structure. The residual ammonia was entrapped inside the layers of magnesium and phosphate, and cannot be removed without collapsing the entire structure.

The water molecules in the struvite structure are responsible for hydrogen bonding and are included in the formation of a unit cell frame; any excessive removal can cause severe damage to the structure and the entire structure may collapse. Moreover, the magnesium atoms present in the struvite structure have a strong affinity towards oxygen, provided by six water molecules of crystallization before thermal decomposition. The excessive release of water due to thermal decomposition forced the phosphate to share the oxygen with magnesium atoms, in order to maintain the magnesium coordination number of 6. Therefore, a very packed, layered structure forms with ammonia in between the layers of magnesium and phosphate. Therefore, the only way to remove the ammonia completely from the struvite structure is to decompose struvite at temperatures above 200°C, where it transforms into magnesium pyrophosphate salt through the release of both water of crystallization, as well as water of constitution. Therefore, it is inferred that high temperatures (<100°C) and prolonged durations of heating (24 hours) were insufficient for complete removal of ammonia from struvite pellets, due to the formation of a 2D amorphous layered structure; this further impedes ammonia evolution belonging to the layered structure.

5.1.2.5 Subsequent heating and rehydration

Ammonia entrapment in the layered structure, and how it prevents the complete transformation struvite to newberyite, have been discussed in the previous section. However, it was also noticed in oven dry experiments that the instability of a layered structure induced from moisture absorption, after being exposed to the atmosphere, caused a disappearance of the layered structure peak in the samples decomposed at 60.5°C for 24 hours (Figure 5.5) and 85.5°C for 7 hours (Figure

5.8, b). Therefore, it was hypothesised that the disappearance of a layered structure, upon rehydration, can increase the ammonia removal efficiency through subsequent heating and rehydration processes. Therefore, the synthetic struvite sample was subsequently heated and rehydrated three times, in order to observe any increase in ammonia removal efficiency. Chemical analysis for the nitrogen and water content of the struvite samples, heated for 24 hours at 60.5°C and subsequently rehydrated with atmospheric moisture, are shown in Figure 5.11 and Figure 5.12.

The N:P content in the raw struvite samples was around 0.9 which decreased to around 0.5 after 24 hours of heating at 60.5°C. There was a small difference in the nitrogen content between the heated and rehydrated struvite samples. The 2 hour rehydrated sample was heated a 2nd time at the same temperature, for 24 hours, resulting in 20% more reduction of ammonia from the previously decomposed sample. There was 30% ammonia left in the struvite structure and the corresponding water content was around 1.8 molecules, which is similar to the struvite samples decomposed at 61.5°C (where a layered structure formation was confirmed). The nitrogen content decreased further to 20%, when the 2 week old rehydrated sample was heated for a 3rd time at 60.5°C, for 24 hours. It was inferred that complete ammonia removal was not possible, due to the formation of a layered structure during the oven dry process. When heating the sample for the 2nd and 3rd times, ammonia that was released from the structure obviously belongs to the struvite structure, rather than the layered structure, and the corresponding water content was similar to the previous oven dry experiment (where the presence of a layered structure was observed).

Therefore, it can be said that subsequent heating and rehydration can increase the extent of ammonia removal up to a certain point, but cannot completely remove all the ammonia, due to the formation of a layered structure during each heating period; it cannot be eliminated upon rehydration. It is believed that subsequent dehydration facilitated the formation of a layered structure, which might have transformed into a more organized layered structure over time (such as dittmarite). Considering all the experiments performed on synthetic struvite samples using the oven dry process, it is evident that complete ammonia removal from the struvite sample cannot be achieved (a) at higher temperatures with prolonged heating durations or (b) following subsequent heating and rehydration. The formation of a layered structure is found to be inevitable through the oven dry process.

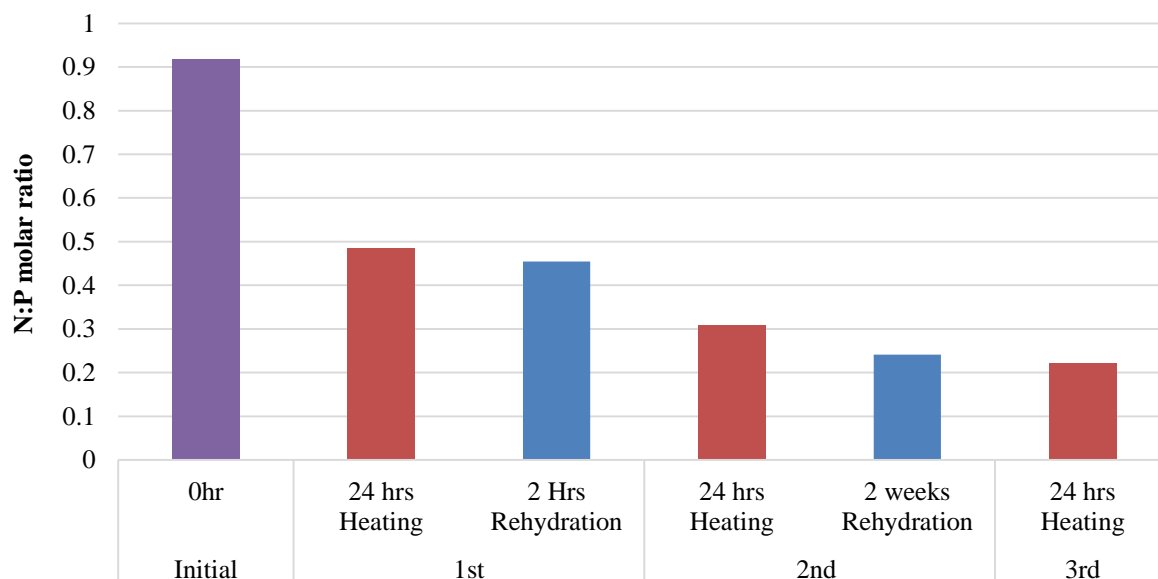


Figure 5.11 N:P molar ratio of synthetic struvite that undergone subsequent heating at 60.5°C followed by rehydration

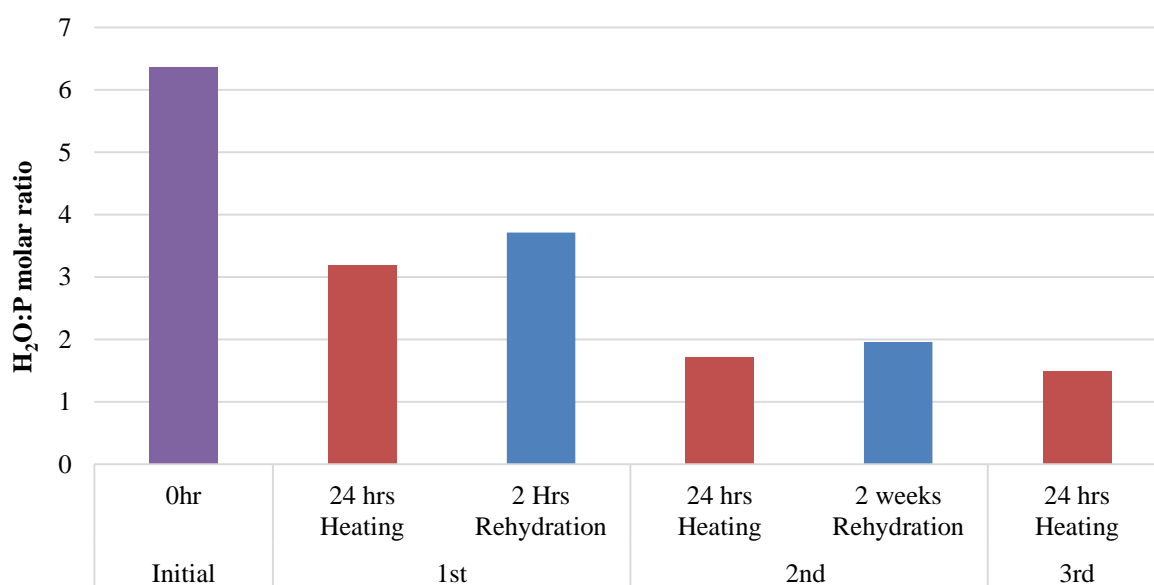


Figure 5.12 H₂O:P molar ratio of synthetic struvite that undergone subsequent heating at 60.5°C followed by rehydration

5.2 Bench-scale experiments with humid air

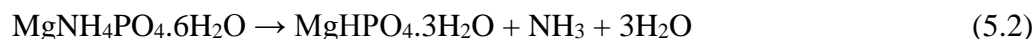
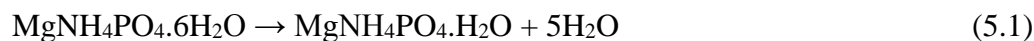
The excessive water removal from the struvite structure (>3 water moles per mole of PO_4), through the oven dry method, led to the formation of a layered structure (confirmed by XRD results). Ammonia was trapped in the compacted layered structure and could not be removed completely, without collapsing the entire structure. In order to accomplish complete ammonia removal from struvite, the formation of a layered structure, including both dittmarite and an amorphous 2D layered structure, must be prevented in the decomposed solid phase.

To prevent layered structure formation, the excess removal of water of crystallization from the struvite structure, causing dehydration, must be prevented. The presence of higher residual water of crystallization in the decomposed struvite sample should prevent the structure from being compacted, so that ammonia can escape easily. The following section briefly reviews the previous studies in which the influencing parameters for preventing dehydration, while performing thermal decomposition of different magnesium phosphate compounds, were investigated.

5.2.1 Background

5.2.1.1 Influence of humidity on dehydration of magnesium phosphate compounds

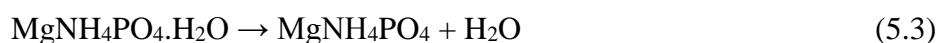
The composition of the solid phase obtained from struvite thermal decomposition depends on the extent of ammonia and water removal from the struvite structure. Excessive water removal, without any ammonia evolution, leads to the formation of dittmarite, as per Equation (5.1). However, the complete release of ammonia, with a controlled release of water, can lead to the formation of newberyite (see Equation 5.2).



In order to prevent the formation of dittmarite type compounds (5.1) and facilitate the formation of newberyite (5.2), the water vapour evolution needs to be minimized. This can be achieved by

providing high water vapour pressure during the struvite decomposition process. Following Le Chatelier's principle, a controlled release of a reaction product can be achieved by altering the surrounding atmospheric conditions, using the other reaction product (which is water in this case). Therefore, if evolution of water can be controlled in Equation (5.1) through altering the surrounding atmospheric conditions, the equilibrium will shift backward, a new equilibrium will be established, and newberyite may form, as per equation (5.2). Therefore, the hypothesis was that struvite decomposition under open atmosphere, with high water vapour pressure, could lead to the formation of newberyite through the continuous release of ammonia from the structure, at high temperatures, in a fluidized bed reactor.

Pysiak et al. (1993), performed experiments on $\text{NH}_4\text{M}^{\text{II}}\text{PO}_4$ (where M^{II} is Mg, Mn, Co, Cu) in air, in a vacuum, and in the atmosphere containing gaseous reaction products (water vapour and ammonia). They wanted to provide conclusive information on the subsequent transformation of $\text{NH}_4\text{M}^{\text{II}}\text{PO}_4$, under the influence of isothermal and non-isothermal heat treatments, under different atmospheric conditions. The transformation process of $\text{MgNH}_4\text{PO}_4 \cdot \text{H}_2\text{O}$ (dittmarite) into several different compounds, upon heat treatment, is necessary to understand in order to perceive the influence of surrounding atmospheric conditions on the final decomposition product. During heating of $\text{MgNH}_4\text{PO}_4 \cdot \text{H}_2\text{O}$, a crystalline or amorphous salt forms when the water of crystallization evolves from the structure, as per Equation (5.3). Further heat treatment causes the formation of an acid salt (MgHPO_4) through the evolution of ammonia gas (Equation 5.4). After, this acid salt (MgHPO_4) transforms into magnesium pyrophosphate, when the water of constitution evolves from the structure (Equation 5.5).



When $\text{MgNH}_4\text{PO}_4 \cdot \text{H}_2\text{O}$ is heated in an atmosphere containing gaseous ammonia, reaction (5.3) governs and causes the formation of MgNH_4PO_4 , due to the loss of water of crystallization. This event suppresses Equation (5.4) through inhibition of ammonia gas evolution (Pysiak et al., 1993). The aforementioned researchers note that the final product of the equations depends on the initial

composition of the material, their degree of dispersion, heating rate, heating duration, the surrounding atmospheric conditions and other factors. These factors can alter the end product of the equations and therefore, Equations (5.3-5.5) may replace each other.

These authors also reported that, during heating of $\text{NH}_4\text{CoPO}_4 \cdot \text{H}_2\text{O}$ in the atmosphere containing gaseous ammonia with pressure $P_{\text{NH}_3} > 40\text{-}50$ hPa, the water of crystallization evolved from the structure, without any loss of ammonia. A simultaneous evolution of ammonia and water vapour occurred when the thermal decomposition was performed under vacuum conditions. The ammonia evolution was more significant compared to water of crystallization, when $\text{NH}_4\text{CoPO}_4 \cdot \text{H}_2\text{O}$ was heated in an atmosphere of water vapour ($P_{\text{H}_2\text{O}} = 20$ hPa), at temperatures lower than 150°C . Therefore, during heat treatment of other magnesium phosphates, the rate of dehydration and ammonia evolution can be controlled by altering the surrounding atmospheric condition via changing the composition and pressure of the atmosphere.

Samuskevich and Lukyanchenko (1998) investigated the chemical and phase transformations of magnesium di-hydrogen-phosphate tetrahydrate ($\text{Mg}(\text{H}_2\text{PO}_4)_2 \cdot 4\text{H}_2\text{O}$) during its iso-thermal and non-isothermal heating in vacuum, water-vapour atmosphere (when $P_{\text{H}_2\text{O}}$ values were fixed) and in air (at a controlled relative humidity) using crystalline samples. $\text{Mg}(\text{H}_2\text{PO}_4)_2 \cdot 4\text{H}_2\text{O}$ was thermally decomposed at a temperature of 60°C in water vapour atmosphere (5hPa), air with 0% and 25% humidity; the corresponding loss of water molecules is shown in Figure 5.13.

It is evident that the evolution of water molecules decreased from 2.5 moles to 1.5 moles, after increasing the relative humidity from 0 to 25% when decomposing at 60°C for 2 hours. Therefore, it was inferred that the expulsion or evolution of excessive water moles from the structure can be prevented or minimized, by increasing the air humidity during thermal decomposition.

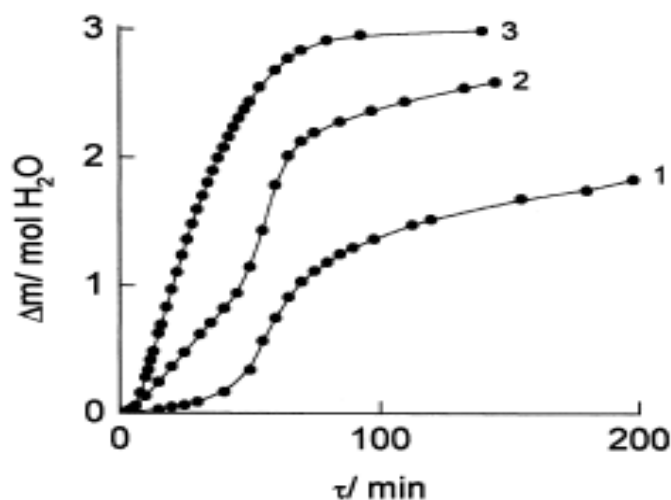


Figure 5.13 The kinetic curves of $\text{Mg}(\text{H}_2\text{PO}_4)_2 \cdot 4\text{H}_2\text{O}$ upon dehydration (1) in air at relative humidity $\text{RH} = 25\%$ (Samuskevich and Lukyanenko, 1998), (2) in air at relative humidity $\text{RH} = 0\%$ and (3) in water vapour atmosphere at $p_{\text{H}_2\text{O}} = 5 \text{ hPa}$

5.2.1.2 Finding operating range for struvite decomposition

In order to prevent dittmarite formation, the struvite thermal decomposition must be performed in such a way that the surrounding water vapour pressure is higher than the equilibrium water vapour pressure, at the surface of struvite crystal at a given temperature. Kiehl and Hardt (1933) performed a study on different magnesium phosphates, to identify the dissociation pressure during transition of orthophosphate to pyrophosphate, upon ignition. A static method was used in order to measure the dissociation pressure. The authors determined the dissociation pressure for the system struvite-dittmarite-newberyite- H_2O - NH_3 . They noted that, at lower temperatures, there was no ammonia gas evolution observed in this system. Therefore, Figure 5.14 can be safely assumed to be the equilibrium water vapour pressure for struvite (up to 60°C) and dittmarite (above 60°C , up to the highest temperature values applied in this study).

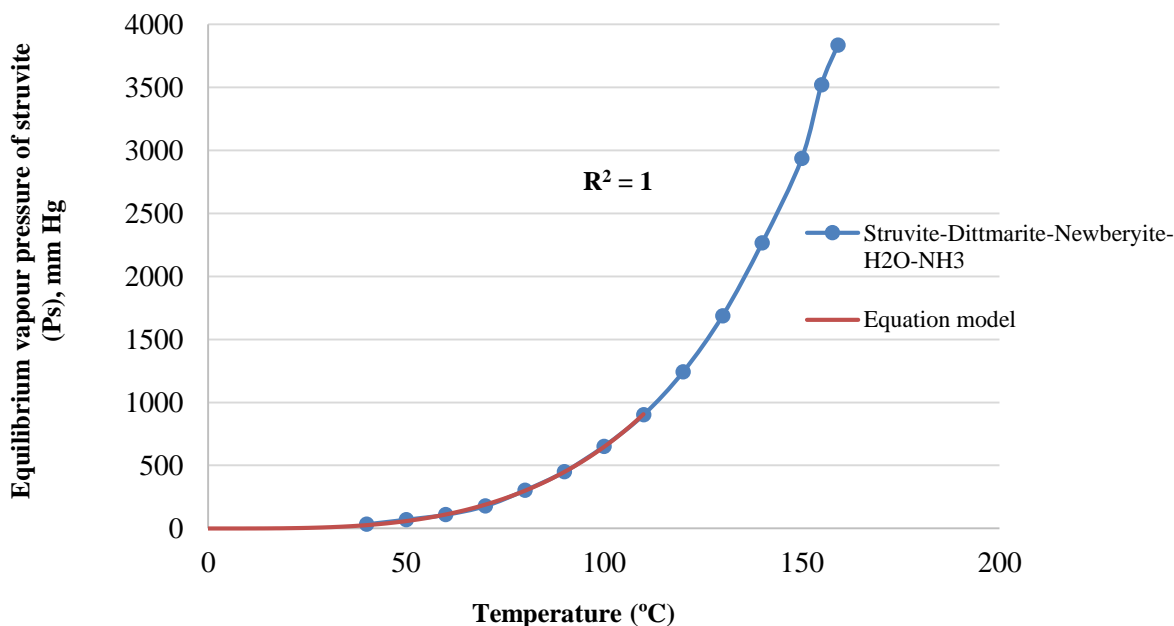


Figure 5.14 Dissociation pressure of struvite-dittmarite-newberyite- $\text{H}_2\text{O-NH}_3$ and the equation model at different temperatures (Kiehl and Hardt, 1933)

The dissociation pressure for the system of struvite-dittmarite-newberyite- $\text{H}_2\text{O-NH}_3$ has been plotted over temperature (Figure 5.14) and the corresponding Equation Model (5.6) was found, through curve fitting, where the R^2 value is unity.

$$y = (a+bx+cx^2+dx^3+ex^4)^2 \quad (5.6)$$

Where,

y = Equilibrium vapour pressure of struvite (mm Hg)

x = Temperature (°C)

a, b, c, d, e = Curve fitting equation constants

a = 1.85E-06; b = 0.000103; c = 0.003985; d = -2.25E-05; e = 8.13E-08

From Figure 5.14, it can be seen that the dissociation pressure of struvite-dittmarite-newberyite- $\text{H}_2\text{O-NH}_3$ overlaps with the dissociation pressure obtained from the equation model. This validates the equation and can be used to measure the struvite equilibrium pressure at any temperature, within the range of this study.

The layered structure formation can be prevented, as long as the water of hydration is retained in the struvite structure. Therefore, to prevent dehydration, steam must be provided to increase the water vapour pressure surrounding the struvite, in such a way that the driving force for dehydration and condensation will remain negative throughout the experiment (which was shown in the Equations 5.7 and 5.8).

$$\text{To prevent Dehydration, } \Delta P = P_s - P_{H_2O} \text{ (negative)} \quad (5.7)$$

$$\text{To prevent Condensation, } \Delta P = P_{H_2O} - P^*_{H_2O} \text{ (negative)} \quad (5.8)$$

Where,

P_s = Struvite equilibrium vapour pressure

P_{H_2O} = Surrounding equilibrium water vapour pressure

$P^*_{H_2O}$ = Saturated water vapour pressure

The negative driving force of dehydration (5.7) and condensation (5.8) will prevent excessive water removal from the struvite structure and partial struvite dissolution in the reactor respectively. The minimum relative humidity below which dehydration could occur has been calculated using the following Equation (5.9).

$$RH_{\min} = \frac{\text{Equilibrium vapor pressure of struvite}(P_s)}{\text{Saturated water vapor pressure}(P_w^*)} \times 100\% \quad (5.9)$$

Saturated water vapour pressure depends on temperature; as the temperature increases, the saturated water vapour pressure increases. At 100% relative humidity, the surrounding water vapour pressure is equal to the saturated or equilibrium water vapour pressure. Dehydration will occur if the surrounding water vapour pressure is lower than the struvite equilibrium vapour pressure, whereas condensation will take place when the surrounding water vapour pressure reaches the saturated water vapour pressure. The minimum relative humidity, at different temperatures, has been calculated using Equation (5.9). The obtained operating range for struvite thermal decomposition, with respect to temperature and relative humidity, is presented in Figure 5.15 (which was used in the bench-scale experiments).

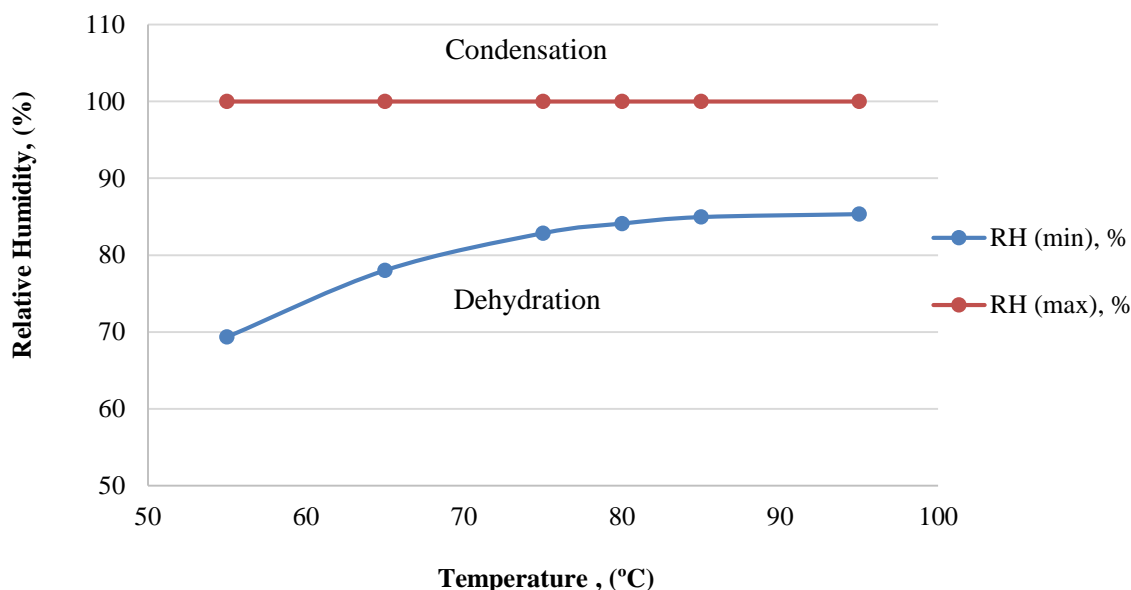


Figure 5.15 Operating temperature and relative humidity for struvite thermal decomposition

From Figure 5.15, it can be seen that, thermal decomposition of struvite can be performed within broader ranges of relative humidity, at lower temperatures, compared to higher temperatures, thus inhibiting the formation of dittmarite. It can be expected that formation of a layered structure can be prevented, if the operating relative humidity is varied between the maximum and minimum relative humidities at the corresponding temperature. For instance, theoretically, dittmarite formation could be prevented at 80°C heating temperature, if the relative humidity is maintained between 80% and 100% (Figure 5.15). Dehydration might occur when the relative humidity decreases below the minimum relative humidity, at a particular temperature. On the other hand, condensation might take place when the relative humidity exceeds the maximum relative humidity limit at 100%.

The presented technology for ammonia recovery relies on the decomposition of struvite to newberyite, without forming a transitional phase of dittmarite or any other layered structure. According to Kiehl and Hardt (1933), struvite to dittmarite transformation occurs below 60°C and ammonia starts to evolve above 60°C. It was also reported that dittmarite may form at temperatures above 90°C (Paulik and Paulik, 1975a; 1975b). Previous researchers have claimed that struvite rapidly decomposes at temperatures between 85 °C and 115 °C (Frost et al., 2004; Bhuiyan et al.,

2008b) where the thermal stability of dittmarite has been observed. Novotny (2011) performed isothermal heat treatment on commercially produced pellets and reported 60°C-80°C, as the temperature range for struvite thermal decomposition. Therefore, a temperature range of 65°C-85°C was selected in this study, to avoid the formation of dittmarite during thermal decomposition of struvite.

The corresponding minimum relative humidity for the decomposition temperature 65°C to 85°C ranged between 80% and 85%, according to Figure 5.15. Therefore, considering the minimum and maximum relative humidity range, as well as high energy consumption from steam incorporation, the experimental relative humidity range was selected to be between 65% and 100%. Furthermore, in order to increase the ammonia removal efficiency, struvite thermal decomposition must be performed in the fluidized bed reactor (FBR), thus increasing the mass and heat transfer throughout the experiment.

5.2.2 Hypotheses and specific objectives

The main purpose of the bench-scale experiments was to prevent dehydration, thus leading to the formation of a layered structure including both dittmarite and a 2D amorphous layered structure. The bench-scale experiments were performed to answer the following questions:

- Can the limitations and experimental factors that prohibit the complete transformation of struvite to newberyite, in the oven dry process, be overcome?
- Can the formation of the layered structure be prevented? Is the hypothesis that high humidity prevents layered structure formation supported?
- Is it possible to remove all of the ammonia from struvite, after incorporating hot air and steam, and if so, what is the optimum temperature and relative humidity corresponding to 100% ammonia removal and struvite to newberyite transformation?
- What are the possible operating conditions for dittmarite formation?
- How does the ammonia removal efficiency vary with different sizes and sources of struvite pellets, and what are the characteristics in terms of size, source, and hardness that correspond to maximum ammonia removal?

- What are the effects of relative humidity on layered structure formation, at a given temperature?

Hypotheses

- Dehydration can lead to the formation of a layered structure including dittmarite or an amorphous 2D layered structure. This can be prevented by introducing steam and suppressing water from leaving the struvite structure.
- Higher water vapour pressure surrounding the struvite will impede excess release of water of crystallization from struvite, thereby retaining it as a crystalline structure. The continuous flow of hot air and steam will facilitate NH_3 removal from the surface of struvite crystals. The fluidized bed reactor (FBR) will also increase mass and heat transfer.
- Incorporation of steam, with hot air, can replace the NH_3 with H_2O and may cause formation of phosphorrosslerite ($\text{MgHPO}_4 \cdot 7\text{H}_2\text{O}$) or newberyite $\text{MgHPO}_4 \cdot 3\text{H}_2\text{O}$.
- Different sources and sizes of pellets can have different ammonia removal efficiencies, due to their differing struvite morphologies, porosities, compactness and hardness.

5.2.3 Results and discussion of bench-scale experiments

5.2.3.1 Identifying optimum condition with respect to temperature and relative humidity

The initial ammonia and water contents in the Lulu Island struvite pellets were around 0.9 and 6.5 mole per 1 mole of $\text{Mg}(\text{PO}_4)$, respectively, but depended on the surrounding atmospheric conditions such as humidity. A higher water content could indicate either moisture entrapment in the struvite pellets or the presence of impurities such as Fe, Al, Ca that might have been considered as water during mass balance calculation (Fattah, 2010). On the other hand, a lower ammonia content could result from surrounding dry atmospheric conditions (Cohen and Ribbe, 1966; Whitaker, 1968; Ribbe, 1969). The effects of temperature, relative humidity and duration of heating on the ammonia removal efficiency in the bench-scale setup are discussed in the following sections.

5.2.3.1.1 Effects of temperature on rate and efficiency of ammonia removal

Figure 5.16 and Figure 5.17 present the residual ammonia and water contents in the decomposed solid samples, when the Lulu Island pellets (<1mm) were heated at different combinations of temperature and relative humidity (RH), for 2 and 4 hours. The bar charts at three different relative humidities, with increasing temperature, have been organized to show the effects of temperature on ammonia removal efficiency, at each relative humidity. In the bench-scale experiments, humidity in the diffuser was manually monitored and adjusted as needed, to maintain the desired experimental conditions. However, fluctuation of the relative humidity ($\pm 8\%$) inside the diffuser was unavoidable. This fluctuating operating condition is referred to as an “unstable regime” in this study. The results presented for 2 and 4 hours duration in Figures 5.16 and Figure 5.17 were generated under an “unstable regime”. A better control of relative humidity ($\pm 3\%$) was achieved later and a few experiments were repeated and presented with the same results as “2 Hr Repeat”. This controlled condition is noted as “stable regime”.

In general, the higher the temperature, the greater the ammonia removal achieved at each humidity, and a significant amount of water evolved from the structure. According to Figure 5.16, maximum ammonia removal was achieved at 85°C, followed by 80°C, 75°C and 65°C, for any particular humidity and duration of heating. For a particular humidity, the ammonia removal efficiency increased with increasing temperature. For example, at 95% RH and 2 hours of heating, the ammonia removal efficiency was 50%, 85%, 87% and 95% at temperatures 65°C, 75°C, 80°C and 85°C, respectively.

However, struvite decomposition performed under higher temperatures, with lower humidity, reduced the ammonia removal efficiency. Figure 5.16 shows that, with 2 hours of heating at 85°C under a “stable regime”, around 100% ammonia removal can be achieved at 95% RH, as opposed to 70% ammonia removed with 65% RH, after 2 hours of heating. The residual water content was found to be exactly 3 moles at 85°C, after 2 hours of heating with 95% RH. Complete removal of ammonia, and three moles of residual water content, indicate that the transformed decomposed struvite compound might be newberyite.

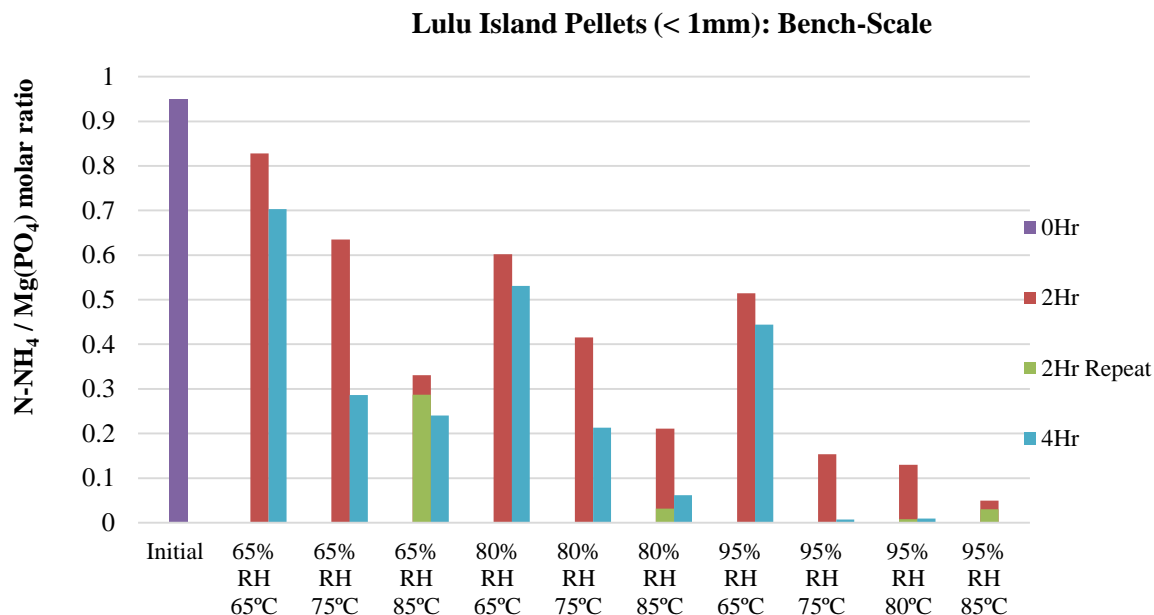


Figure 5.16 N-NH₄ molar ratio with respect to Mg (PO₄) of Lulu Island pellets (<1mm) heated at three different relative humidity with increasing temperatures for different heating durations

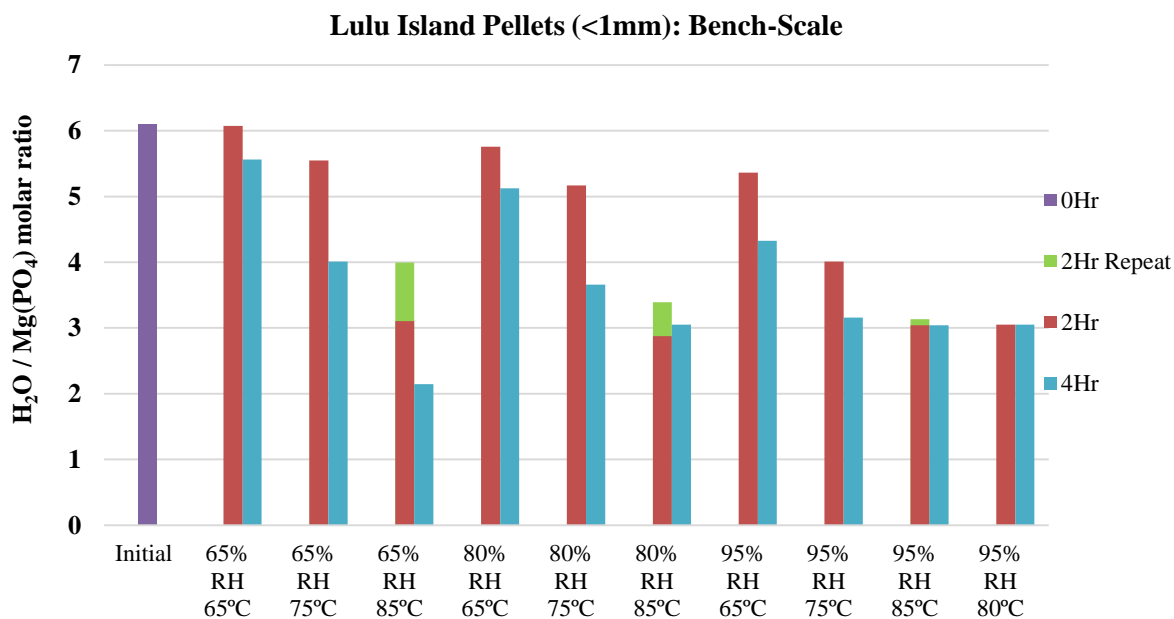


Figure 5.17 H₂O molar ratio with respect to Mg (PO₄) of Lulu Island pellets (<1mm) heated at three different relative humidity with increasing temperatures for different heating durations

On the other hand, complete removal of ammonia could not be achieved at 65% RH, with 4 hours of heating, and a decomposition temperature of 85°C, due to the possibility of a layered structure being formed in the decomposed struvite product, due to excessive removal of water (4 moles in this case). The solid phase of the struvite decomposition product is discussed in Section 5.2.3.1.4.

5.2.3.1.2 Effects of relative humidity on rate and efficiency of ammonia removal

To observe the effect of relative humidity on ammonia removal efficiency at each individual temperature, bar charts were reorganized by temperature, with increasing relative humidity. Figure 5.18 and Figure 5.19 represent residual ammonia and water content after heating Lulu Island pellets (<1mm) at various combinations of temperature and relative humidity, for 2 and 4 hours of heating.

In general, the higher the humidity, the more ammonia removal was achieved at any given temperature. The maximum ammonia removal efficiency was achieved at 95% RH, followed by 80% and 65% RH at any particular temperature and duration of heating. The ammonia removal efficiency was found to be greater at higher relative humidity, with a higher temperature.

In Figure 5.18 and Figure 5.19, the results obtained from heating the Lulu Island struvite pellets at 85°C, with a relative humidity of 65%, 80% and 95%, were obtained under an “unstable regime”. Therefore, dittmarite may have formed during the experiment, which could explain the higher residual ammonia in the decomposed product after 2 hours of heating. To observe the process efficiency under “stable” operating conditions, struvite heating at 85°C with 65%, 80% and 95% RH was repeated for 2 hours and presented with previous results as “2 Hr repeat”. From Figure 5.18, more than 95% ammonia can be removed with 80% and 95% relative humidity with 2 hours of heating at 85°C, under “stable” operating conditions. The residual water content was found to be 3.38 and 3.0 moles, respectively, for 80% and 95% RH with 85°C (Figure 5.19).

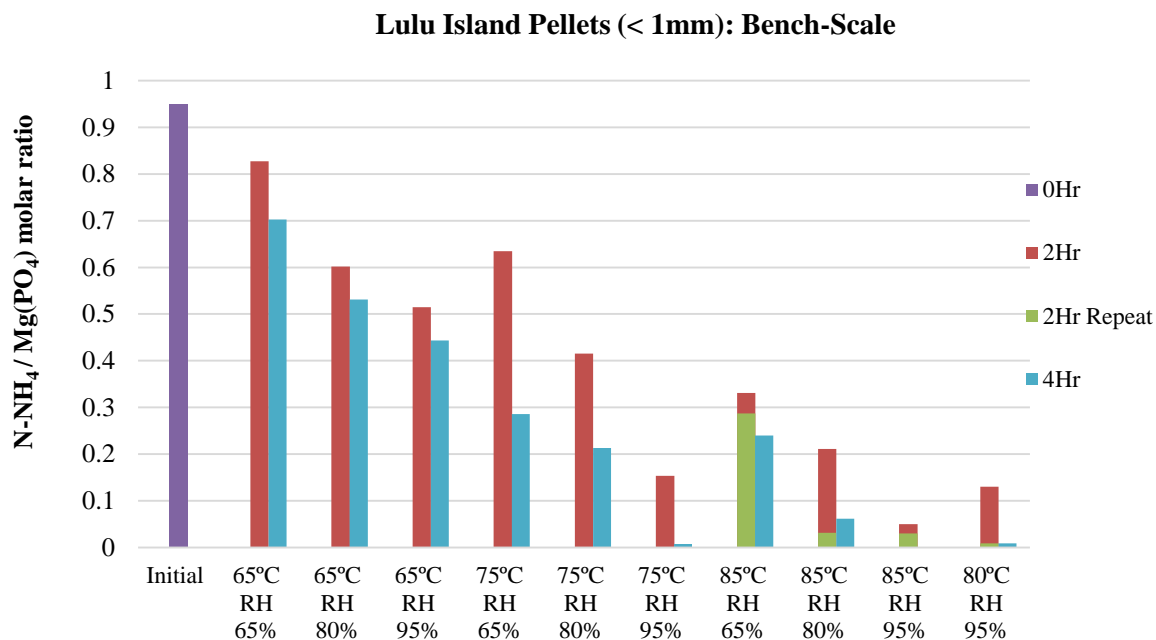


Figure 5.18 N-NH₄ molar ratio with respect to Mg(PO₄) of Lulu Island pellets (<1mm) heated at three different temperatures with increasing relative humidity for different heating durations

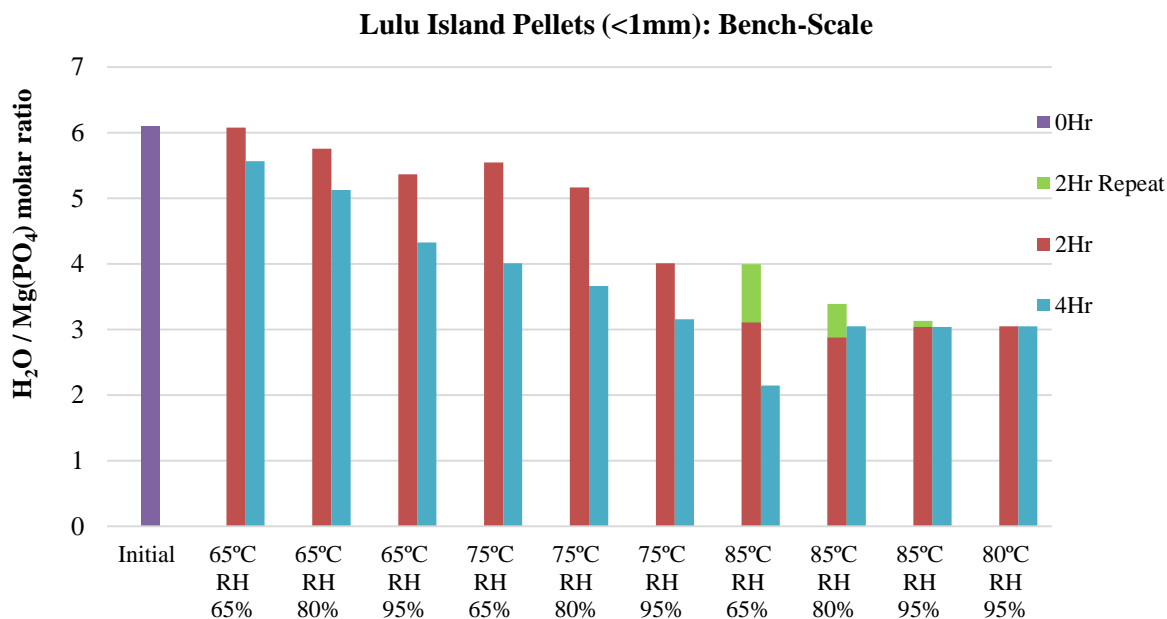


Figure 5.19 H₂O molar ratio with respect to Mg(PO₄) of Lulu Island pellets (<1mm) heated at three different temperatures with increasing relative humidity for different heating durations

During heating of struvite under a “stable regime”, higher ammonia removal was achieved; this might be due to the retention of more water in the decomposed samples, preventing the structure from being compacted and eventually allowing more ammonia removal. Therefore, at higher temperatures and higher humidity, such as 85°C or 80°C with 95% RH, ammonia can be removed completely from Lulu Island struvite pellets smaller than 1mm, under “stable” operating conditions within a short period of time. The composition of the decomposed solid samples is discussed in Section 5.2.3.1.4.

5.2.3.1.3 Effects of struvite heating duration on ammonia removal

The longer the process, the greater the ammonia removal achieved, unless there was some dittmarite formed within a struvite pellet during the heating process. At any given humidity, the ammonia removal efficiency was not significant between 2 and 4 hours of heating, when the decomposition temperature was as low as 65°C. Further increases in temperature, up to 75°C, caused a significant increase in ammonia removal efficiency with the increase in heating duration from 2 to 4 hours. For instance, the difference in ammonia removal efficiency between 2 and 4 hours heating of heating at 65% RH and 65°C was only 12%, while at 65% RH and 75°C it was 30%. The prolonged 4 hours of heating at 95% RH provided a decomposed struvite product devoid of ammonia at 75°C, whereas around 45% ammonia was left in the decomposed struvite samples after heating at 65°C. However, the longer duration of heating, up to 4 hours at higher temperatures with lower humidity, showed a negligible difference in ammonia removal efficiency compared to 2 hours of heating. For instance, the residual ammonia content at 85°C with 65% RH was around 33% at 2 hours heating duration, which decreased to 24% after increasing heating duration to 4 hours. The increase in relative humidity up to 95% at 85°C resulted in about 97% ammonia removal, at 2 hours heating duration. Thus, it can be inferred that the heating of struvite pellets, at high relative humidity, with high temperature, can remove approximately 100% ammonia, within 2 hours of heating. Struvite heating beyond 2 hours could not provide any significant difference in ammonia removal efficiency. In addition, the longer duration of heating not only increased the possibility of dittmarite formation, but also increased the energy consumption. Ammonia can be removed from the struvite structure as long as there was no dittmarite formed during the experiment. From the oven dry experiments, it is clear that ammonia, belonging to the layered

structure, including both dittmarite and a 2D amorphous layered structure, is impossible to remove even after heating for a longer period.

5.2.3.1.4 XRD results

A few decomposed struvite samples were chosen for XRD analyses, based on the results obtained from chemical analysis. The ultimate goal was to find the optimum operating conditions where struvite can be completely transformed into newberyite, through thermal decomposition. The parallel formation of compounds other than struvite and newberyite, such as dittmarite or other layered structures, can reduce the ammonia removal efficiency. The XRD results can validate the optimum operating conditions with respect to temperature, relative humidity and heating duration, where the residual solid phase is entirely newberyite and neither struvite nor dittmarite.

The presence of dittmarite can be expected in the struvite samples that were decomposed either at higher temperatures in a shorter period of time, or at lower temperatures with prolonged heating duration, due to excessive dehydration. Table 5.2 represents the XRD results of selected decomposed solid samples obtained at various combinations of temperatures and relative humidity. The XRD patterns, with detected peak intensity over diffraction angles, can be found in Appendix C.1. The struvite sample, decomposed at 65°C with 95% RH, contained a newberyite compound along with struvite, after 2 hours of heating; whereas, trace amounts of dittmarite, along with struvite and newberyite, were identified after 4 hours of heating (Table 5.2). In general, the decomposed solid sample, containing a high intensity of struvite peak, indicates the presence of a high residual struvite compound in the sample. In contrast, a prominent newberyite peak indicates greater transformation of struvite into newberyite that can be achieved with more extensive ammonia release from struvite. Ammonia evolution from the struvite solid phase starts at the beginning of the experiment, thereby enhancing the formation of newberyite and reducing the struvite portion. Incorporation of steam and hot air caused a decrease in the struvite peak and formation of newberyite in the decomposed solid samples. As a result, newberyite was detected in every sample for each combination of temperature and relative humidity, as shown in Table 5.2. The presence of a pronounced struvite peak in the decomposed samples at 65°C with 95% humidity, for 2 hours and 4 hours of heating, indicates a slower transformation process of struvite

to newberyite; this results in a high residual ammonia content at that operating range (Appendix C.1).

Table 5.2 XRD results of Lulu Island pellets after heating at various temperatures and relative humidity

Lulu Island Pellets (<1mm)			Struvite	Newberyite	Dittmarite
Temperature, °C	Relative Humidity (%)	Duration of Heating, (hours)			
65°C	65%	2, 4	+	+	-
	80%				
	95%	2	+	+	-
		4	+	+	Trace
75°C	65%	2	+	+	-
	80%				
	95%	2	+	+	-
		4	-	+	Trace
80°C	95%	2	+	+	+
		*2 repeat	-	+	-
85°C	65%	2	+	+	+
		*2 Repeat	+	+	-
		4	+	+	+
	80%	2	-	+	+
		*2 repeat	+	+	-
	95%	2	-	+	+
		*2 repeat	-	+	-

+ refers to detected compound, - refers to non-detected compound

For 2 hours and 4 hours decomposed samples, normal angle XRD performed (2θ starting scanning angle 5°)

*For 2 hours repeat, low angle XRD (2θ starting scanning angle 0.8°) performed immediately after decomposition

No trace amounts of dittmarite were found after 2 hours of heating at 65°C and 75°C, with any humidity. However, 4 hours of heating with 95% RH led to the formation of dittmarite in the decomposed solid phase, which prevents complete ammonia removal. The trace amount of dittmarite may become prominent with an increase in heating duration beyond 4 hours. Therefore, the decomposed solid phase containing a higher percentage of dittmarite, compared to newberyite, can no longer be suitable as precipitating agent for the aqueous ammonia removal process, due to the retained ammonia in between the structure. This confirms that low temperatures, with high humidity conditions, will not favour complete ammonia removal, even with prolonged heating. XRD analysis was also conducted on the decomposed struvite samples heated at 85°C, with varying humidity, under stable and unstable operating conditions. Strong peaks of dittmarite, along

with newberyite and struvite, were found when Lulu Island pellets were heated at 85°C with 65% and 80% RH, for 2 hours under an “unstable regime” (Appendix C.1). When struvite is heated at high temperatures under an “unstable regime”, the relative humidity fluctuation may favour the formation of dittmarite within a short period of time. Furthermore, the increase in humidity up to 95% (Table 5.2) caused the disappearance of the struvite peak, indicating the complete decomposition of struvite and the decomposed solid phase containing dittmarite and newberyite.

The same experiments at 85°C, with 65%, 80% and 95% RH, were carried out under a “stable regime” where relative humidity was precisely controlled ($\pm 3\%$). The XRD patterns, with a peak intensities over various scanning angles obtained from freshly decomposed struvite heated at 85°C with 65%, 80% and 95% RH, can be found in Appendix C.2. No dittmarite formation was found in the decomposed solid phase, after heating struvite under this “stable regime”. The accurately controlled operating conditions promoted the formation of newberyite and, eventually, prevented dittmarite formation. At 85°C with 95% RH, the decomposed solid phase was entirely newberyite under “stable” operating conditions (Table 5.2), while the decomposed solid phase contained significant amounts of dittmarite under the “unstable regime” (Table 5.2). To further optimize the operating conditions, the Lulu Island pellets were again heated at 80°C with 95% RH, under “stable regime”. The struvite solid phase completely transformed into newberyite; whereas, a significant amount of struvite was found in the decomposed struvite sample when heated under the “unstable regime”.

In summary, considering the energy consumption and probability of dittmarite formation at 85°C, the optimum operating conditions for struvite to newberyite transformation is recommended to be: 80°C with 95% RH for 2 hours of heating. However, further experiments were conducted to investigate the presence of a layered structure and the corresponding operating conditions, such that the formation of a layered structure can be prevented in decomposed struvite samples. The formation of a layered structure, during the oven dry experiments, was discussed in Section 5.1.2.1.3.1.

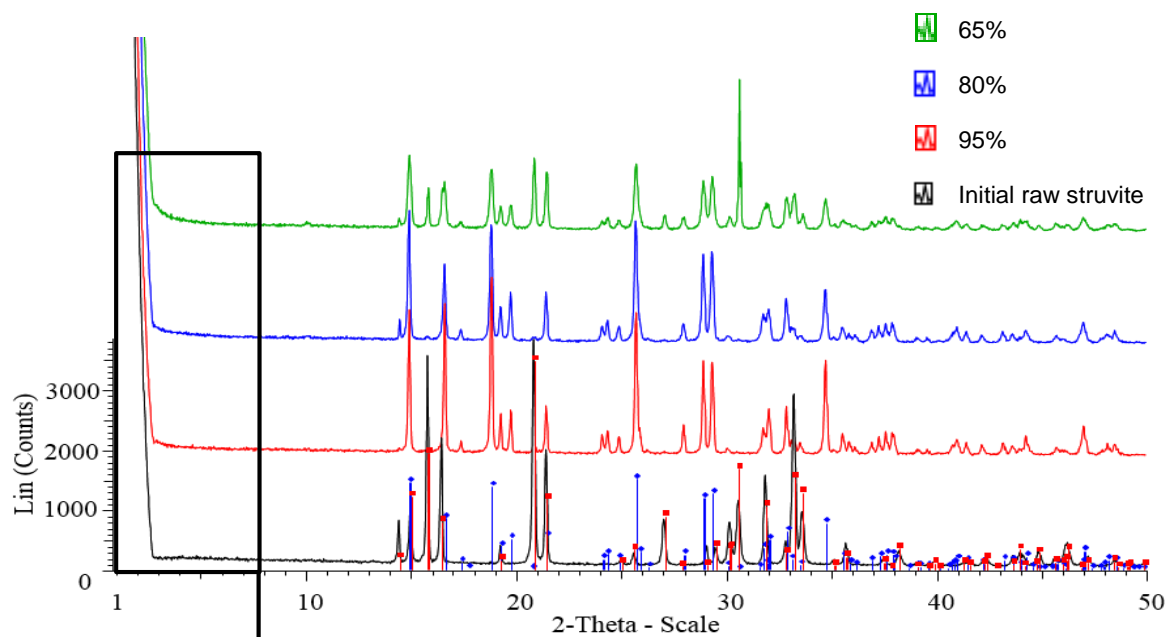
5.2.4 Effects of relative humidity on layered structure formation

In order to observe the presence of a layered structure at higher temperatures, with varying humidity, XRD analysis was performed at low angles (starting scanning angle = 0.8°) on the Lulu Island struvite pellets heated at 85°C with 65%, 80% and 95% RH, for 2 hours, under “stable” operating conditions. Figure 5.20 indicates the intensity of peaks formed at different angles after performing XRD on the decomposed Lulu Island pellets, obtained at the described operating conditions. Figure 5.20 (a) indicates the XRD results from the lowest to highest angle, whereas Figure 5.20 (b) shows the enlarged view of peaks formed at lower angles.

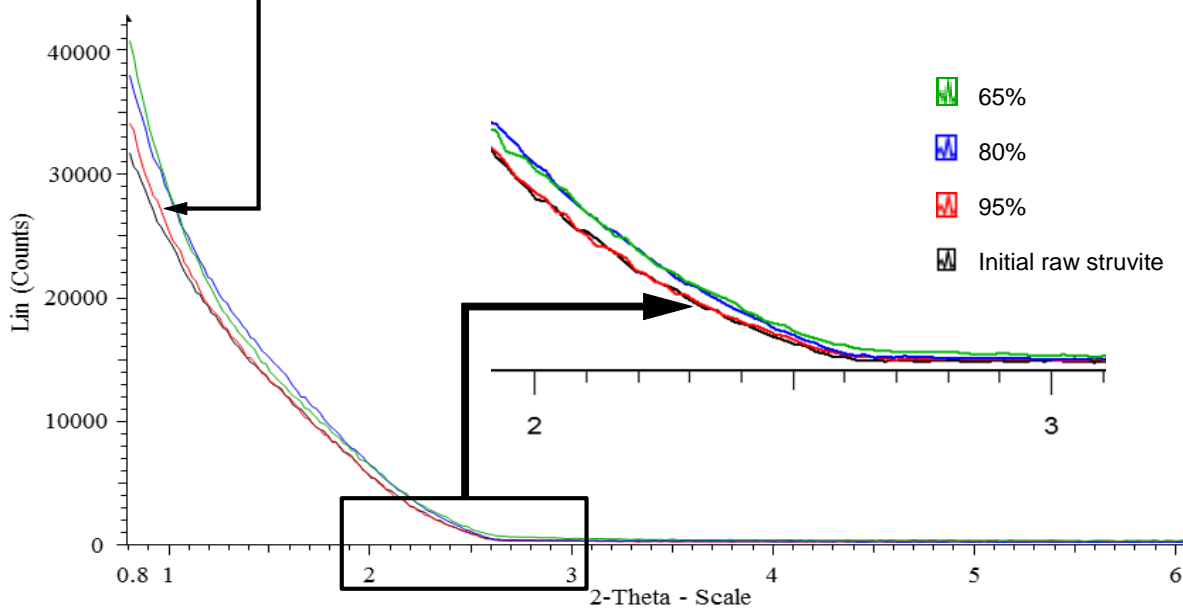
During low angle XRD analysis, no peak of a 2D amorphous layered structure was found in the samples after 3 days of heating these pellets. The struvite pellets decomposed at 85°C contained newberyite, along with struvite, when 65% and 80% RH were introduced. From Figure 5.20 (a), it can be seen that the intensity of the newberyite peak increased, whereas the intensity of the struvite peak decreased simultaneously with the increase in relative humidity. The pronounced newberyite peaks indicate increased newberyite formation and lower struvite residuals. The decomposed solid phase contained only newberyite (neither dittmarite nor struvite) after increasing the humidity up to 95%. No presence of dittmarite was observed in any of the decomposed struvite samples that were shown in Figure 5.20 (a). In Figure 5.20 (b), the shoulder of the initial struvite samples coincides with the shoulder formed at 85°C with 95% RH; however, the shoulder of the struvite samples heated at 65% and 80% RH, moved away from the shoulder of the initial struvite samples. A similar shoulder movement from initial struvite samples was also observed in the oven dry experiments. Furthermore, it was proved that the shoulder movement indicates the presence of a 2D layered structure, which may not appear due to absorption of moisture over the time period.

Considering the movement of the shoulder from the initial state, it can be suspected that the 2D layered structure might have started forming at 65% RH, but due to instability, disappeared after exposure to the atmosphere. Based on the outcomes of the oven dry experiments, it can be assumed that, if there was any layered structure present in the residual solid phase, it would have transformed into a more organized layered structure over time (such as dittmarite).

Lulu Island Pellets (0.5-1mm): T-85°C, RH- 95%, 80%, 65% & 2 hr



(a)



(b)

Figure 5.20 X-ray diffraction patterns of Lulu Island pellets (<1mm) heated at 85°C with 65%, 80% and 95% relative humidity for 2 hours (a) scanning angle 0.8 to 50 degree; ■ standard newberyite, ■ Standard struvite (b) enlarged view of scanning angle 0.8 to 6 degree

Therefore, XRD analysis was also performed on the same samples after 4 months of storage in the desiccator, in order to observe the transformation of the layered structure over time. Figure 5.21 (a) represents the XRD results of the freshly decomposed struvite samples heated at 85°C with 80% RH and Figure 5.21 (b) shows the XRD results of the same decomposed sample after 4 months in the desiccator. The additional XRD results from struvite samples decomposed at 85°C with 65% and 95% RH, can be found in Appendix C.3.

The XRD results obtained 4 months earlier showed that the residual solid phase contained newberyite at 85°C with 95% RH (Appendix C.2), whereas at 65% (Appendix C.2) and 80% RH (Figure 5.21, a), the residual solid phase contained newberyite along with struvite. No presence of dittmarite or a 2D amorphous layered structure was observed at 65%, 80% and 95% RH. The XRD results obtained from the samples decomposed at 85°C with 95% RH, for 2 hours, confirmed that the residual solid phase remained as newberyite even after remaining 4 months in the desiccator. The XRD data (after 4 months) showed the presence of dittmarite in the samples decomposed at 85°C with 80% (Figure 5.21, b) and 65% relative humidity (Appendix C.3) for 2 hours. It is evident that the layered structure formed in the residual solid phase, during heating at 85°C with 65% and 80% RH, was further transformed into a more organized layered structure (i.e. dittmarite) over time.

Therefore, it can be suggested that, at lower humidity with a higher temperature, there is the possibility of a layered structure formation during heating, due to excessive dehydration; this can be confirmed from the movement of the shoulder through performing low angle XRD analysis on the freshly decomposed sample, without any delay. Considering that higher humidity lowers the possibility of layered structure formation, the operating humidity range is suggested to be between 80% and 95%, for complete transformation of struvite to newberyite.

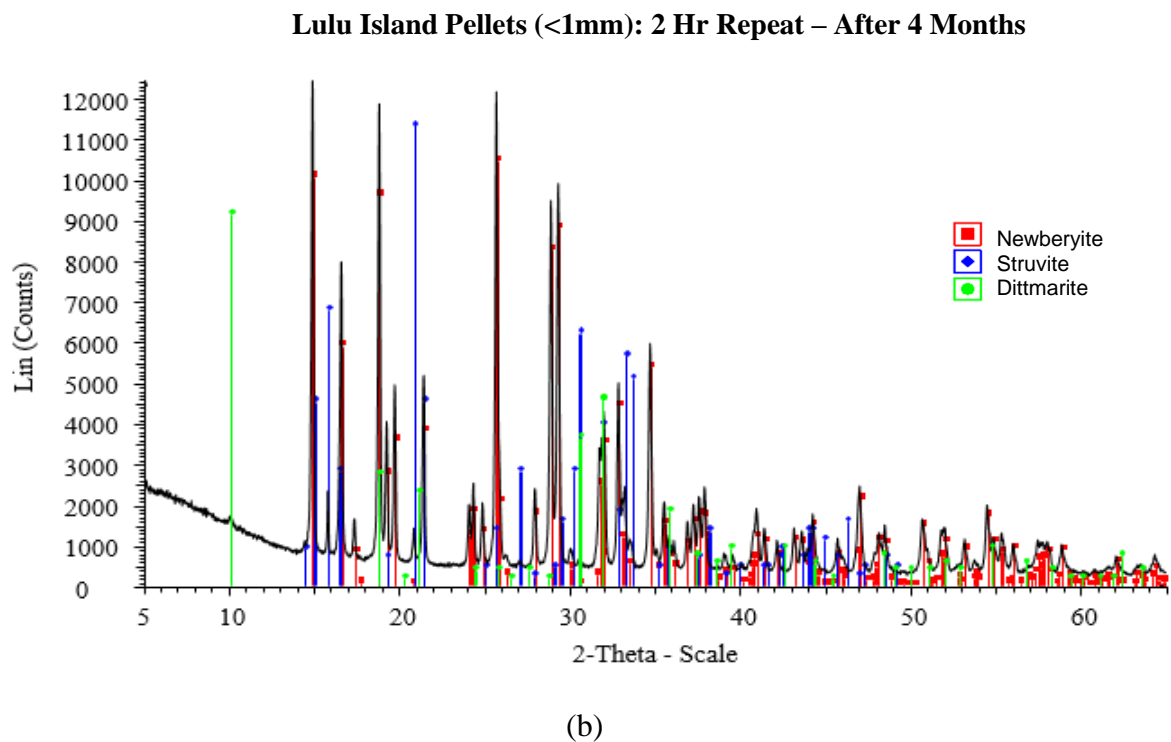
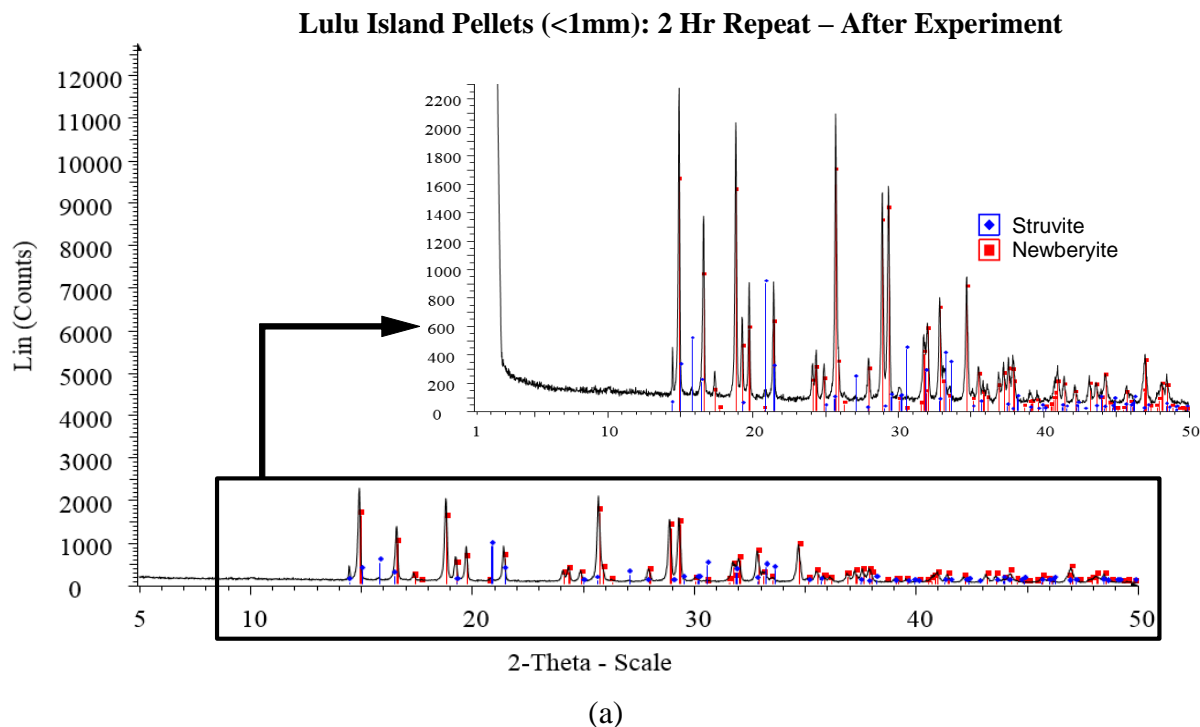


Figure 5.21 X-ray diffraction patterns of Lulu Island pellets after one year (<1mm), decomposed at 85°C with 80% RH for 2hours (a) right after thermal decomposition (b) after four months

5.2.5 Effects of size and sources of different pellets on ammonia removal efficiency

5.2.5.1 Chemical content for different sources and sizes of pellets

In order to observe the ammonia removal efficiency from pellets of different size and source, struvite pellets were heated at the optimum conditions identified from the bench-scale experiments. To evaluate the effect of sizes and sources of struvite pellets, Lulu Island pellets (smaller and larger than 1 mm), Penticton B.C. and Edmonton Gold Bar smaller than 1 mm, and recrystallized pellets larger than 1mm, were heated at 80°C and 95% relative humidity. It was hypothesized that different pellets possess different degrees of porosity, compactness and hardness, due to difference in their sources and sizes, thus affecting ammonia removal efficiencies. Figure 5.22 and Figure 5.23 represent residual ammonia and water content resulting from heating these struvite pellets, under optimum conditions.

In general, the softer and more porous the pellets, the more ammonia will easily escape upon decomposition, thereby increasing removal efficiency. As far as the same source is concerned, smaller pellets are usually softer than larger pellets. For instance, in Figure 5.22 and 5.23, the ammonia and water removal efficiency was found to be higher for smaller (<1mm) Lulu Island pellets, compared to larger Lulu Island pellets (>1mm), when heated under the same experimental conditions. The smaller Lulu Island pellets showed complete ammonia removal within 2 hours, whereas around 30% ammonia remained in the larger pellets. Complete ammonia removal could not be achieved from the larger pellets even after 4 hours. Thus, pellets with different sizes, from the same source, appear to exhibit different ammonia removal efficiencies. The high residual ammonia and water contents after 2 and 4 hours of heating larger Lulu Island pellets indicate that the decomposed solid phase might have contained significant portions of struvite, together with dittmarite, impeding ammonia evolution from the structure.

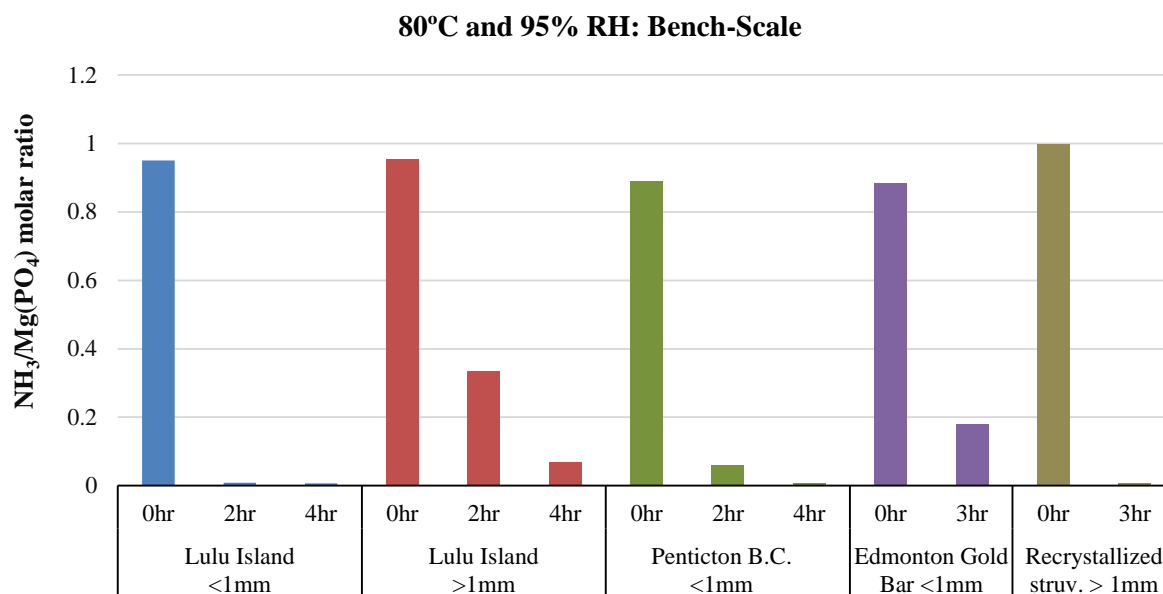


Figure 5.22 N-NH₄ molar ratio with respect to Mg (PO₄) of different sources and sizes of pellets heated at optimum conditions for different heating durations

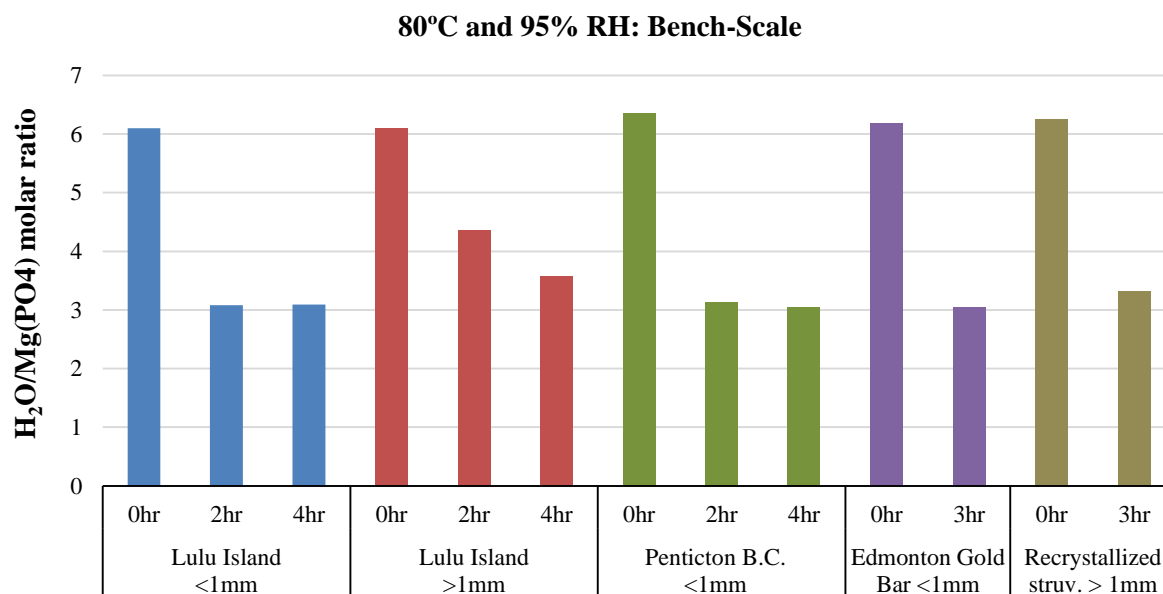


Figure 5.23 H₂O molar ratio with respect to Mg (PO₄) of different sources and sizes of pellets heated at optimum conditions for different heating durations

As far as different sources of struvite pellets are concerned, similar sizes of struvite pellets from different sources may have different ammonia removal efficiencies due to varying hardness, porosity and structural composition. The smaller (<1mm) Edmonton Gold Bar pellets showed lower ammonia removal efficacy in comparison to smaller Lulu Island pellets (<1mm) and Penticton B.C. pellets (<1mm), even after 3 hours of heating.

About 100% and 94% ammonia removal was achieved after decomposing smaller Lulu Island and Penticton B.C. pellets, respectively, for 2 hours, whereas around 70% ammonia removal was attained from decomposition of smaller Edmonton Gold Bar pellets after 3 hours of heating under optimum conditions. However, the larger pellets from the same source may achieve higher ammonia removal efficiencies compared to smaller pellets from different sources. The ammonia removal efficiency seemed to vary among the sizes of different sources of pellets. The smaller pellets could be harder than larger pellets, when the source was different. For instance, complete ammonia removal efficiency was achieved from larger recrystallized pellets (>1mm) after 3 hours of heating, which could not be achieved from smaller Edmonton Gold Bar pellets (<1mm). Without providing any crushing strength, it can be inferred that the Edmonton Gold Bar pellets are harder than recrystallized pellets because they could be easily smashed between two fingers.

The ammonia removal efficiency was found to be higher from smaller Lulu Island pellets followed by Penticton B.C. and Edmonton Gold Bar pellets, even after heating under optimum conditions. The Edmonton Gold Bar pellets contained the highest residual ammonia even after prolonged duration (3 hours) of heating under optimum conditions. For this reason, smaller and harder struvite pellets may not be suitable for complete ammonia removal using the proposed technology. For softer and larger recrystallized pellets, the proper fluidization and possibility of disintegration were major concerns for heating. Based on difficulty of fluidization and possibility of dust formation, the very soft recrystallized pellets were not suitable either, although the ammonia removal efficiency was higher compared to other pellets. Under microscopic view, it was found that the Edmonton Gold Bar pellets possessed a smoother and harder solid surface, whereas the Lulu Island and Penticton B.C. pellets exhibited a porous surface. If the pellets are harder and non-porous, steam cannot permeate and reach the core of the pellets and as a result, struvite is able to start forming in the core. Therefore, it is posited that the ammonia removal efficiency is higher

for porous and softer pellets, relative to those of harder and non-porous pellets. Struvite morphology, in terms of various sizes and sources and their respective ammonia removal capacities, are discussed in Section 5.4.

5.2.5.2 XRD results

XRD analysis was performed on the selected decomposed struvite pellets discussed in the previous section, to identify the best candidate in terms of size and source for complete transformation of struvite to newberyite under optimum heating conditions. The residual solid phase may contain phases such as struvite, newberyite and dittmarite. Table 5.3 represents the XRD results of different sources and sizes of struvite pellets that were decomposed under optimum conditions (80°C and 95% RH) in the bench-scale experiments. The XRD patterns of different compounds, with peak intensity over different scanning angles, are provided in Appendix C.4.

Table 5.3 XRD results of different sources and sizes of struvite pellets after decomposing at 80°C and 95% RH

Samples from Bench-Scale Experiments			Struvite	Newberyite	Dittmarite
Type of Struvite	Size of Struvite Pellets	Duration of Heating, (hours)			
Lulu Island	<1mm	2	-	+	-
		2	+	+	-
		4	+	+	Trace
Penticton B.C.	<1mm	2	+	+	Trace
Edmonton Gold Bar	<1mm	3	-	+	+
Recrystallized	>1mm	3	-	+	Trace

+ refers to detected compound, - refers to non-detected compound

From Table 5.3 it can be observed that the presence of newberyite was detected in all the decomposed solid phases heated under optimum conditions, irrespective of size or source of the struvite pellets. It was found from the chemical analyses discussed in the previous section that ammonia removal efficiency from struvite was found to be dependent on size, hardness and duration of heating. After 2 hours of heating at optimum conditions, the smaller Lulu Island pellets completely transformed into newberyite, whereas the larger pellets contained struvite along with newberyite (Table 5.3). The residual ammonia from the larger Lulu Island pellets could be

removed further through longer heating, as long as the formation of dittmarite was prevented. However, XRD results obtained from 4-hour decomposed Lulu Island pellets (Table 5.3) indicate the presence of dittmarite, confirming that prolonged heating on Lulu Island pellets will not be suitable for the complete removal of ammonia. Therefore, it can be inferred that, with the same source of struvite pellets, different sizes result in different ammonia removal efficiencies due to slower transformation of struvite to newberyite and the formation of dittmarite in the pellet core.

With the same size of pellets, those from different sources also exhibit different ammonia removal efficiencies, as the morphology and hardness of various sources of pellets are different. The Edmonton Gold Bar pellets smaller than 1 mm were harder than Lulu Island, Penticton B.C. and recrystallized pellets (Details of the hardness and morphology of struvite pellets are discussed in Section 5.4 and Section 5.5). A strong peak of dittmarite was identified, along with newberyite, in Edmonton Gold Bar pellets after 3 hours of heating.

It is suspected that the relative humidity might be lower in the core of the Edmonton Gold Bar pellets compared to the surrounding parts of the pellets, because steam is less able to penetrate the harder surface of the pellets, thereby creating favourable conditions for dittmarite formation. However, the larger pellets, such as recrystallized pellets, are softer than any other pellets and contain trace amounts of dittmarite due to improper fluidization and dust formation. The improper fluidization may also lead to the formation of a layered structure including dittmarite or an amorphous layered structure, due to reduced mass and heat transfer (that will provide a similar environment as that of the oven dry experiments).

In summary, ammonia removal efficiency is related to the size of the struvite, as well as the hardness of the pellets. The larger pellets tested required a much higher gas flow velocity, compared to smaller pellets for proper fluidization; this caused more energy consumption due to increased supply of hot air and steam. In addition, the transformation rate of struvite to newberyite, upon decomposition, is very slow for larger pellets and is more susceptible to dittmarite formation with prolonged heating. On the other hand, the softer and smaller pellets are susceptible to dust formation during the experiment; this will reduce the amount of decomposed solid containing newberyite, after consuming a large amount of energy. Therefore, carefully selected size and

hardness of the pellets will provide the most suitable pellets for complete conversion of struvite to newberyite, without forming dittmarite within the shortest period of heating.

5.3 Pilot-scale experiments with humid air

5.3.1 Hypothesis and specific goals

The struvite pellets became fully transformed into newberyite in the bench-scale experiments, after conditioning with hot air with steam. In order to make this technology industrially applicable, the process must be operated efficiently, in a large-scale setup. Therefore, the reactor in the pilot-scale experiment was scaled up 7 folds, compared to the reactor in the bench-scale experiment. This new experimental design was expected to reveal any operational difficulties and energy saving options, with regard to effective ammonia removal.

The pilot-scale experiments were performed to answer the following questions.

- Is it possible to achieve 100% ammonia removal efficiency at pilot-scale using the optimum conditions obtained from the bench-scale experiments?
- How does the ammonia removal efficiency vary with different sizes and sources of struvite pellets at the optimum condition in the pilot-scale setup?
- Is it possible to further optimize the operating conditions with respect to temperature, relative humidity, and heating duration using the most suitable pellets, corresponding to maximum ammonia removal upon heating under optimum conditions?
- How can the process operation be improved by adjusting operating parameters, process design and cost?

Hypotheses

- The optimum temperature and relative humidity identified from bench-scale experiments would remove 100% ammonia from struvite pellets, when applied to the pilot-scale experiments.
- The process will be more energy efficient and economically feasible, if the operating temperature, relative humidity and duration of heating can be reduced further, for complete conversion of struvite to newberyite.
- Uniform heating, uninterrupted steam supply, precise control of temperature, relative humidity and proper fluidization of struvite pellets in FBR will facilitate NH_3 removal from the surface of struvite pellets.

5.3.2 Results and discussion of pilot-scale experiments

5.3.2.1 Process efficiency for different sources and sizes of struvite pellets

The optimum conditions obtained from the bench-scale experiments were 80°C, with 95% RH and 2 hours heating duration. Pilot-scale experiments were conducted using similar pellets, in size and quality; Lulu Island pellets (larger than 1mm, crushed smaller than 1mm), Penticton B.C. (smaller and larger than 1mm), Edmonton Gold Bar pellets (smaller than 1mm), and recrystallized pellets (larger than 1mm). The optimum conditions obtained from the bench-scale experiments were used in the pilot-scale setup, to observe ammonia removal efficiency, identify the appropriate size and source of the pellets and overcome the challenges of operating a pilot-scale reactor.

The process stability in the pilot-scale experiments was also monitored through recording fluctuations of temperature, relative humidity, and air flow, through both the jacket and reactor during thermal decomposition of struvite pellets. Figure 5.24 is a representative graph showing the values of the operating parameters when the Penticton B.C. pellets (<1mm) were heated under optimum conditions (80°C and 95% RH) for two hours. The additional monitored data at other operating conditions are presented in Appendix E. Figure 5.24 shows that the temperature was

stable at $80^{\circ}\pm 1^{\circ}\text{C}$ and the air flow through the reactor and jacket was around 1.2 and 3.6 SCFM, respectively, with small fluctuations. The average relative humidity fluctuated at $95\% \pm 10\%$, with a few outliers.

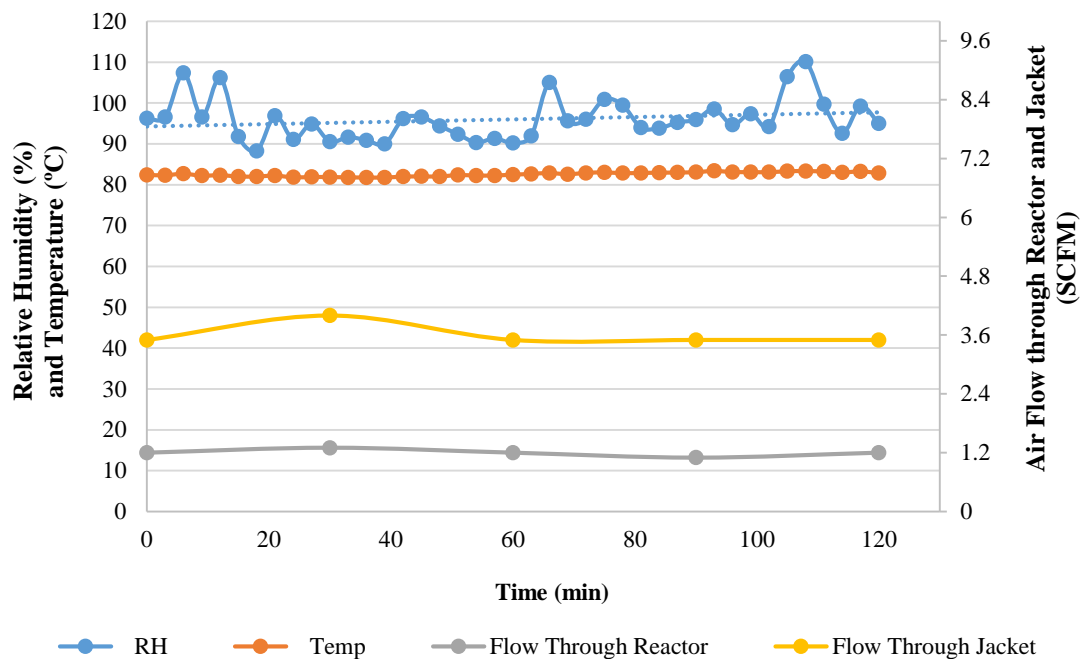


Figure 5.24 Temperature, relative humidity and air flow through reactor and jacket during thermal decomposition of Penticton B.C. pellets (<1mm) at optimum conditions in the pilot-scale setup.

5.3.2.1.1 Chemical results and interpretation

Figure 5.25 and Figure 5.26 represent residual ammonia and water contents with different sources and sizes of struvite pellets, when heated under optimum conditions for different durations.

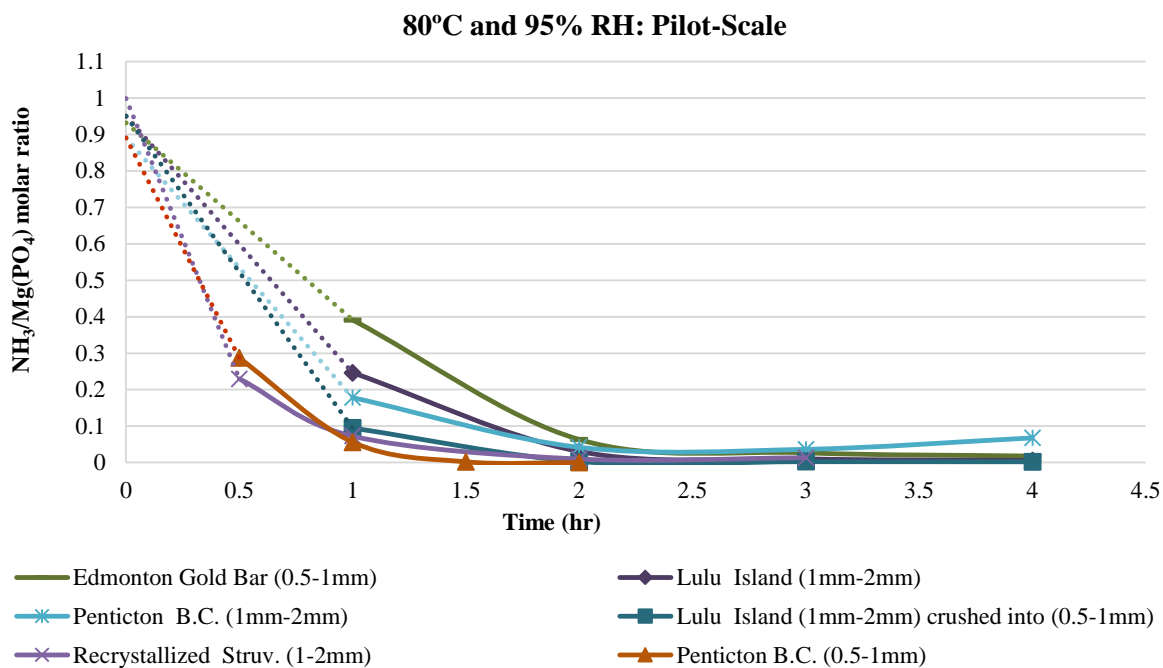


Figure 5.25 N- NH_4 molar ratio with respect to $\text{Mg}(\text{PO}_4)$ of different sources and sizes of struvite pellets heated at optimum conditions for different heating durations

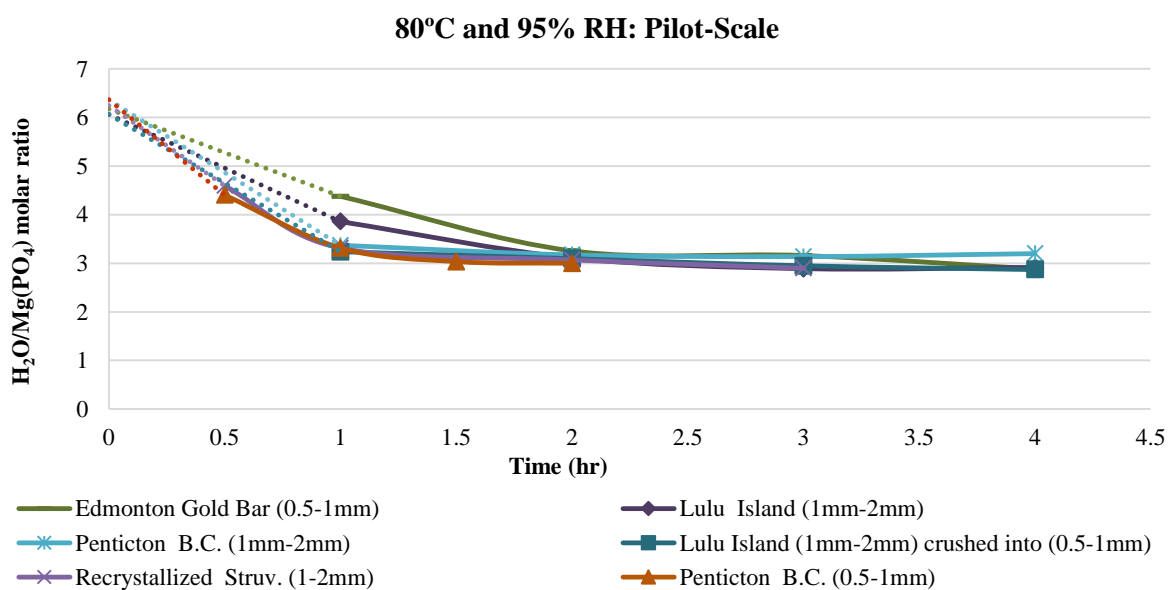


Figure 5.26 H_2O molar ratio with respect to $\text{Mg}(\text{PO}_4)$ of different sources and sizes of struvite pellets heated at optimum conditions for different heating durations

In general, ammonia removal occurred rapidly within the 1st hour of heating for each source and size of pellets. The maximum ammonia removal efficiency was observed from smaller Penticton B.C. pellets, followed by larger recrystallized pellets, crushed Lulu Island pellets, larger Penticton B.C. pellets, larger Lulu Island pellets and finally smaller Edmonton Gold Bar pellets. Overall, the struvite decomposition process was very slow for larger and harder pellets, compared to smaller and softer pellets, consistent with the results obtained from the bench-scale experiments.

The Lulu Island pellets, larger than 1 mm, were crushed into 0.5-1 mm pellets and heated at optimum conditions for 4 hours. The crushed Lulu Island pellets showed a similar trend with respect to ammonia removal in the pilot-scale, to that of the original 0.5-1 mm Lulu Island pellets. The smaller crushed (0.5-1 mm) and larger (1-2 mm) Lulu Island pellets in the pilot-scale setup showed 100% ammonia removal after 2 hours of heating, where the residual water content remained constant at around 3 molecules (Figure 5.25 and Figure 5.26). Based on the slope of the curves, both ammonia and water removal were faster for smaller Lulu Island pellets, compared to larger pellets within 2 hours of heating. After 2 hours however, the ammonia removal efficiency was almost identical for both sizes, under optimum conditions.

The Penticton B.C. pellets, which were softer than Lulu Island pellets, were also heated at 80°C and 95% RH, to observe the effects of size and hardness on ammonia removal efficiency. The Penticton B.C. pellets (<1 mm) showed 100% ammonia removal after 1.5 hours, whereas around 4% ammonia was left in the Penticton B.C. pellets (>1 mm), even after 2 hours of heating. The Penticton B.C. pellets larger than 1 mm showed faster ammonia and water removal compared to Lulu Island pellets of a similar size, within 2 hours of heating. After 2 hours of heating, the ammonia removal from the larger Penticton B.C. pellets was found to be slower. Complete ammonia removal was not achieved from the larger Penticton B.C. pellets, even after 4 hours of heating at optimum conditions, and the residual water content was found to be above 3 moles. The Penticton B.C. pellets larger than 1 mm might have contained some impurities that had been accounted for in water. Therefore, the actual water content in the larger decomposed Penticton B.C. pellets might be less than 3 moles per mole of P (but was considered as 3.2 moles in this experiment).

At the end of the experiments, the struvite pellets were collected from the bottom of the reactor. Some decomposed pellets were left on the extended portion of the metal ring attached to the bottom part of the reactor, where the mixture of fluidizing gases could not reach, and which were believed to be responsible for the residual ammonia concentration at the end of the experiment. Therefore, the ammonia content was found to be higher in larger Penticton B.C. pellets, after 4 hours of heating.

However, the Edmonton Gold Bar pellets, that were less than 1mm, were harder than any other pellets heated at this optimum condition. Initially, the ammonia removal was high and there was around 6% ammonia left at exactly 2 hours; this eventually decreased to less than 3% after 4 hours of heating. This infers that 100% ammonia removal can be achieved from Edmonton Gold Bar pellets, even though the process may require a longer duration of heating; however, this cannot be performed without causing excessive dehydration, leading to the formation of a layered structure. Conversely, in the case of large (>1mm) softer pellets, the ammonia removal was faster, compared to smaller and harder pellets.

Recrystallized struvite pellets (>1mm), synthesized from newberyite, were also heated at the optimum conditions, to observe the ammonia removal efficiency of larger and softer pellets. These recrystallized pellets showed similar ammonia and water removal efficiency as the smaller Penticton B.C. pellets. Complete ammonia removal was achieved from recrystallized pellets after 2 hours of heating. Relative to other pellets, recrystallized pellets were very soft and could be crushed by hand. Therefore, while heating, these recrystallized pellets fell apart and transformed into dust. It was difficult to fluidize these pellets during heating, because of dust formation. This confirms that larger pellets are also suitable for the ammonia removal process, as long as they are neither very hard nor very soft. The size and hardness corresponding to smaller Penticton B.C. pellets were found to be most suitable for 100% ammonia removal and struvite to newberyite transformation. From the previous discussion, it is obvious that struvite morphology and hardness have significant effects on the percentage of ammonia removal upon decomposition as well as the number of cycles of efficiently recycling the decomposed product for struvite reformation. These topics will be discussed in Sections 5.4 and Section 5.5.

5.3.2.1.2 XRD results

In order to identify the formation of solid phases at the beginning of the experiment, XRD analysis was performed on each of the decomposed struvite samples heated for one hour, under optimum conditions. If dittmarite was identified at the beginning of the experiment, the corresponding operating conditions would not be utilized further for struvite to newberyite transformation. The XRD results are presented in Table 5.4. The XRD patterns, along with peak intensity and diffraction angles, are provided in Appendix D.2.

Table 5.4 XRD results of different sources and sizes of pellets after heating at 80°C and 95% RH for 1 hour

Samples from Pilot-scale Experiments		Struvite	Newberyite	Dittmarite
Types of Struvite	Size of Struvite Pellets			
Penticton B.C.	<1mm	Trace	+	-
	>1mm	+	+	+
Lulu Island	>1mm	+	+	Trace
Lulu Island crushed	<1mm			
Edmonton Gold Bar	<1mm			
Recrystallized	>1mm			

+ refers to detected compound, - refers to non-detected compound

In general, the presence of newberyite, along with struvite, was identified with each source and size of pellets. Table 5.4 shows that the smaller Penticton B.C. pellets contained trace amounts of struvite, with newberyite, after decomposition under optimum conditions for one hour. The pronounced newberyite peaks, along with trace struvite peaks, indicate the enhanced formation of newberyite compounds, thereby reducing residual struvite (Appendix D.2). The struvite peaks eventually disappeared with an increase in heating duration and were completely transformed into newberyite after 1.5 hours (Appendix D.2). On the other hand, a strong peak of dittmarite was found for the larger Penticton B.C. pellets, with one hour of heating. Based on the slope of the curves (Figure 5.25) and XRD results, it is evident that the ammonia removal decelerated once dittmarite formation began; this eventually became more prominent as the duration of heating period was increased. This also confirms why 100% ammonia removal from larger Penticton B.C. pellets is not possible, even after heating for 4 hours at optimum conditions, due to the formation

of dittmarite at the beginning of heating. For the same source of Penticton B.C. pellets with smaller size, newberyite was the only identified compound after 1.5 hours of heating.

The similarly-sized, larger Lulu Island pellets also contained a trace amount of dittmarite after one hour of heating at optimum conditions. As a result, greater ammonia removal was achieved from larger Lulu Island pellets, compared to larger Penticton B.C. pellets, for which a strong dittmarite peak was identified after a 1 hour heating period (Appendix D.2). In the case of larger pellets, dittmarite formed at the core of the pellets, where the temperature was high but access of steam was low, providing a favorable condition for dittmarite formation. Therefore, the ammonia removal efficiency for pellets from the same source was found to be higher for smaller sizes, compared to larger sized pellets.

Struvite decomposition was found to be slow for smaller and harder pellets, such as the Edmonton Gold Bar pellets. In Table 5.4, a trace amount of dittmarite, along with struvite, and newberyite was detected in the decomposed Edmonton Gold Bar pellets after one hour of heating. The presence of dittmarite along with struvite is responsible for the high residual ammonia after 1 hour of heating. Similar compounds were identified in the decomposed recrystallized pellets. However, pronounced struvite peaks were identified in the one-hour decomposed Edmonton Gold Bar pellets, whereas reduced peaks of struvite were obtained from decomposition of recrystallized pellets (Appendix D.2). This indicates that most of the struvite had already been transformed into newberyite, within one hour of heating in the recrystallized pellets, but only a small portion of struvite had been transformed into newberyite in the case of Edmonton Gold Bar pellets. Therefore, complete ammonia removal from the Edmonton Gold Bar pellets required a much longer time in comparison to the recrystallized pellets. Complete ammonia removal from the Edmonton Gold Bar pellets was achieved after heating at optimum conditions for more than 3 hours, whereas the recrystallized pellets showed complete ammonia removal after just 2 hours. This suggests that the trace amounts of dittmarite might not have increased over time and, as a result, complete ammonia removal was achieved from both types of pellets.

With regard to size, pellets smaller than 0.5 mm are not suitable, as it is difficult to maintain a stable fluidization regime with such small particles. The harder pellets, such as the Edmonton Gold Bar pellets, required a longer duration of heating, in order to achieve complete ammonia removal (which is not economically feasible). On the other hand, the very soft pellets, such as recrystallized pellets, are not suitable either for thermal decomposition, despite exhibiting high ammonia removal efficiency within a short period of time; these softer pellets easily disintegrate in the reactor and turn into dust during the experiment. Based on the size and hardness, Penticton B.C. and Lulu Island pellets, ranging from 0.5-1 mm, were found to be most suitable for the complete conversion of struvite to newberyite. However, the ammonia removal from smaller Penticton B.C. pellets was faster than for Lulu Island pellets; hence, the former pellets were chosen as the most suitable pellets for process optimization in the pilot-scale setup.

5.3.2.2 Penticton B.C. struvite pellets for process optimization

5.3.2.2.1 Chemical results and interpretation

As described in Section 5.3.2.1.1, the Penticton B.C. struvite pellets smaller than 1 mm, showed 100% ammonia removal potential at optimum conditions, after 1.5 hours of heating (Figure 5.25). The focus of this next phase was to further optimize the operating conditions with respect to temperature, relative humidity and duration of heating, using the smaller Penticton B.C. pellets. Energy consumption can be minimized if the transformation of struvite to newberyite is performed at a higher temperature and higher relative humidity, within a short period of time, rather than with lower temperature and lower relative humidity with prolonged heating. Figure 5.27 and Figure 5.28 represent residual ammonia and water content in the struvite decomposition product after heating at various combinations of temperature and relative humidity.

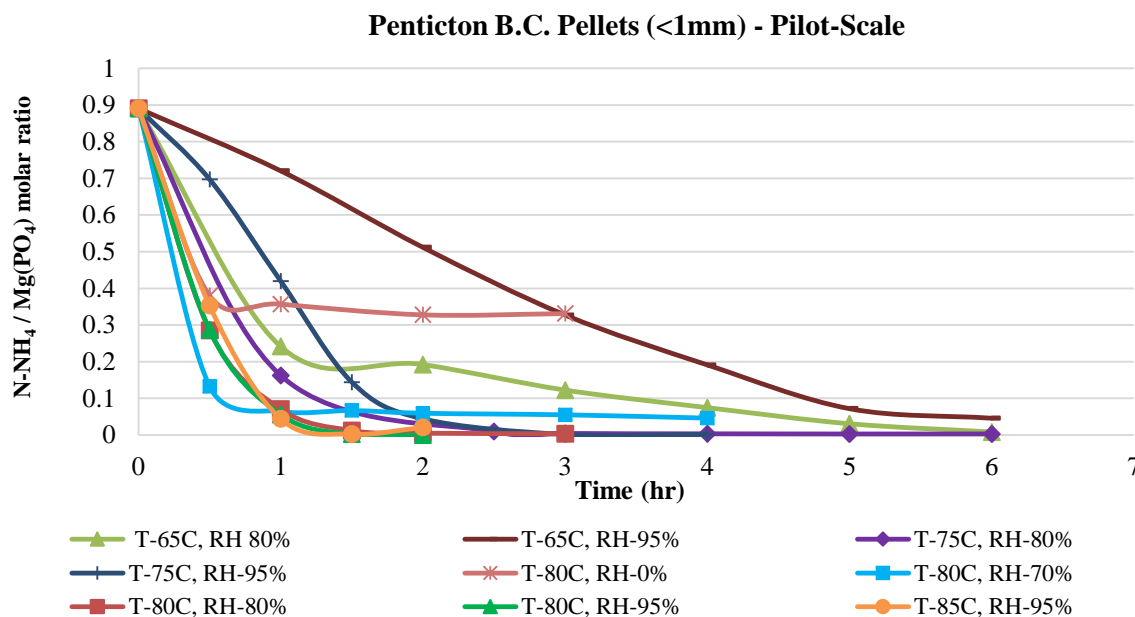


Figure 5.27 N-NH₄ molar ratio with respect to Mg (PO₄) of Penticton B.C. pellets (<1mm) heated at various combinations of temperature and relative humidity for different heating durations

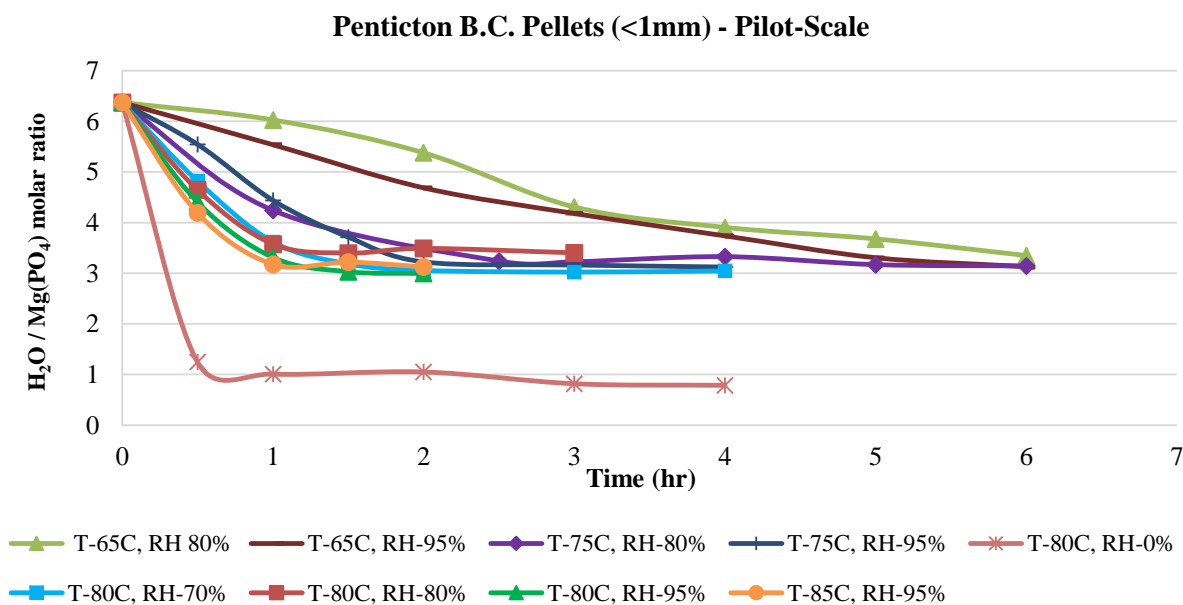


Figure 5.28 H₂O molar ratio with respect to Mg (PO₄) of Penticton B.C. pellets (<1mm) heated at various combinations of temperature and relative humidity for different heating durations

The first experiment was performed using smaller pellets at 80°C without any humidity, resulting in similar ammonia and water removal efficiencies to those of the oven dry experiments. Around 30% ammonia and one mole of water remained in the struvite decomposition product, after 4 hours of heating at 80°C. The use of hot air without steam may have caused the formation of an amorphous 2D layered structure, preventing the residual 30% ammonia removal from the struvite structure (similar to results from the oven dry experiments). From the bench-scale experiments, it was found that the ammonia removal process was much faster at higher humidity, compared to lower humidity, regardless of temperature. Therefore, in the pilot-scale experiments, the Penticton B.C. pellets (0.5-1mm) were heated at temperatures of 65°C, 75°C, 80°C, 85°C with humidities from 70% to 95%, in order to further optimize the operating conditions.

The ammonia and water removal efficiency was highest at 80°C followed by 75°C and 65°C at any particular humidity. The lowest ammonia removal efficiency was found at 70% humidity when struvite pellets were heated at 80°C. The residual ammonia content was found to be around 8% after 1 hour of heating and remained unchanged even after 4 hours of heating, indicating the formation of a layered structure which prevented ammonia evolution upon prolonged heating. The impurities might have been present in the struvite structure (Fattah, 2010) which has been considered as water content; therefore, the actual water content might be lower than 3 molecules as substantial dehydration occurred upon decomposition at 80°C with low humidity (70%).

Further increases in relative humidity up to 80% and 95% with 80°C heating caused 100% or complete ammonia removal within 1.5 hours. In order to confirm the complete conversion of struvite to newberyite, the XRD tests discussed in the following Section 5.3.2.2.2 were performed on the struvite pellets decomposed at 80°C with 80% and 95% RH. There was no significant difference in ammonia or water removal observed between the temperatures of 80°C and 85°C with 95% RH. Therefore, the process would be more energy efficient and economically feasible at 80°C rather than 85°C.

The ammonia removal was found to be much faster at lower humidity compared to higher humidity at temperatures below 80°C. The decomposed struvite samples contained more water molecules at lower humidity compared to higher humidity, which preserved the loose crystalline struvite

structure and promoted ammonia escape from the loose structure. Therefore, ammonia removal efficiency is optimal as long as more water remains in the structure. In Figure 5.27, the ammonia removal was initially faster with 80% RH compared to 95% RH whereas the water removal was slower at 80% compared to 95% RH when struvite decomposition was performed at both 65°C and 75°C. The reason for the high water content during struvite thermal decomposition at lower humidity instead of higher humidity cannot be identified. After 5 hours of heating, no significant difference in ammonia removal efficiency was observed between 80% and 95% RH with 65°C heating and eventually almost 95% ammonia was removed in these conditions. A similar outcome was also observed with 75°C heating with 80% and 95% RH, but complete ammonia was removed after only 3 hours of heating. Therefore, at lower temperature, complete ammonia removal can be achieved with prolonged heating as long as the residual solid phase contains no dittmarite.

5.3.2.2.2 XRD results

Table 5.5 indicates the XRD results of the decomposed solid samples obtained after heating smaller Penticton B.C. pellets at three different temperatures, with varying relative humidity and heating durations. The XRD patterns of decomposed solid samples heated under different conditions, containing peak intensity over different scanning angles, are presented in Appendix D.3. From the chemical analysis, it was found that both ammonia and water removal were very slow at lower temperature with a higher humidity. Likewise, the XRD results also confirmed that struvite to newberyite transformation was very slow during struvite decomposition at 65°C with 80% RH, and no trace amount of dittmarite was found in the decomposed struvite samples.

A high intensity struvite peak, compared to a newberyite peak, was found after heating struvite at 65°C with 80% and 95% RH for 2 hours (Appendix D.3). The intensity of the struvite peak decreased as the duration of heating increased and the newberyite peaks became more prominent after 5 hours of heating; this infers that the transformation process from struvite to newberyite increases with an increase in heating duration. Therefore, it is possible to achieve complete removal of ammonia from struvite at lower temperatures, with higher humidity, although the transformation process is very slow. Struvite heating at lower temperatures, with higher humidity, can save energy, provided it is performed within a short period of time; otherwise, the process will

not be energy efficient if prolonged heating is required. For the mentioned operating conditions, the struvite to newberyite transformation process required more than 6 hours. Similar XRD results were found at 75°C with 80% and 95% RH (Table 5.5), where struvite to newberyite transformation, through the release of 100% ammonia, occurred after 3 hours instead of 6 hours.

Table 5.5 XRD results of Pentiction B.C. pellets after heating at various temperatures and relative humidity

Pentiction B.C. Pellets (<1mm)			Struvite	Newberyite	Dittmarite
Temperature, (°C)	Relative Humidity, (%)	Duration of Heating, (hours)			
65°C	80%	2, 5	+	+	-
	95%				
75°C	80%	1	+	+	-
	95%				
80°C	70%	0.5	+	+	Trace
		1.5	-	+	+
		2, 4	-	+	+
	80%	1.5	-	+	Trace
		2	-	+	Trace
	95%	1.5	-	+	-

+ refers to detected compound, - refers to non-detected compound

Further increases in temperature caused faster and greater removal of ammonia from the struvite structure, within a short period of time. The ammonia removal rate was much greater within one hour of heating at 80°C with 70% RH, compared to 80% RH and 95% RH (Figure 5.27). However, the decomposed solid phase contained dittmarite, along with newberyite, after 1.5 hours of heating at 80°C with 70% RH (Table 5.5). Therefore, the prolonged heating could not release the residual ammonia from the Pentiction B.C. pellets, since the residual ammonia after one hour of heating belonged to the dittmarite compound (further impeding ammonia evolution). The XRD results confirm that struvite heating at higher temperatures, with lower humidity, facilitated dittmarite formation at the beginning of struvite thermal decomposition, causing incomplete ammonia removal (even after longer duration of heating).

At 80°C, both ammonia (Figure 5.27) and water (Figure 5.28) removal were similar with 80% and 95% RH, where 100% ammonia removal was accomplished within 1.5 hours. The XRD results for struvite samples decomposed at 80°C, for 1.5 hours, showed the presence of trace amounts of dittmarite, along with newberyite, after heating with 80% RH; whereas, the residual solid phase was composed of newberyite, when heated with 95% RH. This technology would be efficient only if struvite can be completely transformed into newberyite, without any dittmarite formation. The decomposed solid containing dittmarite, even in trace amounts, could significantly reduce the efficiency of the process. The presence of dittmarite in the decomposed sample may increase after each completion of the cycle and this solid phase (containing dittmarite) cannot be used further in the aqueous ammonia removal process.

The monitored data (Figure 5.24), referring to the relative humidity, showed that the overall relative humidity varied $\pm 10\%$. The fluctuations in relative humidity may have caused trace amounts of dittmarite to be formed at 80% RH. The transformation of struvite to newberyite would be more efficient if the process parameters could be controlled more precisely. After monitoring the relative humidity corresponding to 100% ammonia removal efficiency, the operating range in terms of relative humidity for struvite to newberyite transformation can be varied in between 80% and 100% (Appendix E). Considering energy consumption, desirable end product, and probability of condensation, the relative humidity range can be narrowed down further from 95% to 85%. Therefore, struvite can be fully transformed into newberyite within a short period of time at 80°C with $85\pm 5\%$ RH.

5.4 Struvite morphology

While powder XRD analysis provides information related to phase composition of the solids, some physical properties, such as crystal morphology, size and habitus, can be identified with microscopic analysis. The ammonia removal efficiency is believed to be dependent on the compactness of the pellets, including both the interior and exterior of the pellets. Therefore, the scanning electron microscopy (SEM) analysis performed by different authors, on both interior and exterior surfaces of different sources of struvite pellets, are discussed in the following section, in an attempt to identify the correlation between pellet compactness and ammonia removal efficiency.

5.4.1 Background

The compactness of struvite pellets has been determined through SEM imagery by different authors using harvested pellets produced from different sources, under various controlling conditions. The compactness of the pellets varied depending on size and other controlling factors involved, during struvite harvesting and crystallization (Fattah, 2010). Fattah performed SEM tests on the pellets harvested from the LIWWTP to observe the controlling factors on struvite morphology and hardness. Figure 5.29 represents the SEM images of the interior and exterior surface of the harvested Lulu Island pellets by Fattah.

Different sizes of pellets have different compactness and hardness, depending on both interior and exterior composition of the pellets. The author reported that the exterior surface of the Lulu Island pellets was smooth and coated with an outer layer 0.1mm thick, which might be the reason for a higher hardness value. On the other hand, the interior was found to be composed of small, individual crystals which were loosely packed, softer and less dense.

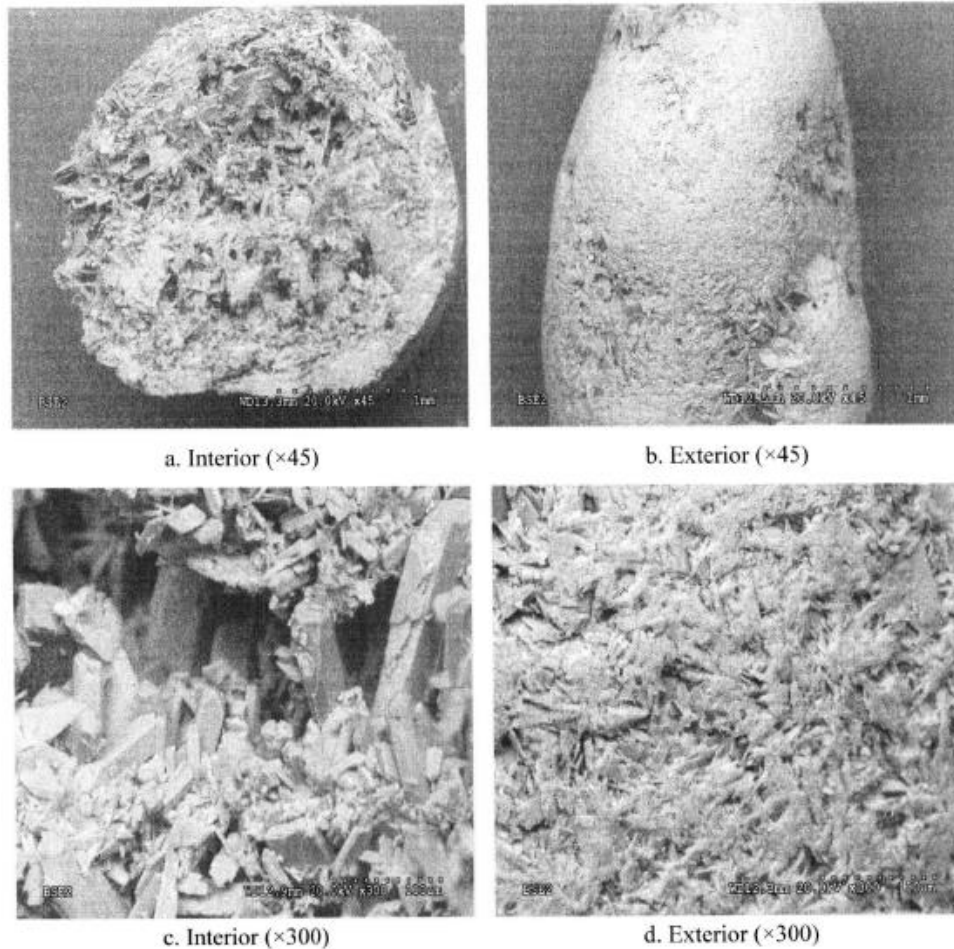


Figure 5.29 SEM images of the interior and exterior of Lulu Island pellets harvested in LIWWTP (Fattah, 2010)

Huang (2003) also harvested Lulu Island pellets and performed SEM on the interior and exterior surfaces. The harvested pellets had a diameter of more than 4.75 mm and exhibited both smooth and coarse surfaces, which are shown in Figure 5.30 (a, b, c and d). The SEM images of the pellet interiors ($4.75\text{mm} > d > 2.83$), obtained by the same author, are presented in Figure 5.30 (e, f). According to Huang (2003), the exterior surface consisted of tightly-aggregated, brick and rod-like crystals, clearly visible under 3000X magnification (Figure 5.30, d). The pellets were loosely aggregated in the core and therefore, weak in terms of structural strength. During harvesting, if both the core and edge of the pellets become tighter, then the entire pellet would be stronger and much more difficult to break.

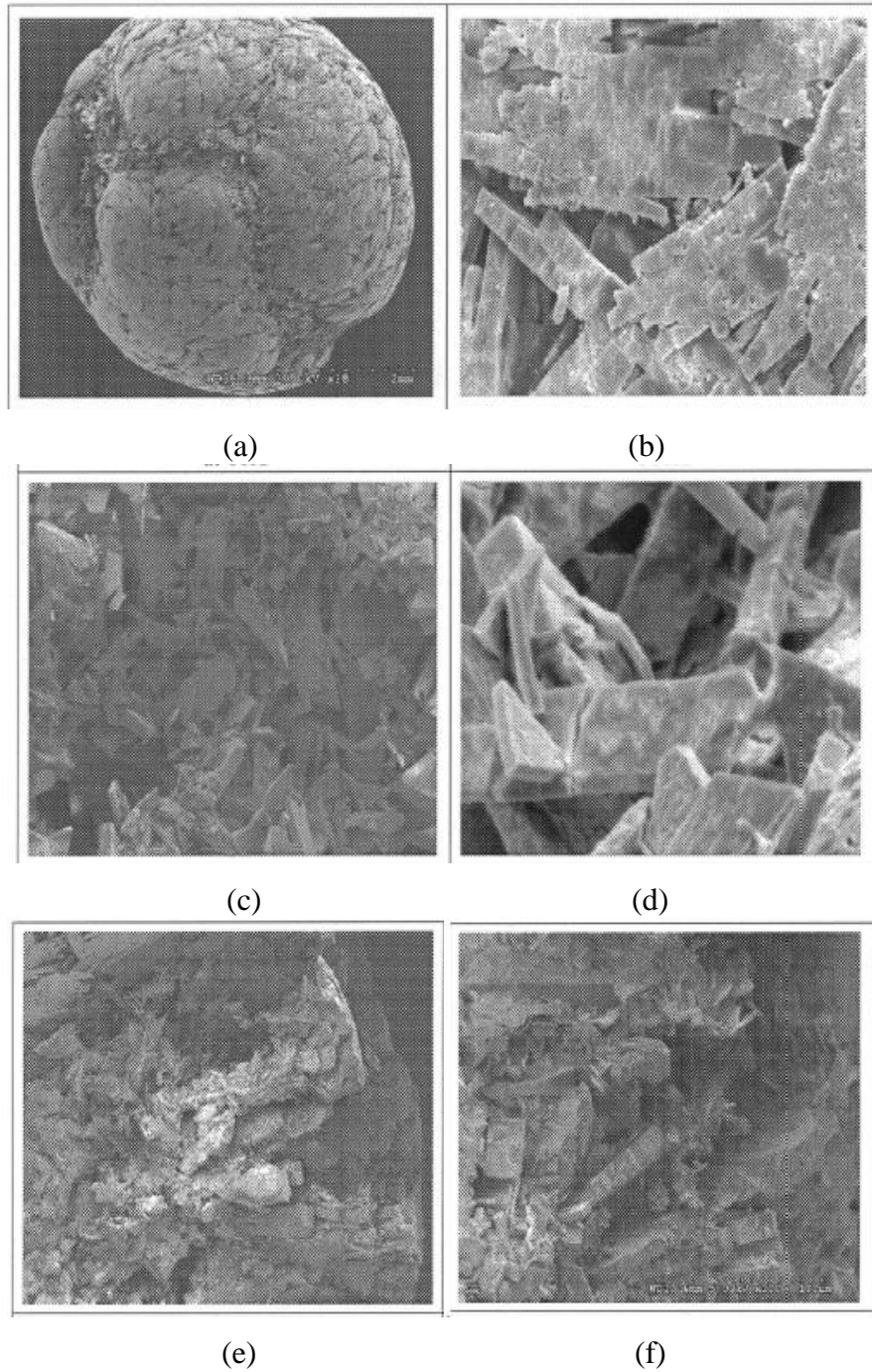


Figure 5.30 SEM images of the Lulu Island pellets (a) exterior surface magnified at 18X (b) exterior smooth surface magnified at 300X (c) exterior coarse surface magnified at 300X (d) exterior coarse surface magnified at 3000X (e) interior surface magnified at 50X and (f) interior surface magnified at 300X (Huang, 2003)

Another study was performed by Novotny (2011) on Edmonton Gold Bar struvite pellets (2-2.36 mm). The SEM images (Figure 5.31 and 5.32) of the interior of the raw pellets are shown in Figure 5.32, specifically. The interior surface of the pellets was very smooth and composed of distinct layers like an onion. There were no cracks or porosity observed for these pellets at 70x (Figure 5.31, b) magnification, whereas these features were visible at 45x magnification (Figure 5.29, b) in Lulu Island pellets. However, hair line cracks were observed in the interior surface after magnifying up to 500x (Figure 5.31, b). The Edmonton Gold Bar pellets seemed to be more compact and dense, compared to the Lulu Island pellets, at 300x (Figure 5.30, b) magnification.

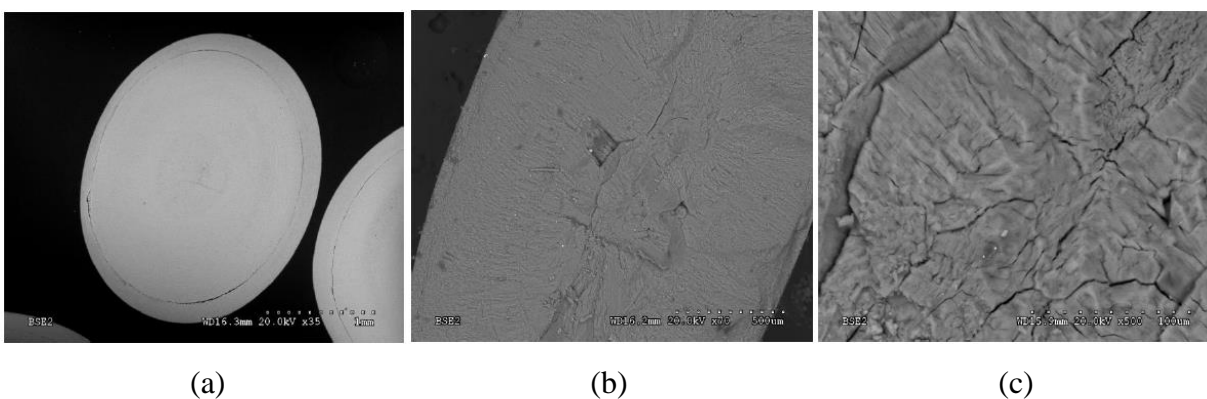


Figure 5.31 SEM images of raw Edmonton Gold Bar struvite interior (a) 35X, (b) 70X and (c) 500X (Novotny, 2011)

Novotny (2011) also performed SEM imagery on the interior surface of heated Edmonton Gold Bar pellets and the images are presented in Figure 5.32. Thermal decomposition of these pellets caused cracks on the surface, that eventually allowed for ammonia and water evolution; whereas, the raw Lulu Island pellets contained a rougher needle-like surface before thermal treatment which might explain the higher ammonia evolution from these pellets compared to the Edmonton Gold Bar pellets.

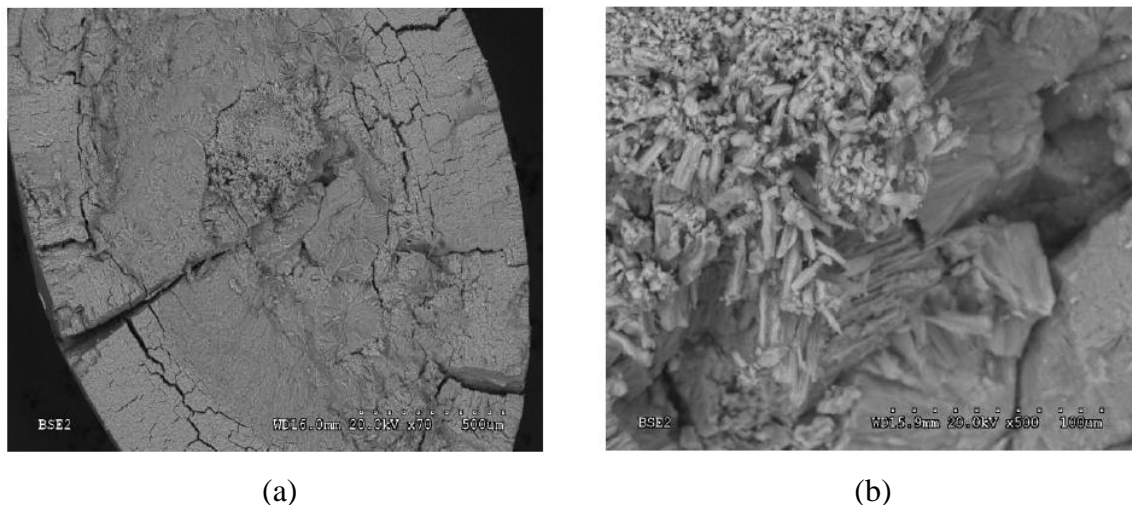


Figure 5.32 SEM images of interior surface of heated Edmonton Gold Bar pellets (a) 70X and (b) 500X (Novotny, 2011)

Britton (2002) also took SEM images of the Penticton B.C. pellets harvested from the COP AWWTP. The core of the pellets consisted of fine, needle-like particles that were loosely packed and weaker than the exterior shell. The exterior shell consisted of tightly-aggregated, smaller, brick-like crystals mentioned by Britton, whereas after re-inspecting the same SEM images, Forrest (2004) concluded that the outer shell of the Penticton B.C. pellets was much less tightly aggregated than previously reported. Britton also performed the SEM under 3000X magnification and the outer surface was visibly covered with cracks and fissures.

5.4.2 Specific objective and hypothesis

The morphology of the struvite pellets decomposed in this study was focused on to answer the following questions.

- How do the struvite pellets of different sources and sizes differ in terms of morphology?
- How does the morphology of various struvite pellets affect the ammonia removal efficiency?

Hypothesis

- The different sources and sizes of pellets are believed to possess different physical characteristics, including both the interior and the exterior surfaces of the pellets; this might explain the different ammonia removal efficiencies.

5.4.3 Results and discussion of struvite morphological studies

In this study, struvite pellets with various size, source and hardness were thermally decomposed, in order to transform the struvite into newberyite through 100% release of ammonia. Previous research show that the Lulu Island and Penticton B.C. pellets are loosely packed (Fattah, 2010; Huang, 2003) whereas the Edmonton Gold Bar pellets are tightly aggregated (Novotny, 2011). To understand how these external structural features affect ammonia removal efficiency, the exterior surface of struvite samples from different sources was examined. Figure 5.33 shows the external appearance of the Edmonton Gold Bar and recrystallized struvite pellets, under microscopic view.

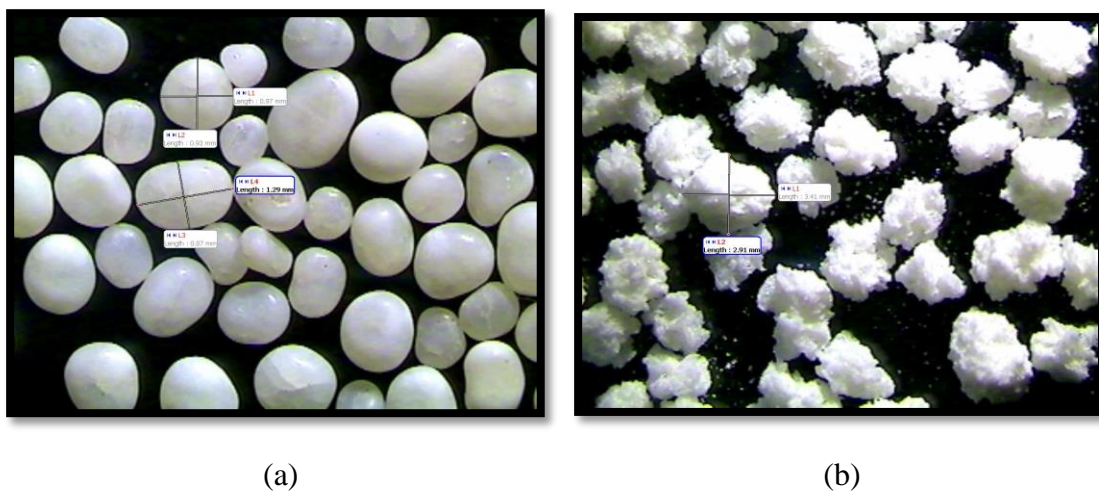


Figure 5.33 Morphology of the struvite pellets from different sources (a) Edmonton Gold Bar pellets (<1mm) (b) recrystallized pellets (>1mm)

The morphology of the Edmonton Gold Bar pellets showed a smooth round surface and no sharp edges, consistent with the SEM results performed by Novotny (2011). There were no cracks or porosity evident on the exterior surface. From the previous section, it was seen that the interior was similar to the exterior making the Edmonton Gold Bar pellets strong in terms of hardness (Novotny, 2011). Therefore, steam could not permeate through the solid round, hard and smooth surface of these pellets and, hence, formation of dittmarite had occurred in both the bench-scale and pilot-scale experiments, in several cases. On the other hand, the recrystallized pellets produced at the pilot plant contained a porous exterior with sharp edges, instead of the round and smooth surfaces of Edmonton Gold Bar pellets. Thus, high ammonia removal efficiency was achieved from the porous, softer recrystallized pellets.

The exterior surface of Lulu Island (size <1mm and size >1mm) and Penticton B.C. pellets (size <1mm and size >1mm) are shown in Figure 5.34 (a, b) and 5.34 (c, d), respectively. The images of pellets smaller than 1 mm and larger than 1 mm were obtained at 2X and 1X magnification, respectively. The smaller and larger pellets from the same source can differ significantly, depending on the exterior physical characteristics. The smaller Lulu Island pellets appeared as small crystals with pores, whereas the larger pellets had a coarse surface and consisted of aggregation of smaller pellets. A similar observation has been reported by previous researchers (Fattah, 2010; Huang, 2003). Both sizes of Lulu Island pellets were porous, which make them softer than the Edmonton Gold Bar pellets in terms of strength. Likewise, pores and sharp edges were found in the smaller Penticton B.C. pellets which also exhibited different shapes such as round, elongated and flaky. The porous and softer surface of smaller Penticton B.C. pellets allowed more ammonia release, compared to the smooth and harder exterior surface of the Edmonton Gold Bar pellets. However, the larger Penticton B.C. pellets varied from smooth and hard (like Edmonton Gold Bar pellets) to round and flaky, with a porous surface, that was similar to the smaller Penticton B.C. pellets. Therefore, the larger Penticton B.C. pellets showed less ammonia removal efficiency than the smaller Penticton B.C. pellets, in the pilot-scale experiment (Figure 5.25). Based on the exterior surface morphology of the smaller Lulu Island and Penticton B.C. pellets, it appears that the steam in the bench and pilot-scale experiments easily passed through the surface of these pellets, preventing dittmarite formation at the core. Therefore, the ammonia

removal efficiency was higher from smaller Lulu Island and Penticton B.C. pellets, during thermal decomposition under optimum conditions.

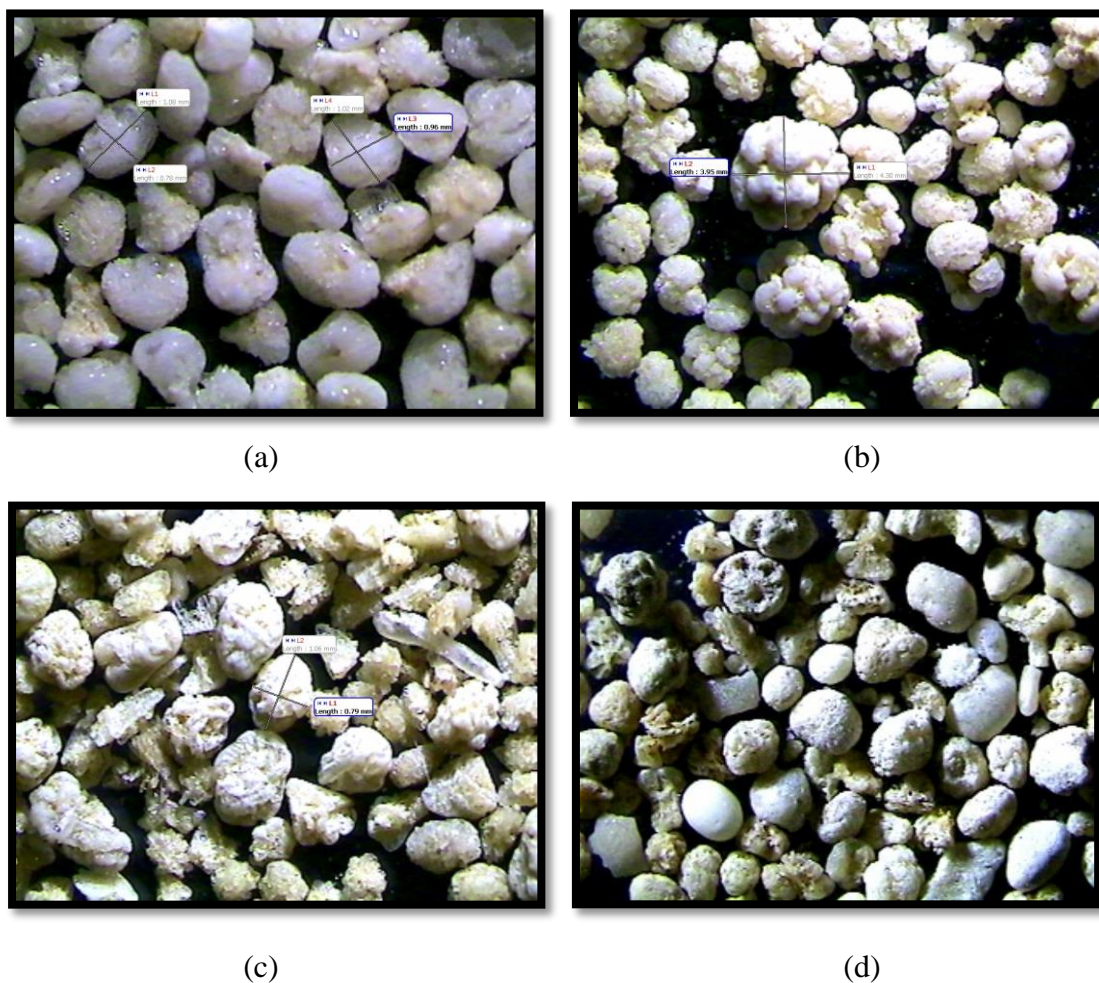


Figure 5.34 Struvite morphology of the raw pellets (a) Lulu Island Pellets (<1mm) (b) Lulu Island pellets (>1mm) (c) Penticton B.C. pellets (<1mm) (d) Penticton B.C. pellets (>1mm)

Figure 5.35 presents the images of the exterior surfaces of decomposed struvite pellets from different sources, after heating at optimum conditions. During thermal decomposition of smaller Penticton B.C. pellets, the sharp edges were transformed into a smooth surface. The pores on the Penticton B.C. pellets became more prominent after 2 hours of thermal decomposition, during which ammonia and water were believed to escape. The smaller Lulu Island pellets, heated under optimum conditions in the bench-scale experiment, showed a similar ammonia removal efficiency

to that of the smaller Penticton B.C. pellets (Figure 5.22). The smaller Lulu Island pellets, which showed complete ammonia removal, were also transformed into a smooth shape, with holes in the exterior surface. In the case of the Edmonton Gold Bar pellets in pilot-scale experiments, their morphology was similar to that of the raw pellets. There was no porosity on the exterior surface of these pellets observed, before or after heating for 4 hours and therefore, they showed the least ammonia removal upon decomposition under optimum conditions.

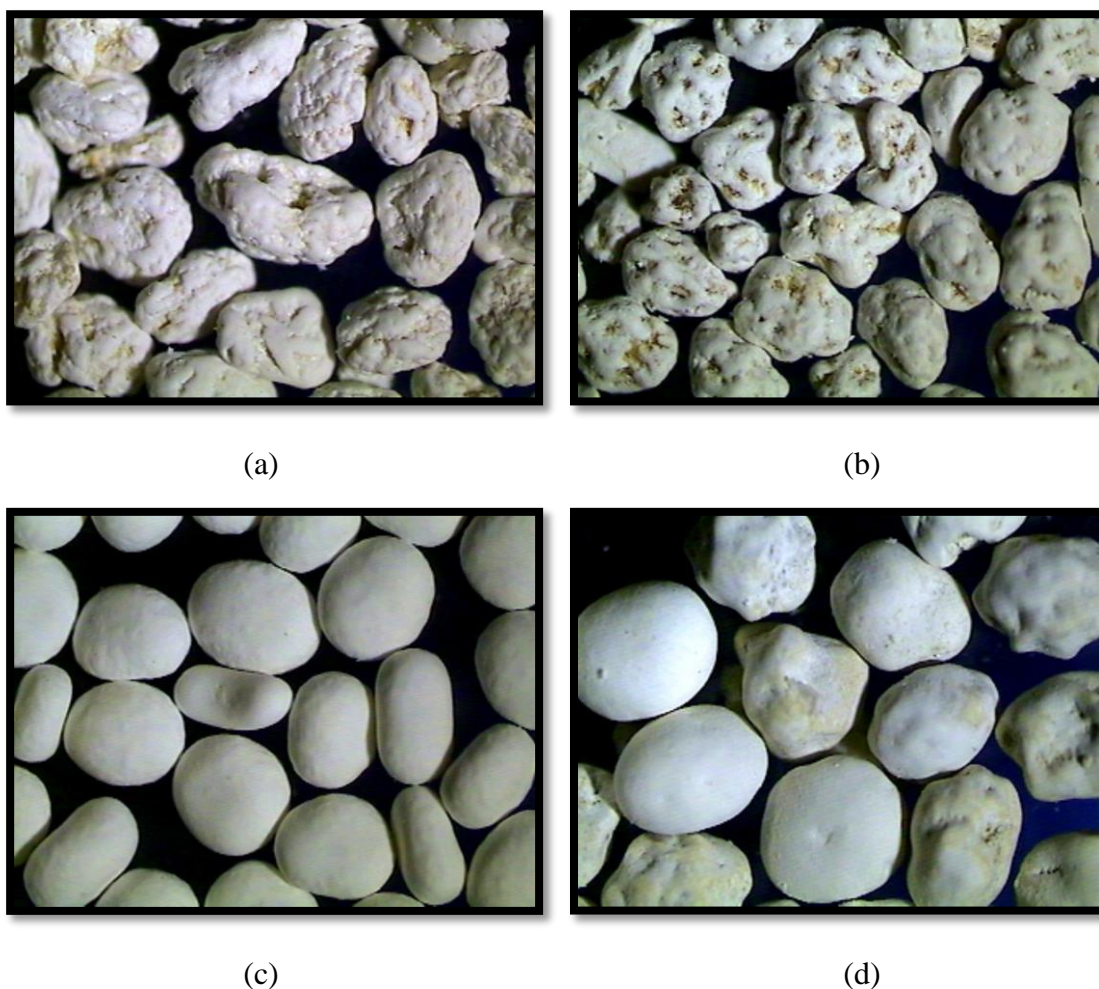


Figure 5.35 Struvite morphology of the pellets after heating at 80°C, 95% RH (a) Penticton B.C. pellets (<1mm)-pilot-scale, 2hr at 3X magnification (b) Lulu Island Pellets-bench-scale (<1mm), 2hr at 3X magnification (c) Edmonton Gold Bar pellets (<1mm), 4hr at 3X magnification (d) Penticton B.C. pellets (>1mm), 4hr at 3X magnification

Some of the larger Penticton B.C. pellets were hard, similar to the Edmonton Gold Bar pellets and showed similar morphology, even after heating at optimum conditions for 4 hours. However, the surface of the Penticton B.C. pellets which was initially rough changed into smooth exterior surface with holes after decomposition process. Therefore, the non-uniform structural characteristics of the larger Penticton B.C. pellets resulted in lower ammonia removal efficiencies, compared to the smaller Lulu Island and Penticton B.C. pellets, upon heating under optimum conditions (Figure 5.25).

In terms of size, porosity and structural characteristics, the smaller Penticton B.C. pellets showed similar properties to those of the small Lulu Island pellets. Larger pellets could be used for thermal decomposition, as long as they possess enough porosity for ammonia evolution. On the other hand, larger pellets that possess higher porosity (i.e. softness), may transform into powder during thermal decomposition, causing improper fluidization and dittmarite formation. Therefore, struvite pellets such as Edmonton Gold Bar (<1mm) and recrystallized (>1mm) pellets cannot be used for thermal decomposition, due to the limited ammonia removal efficiency achievable and the possibility of disintegration upon heating, respectively. Hence, struvite pellets with morphologies that are similar to both smaller Penticton B.C. and Lulu Island pellets, are suitable for complete conversion of struvite to newberyite, within a short period of time.

5.5 Crushing strength of different sources and sizes of pellets

The previous section covered the morphology of various types, sizes and sources of struvite pellets. The strength of struvite pellets is also an important parameter, as it influences the ammonia release capacity of decomposing struvite pellets. The difference in ammonia removal efficiency across different sources and sizes of pellets was explored in Section 5.4, using struvite morphology. To further indicate the importance of struvite morphology in ammonia removal capacity, the strength of the pellets was measured, believed to be influenced by the structural composition of the pellets.

In this section, the crushing strength of different pellets of varying sources and sizes were measured and reported to answer the following questions.

- Why does the ammonia removal efficiency vary with different sizes and sources of struvite pellets?
- Is there any correlation among structural character, crushing strength and ammonia removal capacity?

Hypothesis

- Different sources and sizes of pellets are believed to have different crushing strengths. During struvite thermal decomposition, the crushing strength of struvite is believed to be one of the major influencing factors for maximizing ammonia removal efficiency.

5.5.1 Influence of parameters on crushing strength of struvite pellets

Variations in the crushing strength across different sources and sizes of struvite pellets indicate that the structural strength of the pellets is influenced by size, physical characteristics and compactness. Struvite from different wastewater streams produced, under different operating conditions, can possess different structural strengths. The crushing strength is expected to be lower if the pellets are loosely packed, whereas it is expected to be higher for tightly-packed pellets (Fattah, 2010). Variations in size and shape and the prevalence of pores and defects, may result in differences in the crushing strength of different sources of struvite pellets.

5.5.2 Influence of size, shape and structural composition on crushing strength

Figure 5.36 illustrates the relationship between the size of different sources of pellets and crushing strength. The crushing strength data are based on resistance obtained from crushing 100 or more pellets of each category. In general, there was no significant difference between the average and median crushing strength value at each source and size of pellets. The average crushing strength was found to be highest for smaller Edmonton Gold Bar pellets (1000 g), followed by larger

Penticton B.C. (827 g), larger Lulu Island (800 g), smaller Lulu Island (545 g) and finally, smaller Penticton B.C. pellets (395 g). The standard deviation of the crushing strength value was found to be high in each set of pellets, due to variations in shape such as elongated, flaky and round.

From the SEM images, the exterior pellet surface was thought to be much harder than the interior, except for Edmonton Gold Bar pellets that had similar physical characteristics and compactness both inside and outside. The maximum crushing strength value was obtained for the Edmonton Gold Bar pellets and varied between 650 g and 1350 g. The exterior surfaces of the Edmonton Gold Bar pellets were round and smooth, without any porosity or cracks. The thicker coating of these pellets may have increased the crushing strength value, reducing the ammonia removal efficiency by blocking the interior and exterior pores of the pellets (Fattah, 2010). In addition, the Edmonton Gold Bar pellets smaller than 1mm were much less porous than other pellets of similar size, such as Penticton B.C. and Lulu Island pellets, resulting in the lowest ammonia removal efficiency under the optimum conditions at the pilot plant.

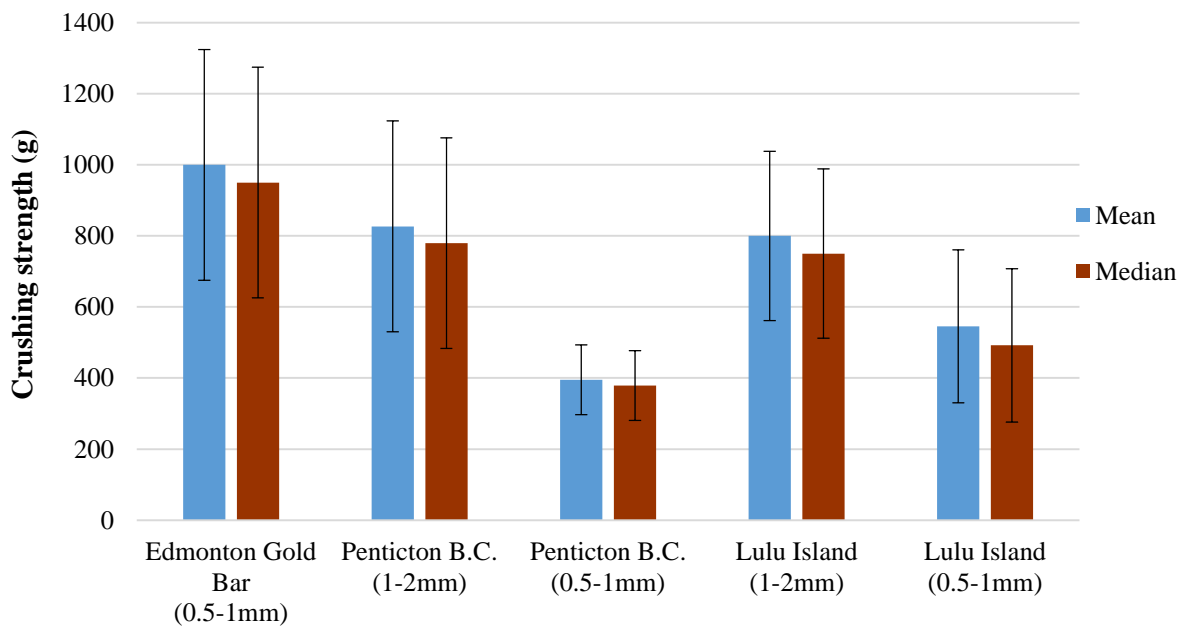


Figure 5.36 Influence of pellet size and sources on crushing strength. Error bars: 95% confidence interval

For pellets from a single source, smaller pellets showed lower crushing strength, compared to larger pellets. However, similarly sized pellets from different sources may have the same or a different crushing strength value. For both Penticton B.C. and Lulu Island pellets, the larger pellets showed more resistance (827 g) than smaller pellets (395 g) upon crushing, using the UBC hardness tester. The larger Penticton B.C. pellets included different shapes of pellets and some of them were as hard as the Edmonton Gold Bar pellets, as noted in Section 5.4.3. The crushing strength value was found to be similar in the larger Lulu Island (800 g) and Penticton B.C. pellets (827 g), which also showed similar ammonia removal efficiencies (Figure 5.25). On the other hand, the smaller Penticton B.C. pellets were more consistent in size, shape and porosity; hence, the standard deviation was also smaller, compared to other sources and sizes; in addition ammonia removal efficiency was highest with these pellets, under heating at optimum conditions. The struvite pellets formed in the UBC pilot plant from synthetic newberyite (i.e. recrystallized pellets) were crushable between one's fingers, in order to acquire a qualitative measure of hardness. These pellets were too soft to measure the hardness using the UBC hardness tester and showed no value during crushing. The pellets transformed into powder due to attrition during heating for 3 hours, at optimum conditions, in both the pilot and bench-scale reactors. Therefore, without any quantitative hardness measure, it can be assumed that the recrystallized pellets are softest, and hence, provided similar ammonia removal efficiencies as smaller Penticton B.C. pellets.

5.6 Cost estimation and economic benefits over other ammonia removal and recovery methods

The proposed ammonia recovery technology would require three different stages, for which the operating costs will differ, depending on the controlling parameters. The process involved at each stage is presented in Figure 5.37. In the Stage 1: struvite thermal decomposition - the operating cost involves high energy consumption, due to the need for hot air and steam. Stage 2: struvite recrystallization - requires chemicals such as acid and caustic, as well as energy consumption through operating pumps. Stage 3: this involves ammonia capture evolving from Stage 1. The recovery of ammonia gas evolving from Stage 1 requires the cost of an adsorbent but revenue can be generated through using the recovered ammonia as a liquid fertilizer or fuel.

The 1st and 3rd stages of this ammonia recovery technology are interdependent and currently under development. During stage 1 of struvite thermal decomposition, ammonia and moist air are evolved and released into the atmosphere. The ammonia-containing moist air would be captured in the 3rd stage, through an adsorption method, where moist air will be separated from the ammonia gas. The separated moist air can be recycled and reused further after passing through the humidifier; this will eventually reduce the cost of the external steam supply by recycling 50% of the steam. In this study, steam was supplied continuously without any recycling, since Stage 3 is still under development. Therefore, the major cost in the 1st stage (struvite thermal decomposition), comes from steam generation; it has been roughly estimated that the operating cost of N removal, without steam recycling, is 34-40 CAD/kg N removed.

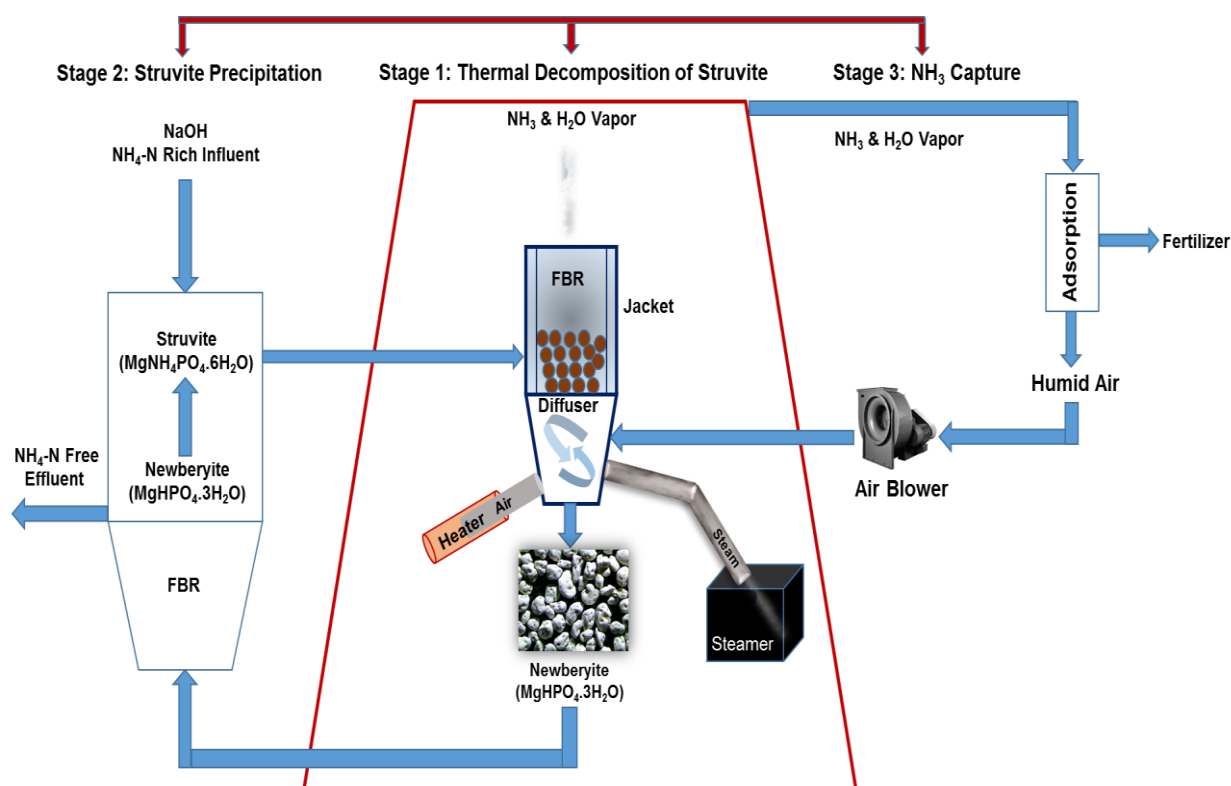


Figure 5.37 Process flow diagram of proposed ammonia recovery technology

In addition to the steam consumption, the jacket temperature must be constantly maintained at a higher temperature than the reactor, to prevent condensation. For this purpose, hot air is introduced continuously inside the jacket, which is released into the atmosphere without any recycling. The

hot air exiting from the jacket can either be returned to the reactor or recycled through the jacket. Therefore, the cost involved in the 1st stage can be reduced further by recycling the hot air exiting the jacket and the moist air leaving the reactor. The costs involved in the 2nd generation system for struvite thermal decomposition with heat, moist air recycling, and struvite recrystallization, with reduced chemical consumption, have been estimated in this work and are presented in Table 5.6. Details of cost estimation can be found in Appendix F.

Table 5.6 The operating cost involves in the 2nd generation of proposed ammonia recovery technology

Present technology detailed layout	Parameters	Operating costs, CAD/kg N removed
1 st stage of struvite thermal decomposition	Energy (heat, steam)	3.0
2 nd stage of struvite recrystallization	Chemicals (acid, caustic)	4.5
	Energy (pumps)	0.5
3 rd stage of ammonia recovery	Adsorbent (Oxalic acid)	3.0
Total Cost (1 st + 2 nd)		8.0
Total Cost (1 st + 2 nd + 3 rd)		11.0
Total cost after deducting the market value of recovered ammonia: 19 CAD/kg (Fertilizer/Fuel)		-8*

*Total cost = operational cost including 3rd stage ammonia capture – market value of recovered ammonia

The costs at the 2nd stage of struvite recrystallization can be reduced further by lowering chemical costs, which is currently being investigated at UBC. The operating costs of the entire system are interrelated. The 3rd stage of the cost is due to the adsorbent which is around 3 CAD whereas the economic value of the extracted product would be around 19 CAD/kg (used as liquid fertilizer). The economic value of the recovered ammonia depends on the form of the extracted product. After recovering ammonia as a commercially available product, the overall operating cost of the entire technology could be a negative 8 CAD/kg of N removed; in other words, the overall cost could be transformed into revenue. The greatest advantage of this entire technology might be the revenue earned during ammonia removal from wastewater.

A comparison of operating costs between different ammonia removal and recovery technologies from wastewater is presented in Table 5.7. It should be noted that the operating costs of the proposed recovery technology presented in the Table 5.7, only considers the costs involved in stage 1 and 2; the price of recovered product (fertilizer) is not included. The proposed ammonia

recovery technology would be economically feasible; compared to the current ammonia recovery technologies involving struvite crystallization, using commercially available Mg and PO_4 . The other ammonia recovery methods, such as ion exchange and the membrane method, have limitations with treating highly-concentrated, ammonia-rich wastewater. During treatment of centrate, the possibility of plugging membranes and ion exchange resins by the solids present in typical WWTP centrate, cannot be avoided and will increase the maintenance cost, or require more sophisticated filtration.

Table 5.7 Operating cost comparison among different ammonia removal and recovery methods

Technology for ammonia removal/recovery	Operating costs, CAD/kg N removed	References
Conventional air stripping *	13	Cilona et al., 2009
Nitrification/denitrification	6-13	
ANAMMOX	1-8	
Struvite crystallization (no Mg, no P reuse) *	13	
Struvite crystallization (with Mg, P reuse) – present technology *	8	Present study
* added value of recovered product not accounted for		

As far as ammonia removal methods are concerned, the proposed recovery method is economically feasible compared to a conventional air stripping method. However, the operating cost of the proposed technology is comparable to other ammonia removal methods, such as nitrification/denitrification and ANAMMOX, even if the economic value of the recovered commercially available product is not considered. The proposed technology would be economically and energetically more efficient, compared to other methods, due to successful process development at each stage, process optimization, heat and moist air reuse, and reduction of chemical consumption.

5.7 Options for increasing ammonia recovery efficiency and the reduction of operational costs

The purpose of this study was to identify and evaluate all of the essential operating parameters for struvite thermal decomposition, these providing sufficient information for practical implementation of a cost-effective ammonia recovery process. It should be noted that 100% ammonia removal from struvite can maximize the aqueous ammonia recovery efficiency from wastewater, which represents the combined N recovery efficiency of the entire technology. However, 100% ammonia removal from struvite, upon thermal decomposition, may increase operational costs which, in turn, may hinder wide application of the technology. From an economic perspective, the decomposed product, containing small amounts of ammonia, could still be used in the ammonia recovery process. The overall challenges associated with various N recovery options, based on the first two stages (struvite decomposition and recrystallization) of the entire technology, are summarized in Table 5.8.

Table 5.8 Advantages and disadvantages associated with different options for combined ammonia recovery processes

Different options for combined N recovery process		Struvite thermal decomposition stage	
		Residual NH ₃ associated with struvite	Residual NH ₃ associated with dittmarite or a 2D amorphous layered structure
Struvite recrystallization stage	Without acid dissolution	+ High recovery efficiency can be achieved subject to N residual percentage	- Limited number of cycles
		- May increase the operational cost of decomposition	+ Possible reduction of operational costs at decomposition stage
	With acid dissolution	- Limited N recovery efficiency Or addition of excess decomposed product	
		- Increased operational costs of struvite recrystallization	

+ refers to advantages and – refers to disadvantages of the different options for ammonia recovery process.

Case 1: Without acid dissolution of decomposed products containing layered structure

The efficiency of this entire technology depends on the maximum number of cycles that can be performed by recycling the decomposed product as a source of magnesium and phosphate, for additional struvite reformation. Greater re-use of the decomposed product will make this process more economically and energetically efficient, as well as industrially applicable. The recyclability of the decomposed product not only depends on the ammonia removal efficiency from struvite during thermal decomposition, but also on the final composition of the decomposed solid phase. The number of re-use cycles that can be utilized for ammonia recovery, by recycling the decomposed product with varying residual ammonia content (in the form of struvite or dittmarite), are presented in Figure 5.38. It should be noted that Figure 5.38 represents only the theoretical estimation of combined N recovery efficiency, based on various ammonia removal efficiencies (70%, 80% and 95%) and composition of the final decomposed products (struvite, or dittmarite along with newberyite).

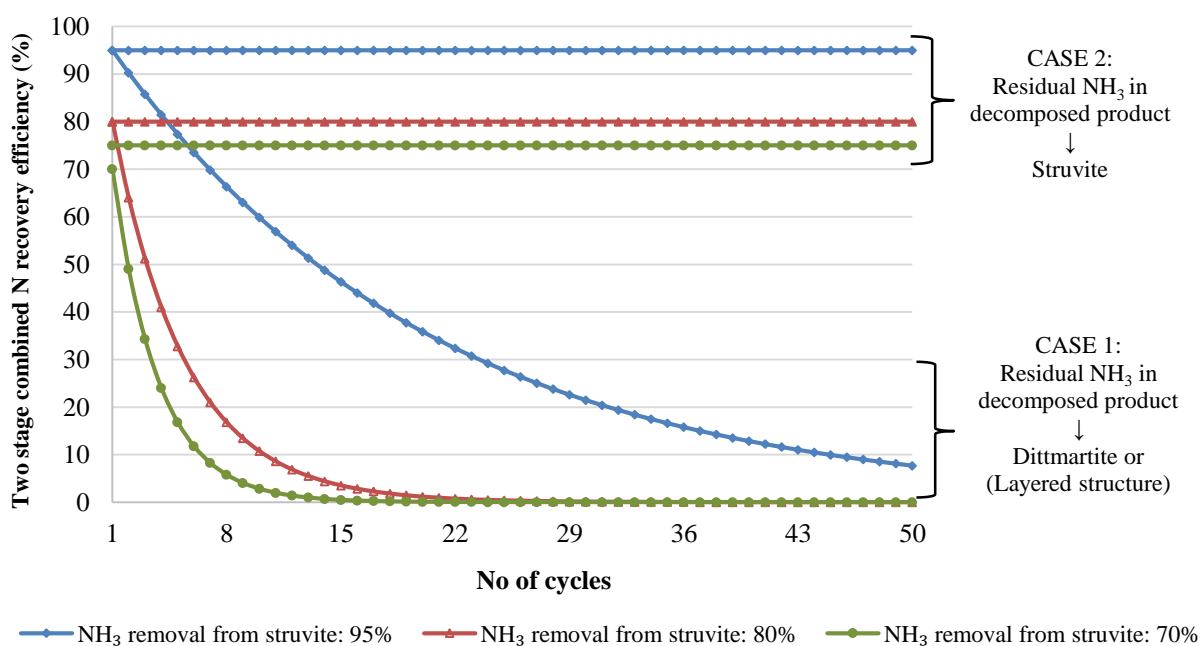


Figure 5.38 Combined nitrogen recovery efficiency over number of cycles at different ammonia removal efficiencies from struvite (without addition of excess decomposed product)

The decomposed product is assumed to be a combination of newberyite and a layered structure (including dittmarite or a 2D amorphous layered structure), or a combination of newberyite and struvite. For instance, at 95% ammonia removal efficiency from struvite, the 5% residual ammonia could be in the form of either struvite or dittmarite, depending on the manner of struvite thermal decomposition utilized. In the struvite recrystallization stage, it is also assumed that the percentage of newberyite present in the decomposed product will be completely transformed into struvite through recrystallization, representing a combined N recovery efficiency from wastewater. The higher the ammonia removal efficiency from struvite, the higher the combined N recovery efficiency achieved over the cycle.

In Figure 5.38, the combined N recovery percentage decreases with an increase in number of re-use cycles; this indicates that the decomposed product is losing its ability for use as a source of magnesium and phosphate over the cycle. In the struvite recrystallization stage, only newberyite can be transformed into struvite, but the dittmarite compound present in the decomposed product remains the same, since no acid is added for dittmarite dissolution. Further decomposition of the obtained recrystallized product, containing dittmarite, causes a further increase in the percentage of dittmarite in the decomposed product at each cycle. Therefore, the decomposed product becomes inefficient as a precipitating agent, due to enhanced accumulation of dittmarite with the increase in number of cycles. The combined N recovery efficiency is expected to decrease from 95% to 8% by the end of the 50th cycle, when ammonia removal efficiency from struvite is 95%; this infers that after 50 cycles, the recrystallized product will contain 92% dittmarite and only 8% struvite. Further reduction in ammonia removal efficiency at 80% and 70%, can cause a reduction in the number of cycles to 17 and 7, corresponding to a recrystallized product containing 92% dittmarite, respectively. When ammonia removal efficiency from struvite during thermal decomposition is about 70%, only 14 cycles can be applied without converting all of the recrystallized product into dittmarite. Further N recovery through struvite recrystallization can be achieved with the excess addition of decomposed product at each cycle; however, this increases overall operating costs.

Case 2: Without acid dissolution of decomposed product containing struvite

During struvite recrystallization, the accumulation of dittmarite during each cycle can be avoided through the prevention of dittmarite formation in the decomposed product; this requires the utilization of humid air at the struvite decomposition stage. The decomposed product containing newberyite, along with struvite, is an efficient source of magnesium and phosphate since the entire decomposed product can be transformed into struvite through recrystallization. In this way, the combined N recovery efficiency is not limited to the number of cycles but depends on the percentage of N residual in the decomposed product, as shown in Figure 5.38. Therefore, the utilization of humid air during struvite thermal decomposition, would be essential in order to recover a higher percentage of aqueous ammonia at each cycle, without forming and accumulating dittmarite. The formation of a decomposed product, devoid of any layered structure, may initially increase the operational cost at the decomposition stage; however, this can be mitigated through recycling the humid air over the cycle, as discussed in the previous section.

Case 3: With acid dissolution of decomposed product at stoichiometric amount

The N recovery efficiency from wastewater through complete dissolution of the decomposed product, by acid addition prior to struvite recrystallization, is evaluated in this section. The combined N recovery process with the addition of stoichiometric amounts of decomposed product containing 30% residual ammonia (either belonging to struvite or any layered structure), is presented in Figure 5.39.

The complete dissolution of the decomposed product can prevent the accumulation of dittmarite in the recrystallized product, but introduces additional nitrogen to the wastewater that is associated with either dittmarite or struvite in the decomposed product. For instance, in order to treat 700 mg/L (50 mmol/L) of nitrogen in wastewater, a decomposed product containing 50 mmol of magnesium and phosphorus with 15 mmol of nitrogen is added to the solution, as shown in Figure 5.39. It is assumed that 50 mmol of nitrogen can be completely recovered through struvite recrystallization at a Mg:N:P ratio of 1:1:1. However, the additional 15 mmol (30%) of nitrogen from the decomposed product will remain in the solution. The overall N recovery efficiency in

each cycle is 70%. The N recovery efficiency in this process is thus dependent on ammonia removal efficiency from struvite in the decomposition stage. For example, the decomposed struvite product, with 10% residual ammonia, will provide 90% N recovery efficiency in each cycle.

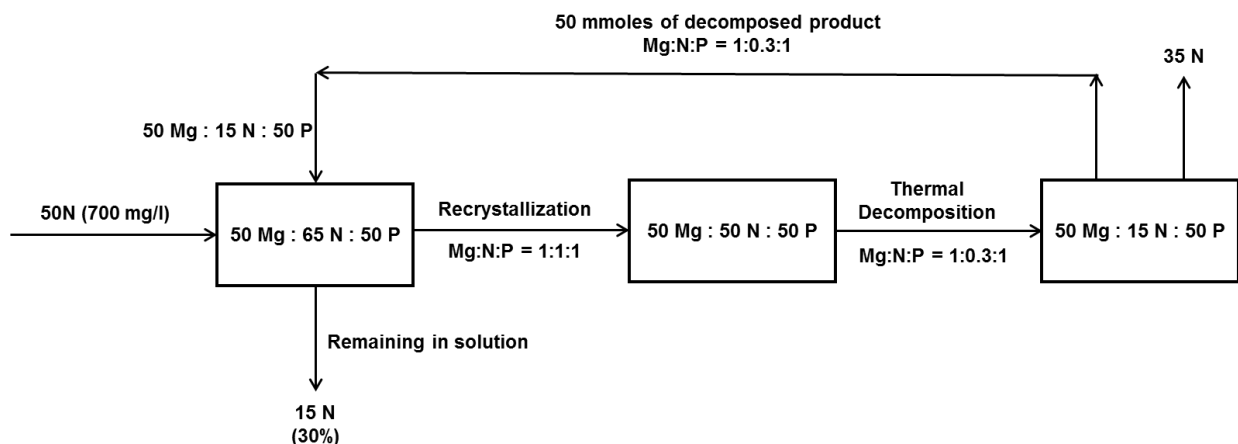


Figure 5.39 Mole balance of the combined ammonia recovery process with addition of stoichiometric amount of decomposed product

Case 4: With acid dissolution of decomposed product in excess for complete nitrogen recovery

The addition of a stoichiometric amount of decomposed product requires the production of 30% more struvite at every cycle, in order to recover the 30% excess nitrogen that is being introduced from the decomposed product with 70% ammonia removal efficiency. As discussed in the previous case, the addition of a stoichiometric amount of decomposed struvite product, containing ammonia, contributes excess nitrogen in the recrystallization stage. The addition of the decomposed product in excess, compared to the stoichiometric amount, can completely remove the initial 50 mmol/L of nitrogen from wastewater at each cycle, as shown in Figure 5.40.

The addition of a decomposed product containing 30% residual ammonia can completely remove 50 mmol/L nitrogen from solution through struvite recrystallization, provided that at each cycle, an excess of 42% more decomposed product than the stoichiometric amount is added. In addition, 30% more struvite must be produced at each cycle, thereby increasing chemical cost by 30%. These two stages, with acid dissolution, require further economic comparisons between 30% more

struvite production in the recrystallization stage and 100% ammonia removal from the struvite, with steam incorporation.

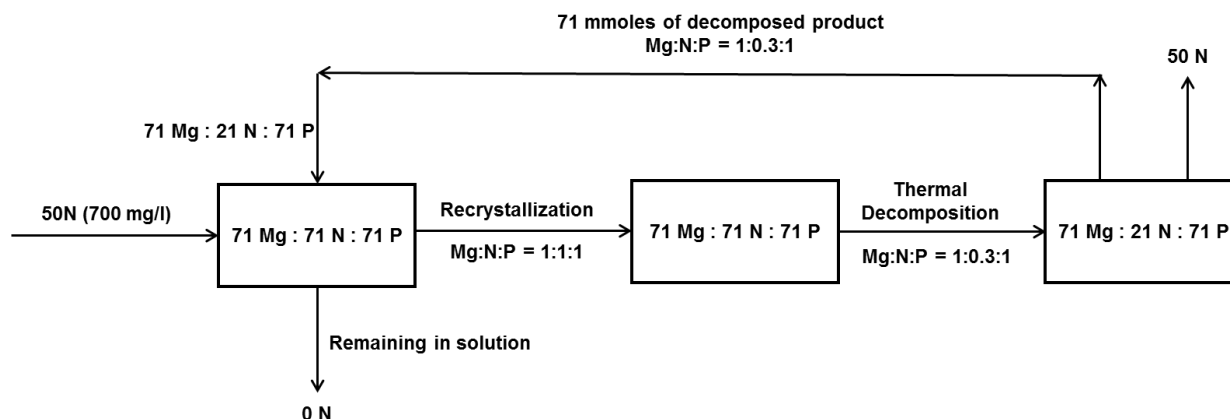


Figure 5.40 Mole balance of combined ammonia recovery process with addition of excess decomposed product

Considering the above four cases, it is apparent that the recycling of a decomposed product containing newberyite along with struvite, without acid addition (Case 2), can provide high N recovery efficiency at each cycle, but may increase the operational costs at the decomposition stage, due to steam incorporation. The addition of acid (Cases 3 and 4) will definitely increase the operational costs; finally, usage of a decomposed product containing dittmarite or layered structure (Case 1) will significantly reduce the N recovery efficiency, with each increasing cycle. However, it should be noted that the focus of this present study was to identify the optimum conditions, corresponding to maximum ammonia removal from struvite, in the first stage (thermal decomposition) of the technology. The economic feasibility of the entire technology cannot be determined with certainty at this time, since the second and third stages are under development and further investigation is required to identify the most suitable approach of the aforementioned N recovery options.

Chapter 6: Conclusions and Recommendations

Based on this 3 step study, the following conclusions can be made at this time.

Conclusions

Oven dry experiments

- Struvite was thermally stable at temperatures below 60.5°C, for up to 24 hours of oven dry heating. During thermal decomposition of struvite, ammonia and water started to escape from struvite around 60°±0.5°C, and the mass loss percentage was significant. Around 60%-70% ammonia removal from the struvite was achieved after 24 hours of heating, from 60.5°C up to 71.1°C. The final composition of the decomposed struvite solid phase was $\text{MgH}(\text{NH}_3)_x\text{PO}_4.y(\text{H}_2\text{O})$, with a 25-35% ammonia content and 1-1.3 water molecules.
- The layered structure of struvite was thermally stable during the oven dry experiment, but was unstable after exposure to atmospheric conditions. This layered structure, which started forming at 60.5°C, was very unstable due to absorption of moisture. A pronounced layered structure peak was observed in the freshly-heated struvite samples decomposing at 61.5°C; the intensity of the layered structure peak continued to increase with an increase in heating duration. No formation of dittmarite and newberyite was observed during initial XRD analysis.
- As the temperature of decomposition increased, the formation of the layered structure progressed. The part of the layered structure devoid of ammonia was transformed into newberyite, whereas the part with entrapped ammonia was transformed into a more organized structure, such as dittmarite, over time. Subsequent heating at 60.5°C for 24 hours and rehydration with atmospheric moisture three times, could not enhance the ammonia removal efficiency. The formation of this layered structure impeded the removal of the residual 30%-40% ammonia, even after 24 hours of heating at temperatures below 100°C.

Bench-scale experiments

- The higher the temperature and relative humidity, the faster the ammonia removal was from the struvite pellets, without forming any layered structure. Lower temperature and lower humidity also resulted in ammonia removal, but only with a longer duration of heating. Higher temperature with lower humidity, resulted in a layered structure formation, which reorganized and transformed into dittmarite, over time.
- The complete transformation of struvite to newberyite seemed to occur at 80°C and 85°C, with 95% RH, after heating the smaller Lulu Island pellets for 2 hours, under stable operating conditions. However, prolonged duration of heating and improper fluidization can lead to the formation of layered structures (i.e. dittmarite and an amorphous 2D layered structure) as observed in this study.
- The larger and harder the pellets, the higher the possibility of dittmarite formation and the more difficult it was to remove ammonia, even after heating under the same optimum conditions. The Lulu Island struvite pellets, in 0.5-1 mm range, appeared to be the most suitable for newberyite formation (not dittmarite) under the optimum conditions studied.

Pilot-scale experiments

- Penticton B.C. struvite pellets (0.5-1 mm) were completely transformed into newberyite, within 1.5 hours of heating at a temperature of $80\pm 2^{\circ}\text{C}$ and $95\pm 7\%$ RH. Complete ammonia removal also can be achieved at lower temperatures and lower humidity, with prolonged heating, but this increased energy consumption and the possibility of dittmarite formation. Struvite heating, at a higher temperature and with lower humidity, can also favour dittmarite formation within a short period of time and this became more prominent with increased heating duration in this work.
- The larger and harder the pellets, the more difficult it was to achieve complete ammonia removal from struvite, even with prolonged heating at optimum conditions; this was due to

the formation of dittmarite at the beginning of the experiment. Softer pellets were not suitable either, due to disintegration and dust formation inside the reactor during the thermal decomposition process. Hence, optimized operating conditions for struvite to newberyite transformation, using smaller Penticton B.C. pellets, is recommended as 80°C, 85±5% RH and 1.5 hours of heating.

Struvite morphology

- The exterior structural characteristics of the struvite pellets can significantly influence the ammonia removal efficiency, during thermal decomposition. Ammonia removal was highest from those struvite pellets that contained sharp edges with a porous exterior surface, instead of a smooth and hard surface.
- The loosely-packed pellets were more suitable for struvite to newberyite transformation, than tightly aggregated pellets, in the fluidized bed reactor.

Hardness of the struvite pellets

- Hardness of struvite is associated with the size and morphology of different, struvite-sourced pellets. The larger struvite pellets, from the same source, exhibited a higher crushing strength, compared to smaller pellets.
- The smaller, tightly-compacted struvite pellets showed higher resistance upon crushing, compared to larger loosely-packed pellets. Overall, the smaller Penticton B.C. pellets (395 g) tested showed highest ammonia removal efficiency within a short period of time, whereas the smaller Edmonton Gold Bar pellets (1000 g) showed the lowest.

Recommendations for future work

The following research goals are recommended for the development of the 2nd generation reactor, and possible commercial adoption, for thermal decomposition of struvite and transformation into newberyite.

- To produce larger batches of newberyite, the diameter of the reactor needs to be increased. A reactor with a larger diameter will also facilitate better fluidization of the pellets.
- To prevent heat loss, the height of the reactor should be reduced, if at all possible.
- Automatic control of humidity must be provided to stabilize operating conditions; the hot air exiting the jacket and moist air exiting the reactor need to be recycled, to reduce energy consumption.
- Proper mixing devices, such as gas distribution devices, are needed to mix the air and steam properly, before entering to the reactor.
- The economic feasibility of this process after modifying the reactor, diffuser, hot air and steam recirculation, needs to be fully assessed at larger pilot-scale.

References

- Abbona, F., Boistelle, R., 1979. Growth morphology and crystal habit of struvite crystals ($\text{MgNH}_4\text{PO}_4 \cdot 6\text{H}_2\text{O}$). *J. Cryst. Growth* 46, 339–354. doi:10.1016/0022-0248(79)90082-4
- Abdelrazig, B.E.I., Sharp, J.H., 1988. Phase changes on heating ammonium magnesium phosphate hydrates. *Thermochim. Acta* 129, 197–215. doi:10.1016/0040-6031(88)87336-2
- Adnan, A., Mavinic, D.S., Koch, F.A., 2003. Pilot-scale study of phosphorus recovery through struvite crystallization — examining the process feasibility. *J. Environ. Eng. Sci.* 2, 315–324. doi:10.1139/s03-040
- Agricultural and Agri-Food Canada, 2013. Canadian farm fuel and fertilizer: Prices and expenses. [WWW Document]. *Mark. Outlook Rep.* URL http://www.agr.gc.ca/resources/prod/doc/misb/mag-gam/mor-rmar/pdf/rmar_04_01_2012-03_eng.pdf (accessed 7.15.15).
- Aiking, H., 2011. Future protein supply. *Trends Food Sci. Technol.* 22, 112–120. doi:10.1016/j.tifs.2010.04.005
- Allar, A.D., Beler-Baykal, B., 2013. Phosphorus recovery from source separated human urine upon processing with clinoptilolite. *Proc. Water Environ. Fed.* 2013, 117–124. doi:10.2175/193864713813525563
- APHA, 2005. Standard methods for the examination of water and wastewater, 21st ed. ed. American Public Health Association, Washington DC.
- Avidan, A.A., King, D.F., Knowlton, T.M., Pell, M., 2000. Kirk-Othmer encyclopedia of chemical technology-Fluidization. John Wiley & Sons, Inc., Hoboken, NJ, USA. doi:10.1002/0471238961.0612210901220904.a01
- Babić-Ivančić, V., Kontrec, J., Kralj, D., Brečević, L., 2002. Precipitation diagrams of struvite and dissolution kinetics of different struvite morphologies. *Croat. Chem. Acta* 75, 89–106.
- Babić-Ivančić, V., Kontrec, J., Brečević, L., Kralj, D., 2006. Kinetics of struvite to newberyite transformation in the precipitation system $\text{MgCl}_2\text{-NH}_4\text{H}_2\text{PO}_4\text{-NaOH-H}_2\text{O}$. *Water Res.* 40, 3447–55. doi:10.1016/j.watres.2006.07.026
- Banks, E., Chianelli, R., Korenstein, R., 1975. Crystal chemistry of struvite analogs of the type $\text{MgMPO}_4 \cdot 6\text{H}_2\text{O}$. *Inorg. Chem.* 14, 1634–1639. doi:10.1021/ic50149a041
- Barnes, D., Li, X., Chen, J., 2007. Determination of suitable pretreatment method for old-intermediate landfill leachate. *Environ. Technol.* 28, 195–203. doi:10.1080/09593332808618782
- Beler-Baykal, B., Allar, A. D., Bayram, S., 2011. Nitrogen recovery from source-separated human urine using clinoptilolite and preliminary results of its use as fertilizer. *Water Sci. Technol.* 63, 811–817. doi:10.2166/wst.2011.324

- Bensalem, A., Iyer, G., 1995. Ambient pressure and temperature synthesis of new layered magnesium phosphate: $\text{MgHPO}_4 \cdot 0.78\text{H}_2\text{O}$. *J. Solid State Chem.* 114, 598–600. doi:10.1006/jssc.1995.1092
- Bensalem, A., Iyer, G., Amar, S., 1995. Synthesis of layered $\text{MgHPO}_4 \cdot 1.2\text{H}_2\text{O}$ under ambient conditions. *Mater. Res. Bull.* 30, 1471–1479. doi:10.1016/0025-5408(95)00168-9
- Bhuiyan, M.I.H., Mavinic, D.S., Beckie, R.D., 2007. A solubility and thermodynamic study of struvite. *Environ. Technol.* 28, 1015–26. doi:10.1080/09593332808618857
- Bhuiyan, M.I.H., Mavinic, D.S., Beckie, R.D., 2008a. Nucleation and growth kinetics of struvite in a fluidized bed reactor. *J. Cryst. Growth* 310, 1187–1194. doi:10.1016/j.jcrysgro.2007.12.054
- Bhuiyan, M.I.H., Mavinic, D.S., Koch, F.A., 2008b. Thermal decomposition of struvite and its phase transition. *Chemosphere* 70, 1347–56. doi:10.1016/j.chemosphere.2007.09.056
- Bilyk, K., Taylor, R., Pitt, P., Wankmuller, D., 2012. Process and economic benefits of sidestream treatment. *Proc. Water Environ. Fed.* 2012, 889–906. doi:10.2175/193864712811694280
- Boistelle, R., Abbona, F., 1981. Morphology, habit and growth of newberyite crystals ($\text{MgHPO}_4 \cdot 3\text{H}_2\text{O}$). *J. Cryst. Growth* 54, 275–295. doi:10.1016/0022-0248(81)90472-3
- Boistelle, R., Abbona, F., Lundager Madsen, H.E., 1983. On the transformation of struvite into newberyite in aqueous systems. *Phys. Chem. Miner.* 9, 216–222. doi:10.1007/BF00311958
- Boistelle, R., Abbona, F., 1985. Nucleation of struvite ($\text{MgNH}_4\text{PO}_4 \cdot 6\text{H}_2\text{O}$) single crystals and aggregates. *Cryst. Res. Technol.* 20, 133–140. doi:10.1002/crat.2170200204
- Bonmatí, A., Flotats, X., 2003. Air stripping of ammonia from pig slurry: Characterisation and feasibility as a pre- or post-treatment to mesophilic anaerobic digestion. *Waste Manag.* 23, 261–72. doi:10.1016/S0956-053X(02)00144-7
- Borgerding, J., 1972. Phosphate deposits in digestion systems. *J. Water Pollut. Control Fed.* 44, 813–819. doi:10.1016/S0043-1354(01)00143-9
- Bouropoulos, N.C., Koutsoukos, P.G., 2000. Spontaneous precipitation of struvite from aqueous solutions. *J. Cryst. Growth* 213, 381–388. doi:10.1016/S0022-0248(00)00351-1
- Britton, A.T., 2002. Pilot scale struvite recovery trials from a full-scale anaerobic digester supernatant at the City of Penticton Advanced Wastewater Treatment Plant. M.A.Sc. Thesis, Department of Civil Engineering, The University of British Columbia, Vancouver, BC, Canada
- Bumb, B.L., Baanante, C.A., 1996. The role of fertilizer in sustaining food security and protecting the environment to 2020. *Intl Food Policy Res Inst.*
- CCME, 2010. Canadian water quality guidelines for the protection of aquatic life: ammonia. *Can. Environ. Qual. Guidel. Can. Coun. Minist. Environ.*
- Celen, I., Türker, M., 2001. Recovery of ammonia as struvite from anaerobic digester effluents. *Environ. Technol.* 22, 1263–72. doi:10.1080/09593332208618192

- Cervantes, F.J., 2009. Environmental technologies to treat nitrogen pollution: Principles & engineering, Integrated Environmental Technology Series. IWA Publishing.
- Chang, C.D., Hellring, S.D., 1989. Layered divalent metal hydrogen phosphates. US 4846853 A.
- Chen, J., Natarajan, S., Wright, P.A., Jones, R.H., Thomas, J.M., Catlow, C.R.A., Townsend, R.P., 1993. Preparation and characterization of a new layered magnesium phosphate: $\text{MgHPO}_4 \cdot 1.2\text{H}_2\text{O}$. *J. Solid State Chem.* 103, 519–522. doi:10.1006/jssc.1993.1130
- Cheung, K.C., Chu, L.M., Wong, M.H., 1997. Ammonia stripping as a pretreatment for landfill leachate. *Water. Air. Soil Pollut.* 94, 209–221. doi:10.1007/BF02407103
- Christensen, C.H., Johannessen, T., Sørensen, R.Z., Nørskov, J.K., 2006. Towards an ammonia-mediated hydrogen economy? *Catal. Today* 111, 140–144. doi:10.1016/j.cattod.2005.10.011
- Cilona, A., Nilsson, S., Malpei, F., Levlin, E., 2009. Gas transfer membrane for ammonia removal of condensed flue gas. URL http://rymd.lwr.kth.se/Publikationer/PDF_Files/LWR_EX_09_27.pdf
- Cohen, L.H., Ribbe, P.H., 1966. Magnesium phosphate mineral replacement at Mono Lake, California. *Am. Miner.* 51, 1755–1765.
- Constantine, T.A., 2006. North American experience with centrate treatment technologies for ammonia and nitrogen removal. *Proc. Water Environ. Fed.* 2006, 5271–5281. doi:10.2175/193864706783763291
- Dean, J.A., 1985. *Lange's handbook of chemistry*. McGraw Hill Book Co., New York.
- Elmøe, T.D., Sørensen, R.Z., Quaade, U., Christensen, C.H., Nørskov, J.K., Johannessen, T., 2006. A high-density ammonia storage/delivery system based on $\text{Mg}(\text{NH}_3)_6\text{Cl}_2$ for – in vehicles. *Chem. Eng. Sci.* 61, 2618–2625. doi:10.1016/j.ces.2005.11.038
- Elston, J., Karmarkar, D., 2003. Aqueous ammonia stripping technology for SCR applications, in: *The Electric Power Conference*, Houston, TX.
- Environment Canada, 2001. Canadian environmental protection act, 1999: Priority substances list assessment report: Ammonia in the aquatic environment [WWW Document]. URL http://www.hc-sc.gc.ca/ewh-semt/pubs/contaminants/psl2-lsp2/road_salt_sels_voirie/index-eng.php (accessed 7.21.15).
- Erisman, J.W., Sutton, M.A., Galloway, J., Klimont, Z., Winiwarter, W., 2008. How a century of ammonia synthesis changed the world. *Nat. Geosci.* 1, 636–639. doi:10.1038/ngeo325
- Evans, T.D., Thompson, A., 2009. Recovering ammonium fertiliser – an alternative to blowing it away, in: *14th European Biosolids & Organic Resources Conference*.
- Fassbender, A.G., 2001. ThermoEnergy ammonia recovery process for municipal and agricultural wastes. *Sci. World J.* 1 Suppl 2, 908–913. doi:10.1100/tsw.2001.287

- Fattah, K.P., 2010. Development of control strategies for the operation of a struvite crystallization process. Ph.D. Thesis, Department of Civil Engineering, University of British Columbia, Vancouver, Canada.
- Fattah, K.P., 2004. Pilot scale struvite recovery potential from centrate at lulu island wastewater treatment plant. M.A.Sc. Thesis, Department of Civil Engineering, The University of British Columbia, Vancouver, BC, Canada.
- Fattah, K.P., Zhang, Y., Mavinic, D.S., Koch, F.A., 2008a. Application of carbon dioxide stripping for struvite crystallization - I: Development of a carbon dioxide stripper model to predict CO₂ removal and pH changes. *J. Environ. Eng. Sci.* 7, 345–356. doi:10.1139/S08-009
- Fattah, K.P., Mavinic, D.S., Koch, F. A., Jacob, C., 2008b. Determining the feasibility of phosphorus recovery as struvite from filter press centrate in a secondary wastewater treatment plant. *J. Environ. Sci. Health. A. Tox. Hazard. Subst. Environ. Eng.* 43, 756–764. doi:10.1080/10934520801960052
- Ferraris, G., Fuess, H., Joswig, W., 1986. Neutron diffraction study of MgNH₄PO₄·6H₂O (struvite) and survey of water molecules donating short hydrogen bonds. *Acta Crystallogr. Sect. B Struct. Sci.* 42, 253–258. doi:10.1107/S0108768186098269
- Finch, T., Sharp, J.H., 1989. Chemical reactions between magnesia and aluminium orthophosphate to form magnesia-phosphate cements. *J. Mater. Sci.* 24, 4379–4386. doi:10.1007/BF00544516
- Fisheries and Oceans Canada, 2007. Whites point quarry joint panel review public hearings [WWW Document]. URL <http://www.ceaa.gc.ca/B4777C6B-docs/WP-1815-034.pdf> (accessed 7.21.15).
- Forrest, A.L., 2004. Process optimization of a technical scale phosphorus recovery system through struvite crystallization at the City of Penticton Advanced Wastewater Treatment Plant. M.A.Sc. Thesis, Department of Civil Engineering, University of British Columbia, Vancouver, BC.
- Frigon, M., 2007. Fertilizers, ethanol and the peaking of natural gas production in Alberta, Library of Parliament Background Paper No. 2007-49-E.
- Frost, R.L., Palmer, S.J., Pogson, R.E., 2012. Thermal stability of newberyite Mg(PO₃OH)·3H₂O. *J. Therm. Anal. Calorim.* 107, 1143–1146. doi:10.1007/s10973-011-1593-7
- Frost, R.L., Weier, M.L., Erickson, K.L., 2004. Thermal decomposition of struvite: Implications for the decomposition of kidney stones. *J. Therm. Anal. Calorim.* 76, 1025–1033. doi:10.1023/B:JTAN.0000032287.08535.b3
- Fux, C., Siegrist, H., 2004. Nitrogen removal from sludge digester liquids by nitrification / denitrification or partial nitrification / anammox : Environmental and economical considerations. *Water Sci. Technol.* 50, 19–26.
- Gunay, A., Karadag, D., Tosun, I., Ozturk, M., 2008. Use of magnesit as a magnesium source for ammonium removal from leachate. *J. Hazard. Mater.* 156, 619–623. doi:10.1016/j.jhazmat.2007.12.067

- Hassan, P., 2013. Simultaneous management of nitrogen and phosphorus in dewatered sludge liquor by combining anammox process with struvite crystallization. M.A. Sc. Thesis, Department of Civil Engineering, The University of British Columbia, Vancouver, BC, Canada.
- He, S., Zhang, Y., Yang, M., Du, W., Harada, H., 2007. Repeated use of MAP decomposition residues for the removal of high ammonium concentration from landfill leachate. *Chemosphere* 66, 2233–2238. doi:10.1016/j.chemosphere.2006.09.016
- Huang, H., 2003. Pilot scale phosphorus recovery from anaerobic digester supernatant. M.A.Sc. Thesis, Department of Civil Engineering, University of British Columbia, Vancouver, BC, Canada.
- Huang, H.M., Xiao, X.M., Yan, B., 2009. Recycle use of magnesium ammonium phosphate to remove ammonium nitrogen from rare-earth wastewater. *Water Sci. Technol.* 59, 1093–1099. doi:10.2166/wst.2009.086
- Huang, H.M., Song, Q.W., Xu, C.L., 2011a. The mechanism and influence factors of struvite precipitation for the removal of ammonium nitrogen, in: *Advanced Materials Research*. pp. 2613–2620. doi:10.4028/www.scientific.net/AMR.189-193.2613
- Huang, H., Xu, C., Zhang, W., 2011b. Removal of nutrients from piggery wastewater using struvite precipitation and pyrogenation technology. *Bioresour. Technol.* 102, 2523–2528. doi:10.1016/j.biortech.2010.11.054
- Huang, H., Song, Q., Xu, C., 2011c. Removal of ammonium from aqueous solutions using the residue obtained from struvite pyrogenation. *Water Sci. Technol.* 64, 2508–2514. doi:10.2166/wst.2011.811
- Jaffer, Y., Clark, T. A., Pearce, P., Parsons, S. a., 2002. Potential phosphorus recovery by struvite formation. *Water Res.* 36, 1834–1842. doi:10.1016/S0043-1354(01)00391-8
- Johnson, R.G., 1959. The solubility of magnesium ammonium phosphate hexahydrate at 38°C with considerations pertaining to the urine and the formation of urinary calculi. *J. Urol.* 81, 681–90.
- Kessler, K., 2010. Analysis of nitrogen loading reductions for wastewater treatment facilities and non-point sources in the great bay estuary watershed - Appendix E : Capital and operation/maintenance costs associated with nitrogen removal at 18 municipal wastewater treatment facilities discharging to the Great Bay Estuary [WWW Document]. New Hampsh. Dep. Environ. Serv. URL http://des.nh.gov/organization/divisions/water/wmb/coastal/documents/gbnla_appendix_e.pdf (accessed 7.21.15).
- Khan, F. A., Ansari, A.A., 2005. Eutrophication: An ecological vision. *Bot. Rev.* 71, 449–482. doi:10.1663/0006-8101(2005)071[0449:EAEV]2.0.CO;2
- Kiehl, S.J., Hardt, H.B., 1933. The Dissociation Pressures of Magnesium Ammonium Phosphate Hexahydrate and Some Related Substances. VII. *J. Am. Chem. Soc.* 55, 605–618. doi:10.1021/ja01329a022
- Kim, B.U., Lee, W.H., Lee, H.J., Rim, J.M., 2004. Ammonium nitrogen removal from slurry-type swine wastewater by pretreatment using struvite crystallization for nitrogen control of anaerobic digestion. *Water Sci. Technol.* 49, 215–222.

- Kim, D., Ryu, H.D., Kim, M.S., Kim, J., Lee, S.I., 2007. Enhancing struvite precipitation potential for ammonia nitrogen removal in municipal landfill leachate. *J. Hazard. Mater.* 146, 81–85. doi:10.1016/j.jhazmat.2006.11.054
- Knight, H., 2013. Portable ammonia factories could fuel clean cars [WWW Document]. *New Sci.* URL <https://www.newscientist.com/article/mg21128285.100-portable-ammonia-factories-could-fuel-clean-cars#.VPgHQfldVhY>. (accessed 7.21.15).
- Koch, F.A., Mavinic, D.S., Yonemitsu, N., Britton, A.T., 2011. Fluidized bed wastewater treatment apparatus. US 7922897 B2.
- Koleva, V.G., 2007. Vibrational behavior of the phosphates ions in dittmarite-type compounds $M'M''PO_4 \cdot H_2O$ ($M' = K^+, NH_4^+$; $M'' = Mn^{2+}, Co^{2+}, Ni^{2+}$). *Spectrochim. Acta - Part A Mol. Biomol. Spectrosc.* 66, 413–418. doi:10.1016/j.saa.2006.03.015
- Komarowski, S., Yu, Q., 1997. Ammonium ion removal from wastewater using Australian natural zeolite: Batch equilibrium and kinetic studies. *Environ. Technol.* 18, 1085–1097. doi:10.1080/09593331808616628
- Kongshaug, K. O., Fjellvåg, H., Lillerud, K.P., 2000. Synthesis and ab-initio structure determination of organically templated magnesium phosphates from powder diffraction data. *J. Mater. Chem.* 10, 1915–1920. doi:10.1039/b001715i
- Königsberger, E., Königsberger, L., 2006. *Biomineralization – Medical aspects of solubility*. John Wiley & Sons, Ltd, Chichester, UK. doi:10.1002/0470092122
- Kontrec, J., Babić-Ivancić, V., Brecević, L., 2005. Formation and morphology of struvite and newberyite in aqueous solutions at 25°C and 37°C. *Coll. Antropol.* 29, 289–294.
- Koutsoukos, P.G., Kofina, A.N., Kanellopoulou, D.G., 2007. Solubility of salts in water: Key issue for crystal growth and dissolution processes. *Pure Appl. Chem.* 79, 825–850. doi:10.1351/pac200779050825
- Kurtulus, G., Tas, A. C., 2011. Transformations of neat and heated struvite ($MgNH_4PO_4 \cdot 6H_2O$). *Mater. Lett.* 65, 2883–2886. doi:10.1016/j.matlet.2011.06.086
- Lan, R., Irvine, J.T.S., Tao, S., 2012. Ammonia and related chemicals as potential indirect hydrogen storage materials. *Int. J. Hydrogen Energy* 37, 1482–1494. doi:10.1016/j.ijhydene.2011.10.004
- Le Corre, K.S., Valsami-Jones, E., Hobbs, P., Parsons, S. A., 2009. Phosphorus recovery from wastewater by struvite crystallization: A review. *Crit. Rev. Environ. Sci. Technol.* 39, 433–477. doi:10.1080/10643380701640573
- Lee, S.I., Weon, S.Y., Lee, C.W., Koopman, B., 2003. Removal of nitrogen and phosphate from wastewater by addition of bittern. *Chemosphere* 51, 265–271. doi:10.1016/S0045-6535(02)00807-X
- Lei, X., Sugiura, N., Feng, C., Maekawa, T., 2007. Pretreatment of anaerobic digestion effluent with ammonia stripping and biogas purification. *J. Hazard. Mater.* 145, 391–397. doi:10.1016/j.jhazmat.2006.11.027

- Li, X.Z., Zhao, Q.L., 2002. MAP precipitation from landfill leachate and seawater bittern waste. *Environ. Technol.* 23, 989–1000. doi:10.1080/09593332308618348
- Li, Y., Yi, L., Ma, P., Zhou, L., 2007. Industrial wastewater treatment by the combination of chemical precipitation and immobilized microorganism technologies. *Environ. Eng. Sci.* 24, 736–744. doi:10.1089/ees.2005.0026
- Liu, Y., Kumar, S., Kwag, J.H., Ra, C., 2013. Magnesium ammonium phosphate formation, recovery and its application as valuable resources: A review. *J. Chem. Technol. Biotechnol.* 88, 181–189. doi:10.1002/jctb.3936
- Lobanov, S. A., Poilov, V.Z., 2006. Treatment of wastewater to remove ammonium ions by precipitation. *Russ. J. Appl. Chem.* 79, 1473–1477. doi:10.1134/S1070427206090151
- Lobanov, S., Koch, F., Mavinic, D., 2013. The implication of aqueous equilibrium modelling to evaluate the potential for nutrient recovery from wastewater streams., in: *WEF/IWA Nutrient Removal and Recovery: Trends in Resource Recovery and Use*. p. (USB proceedings).
- Lobanov, S., Koch, F., Mavinic, D., 2014. Nutrient recovery from wastewater streams by crystallisation. *J. Environ. Eng. Sci.* 00, 1–4. doi:10.1680/jees.13.00008
- Mavinic, D.S., Koch, F. A., Huang, H., Lo, K. V., 2007. Phosphorus recovery from anaerobic digester supernatants using a pilot-scale struvite crystallization process. *J. Environ. Eng. Sci.* 6, 561–571. doi:10.1139/S07-007
- Maxwell, G.R., 2004. *Synthetic nitrogen products: A practical guide to the products and processes*. Springer Science & Business Media. doi:10.1007/b106641
- McVeigh, R., Weatherley, L., 1999. Ammonium ion (NH_4^+) removal from secondary effluent through ion-exchange: The effect of biological activity and the presence of other cations. *Water Sci. Technol.* 40, 143–149. doi:10.1016/S0273-1223(99)00475-8
- Minocha, V. K., Rao, A. P., 1988. Ammonia removal and recovery from urea fertilizer plant waste. *Environ. Technol.* 9, 655–664. doi:10.1080/09593338809384616
- Moerman, W., 2013. Method for purifying wastewater with ammonium removal. EP 2 619 144 B1. doi:10.1016/j.jcis.2005.05.073
- Mohajit, Bhattarai, K.K., Taiganides, E.P., Yap, B.C., 1989. Struvite deposits in pipes and aerators. *Biol. Wastes* 30, 133–147. doi:10.1016/0269-7483(89)90067-0
- Mosier, A., Kroeze, C., 2000. Potential impact on the global atmospheric N_2O budget of the increased nitrogen input required to meet future global food demands. *Chemosph. - Glob. Chang. Sci.* 2, 465–473. doi:10.1016/S1465-9972(00)00039-8
- Nguyen, M.L., Tanner, C.C., 1998. Ammonium removal from wastewaters using natural New Zealand zeolites. *New Zeal. J. Agric. Res.* 41, 427–446. doi:10.1080/00288233.1998.9513328

- Novotny, C., 2011. Ammonia removal and recovery using heated struvite as an adsorbent. M.A.Sc. Thesis, Department of Civil Engineering, University of British Columbia, Vancouver, BC, Canada.
- Ohlinger, K.N., Young, T.M., Schroeder, E.D., 1998. Predicting struvite formation in digestion. *Water Res.* 32, 3607–3614. doi:10.1016/S0043-1354(98)00123-7
- Ohlinger, K.N., Young, T.M., Schroeder, E.D., 1999. Kinetics effects on preferential struvite accumulation in wastewater. *J. Environ. Eng.* 730–737.
- Orentlicher, M., 2012. Overview of nitrogen removal technologies and application/use of associated end products, in: *Got Manure? Enhancing Environmental and Economic Sustainability Conference*.
- Palmer, S. A. K., Breton, M. A., Nunno, T. J., Sullivan, D. M., Surprenant, N.F., 1988. Metal/cyanide containing wastes: Treatment technologies, Noyes Data Corp.
- Paulik, F., Paulik, J., 1975a. TG and EGA investigations of the decomposition of magnesium ammonium phosphate hexahydrate by means of the derivatograph under conventional and quasi-isothermal-quasi-isobaric conditions. *J. Therm. Anal.* 8, 557–566.
- Paulik, J., Paulik, F., 1975b. TG and EGA investigations of the decomposition of some metal ammonium phosphate monohydrates by means of the derivatograph under conventional and quasi-isothermal-quasi-isobaric conditions. *J. Therm. Anal. Calorim.*
- Perry, R. H., Green, D. W., Maloney, J.O., 1997. *Chemical engineers' handbook*, 7th ed. McGraw-Hill. doi:10.1021/ed027p533.1
- Pysiak, J., Prodan, E. A., Samuskevich, V.V., Pacewska, B., Shkorik, N. A., 1993. Thermal transformations of $\text{NH}_4\text{M}^{\text{II}}\text{PO}_4 \cdot \text{H}_2\text{O}$ (where M^{II} is Mg, Mn, Co, Cu). *Thermochim. Acta* 222, 91–103. doi:10.1016/0040-6031(93)80543-J
- Randall, D.J., Tsui, T.K.N., 2002. Ammonia toxicity in fish. *Mar. Pollut. Bull.* 45, 17–23. doi:10.1016/S0025-326X(02)00227-8
- Ribbe, P.H., 1969. The decomposition of struvite: Further evidence. *Mineral. Mag.* 37, 290–291. doi:10.1180/minmag.1969.037.286.24
- Ryu, H.D., Kim, D., Lee, S.I., 2008. Application of struvite precipitation in treating ammonium nitrogen from semiconductor wastewater. *J. Hazard. Mater.* 156, 163–169. doi:10.1016/j.jhazmat.2007.12.010
- Sales, B.C., Chakoumakos, B.C., Boatner, L. A., Ramey, J.O., 1993. Structural properties of the amorphous phases produced by heating crystalline $\text{MgHPO}_4 \cdot 3\text{H}_2\text{O}$. *J. Non. Cryst. Solids* 159, 121–139. doi:10.1016/0022-3093(93)91289-F
- Samuskevich, V. V., Lukyanchenko, O. A., 1998. Thermal transformations of $\text{Mg}(\text{H}_2\text{PO}_4)_2 \cdot 4\text{H}_2\text{O}$. *Thermochim. Acta* 311, 87–95. doi:10.1016/S0040-6031(97)00420-6
- Saracco, G., Genon, G., 1994. High temperature ammonia stripping and recovery from process liquid wastes. *J. Hazard. Mater.* 37, 191–206. doi:10.1016/0304-3894(94)85048-8

- Sarkar, A.K., 1991. Hydration/dehydration characteristics of struvite and dittmarite pertaining to magnesium ammonium phosphate cement systems. *J. Mater. Sci.* 26, 2514–2518. doi:10.1007/BF01130204
- Schindler, D., 1974. Eutrophication and recovery in experimental lakes: Implications for lake management. *Science* 184, 897–899.
- Shand, M.A., 2006. *The Chemistry and Technology of Magnesia*. John Wiley & Sons, Ltd.
- Smil, V., 1999. Nitrogen in crop production: An account of global flows. *Global Biogeochem. Cycles* 13, 647. doi:10.1029/1999GB900015
- Smil, V., 2001. *Enriching the earth: Fritz Haber, Carl Bosch, and the transformation of world food production*. MIT Press.
- Smil, V., 2011. Nitrogen cycle and world food production [WWW Document]. *World Agric.* URL https://www.google.ca/url?sa=t&rct=j&q=&esrc=s&source=web&cd=1&cad=rja&uact=8&ved=0CB0QFjAAahUKEwiclfeD7u_GAhWKFj4KHTpECI8&url=http%3A%2F%2Fwww.vaclavsmil.com%2Fwp-content%2Fuploads%2Fdocs%2Fsmil-article-worldagriculture.pdf&ei=5SKwVdyOLiqtAG6iKn4BQ&usg=AFQjCNFKIihmExnx82oRJrudWLDQLsdK7g&sig2=ge15gPxIp0NIMzIlgkuyY2w&bvm=bv.98197061,d.cWw (accessed 7.22.15).
- Šoptrajanov, B., Stefov, V., Kuzmanovski, I., Jovanovski, G., Lutz, H.D., Engelen, B., 2002. Very low H-O-H bending frequencies. IV. Fourier transform infrared spectra of synthetic dittmarite. *J. Mol. Struct.* 613, 7–14. doi:10.1016/S0022-2860(02)00136-9
- Stefanowicz, T., Napieralska-Zagozda, S., Osińska, M., Samsonowska, K., 1992a. Ammonium removal from waste solutions by precipitation of MgNH_4PO_4 I. Ammonium removal with use of commercial reagents. *Resour. Conserv. Recycl.* 6, 329–337. doi:10.1016/0921-3449(92)90056-8
- Stefanowicz, T., Napieralska-Zagozda, S., Osińska, M., Samsonowska, K., 1992b. Ammonium removal from waste solutions by precipitation of MgNH_4PO_4 II. Ammonium removal and recovery with recycling of regenerate. *Resour. Conserv. Recycl.* 6, 339–345. doi:10.1016/0921-3449(92)90057-9
- Sugiyama, S., Manabe, T., Ioka, D., Nakagawa, K., Sotowa, K.-I., Shigemoto, N., 2009. Removal of aqueous ammonium from industrial wastewater with magnesium hydrogen phosphate. *Phosphorus Res. Bull.* 23, 15–19. doi:10.3363/prb.23.15
- Sugiyama, S., Yokoyama, M., Fujii, M., Seyama, K., Sotowa, K.I., 2007. Recycling of thin-layer of magnesium hydrogenphosphate for removal and recovery of aqueous ammonium. *J. Chem. Eng. Japan* 40, 198–201. doi:10.1252/jcej.40.198
- Sugiyama, S., Yokoyama, M., Ishizuka, H., Sotowa, K.I., Tomida, T., Shigemoto, N., 2005. Removal of aqueous ammonium with magnesium phosphates obtained from the ammonium-elimination of magnesium ammonium phosphate. *J. Colloid Interface Sci.* 292, 133–138. doi:10.1016/j.jcis.2005.05.073
- Sutor, D.J., 1967. The crystal and molecular structure of newberyite, $\text{MgHPO}_4 \cdot 3\text{H}_2\text{O}$. *Acta Crystallogr.* 23, 418–422. doi:10.1107/S0365110X67002889

- Suzuki, T., Yano, M., Sumi, S., Honda, M., Hosoya, Y., Yoshida, K. I., 1997. Study of the structure of struvite stones with scanning electron microscopy and energy-dispersive x-ray microanalysis. *Urol. Int.* 58, 88–92. doi:10.1159/000282957
- Swartz, E., Shi, Q., Davidovits, P., Jayne, J.T., Worsnop, D.R., Kolb, C.E., 1998. Uptake of gas-phase ammonia by aqueous/acidic solutions. *J. Aerosol Sci.* 29, S985–S986. doi:10.1016/S0021-8502(98)90675-9
- Taylor, A. W., Frazier, A. W., Gurney, E.L., 1963a. Solubility products of magnesium ammonium and magnesium potassium phosphates. *Trans. Faraday Soc.* doi:10.1039/tf9635901580
- Taylor, A. W., Frazier, A. W., Gurney, E.L., Smith, J.P., 1963b. Solubility products of di- and trimagnesium phosphates and the dissociation of magnesium phosphate solutions. *Trans. Faraday Soc.* doi:10.1039/tf9635901585
- Tchobanoglous, G., 1985. *Water quality: Characteristics, modeling, modification*. Addison-Wesley.
- ThermoEnergy Corporation, 2007. Ammonia recovery process: Cost benefits to the operation of a typical wastewater treatment plant [WWW Document]. URL https://www.google.ca/url?sa=t&rct=j&q=&esrc=s&source=web&cd=5&cad=rja&uact=8&ved=0C DUQFjAEahUKEwjuhseX3_GAhXGNz4KHRAEB64&url=http%3A%2F%2Fcontent.stockpr.com%2Ftmen%2Fmedia%2F457ec4d86ea0990d31d580b31bd5dca3.pdf&ei=VBOWVe6MFcbvAGQiJzwCg&usg=AFQjCNENY4hmk (accessed 7.22.15).
- Tünay, O., Kabdasli, I., Orhon, D., Kolçak, S., 1997. Ammonia removal by magnesium ammonium phosphate precipitation in industrial wastewaters. *Water Sci. Technol.* 36, 225–228. doi:10.1016/S0273-1223(97)00391-0
- Türker, M., Çelen, I., 2007. Removal of ammonia as struvite from anaerobic digester effluents and recycling of magnesium and phosphate. *Bioresour. Technol.* 98, 1529–1534. doi:10.1016/j.biortech.2006.06.026
- Ulbricht, M., Schneider, J., Stasiak, M., Sengupta, A., 2013. Ammonia recovery from industrial wastewater by transMembranechemiSorption. *Chemie-Ingenieur-Technik* 85, 1259–1262. doi:10.1002/cite.201200237
- Uludag-Demirer, S., Demirer, G.N., Chen, S., 2005. Ammonia removal from anaerobically digested dairy manure by struvite precipitation. *Process Biochem.* 40, 3667–3674. doi:10.1016/j.procbio.2005.02.028
- USDA ERS, 2013. Fertilizer use and price [WWW Document]. URL <http://www.ers.usda.gov/data-products/fertilizer-use-and-price.aspx> (accessed 7.22.15).
- USEPA, 1993. *Manual: Nitrogen control*, Office of Research and Development. Washington, D.C. doi:EPA/625/R-93/010
- USEPA, 1999. EPA 1999 update of ambient water quality criteria for ammonia, Environmental Protection. DIANE Publishing. doi:EPA-822-R-99-014

- Verbeeck, R.M.H., De Bruyne, P.A.M., Driessens, F.C.M., Verbeek, F., 1984. Solubility of magnesium hydrogen phosphate trihydrate and ion-pair formation in the system magnesium hydroxide-phosphoric acid-water at 25°C. *Inorg. Chem.* 23, 1922–1926. doi:10.1021/ic00181a026
- WEF, 2005. Biological nutrient removal (BNR) operation in wastewater treatment plants WEF manual of practice no. 29. McGraw-Hill, Alexandria, VA.
- WERF, 2009. Nutrient removal: Operation and control [WWW Document]. Water Environ. Res. Fed. URL https://www.werf.org/c/KnowledgeAreas/NutrientRemoval/compendium/09-Operation_and_Control_of_BNR.aspx (accessed 7.21.15).
- WERF, 2010. Nutrient recovery state of the knowledge as of December 2010 [WWW Document]. Water Environ. Res. Fed. URL www.werf.org/c/2011Challenges/Nutrient_Recovery.aspx (accessed 7.15.15).
- Whitaker, A., 1968. The Decomposition of Struvite. *Mineral. Mag.* 820–824. doi:10.1180/minmag.1969.037.286.24
- Whitaker, A., Jeffery, J.W., 1970. The crystal structure of struvite, $\text{MgNH}_4\text{PO}_4 \cdot 6\text{H}_2\text{O}$. *Acta Crystallogr. Sect. B Struct. Crystallogr. Cryst. Chem.* 26, 1429–1440. doi:10.1107/S0567740870004284
- Wilson, C.W., 2013. Ammonia recovery from municipal wastewater through a struvite formation-thermal decomposition cycle. M.A.Sc. Thesis, Department of Civil Engineering, The University of British Columbia, Vancouver, BC.
- Wood, S., Cowie, A., 2004. A review of greenhouse gas emission factors for fertiliser production. IEA Bioenergy Task, 38.
- Yetilmezsoy, K., Sapci-Zengin, Z., 2009. Recovery of ammonium nitrogen from the effluent of UASB treating poultry manure wastewater by MAP precipitation as a slow release fertilizer. *J. Hazard. Mater.* 166, 260–269. doi:10.1016/j.jhazmat.2008.11.025
- Yin, S.F., Xu, B.Q., Zhou, X.P., Au, C.T., 2004. A mini-review on ammonia decomposition catalysts for on-site generation of hydrogen for fuel cell applications. *Appl. Catal. A Gen.* 277, 1–9. doi:10.1016/j.apcata.2004.09.020
- Zallen, R., 1998. The physics of amorphous solids. *Am. J. Phys.* 54, 318. doi:10.1002/9783527617968
- Zamfirescu, C., Dincer, I., 2008. Using ammonia as a sustainable fuel. *J. Power Sources* 185, 459–465. doi:10.1016/j.jpowsour.2008.02.097
- Zamfirescu, C., Dincer, I., 2009. Ammonia as a green fuel and hydrogen source for vehicular applications. *Fuel Process. Technol.* 90, 729–737. doi:10.1016/j.fuproc.2009.02.004
- Zengin, G., Ölmez, T., Doğruel, S., Kabdaşlı, I., Tünay, O., 2002. Assessment of source-based nitrogen removal alternatives in leather tanning industry wastewater. *Water Sci. Technol.* 45, 205–215.
- Zhang, S., Yao, C., Feng, X., Yang, M., 2004. Repeated use of $\text{MgNH}_4\text{PO}_4 \cdot 6\text{H}_2\text{O}$ residues for ammonium removal by acid dipping. *Desalination* 170, 27–32. doi:10.1016/j.desal.2003.12.009

- Zhang, T., Ding, L., Ren, H., 2009a. Pretreatment of ammonium removal from landfill leachate by chemical precipitation. *J. Hazard. Mater.* 166, 911–915. doi:10.1016/j.jhazmat.2008.11.101
- Zhang, T., Ding, L., Ren, H., Xiong, X., 2009b. Ammonium nitrogen removal from coking wastewater by chemical precipitation recycle technology. *Water Res.* 43, 5209–5215. doi:10.1016/j.watres.2009.08.054

Appendices

Appendix A : Operational settings for instruments

Table A.1 Settings for x-ray diffraction (XRD), using a Bruker D8 Advance X-ray diffractometer

Parameter	Setting
Type of radiation	CuK α
Starting scanning angle, 2θ min ⁻¹ (Low angle XRD)	0.8°
Scanning angle, 2θ min ⁻¹ (Normal angle XRD)	5°
Average scanning rate	0.019°

Table A.2 Settings for magnesium analysis using flame atomic absorption spectrophotometer

Parameter	Setting
Mode	Absorbance
Measurement	Mode Integration
Flame Type	Air/C ₂ H ₂
Lamp Current	4.0 mA
Wavelength	202.6 nm
Calibration Range	0-250 mg/L

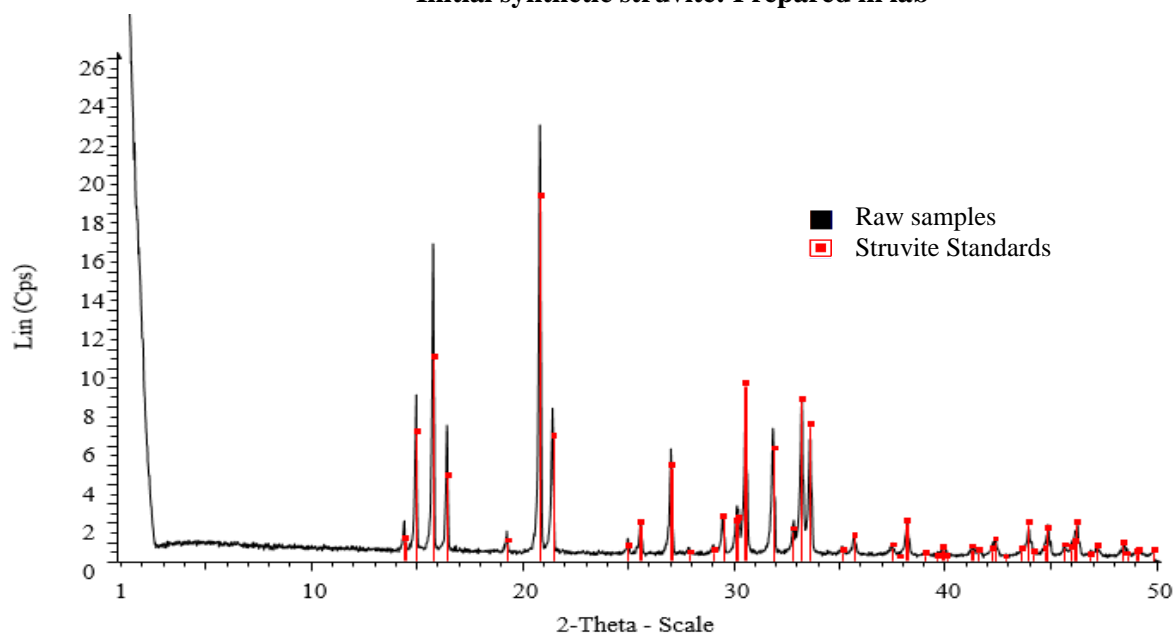
Table A.3 Settings for ammonia and orthophosphate analysis using flow injection analysis

Parameter	NH ₄ -N	PO ₄ -P
Method	4500-NH ₃ H ¹	4500-P G ¹
Temperature	63° C	63° C
Calibration Range	0-50 mg/L	0-25 mg/L

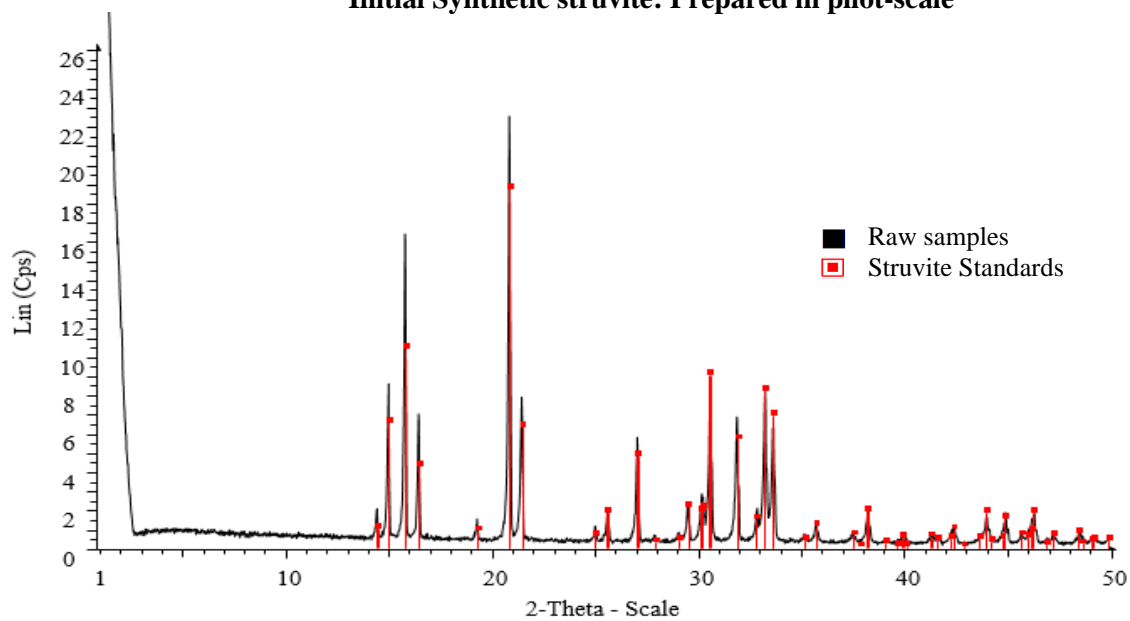
Appendix B : Oven dry experiments

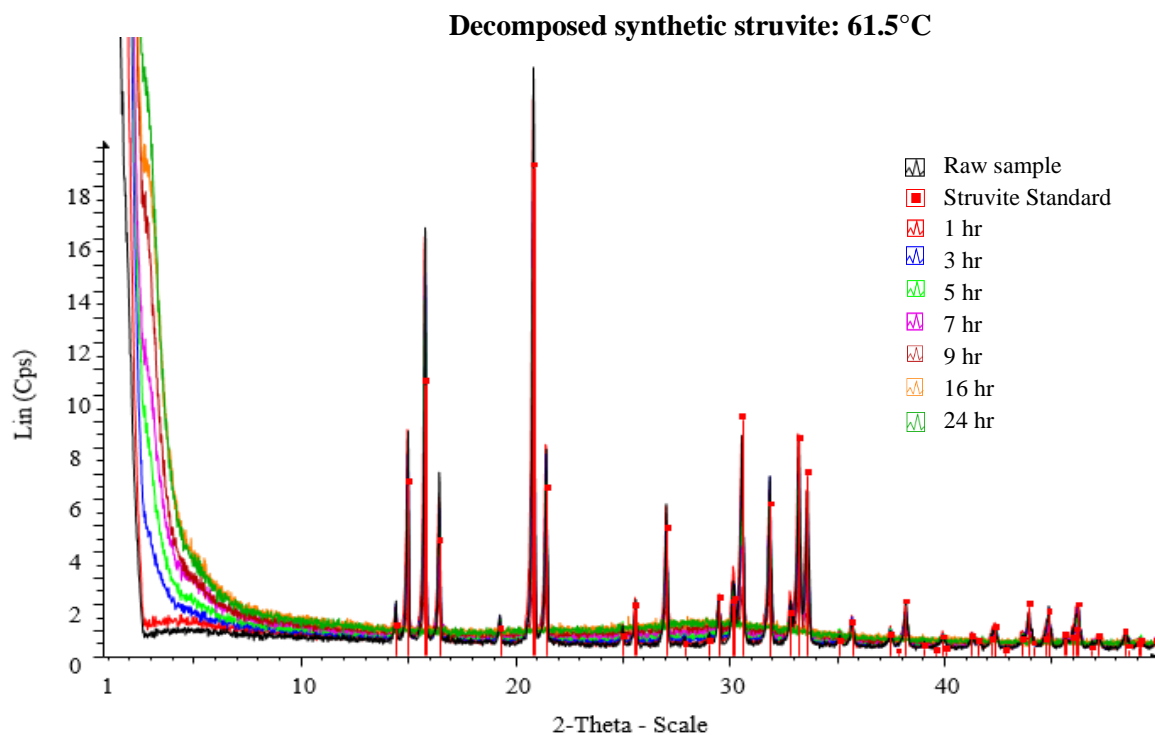
B.1 Formation of layered structure

Initial synthetic struvite: Prepared in lab

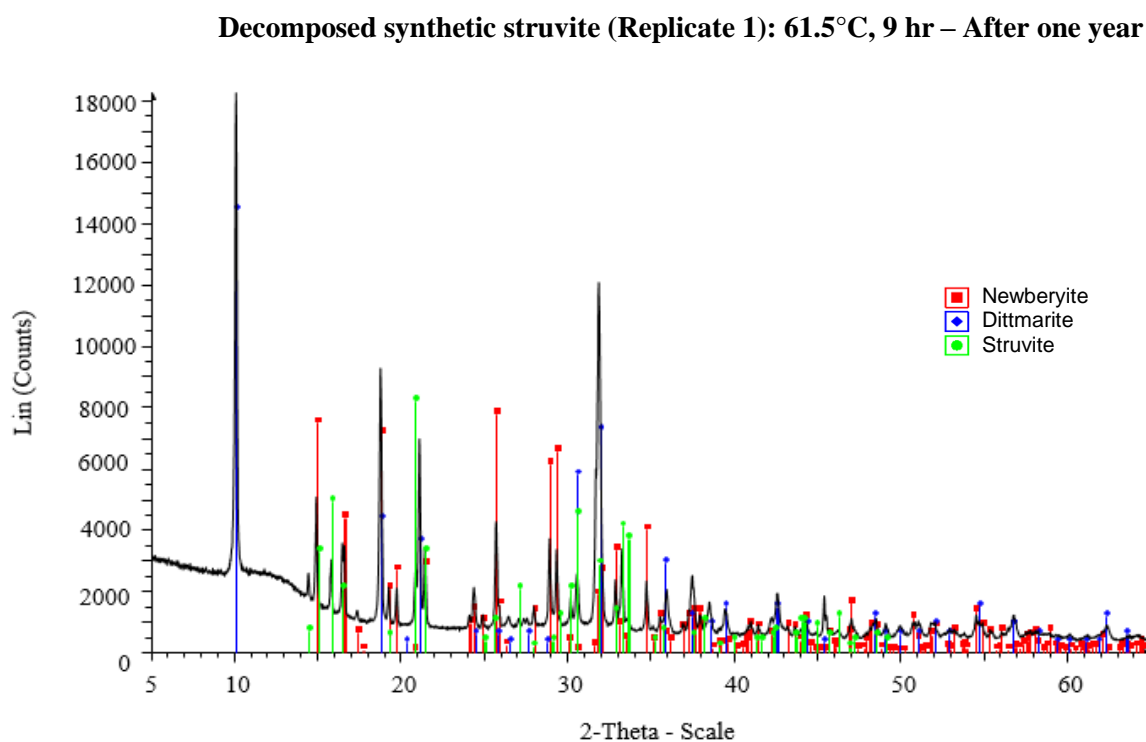


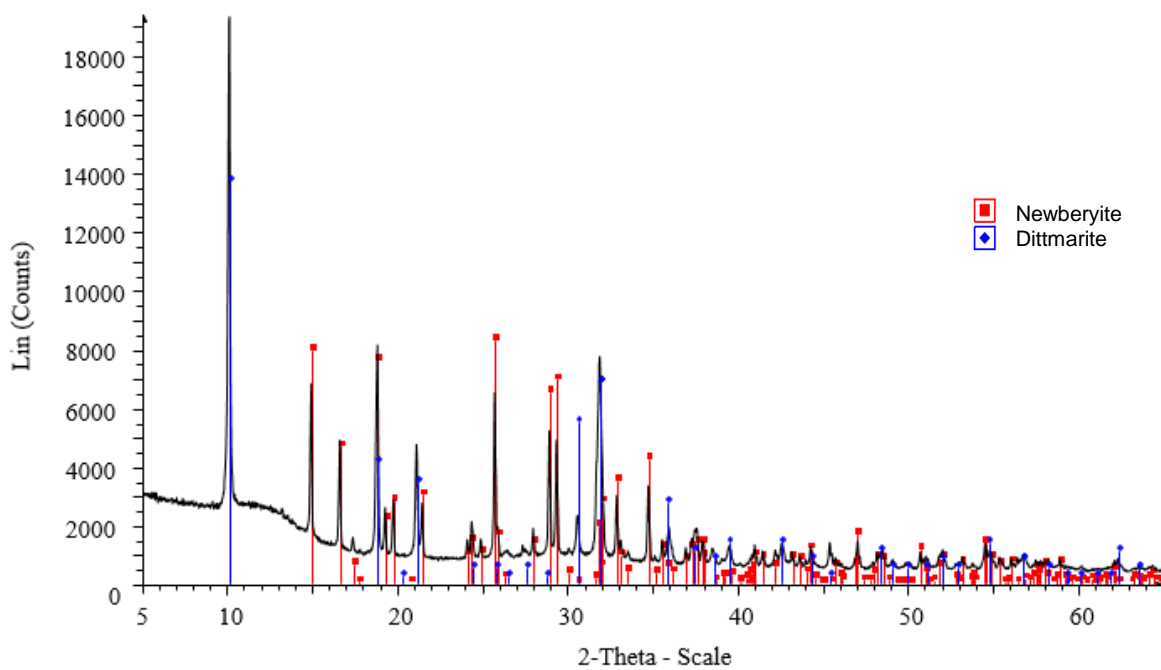
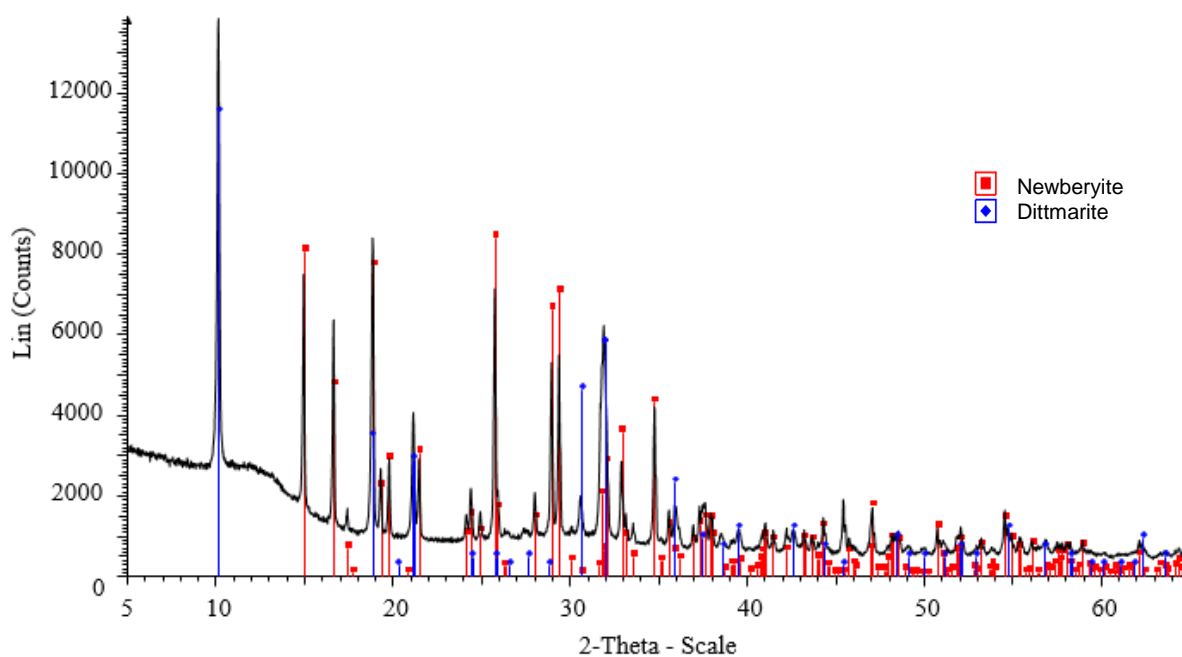
Initial Synthetic struvite: Prepared in pilot-scale

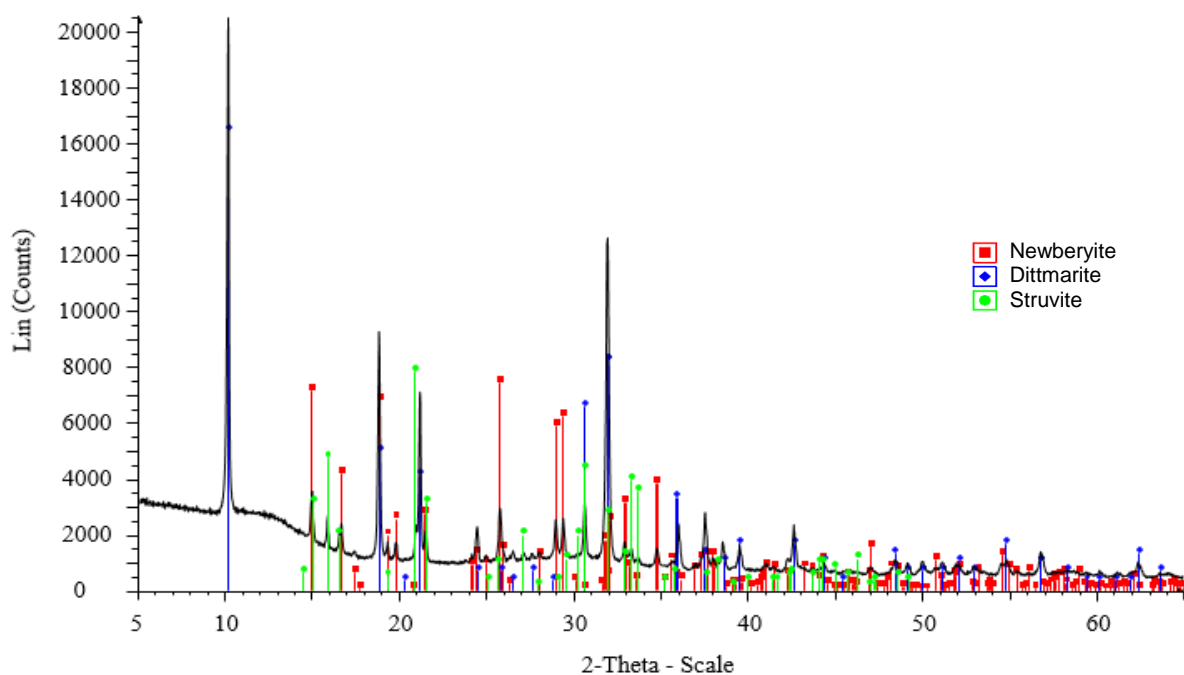
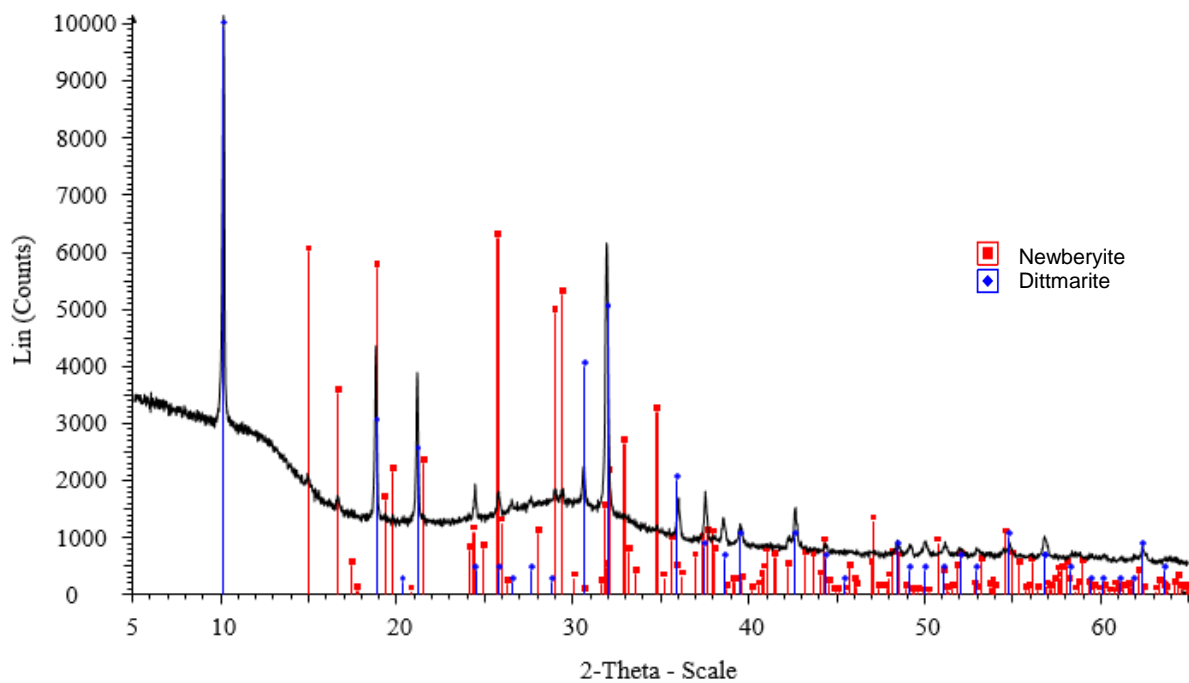


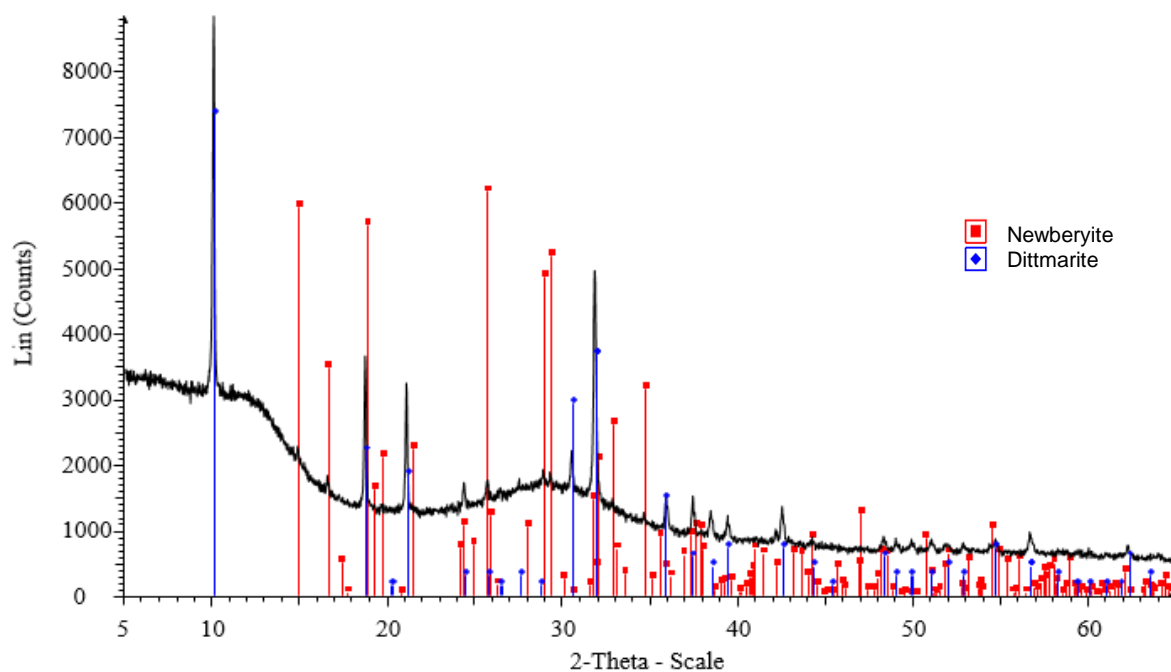
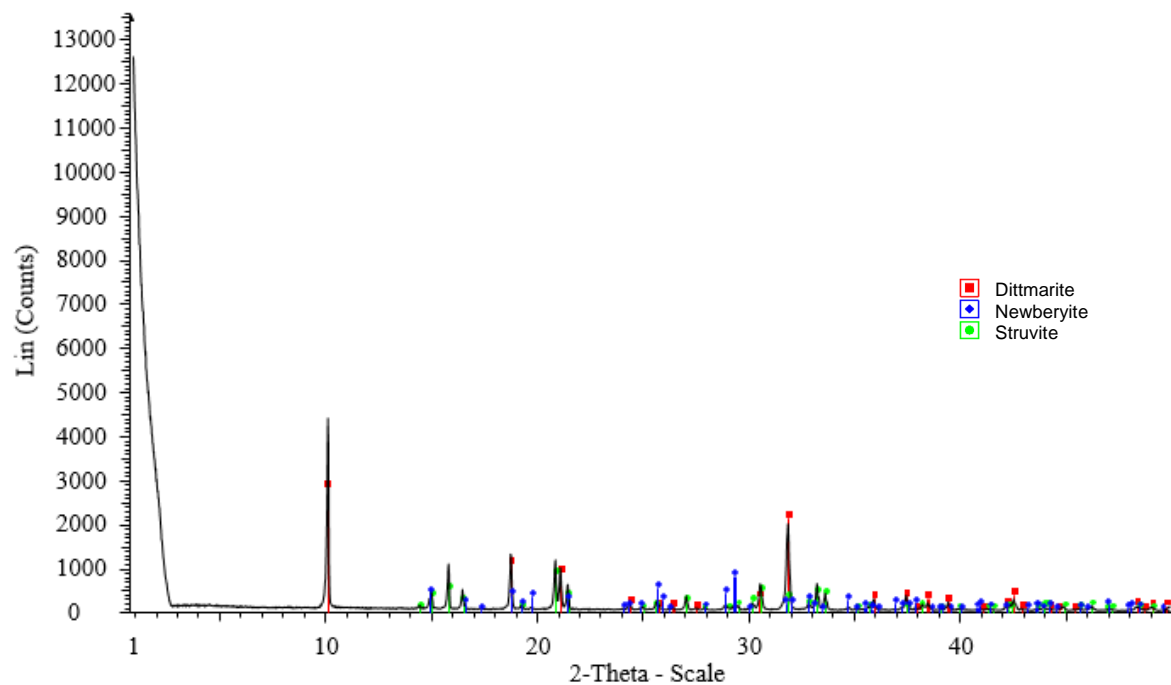


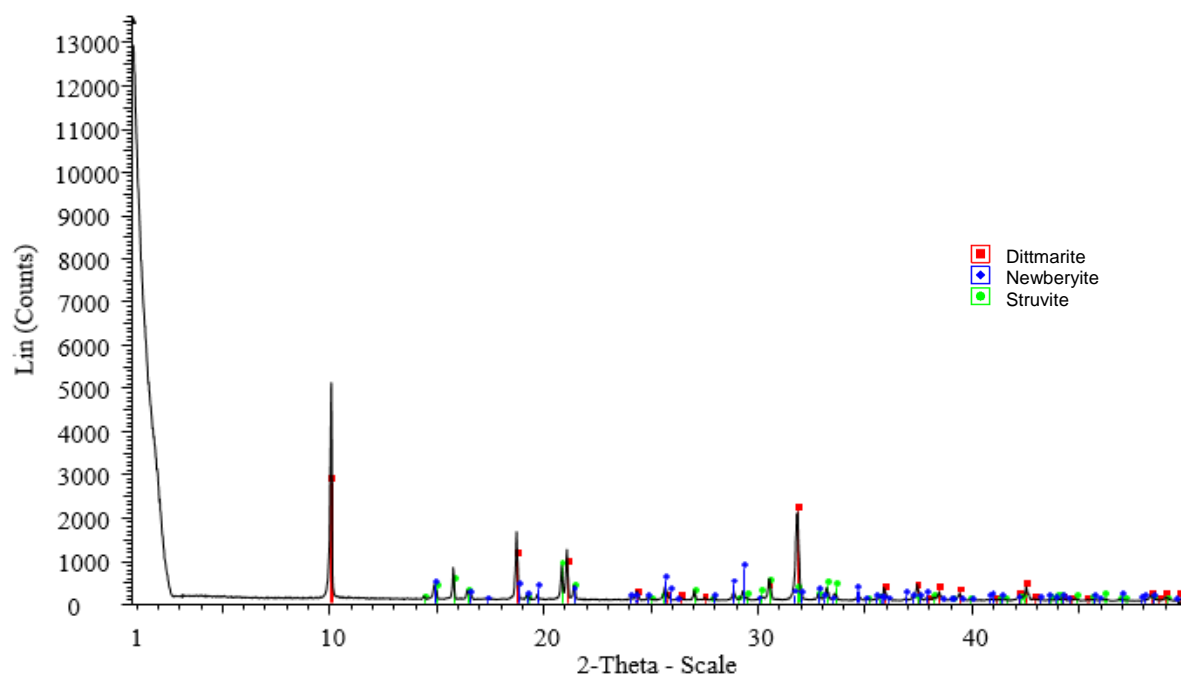
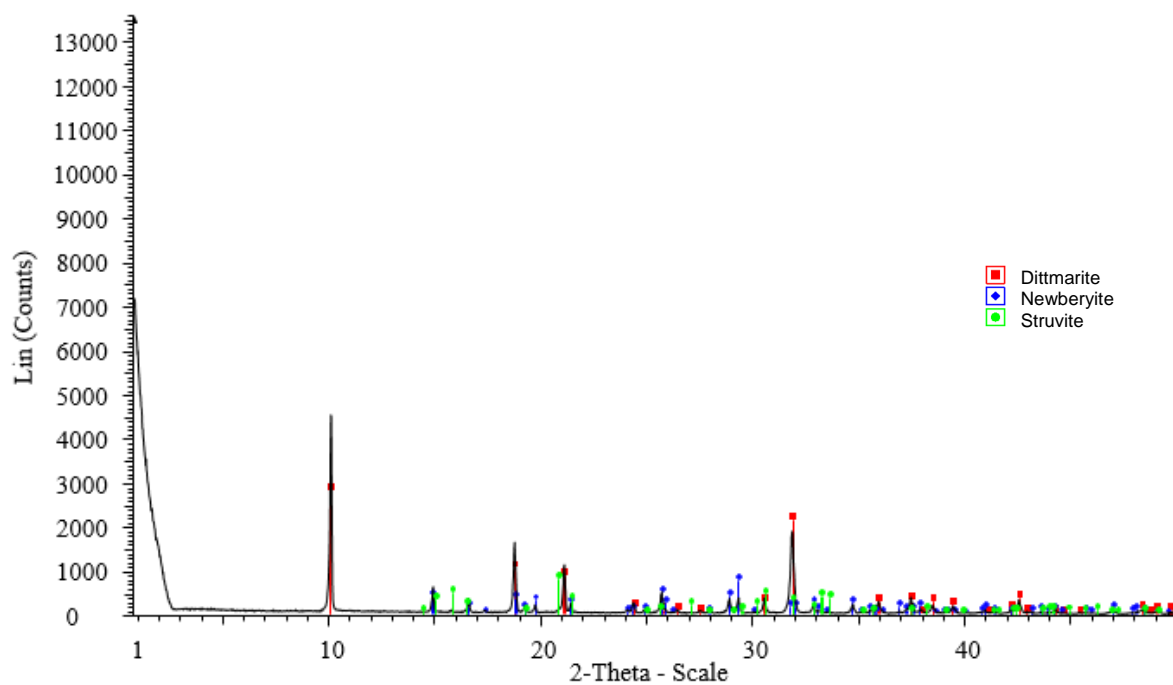
B.2 Transformation of layered structure over time

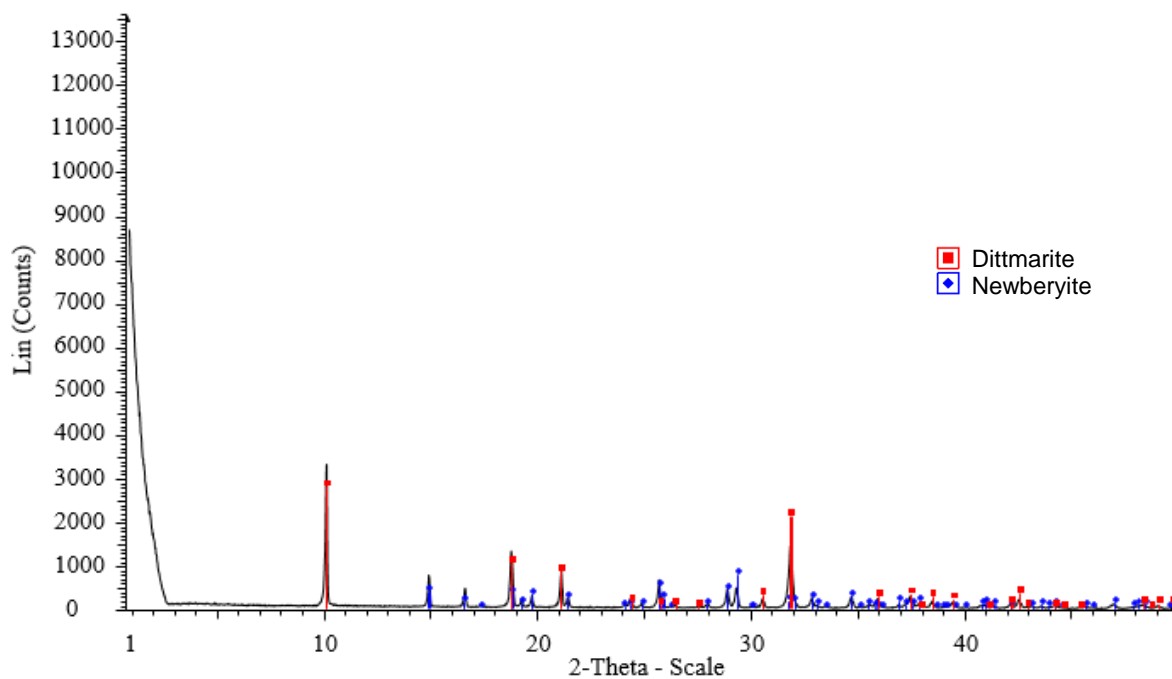
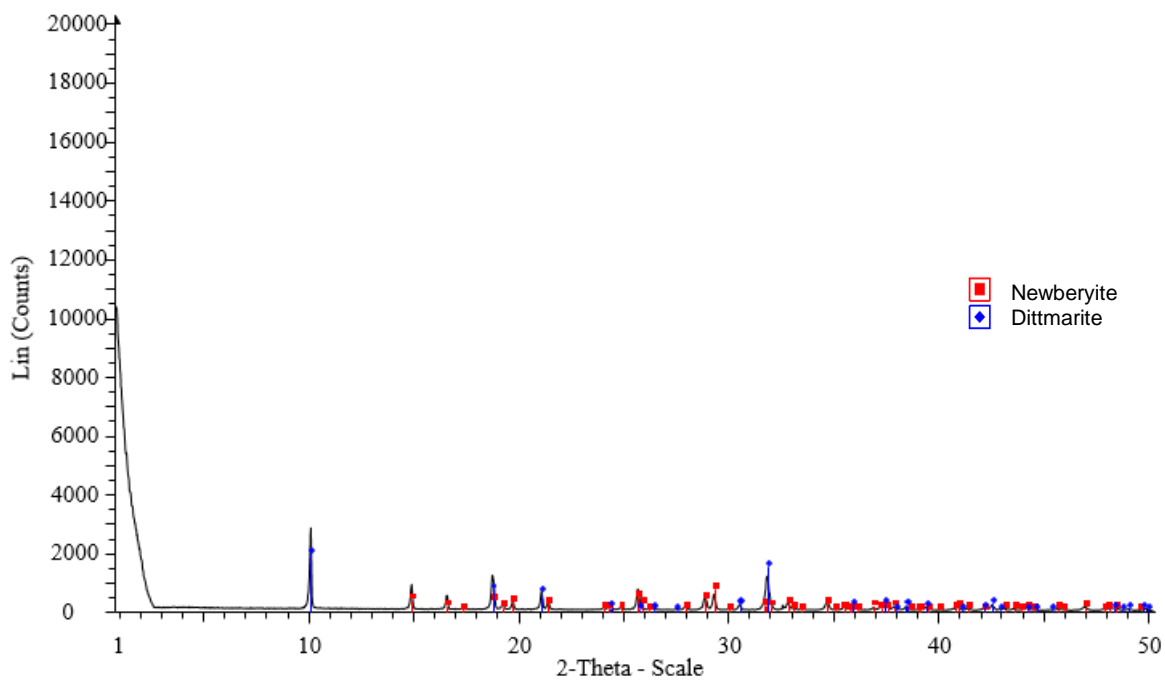


Decomposed synthetic struvite (Replicate 1): 61.5°C, 16 hr – After one year**Decomposed synthetic struvite (Replicate 1): 61.5°C, 24 hr – After one year**

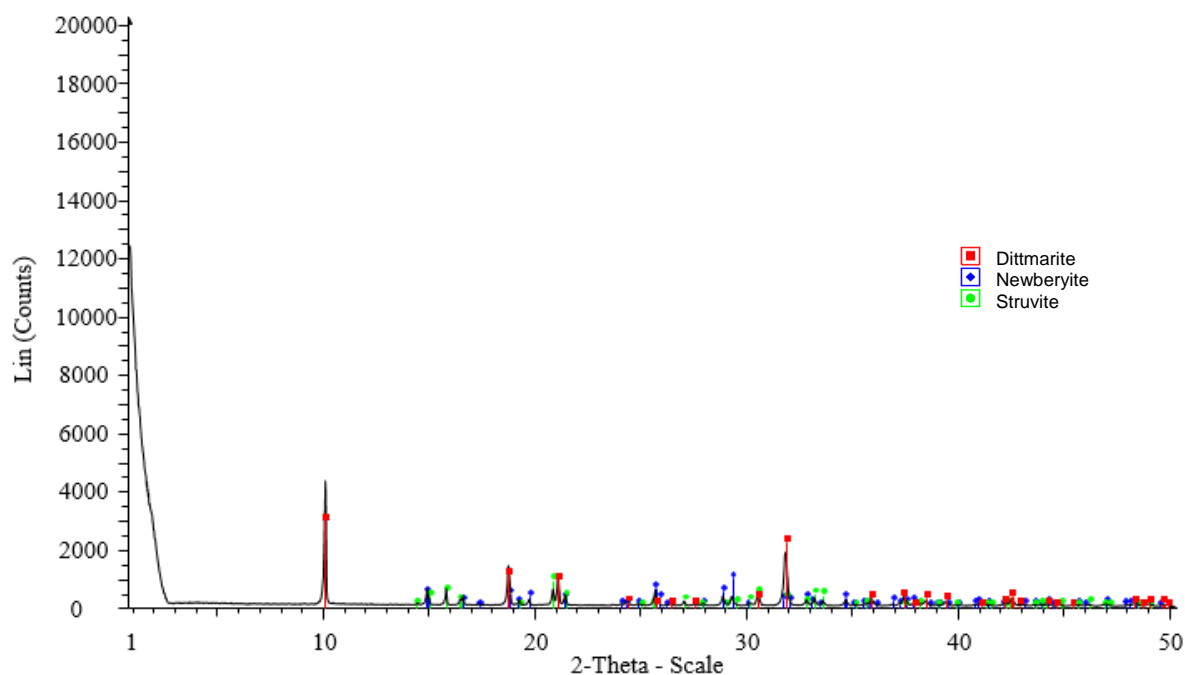
Decomposed synthetic struvite: 61.5°C (Replicate 2), 9 hr – After one year**Decomposed synthetic struvite: 61.5°C (Replicate 2), 16 hr – After one year**

Decomposed synthetic struvite: 61.5°C (Replicate 2), 24 hr – After one year**Decomposed synthetic struvite: 62.5°C, 3 hr – After 3 months**

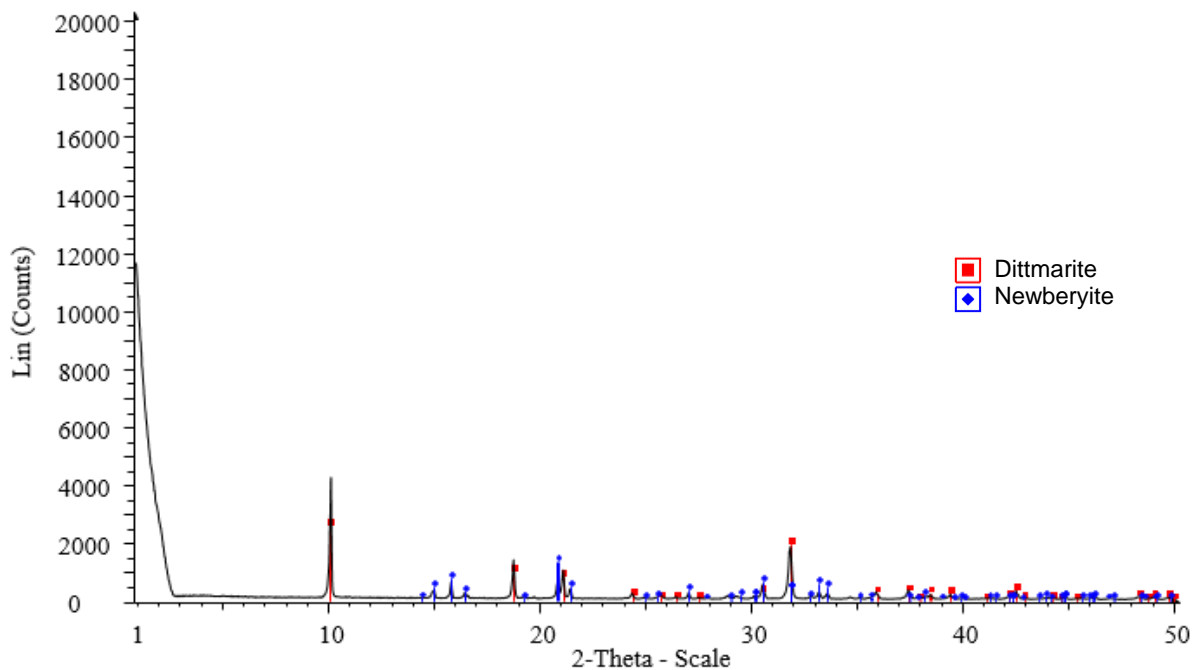
Decomposed synthetic struvite: 62.5°C, 6 hr – After 3 months**Decomposed synthetic struvite: 62.5°C, 9 hr – After 3 months**

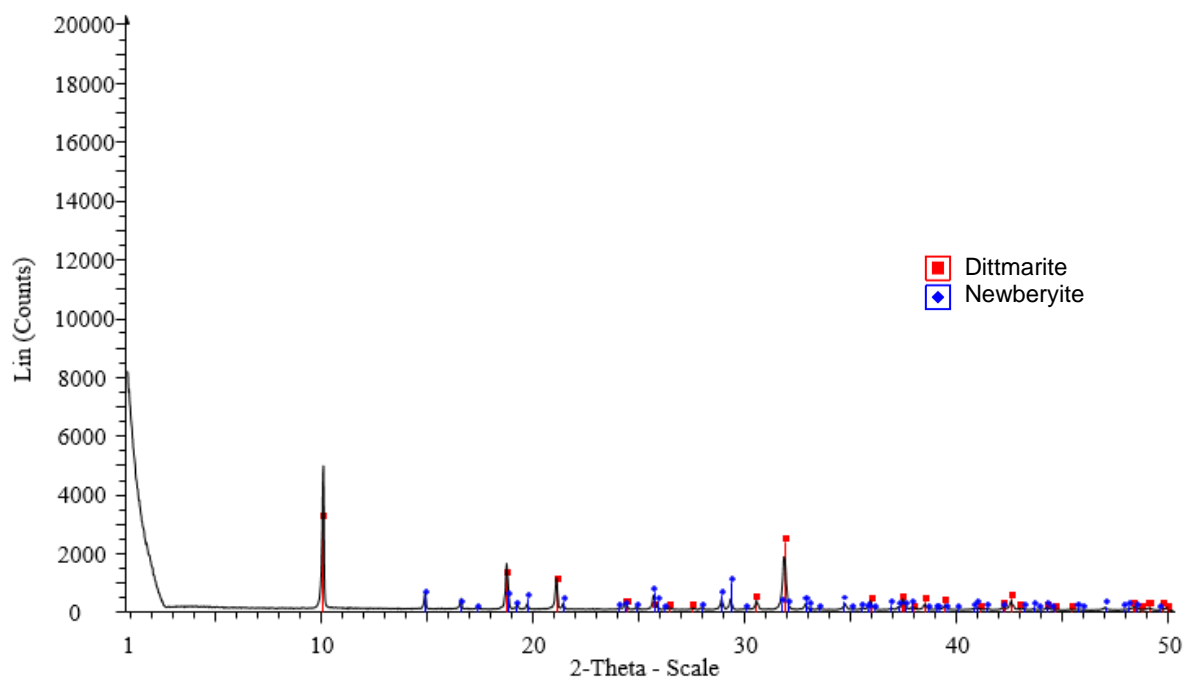
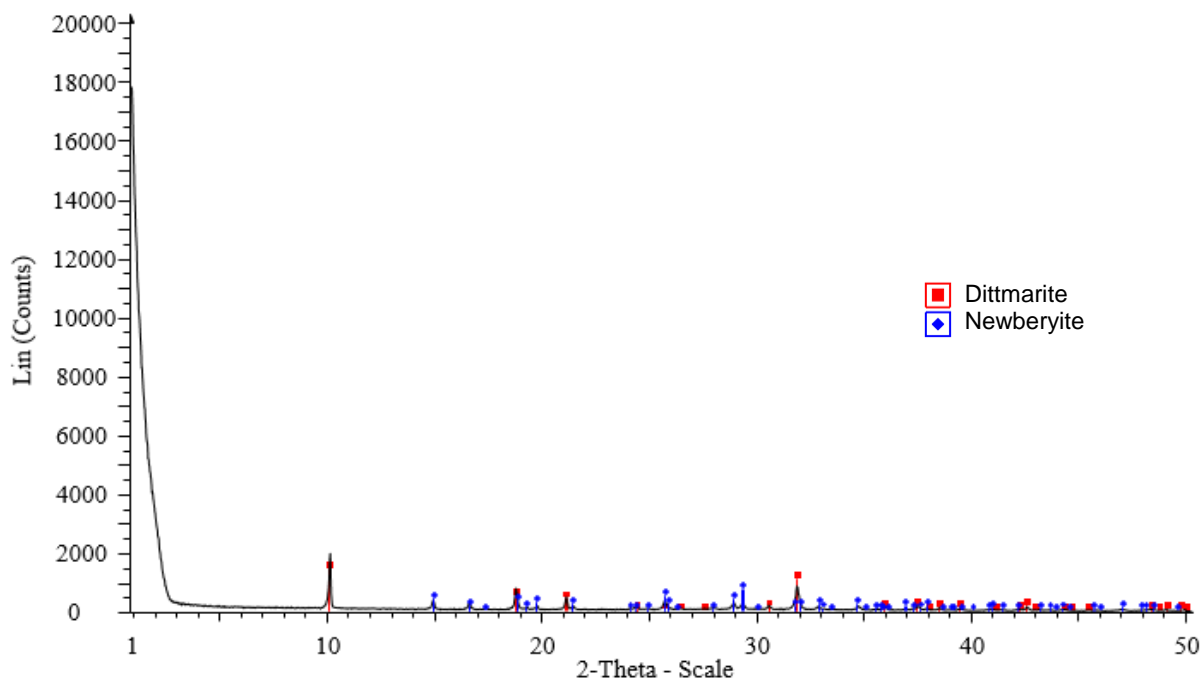
Decomposed synthetic struvite: 62.5°C, 16 hr – After 3 months**Decomposed synthetic struvite: 62.5°C, 24 hr – After 3 months**

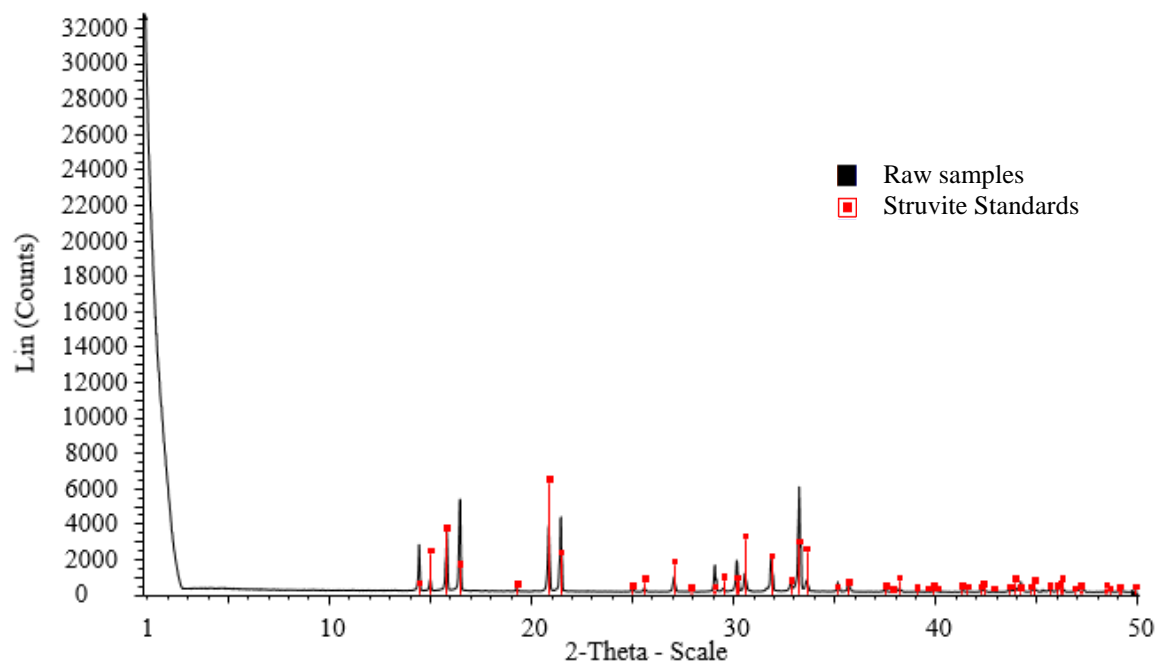
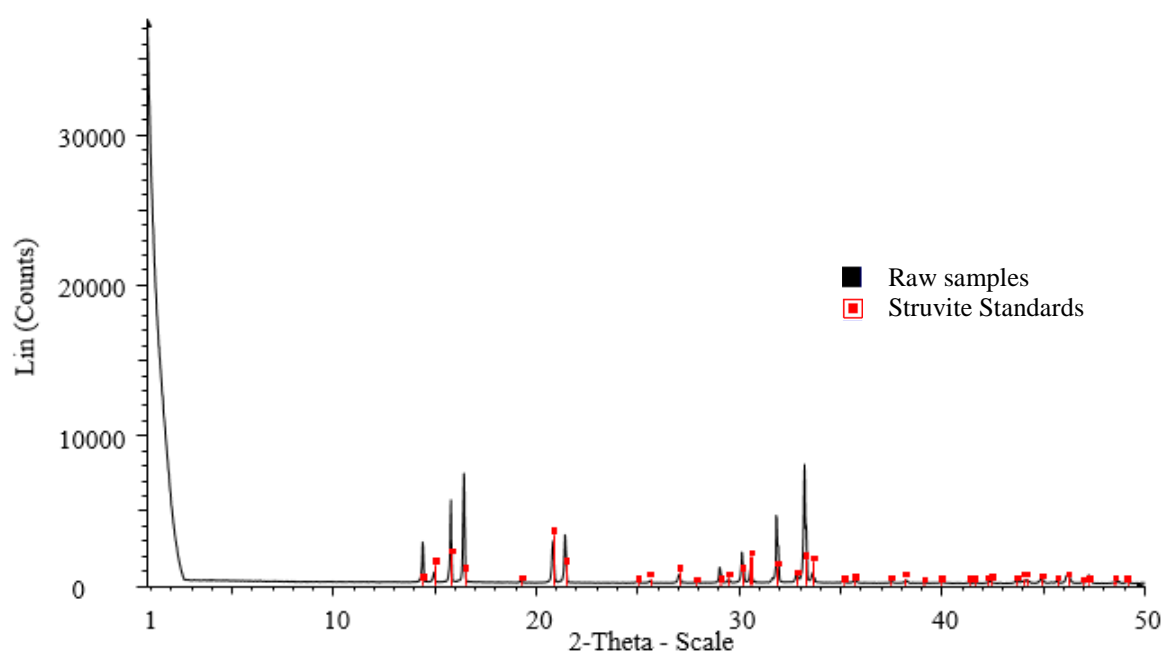
Decomposed synthetic struvite: 66.2°C, 5 hr – After 3 months

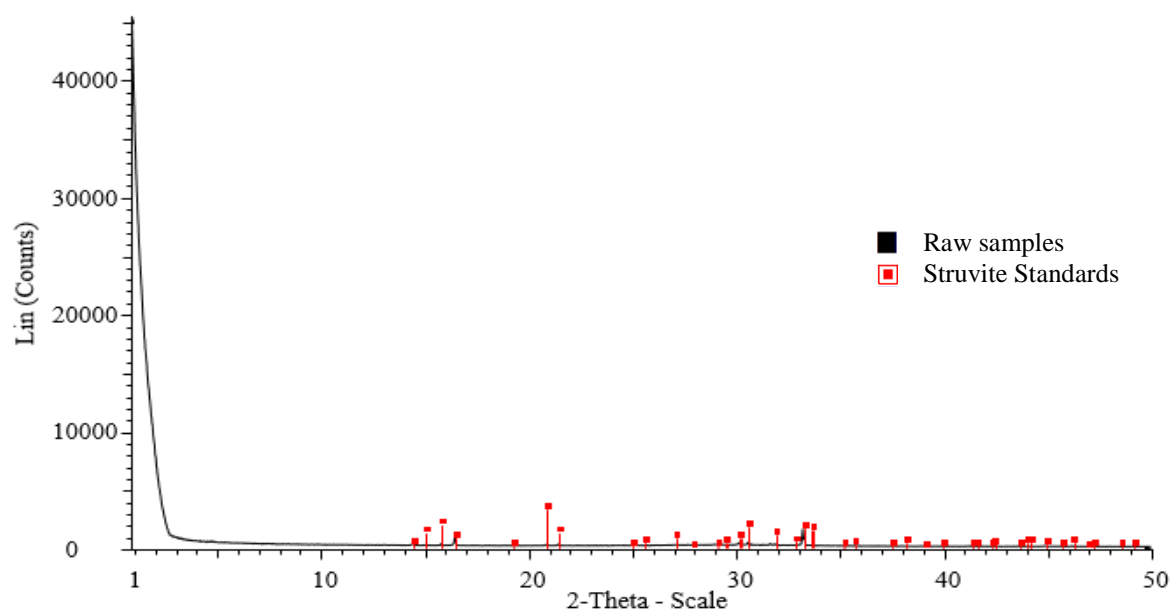


Decomposed synthetic struvite: 71.1°C, 1 hr – After 3 months



Decomposed synthetic struvite: 71.1°C, 3 hr – After 3 months**Decomposed synthetic struvite: 71.1°C, 9 hr – After 3 months**

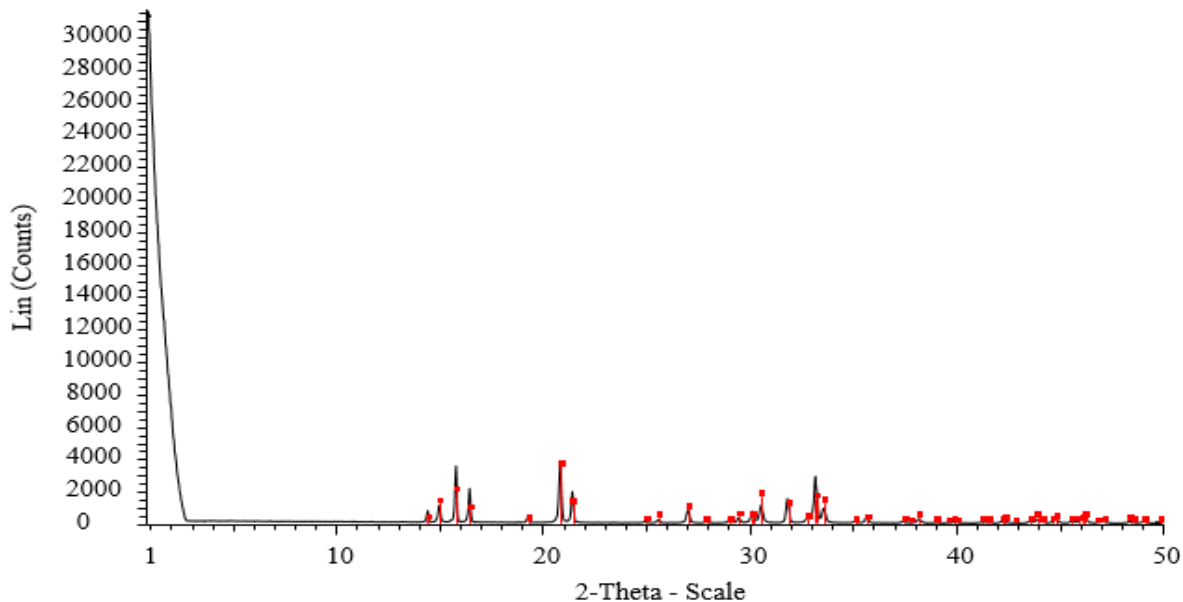
B.3 Temperature influence on layered structure formation**Synthetic struvite: Initial****Decomposed synthetic struvite: 59.6°C, 7 hr**

Decomposed synthetic struvite: 70.1°C, 7 hr

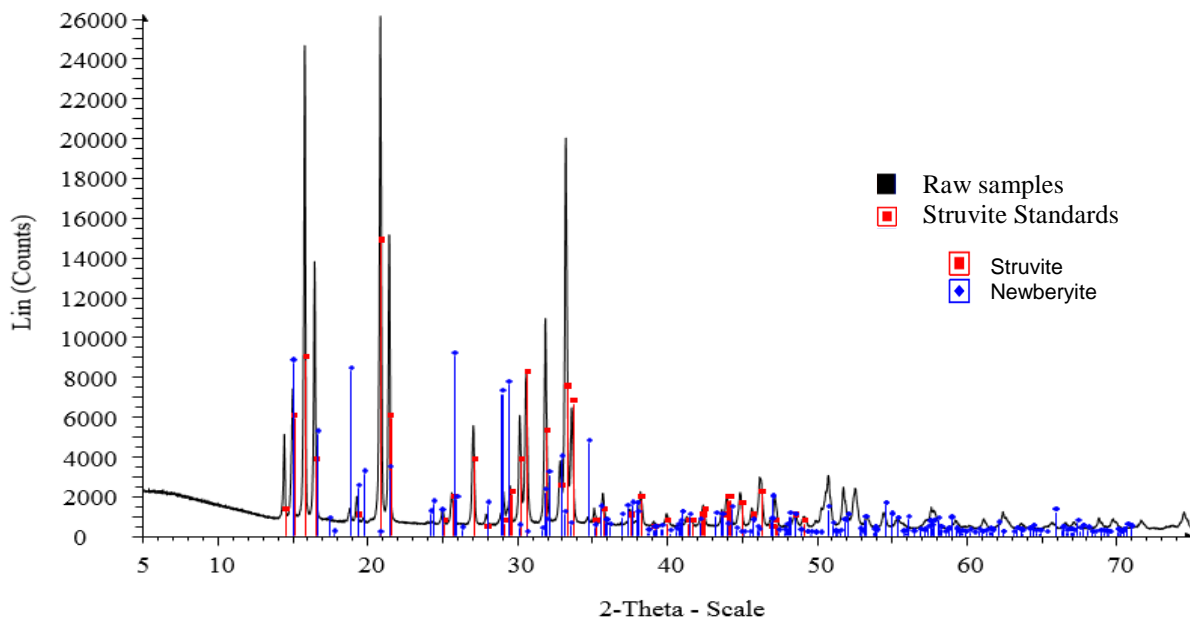
Appendix C : Bench-scale experiments

C.1 XRD results of decomposed samples using different combination of temperature and relative humidity

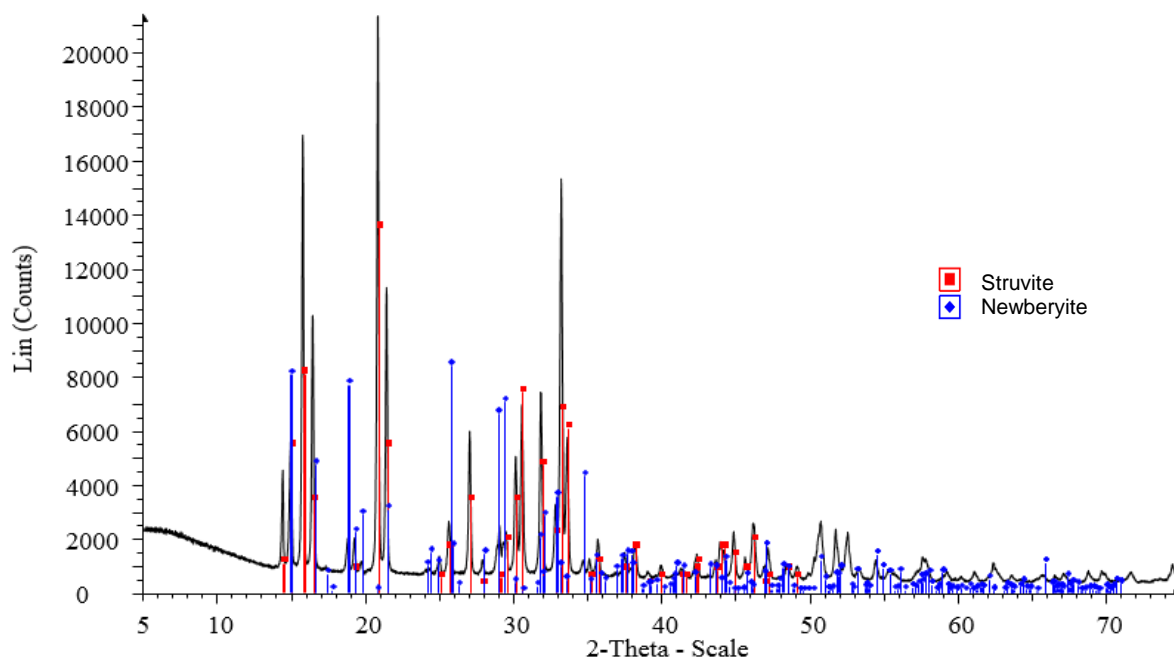
Lulu Island struvite (<1mm): Initial



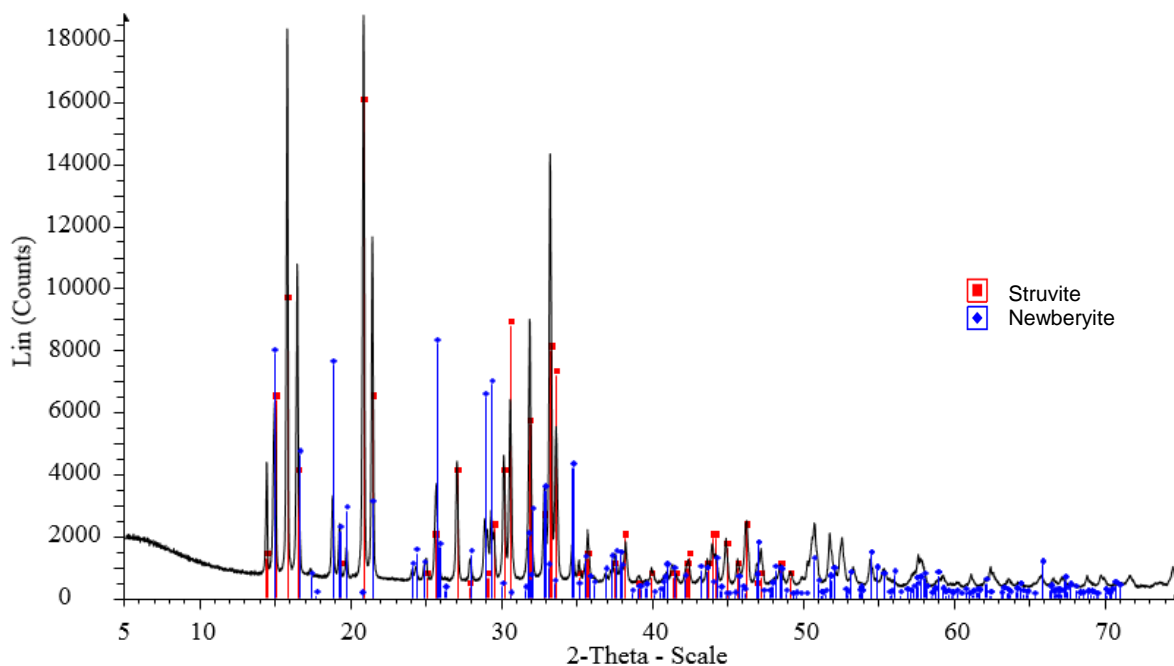
Lulu Island pellets (<1mm): T - 65°C, RH - 65%, 2 hr

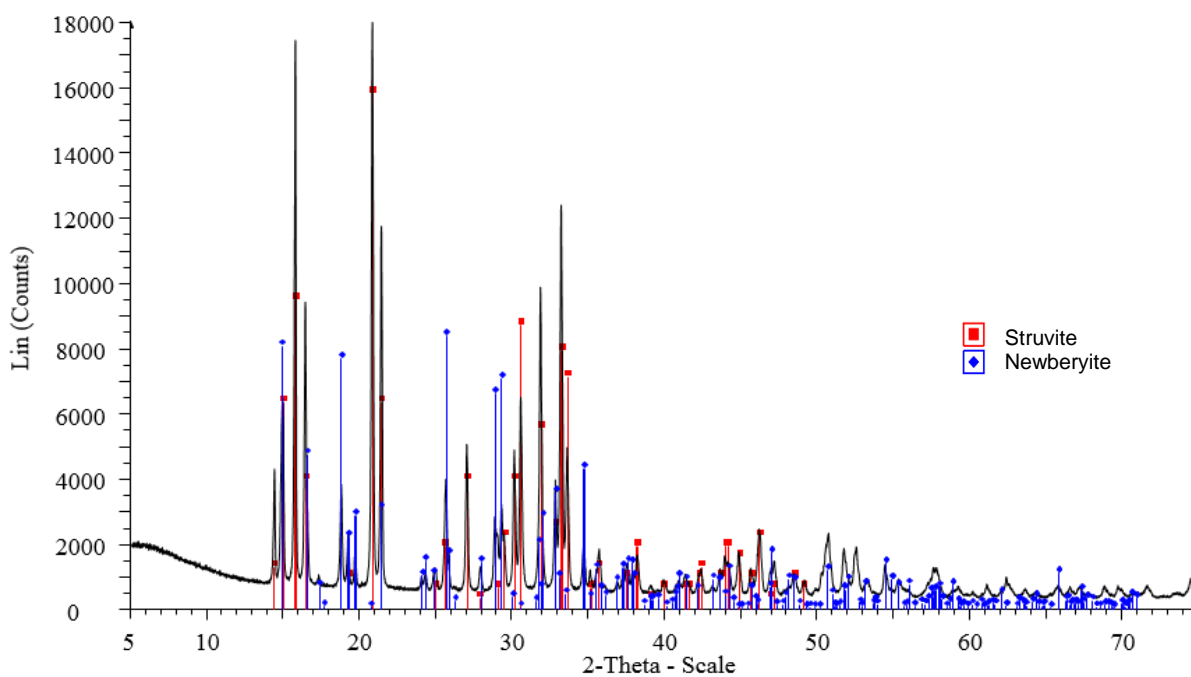
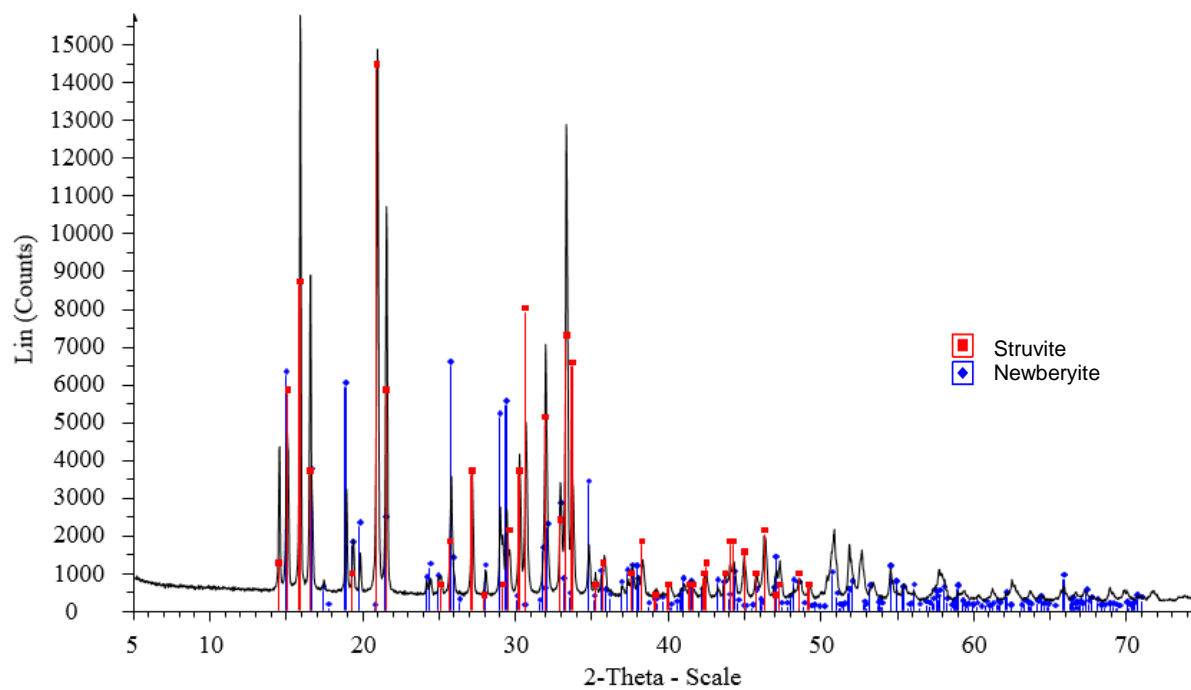


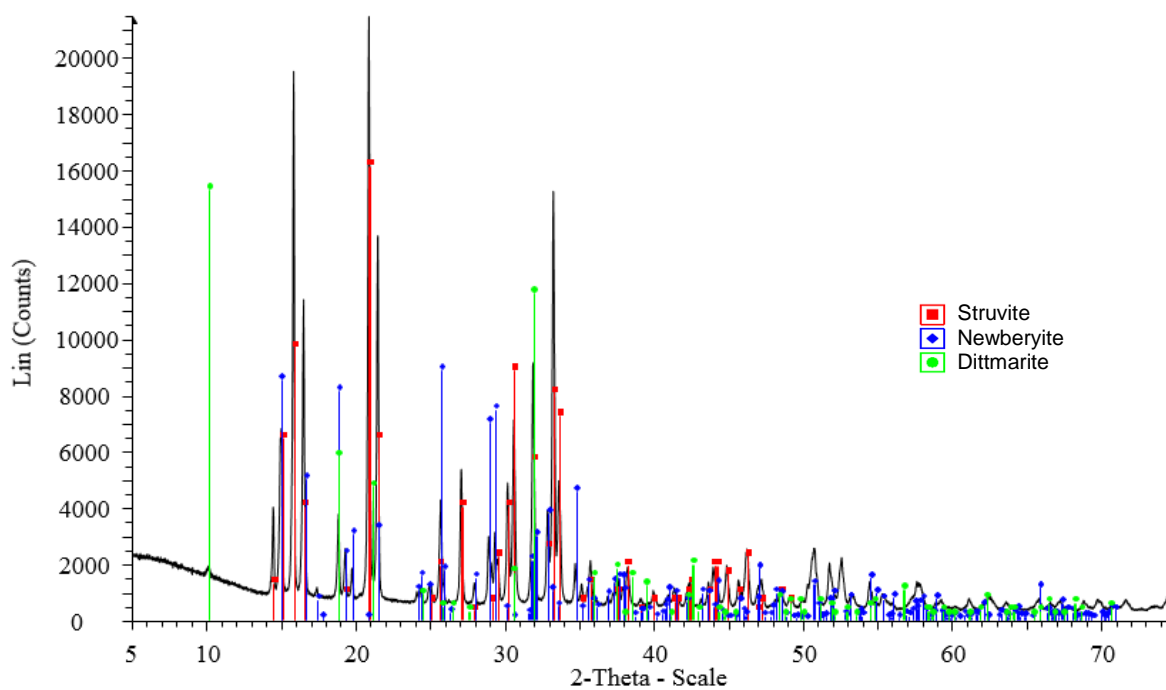
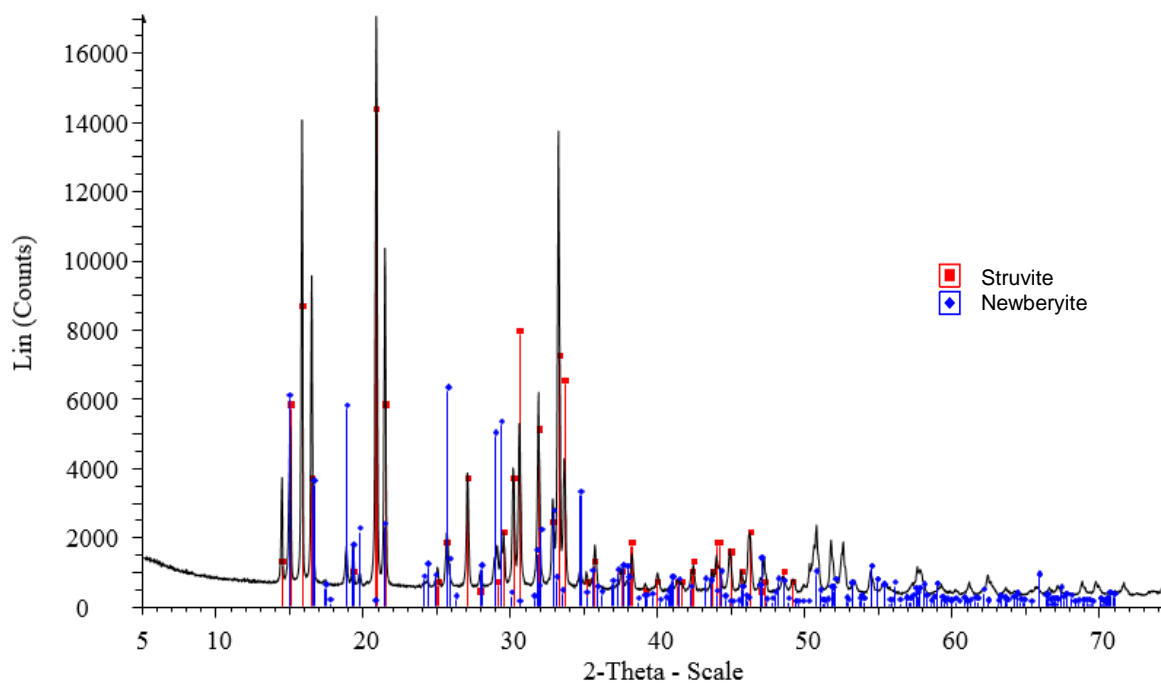
Lulu Island pellets (<1mm): T - 65°C, RH - 65%, 4 hr

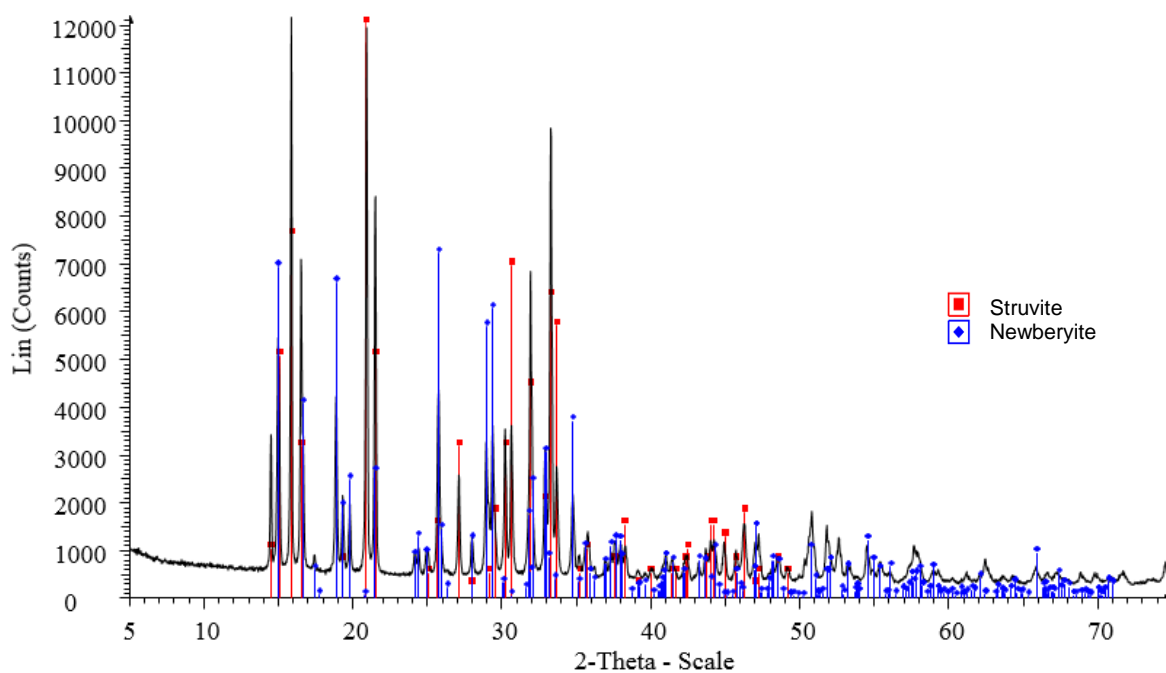
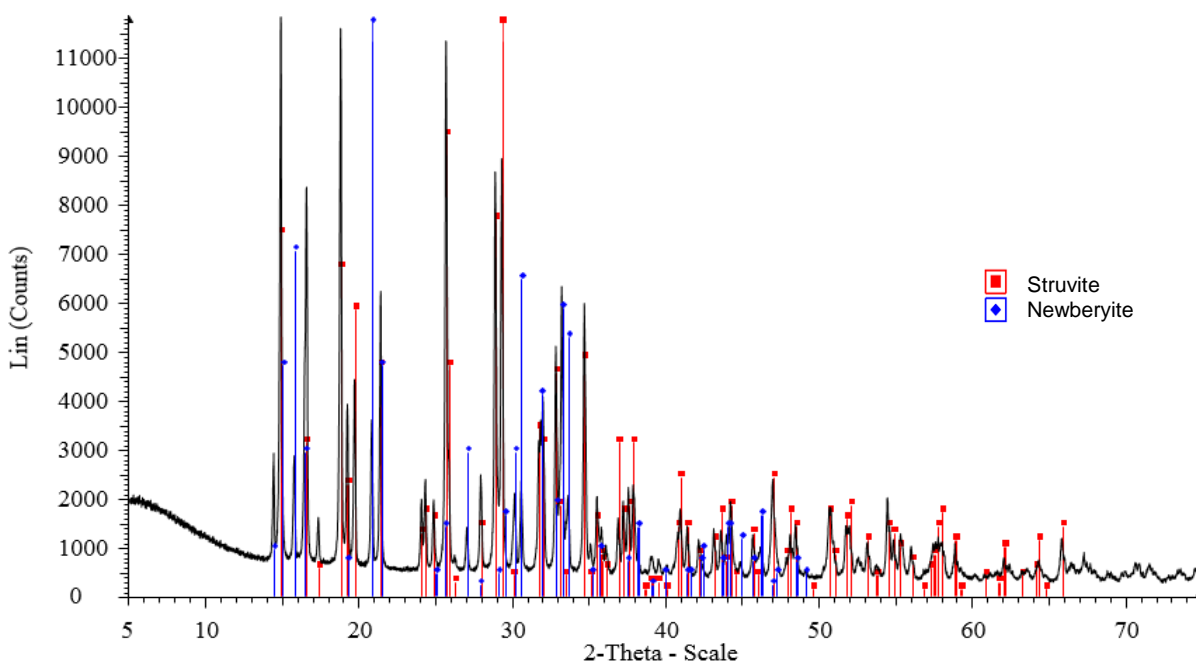


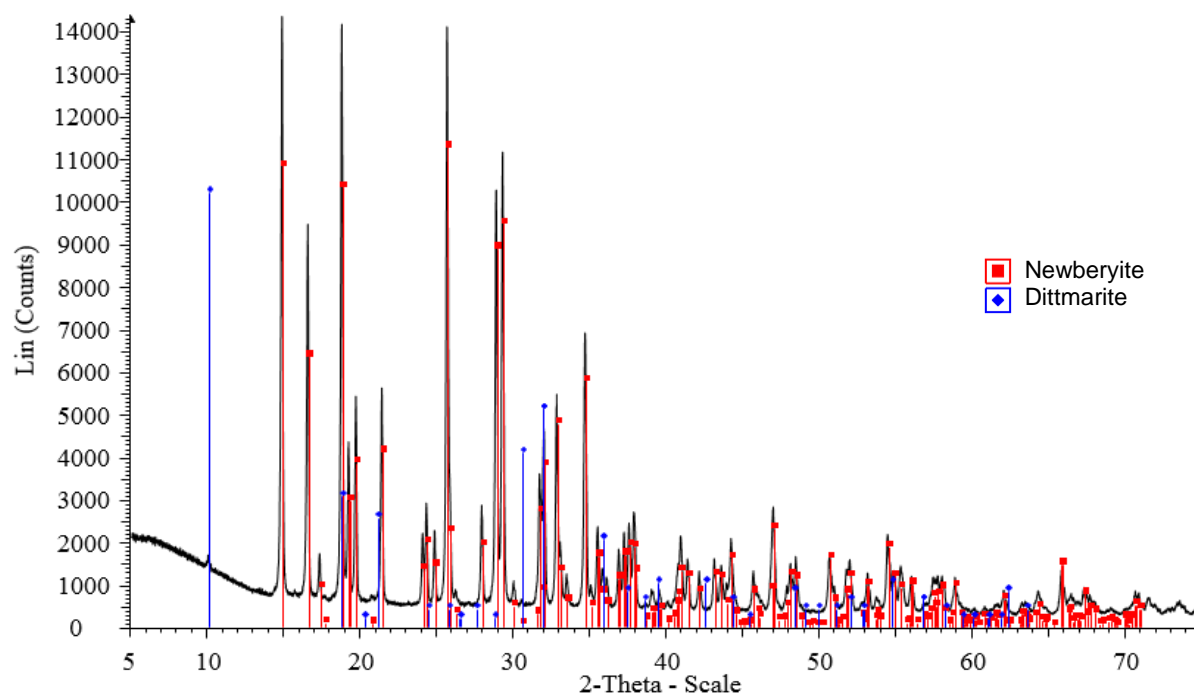
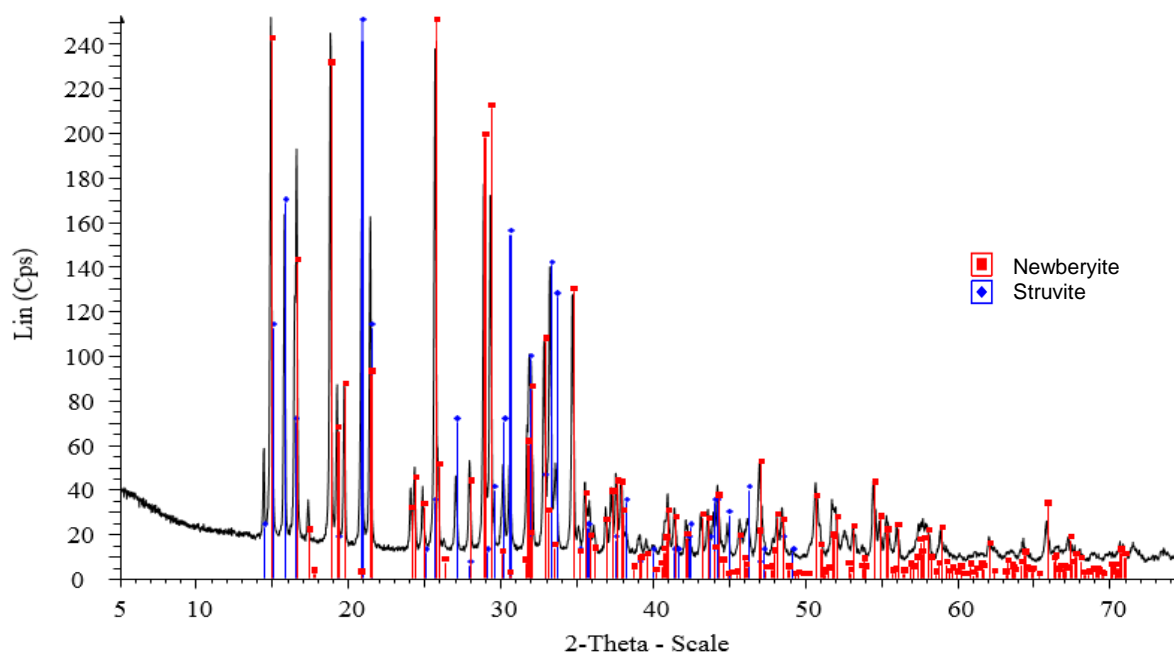
Lulu Island pellets (<1mm): T - 65°C, RH - 80%, 2 hr

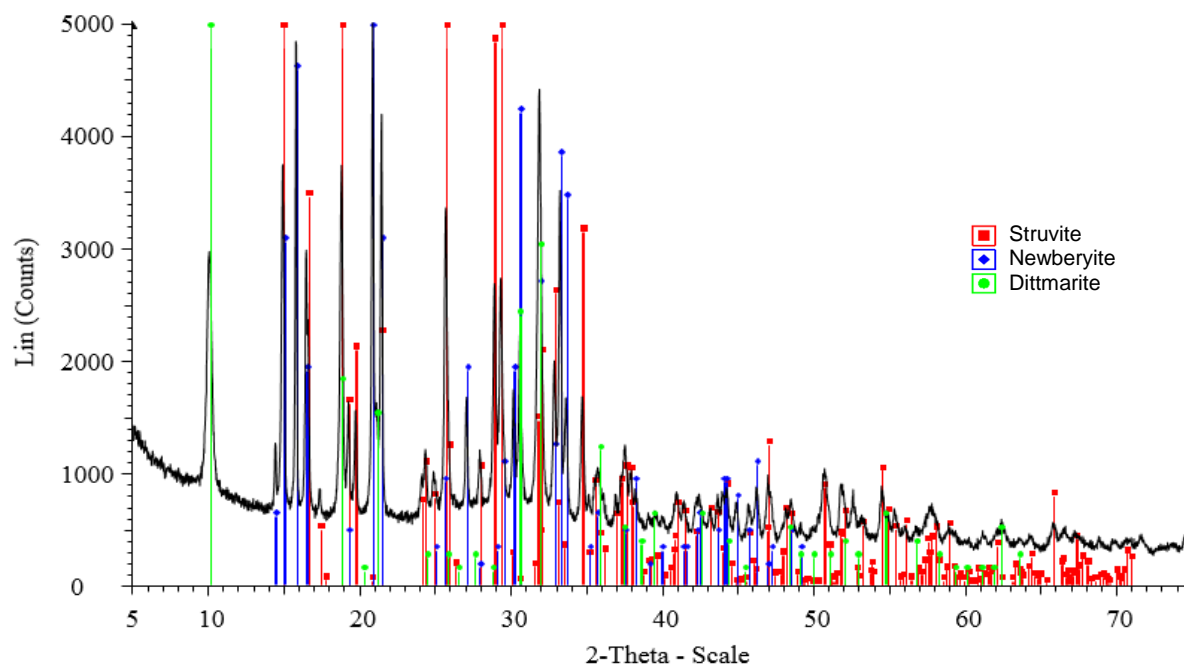
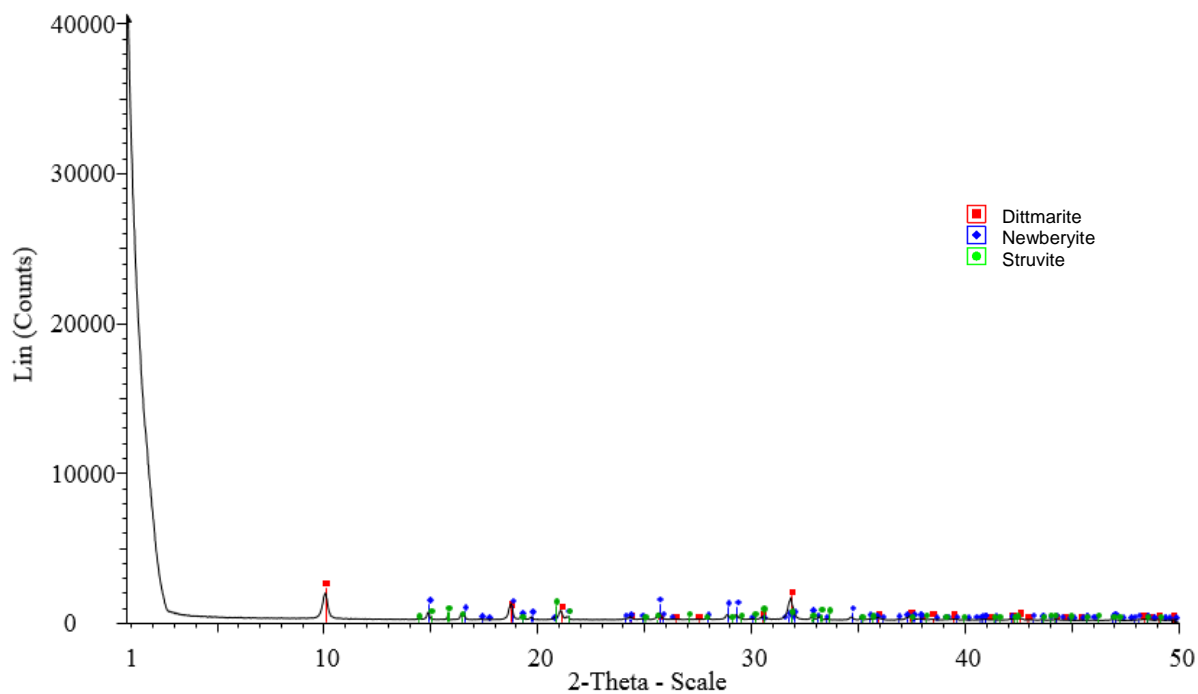


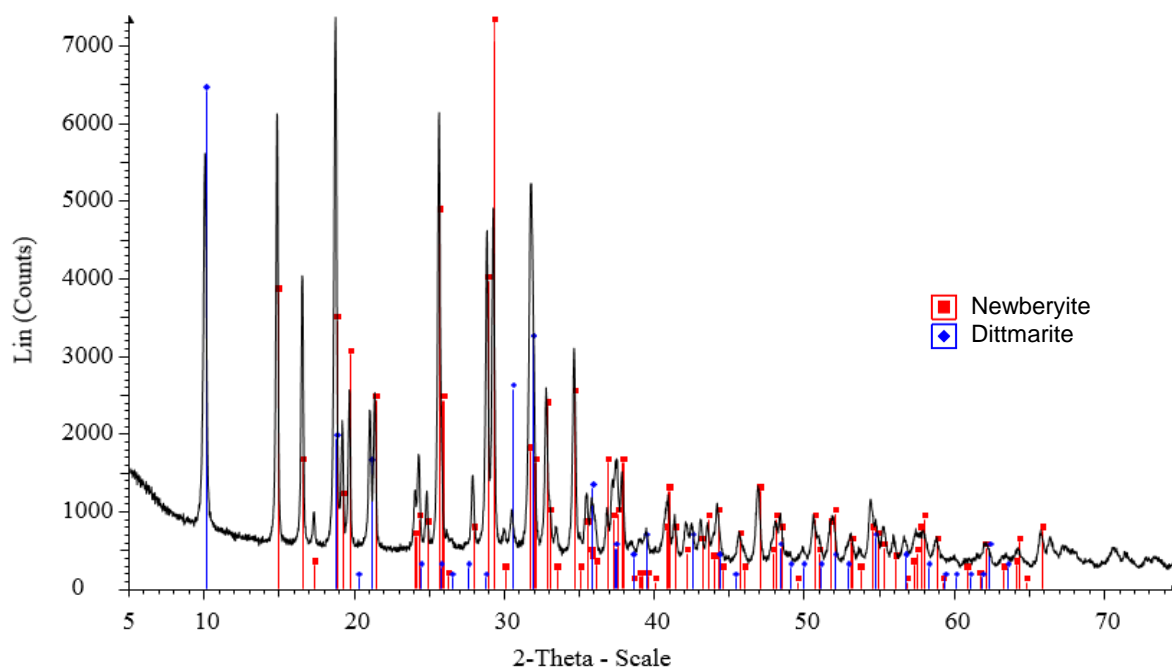
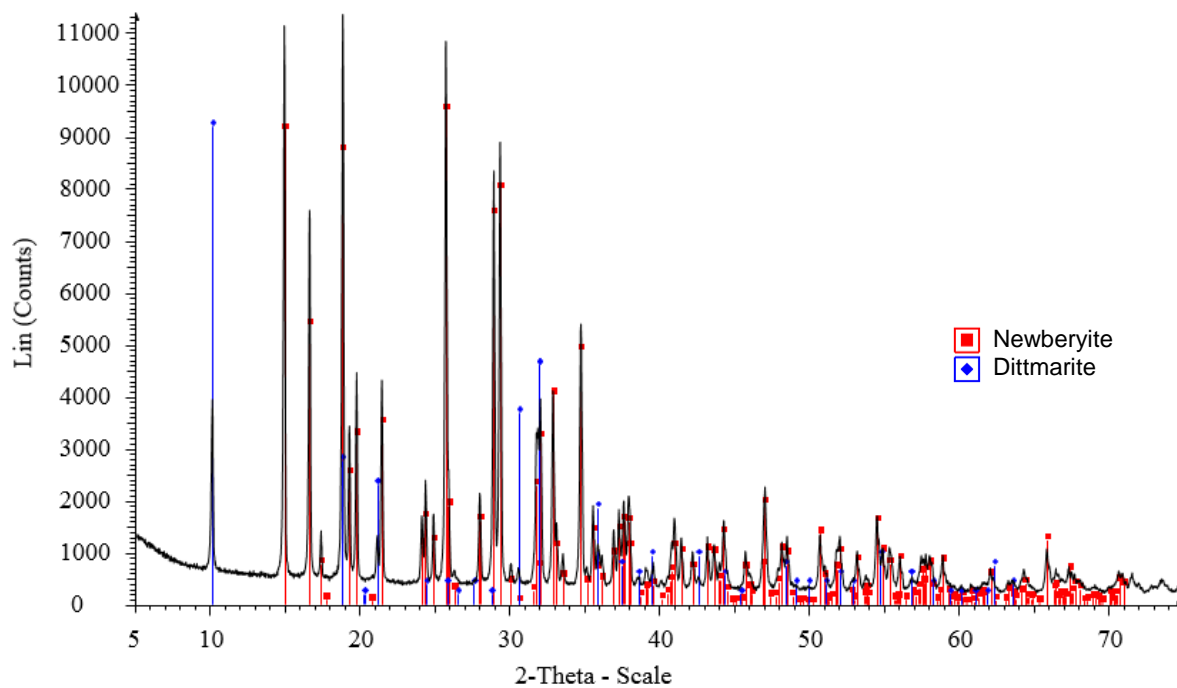
Lulu Island pellets (<1mm): T - 65°C, RH - 80%, 4 hr**Lulu Island pellets (<1mm): T - 65°C, RH - 95%, 2 hr**

Lulu Island pellets (<1mm): T - 65°C, RH - 95%, 4 hr**Lulu Island pellets (<1mm): T - 75°C, RH - 65%, 2 hr**

Lulu Island pellets (<1mm): T - 75°C, RH - 80%, 2 hr**Lulu Island pellets (<1mm): T - 75°C, RH - 95%, 2 hr**

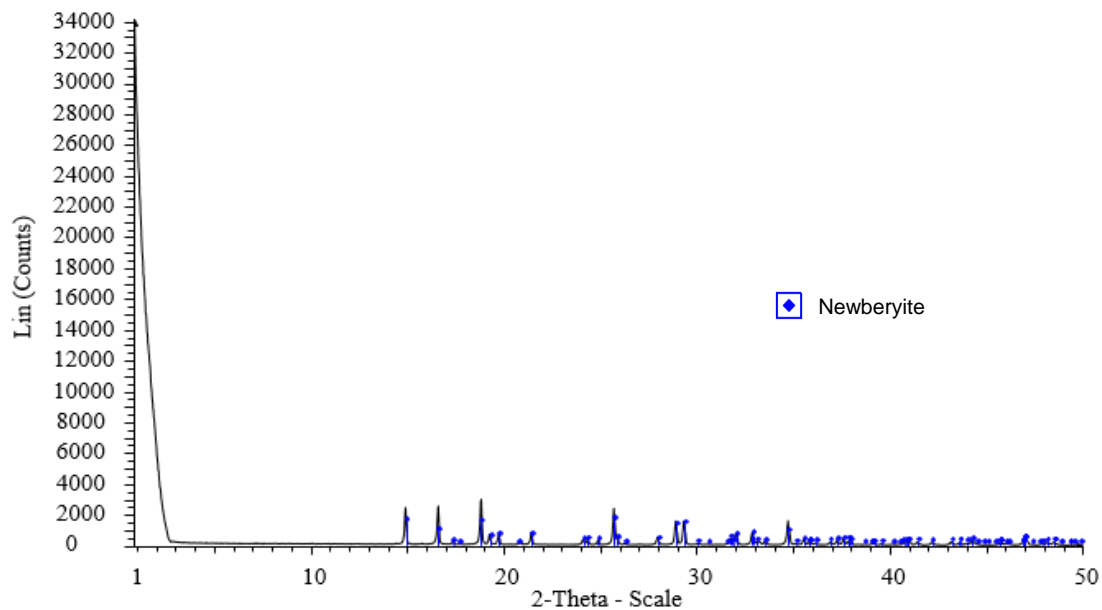
Lulu Island pellets (<1mm): T - 75°C, RH - 95%, 4 hr**Lulu Island pellets (<1mm): T - 80°C, RH - 95%, 2 hr**

Lulu Island pellets (<1mm): T - 85°C, RH - 65%, 2 hr**Lulu Island pellets (<1mm): T - 85°C, RH - 65%, 4 hr**

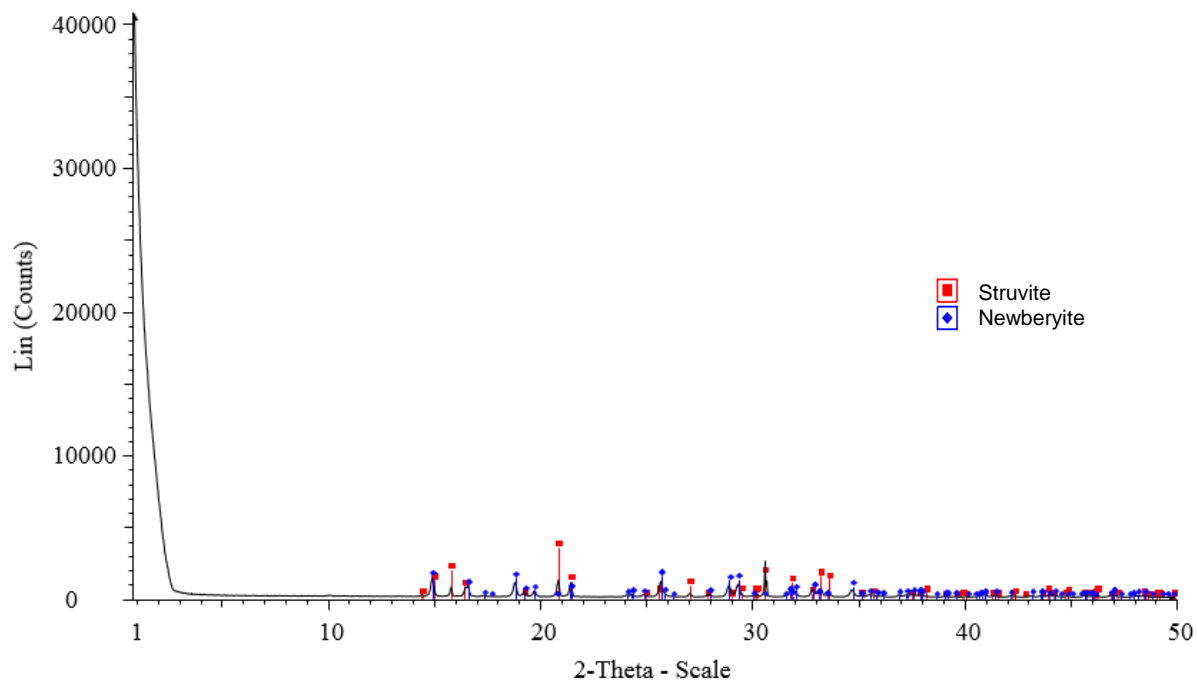
Lulu Island pellets (<1mm): T - 85°C, RH - 80%, 2 hr**Lulu Island pellets (<1mm): T - 85°C, RH - 95%, 2 hr**

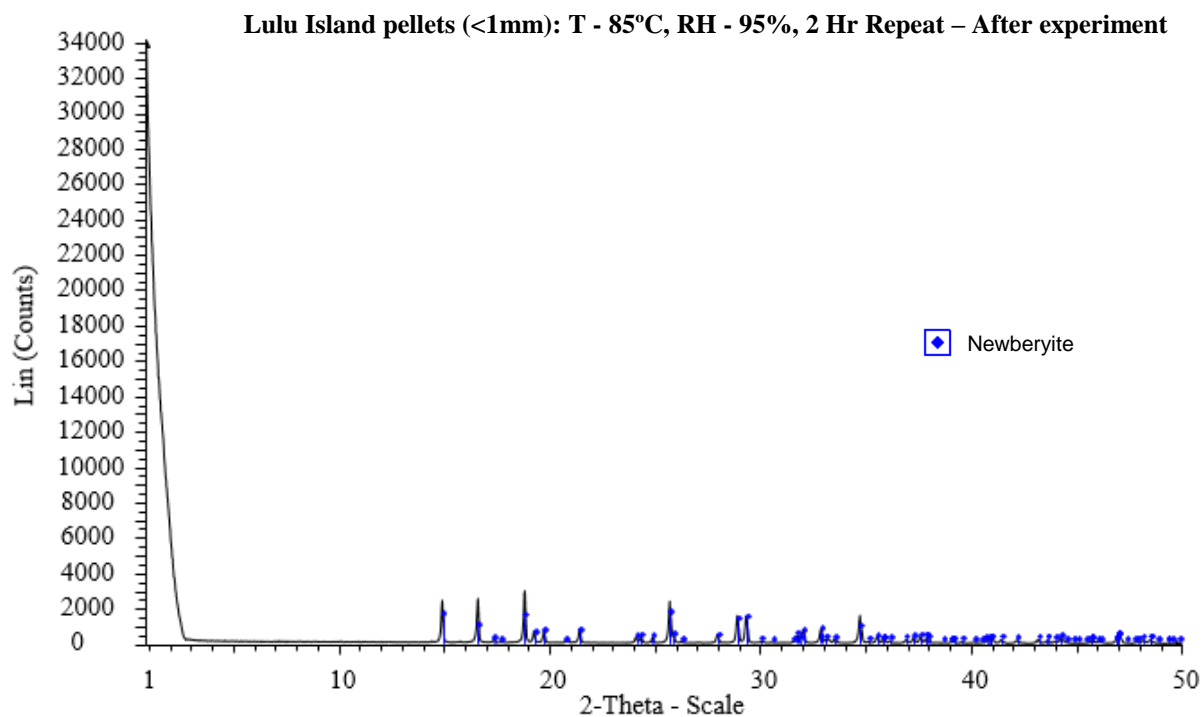
C.2 Relative humidity effects on layered structure formation

Lulu Island pellets (<1mm): T - 80°C, RH - 95%, 2 Hr Repeat – After experiment

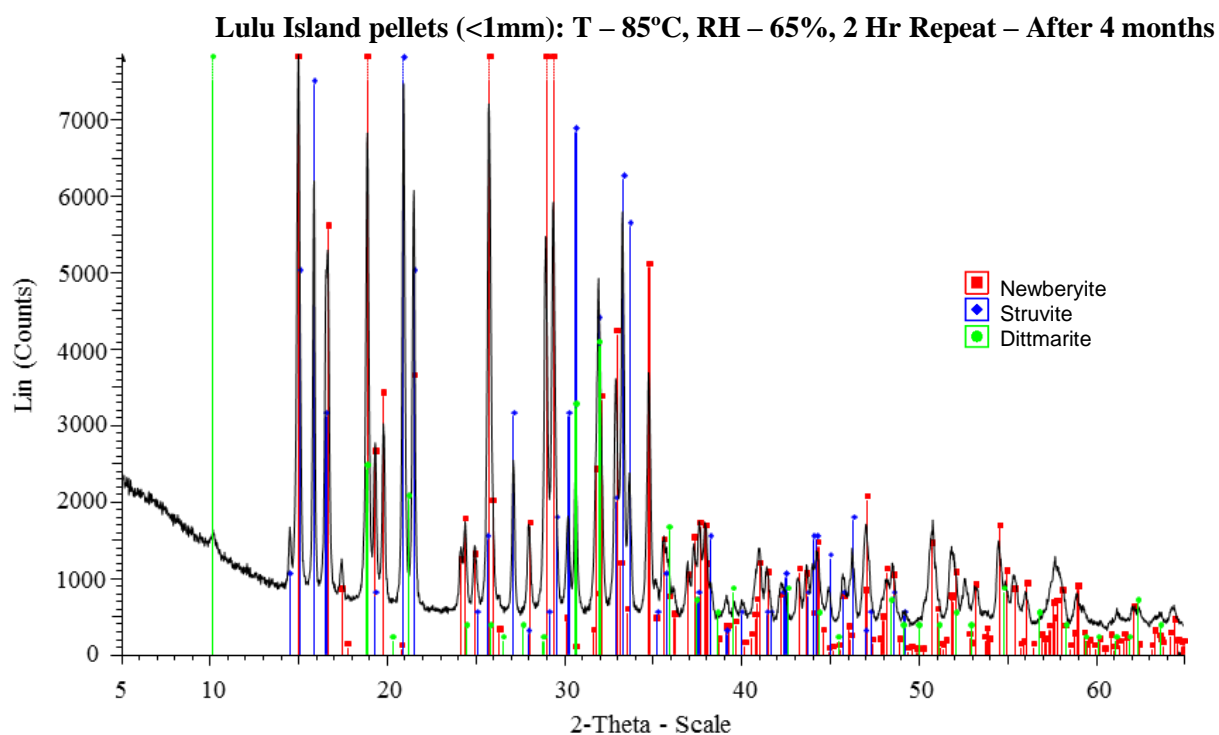


Lulu Island pellets (<1mm): T - 85°C, RH - 65%, 2 Hr Repeat – After experiment

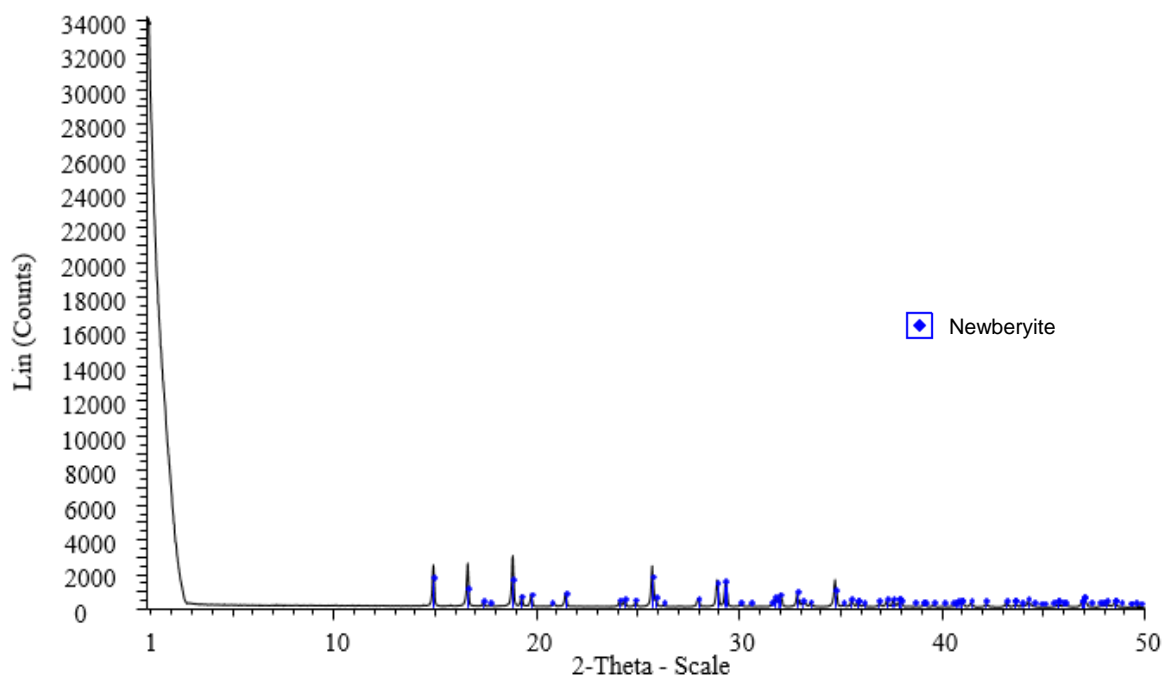




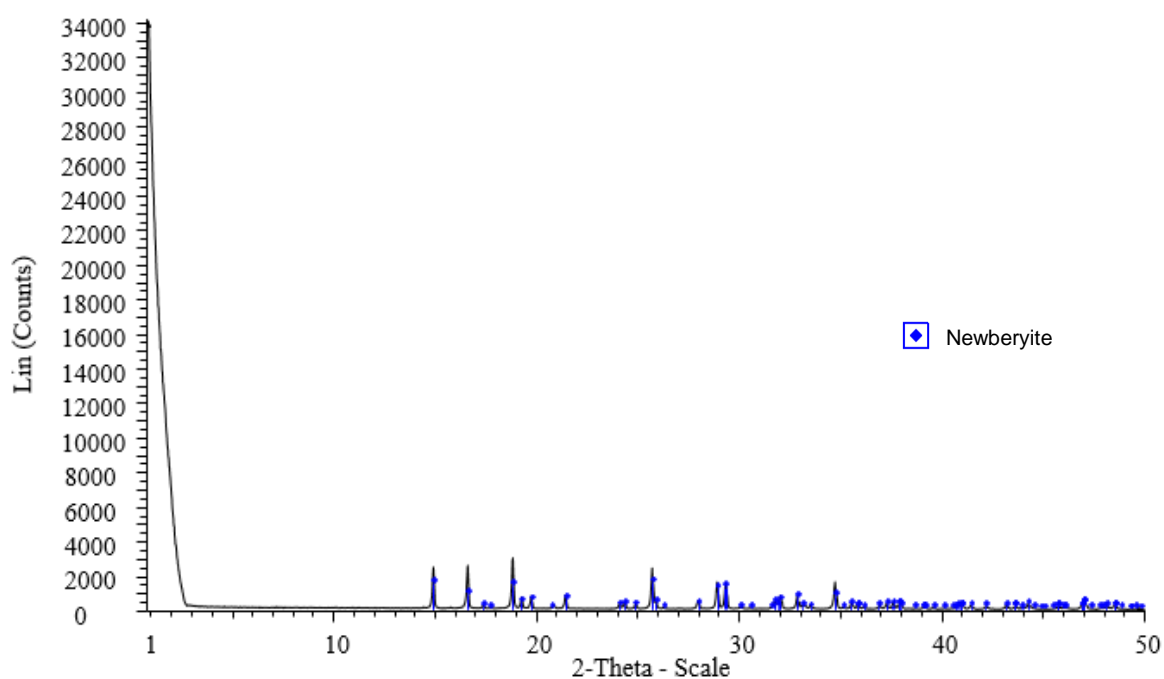
C.3 Layered structure transformation



Lulu Island (0.5-1 mm): T-80°C, RH- 95%, 2 Hr Repeat – After 4 months

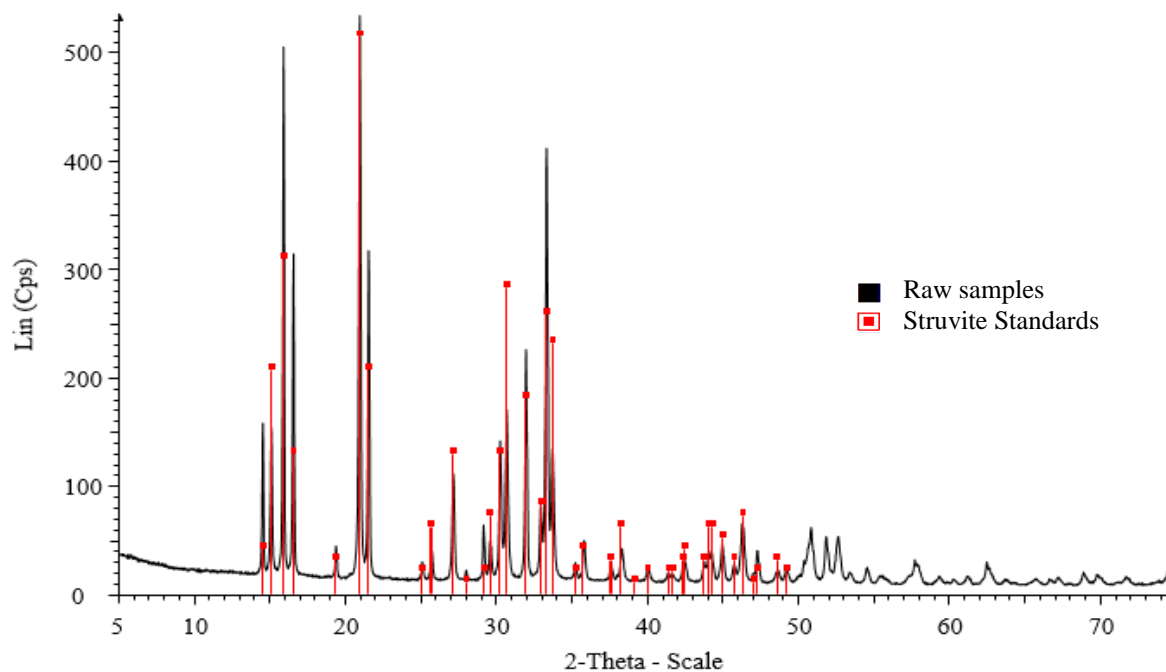


Lulu Island (0.5-1 mm): T-85°C, RH- 95%, 2 Hr Repeat – After 4 months

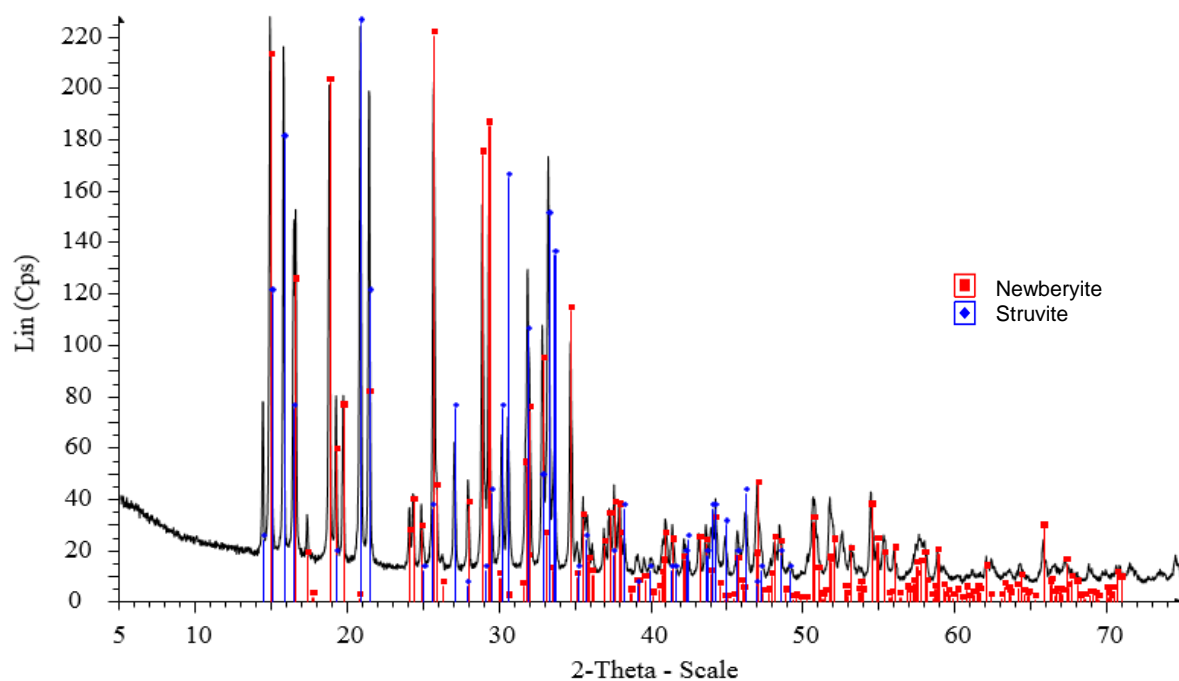


C.4 Different sources and sizes of struvite pellets

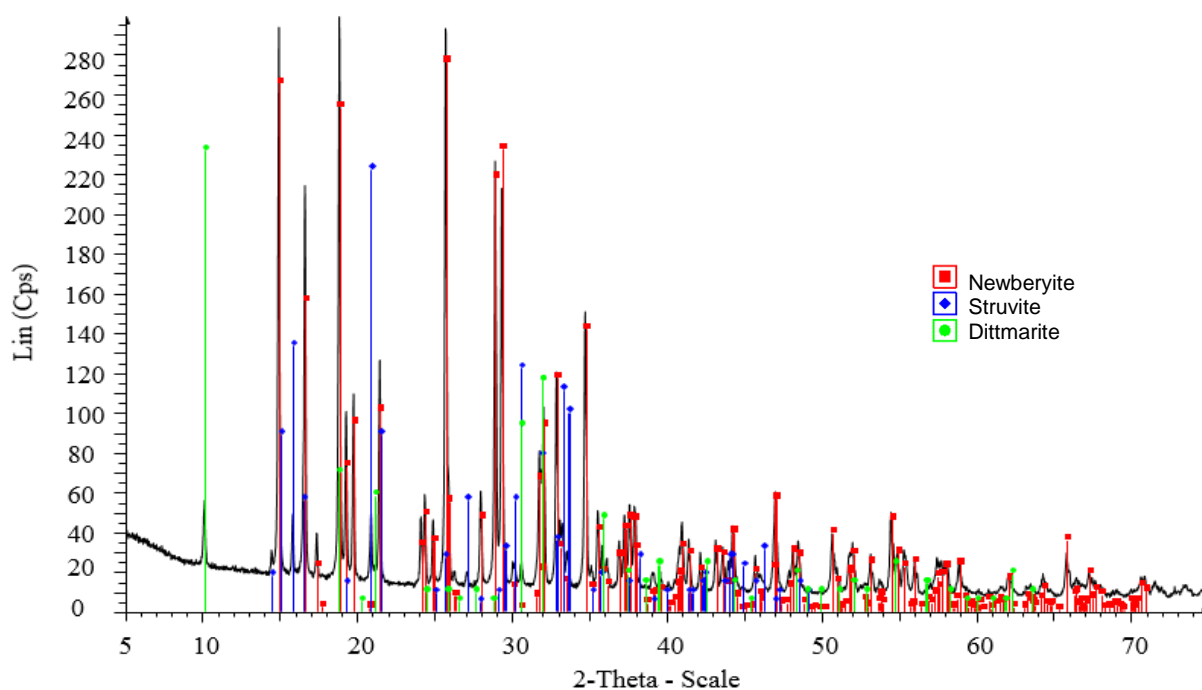
Lulu Island struvite (>1mm): Initial



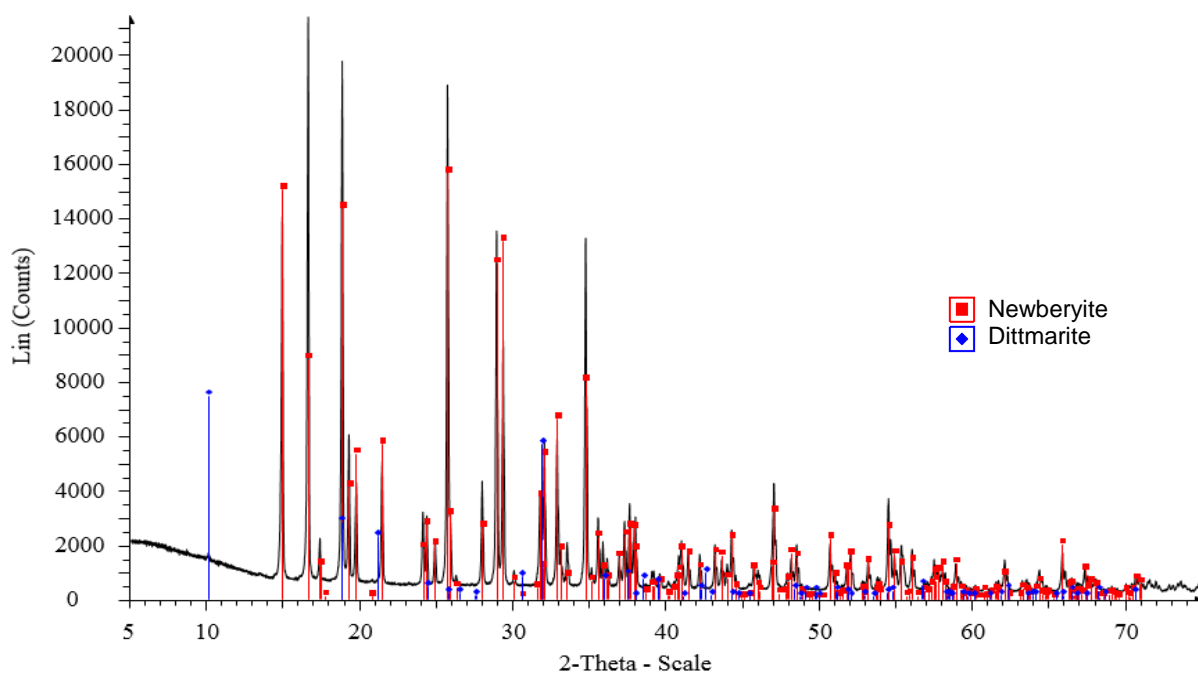
Lulu Island pellets (>1mm): T - 80°C, RH - 95%, 2 hr

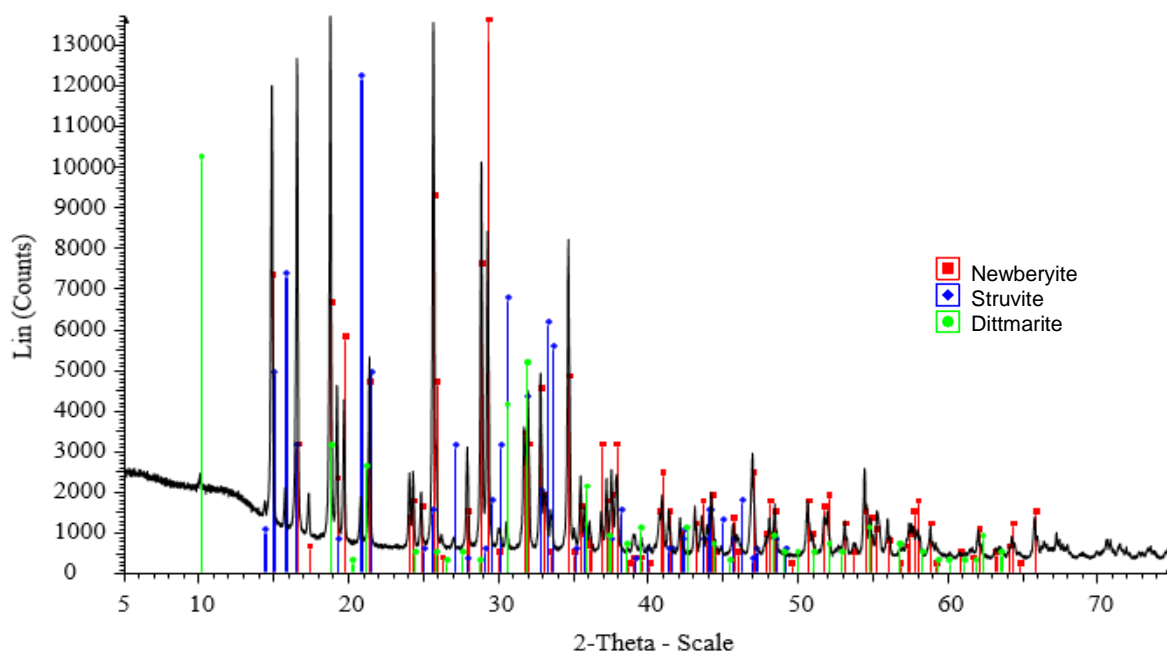
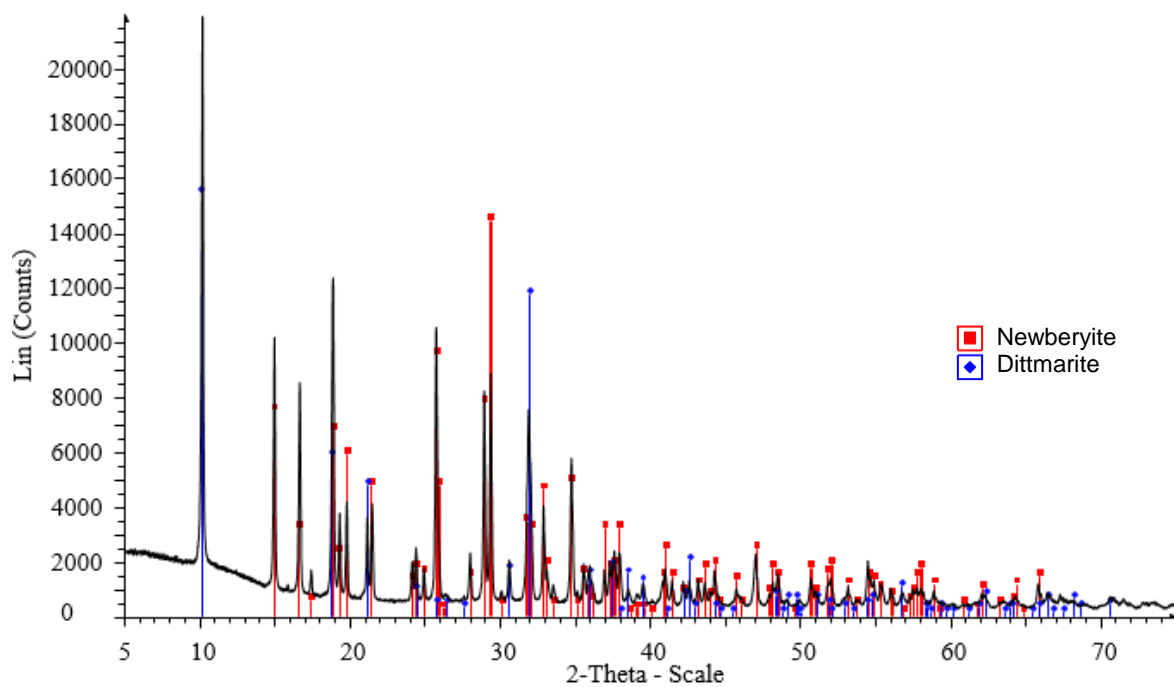


Lulu Island pellets (>1mm): T - 80°C, RH - 95%, 4 hr



Recrystallized pellets (>1mm): T - 80°C, RH - 95%, 3 hr



Penticton B.C. pellets (<1mm): T - 80°C, RH - 95%, 2 hr**Edmonton Gold Bar pellets (<1mm): T - 80°C, RH - 95%, 3 hr**

Appendix D : Pilot-scale experiments

D.1 Identifying operational parameters for FBR

Available inside diameter of the fluidized bed reactor (FBR), $r = 1.6 \text{ in} = 0.04 \text{ m}$

Area of the inside reactor $= \pi r^2 = 0.0013 \text{ m}^2$

Diameter of the struvite pellets, $d = 1 \text{ mm} = 0.001 \text{ m}$

Struvite density considering porosity, $\rho_s = 1400 \text{ kg/m}^3$

Steam density at 100°C , $\rho = 0.6 \text{ kg/m}^3$

Steam viscosity, $\mu = 1.23 \times 10^{-5} \text{ Pa}\cdot\text{sec}$

Operating velocity calculation

The operating velocity, $W_{op} = \text{Operating fluidization No (f)} * \text{Minimum velocity (} w_{min} \text{)}$

Where,

$$\text{Fluidization number limit} = \frac{\text{Maximum velocity}}{\text{Minimum velocity}} = \frac{w_{max}}{w_{min}}$$

$$\text{Minimum velocity, } w_{min} = \frac{Re_{min} * \mu}{\rho * d}$$

$$\text{Maximum velocity, } w_{max} = \frac{Re_{max} * \mu}{\rho * d}$$

Therefore,

$$\text{The Archimedes number, } Ar = \frac{d^3 * \rho * (\rho_s - \rho) g}{\mu^2} = 54710.79$$

$$\text{Reynolds no for minimum velocity, } Re_{min} = \frac{Ar}{1400 + 5.22 * \sqrt{Ar}} = 20.87$$

$$\text{Reynolds no for maximum velocity, } Re_{max} = \frac{Ar}{18 + 0.61 * \sqrt{Ar}} = 340.49$$

$$\text{Minimum velocity, } w_{min} = \frac{Re_{min} * \mu}{\rho * d} = 0.43 \text{ m/sec}$$

$$\text{Maximum velocity, } w_{max} = \frac{Re_{max} * \mu}{\rho * d} = 7 \text{ m/sec}$$

$$\text{Fluidization number limit} = \frac{w_{max}}{w_{min}} = 11.52 < 20$$

Therefore the operating fluidization number can be chosen between 1.5 and 3.

So, the operating fluidization no, $f = 2.8$

$$\begin{aligned} \text{The operating velocity, } W_{op} &= \text{Operating fluidization No (f)} * \text{Minimum velocity (} w_{min} \text{)} \\ &= 2.8 * 0.43 = 1.18 \text{ m/sec} \end{aligned}$$

Flow rates calculation

$$\text{The flow rate, } Q = A * W_{op} = 0.0013 * 1.18 = 0.0016 \text{ m}^3/\text{sec} = 1.57 \text{ L/sec} = 94.43 \text{ L/min} = 3.33 \text{ SCFM}$$

Steam capacity calculation

$$\text{Steam capacity} = \text{Flow rate (Q)} * \text{Steam density (}\rho\text{)} = 0.0016 * 0.6 * 3600 = 3.40 \text{ kg/hr} = 7.49 \text{ lb/hr}$$

$$\text{Actual steam capacity with 75\% nominal for water at } 15^\circ\text{C} = 3.40/0.75 = 4.53 \text{ kg/hr} = 9.99 \text{ lb/hr}$$

Current operating velocity at the pilot-scale experiments

$$\text{Air steam ratio} = 1:1$$

$$\text{Flow rate required for proper fluidization} = 1.4\text{-}1.6 \text{ SCFM (Flow meter monitoring)}$$

$$\text{Operating flow rate, } q = 1.6 * 2 = 3.2 \text{ SCFM} = 0.0015 \text{ m}^3/\text{sec}$$

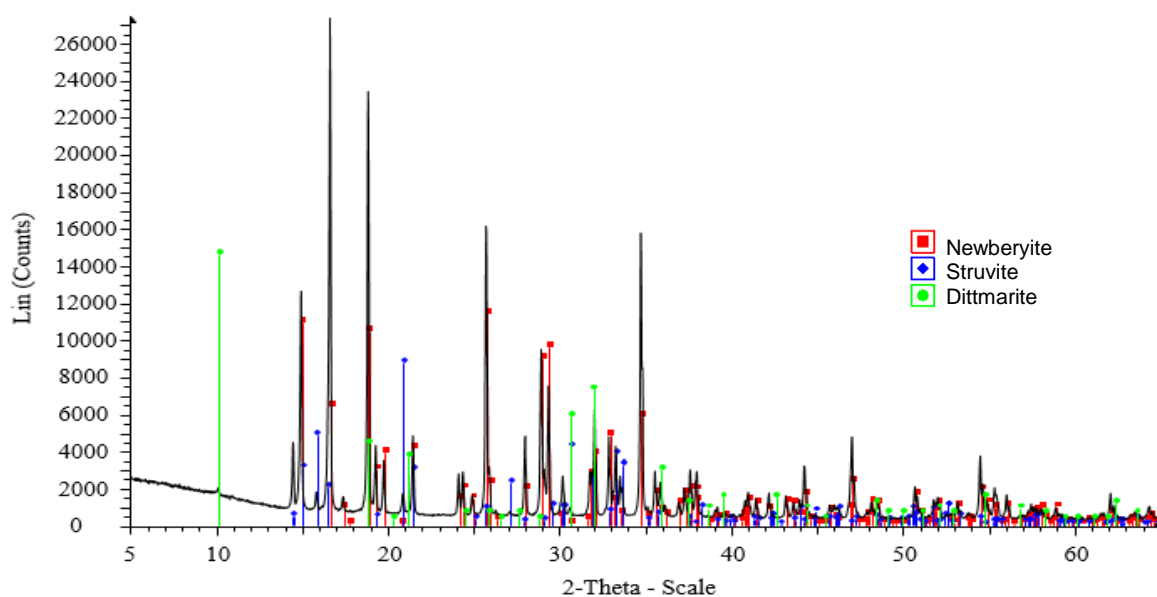
$$\text{Area of the inside reactor, } A = \pi r^2 = 0.0013 \text{ m}^2$$

$$\text{The current operating velocity inside the reactor, } v = q/A = 0.0015/0.0013 = 1.13 \text{ m/sec} \sim 1.18 \text{ m/sec}$$

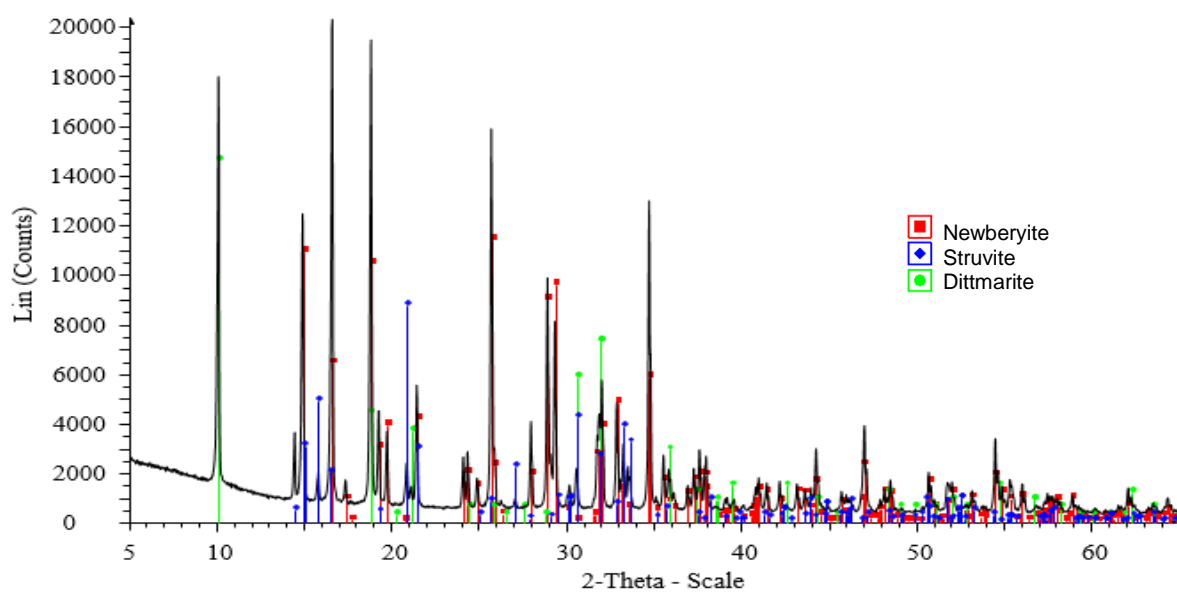
This operating velocity obtained from experiment is in a good agreement with the theoretical value calculated above.

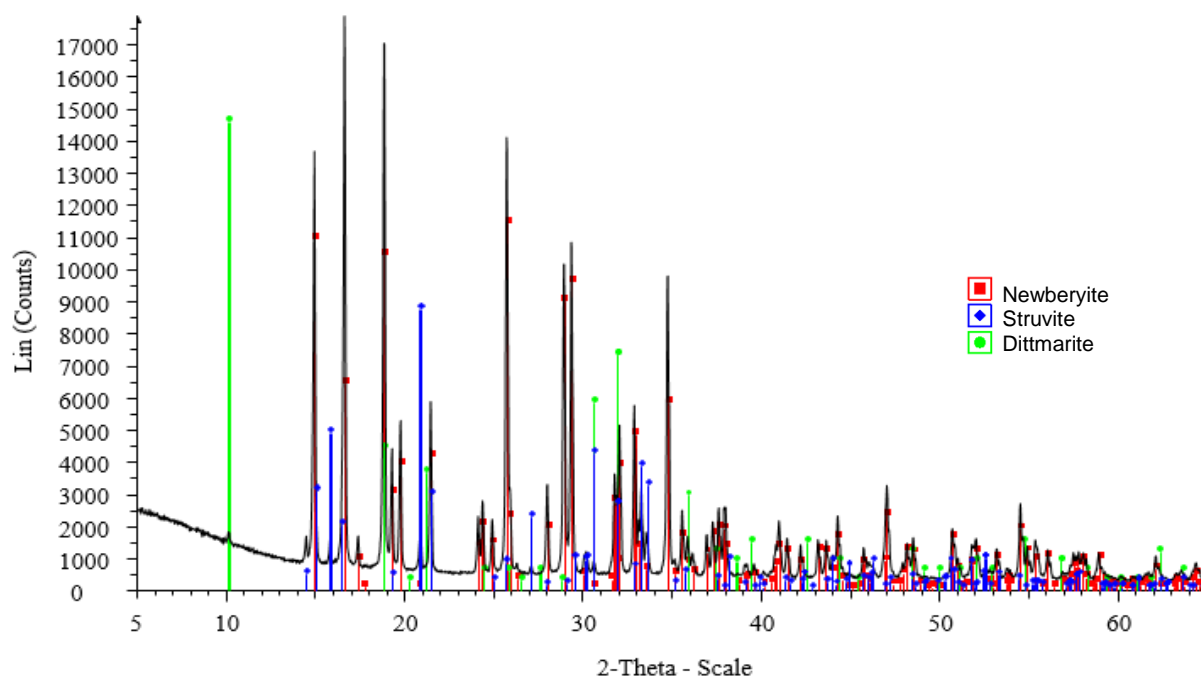
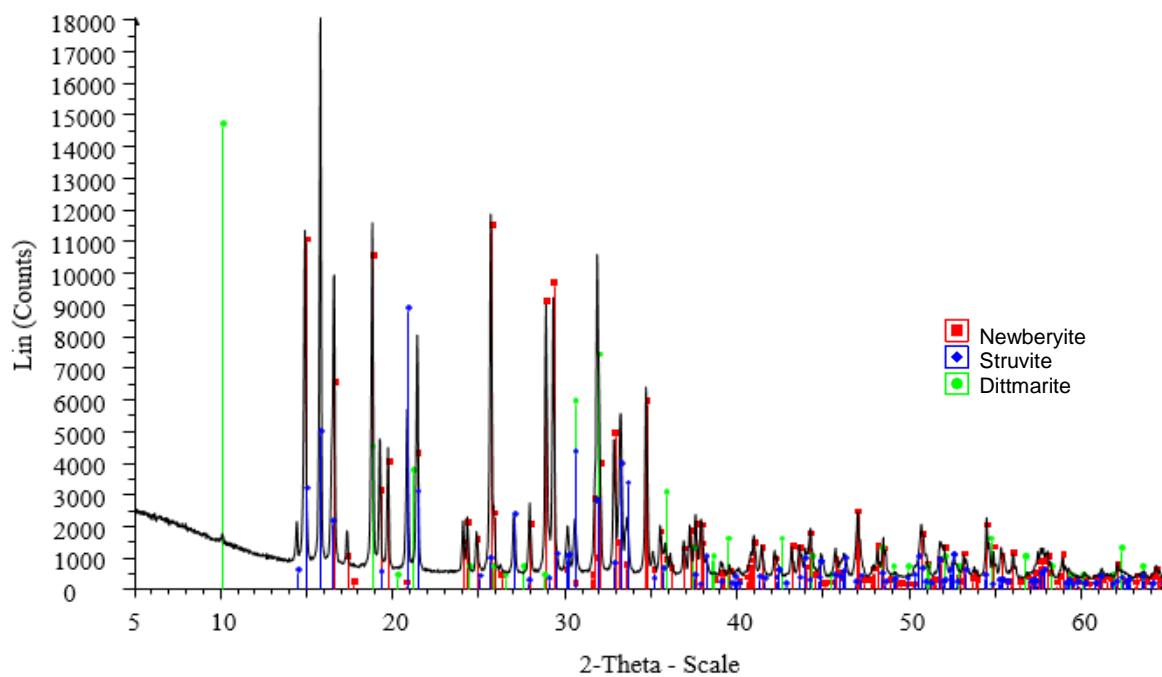
D.2 XRD results of decomposed struvite pellets from different sources and sizes at optimum conditions

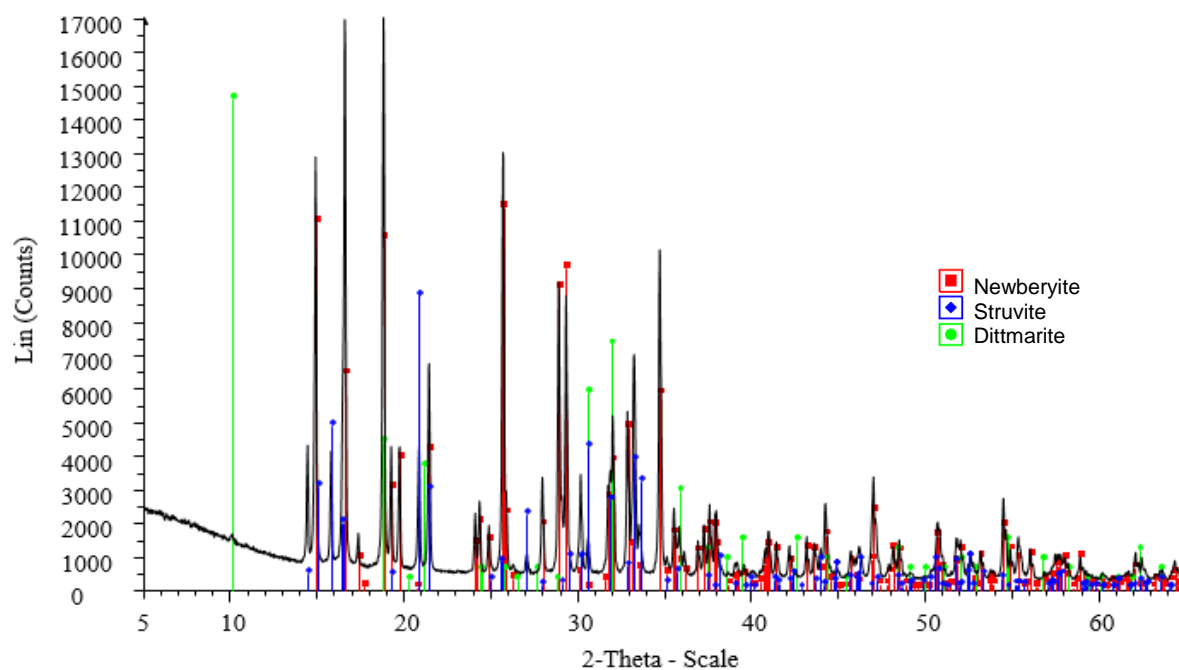
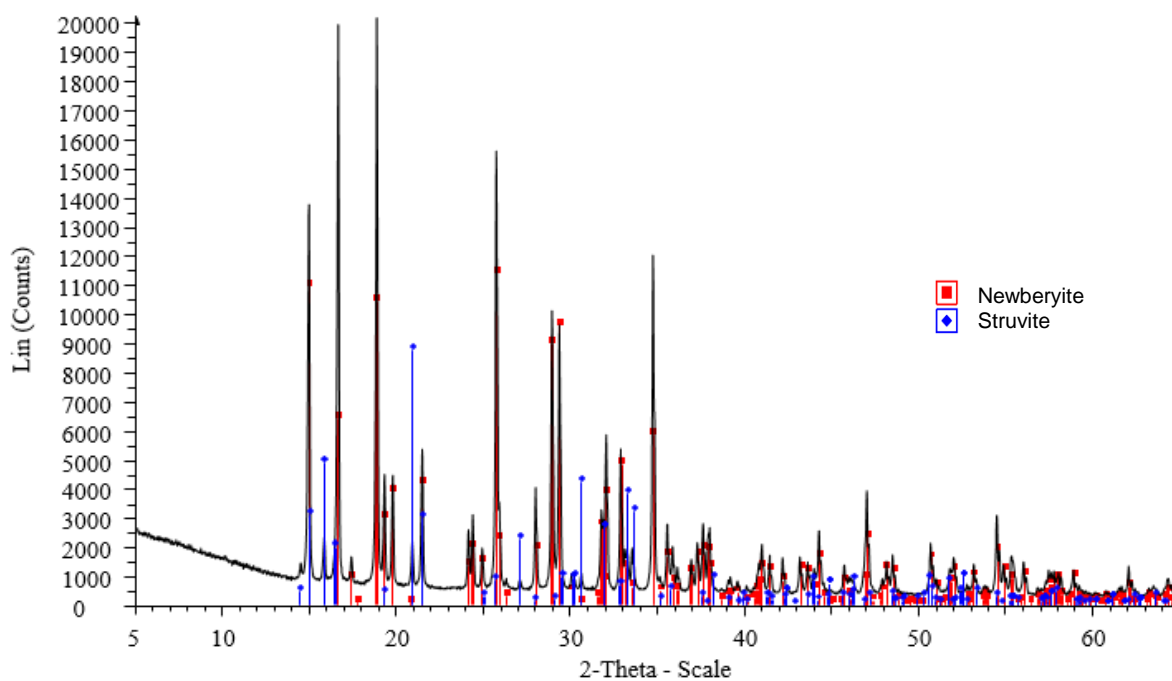
Recrystallized pellets (>1mm): T - 80°C, RH - 95%, 1 hr



Penticton B.C. pellets (>1mm): T - 80°C, RH - 95%, 1 hr

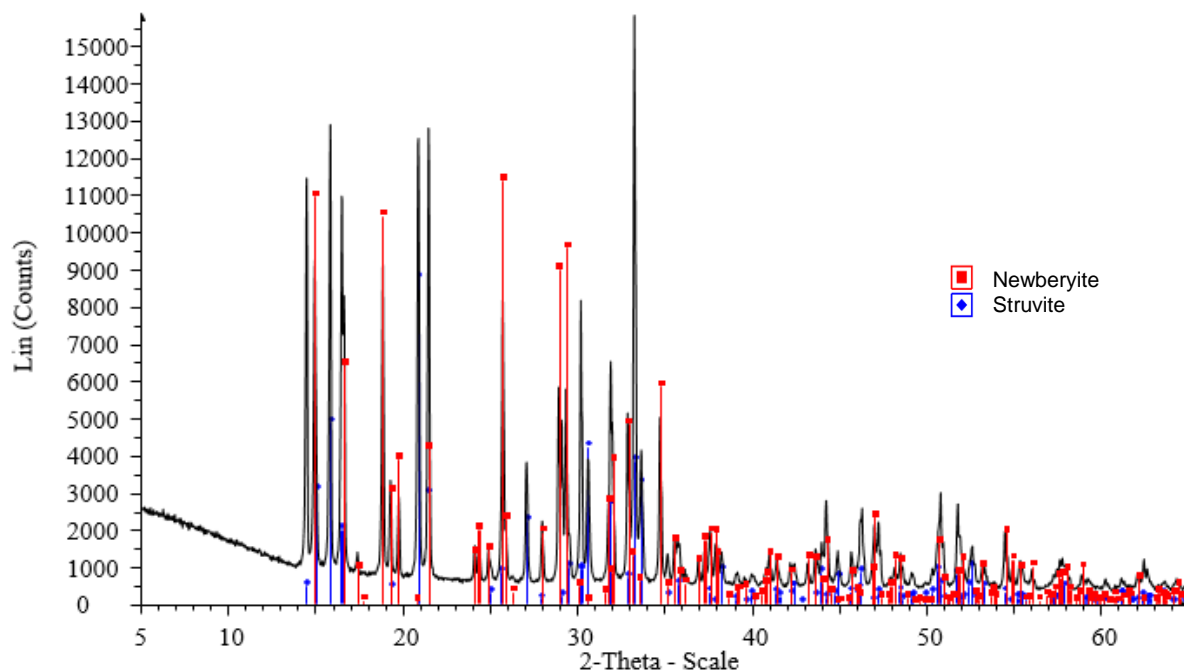


Lulu Island pellets crushed (<1mm): T - 80°C, RH - 95%, 1 hr**Edmonton Gold Bar pellets (<1mm): T - 80°C, RH - 95%, 1 hr**

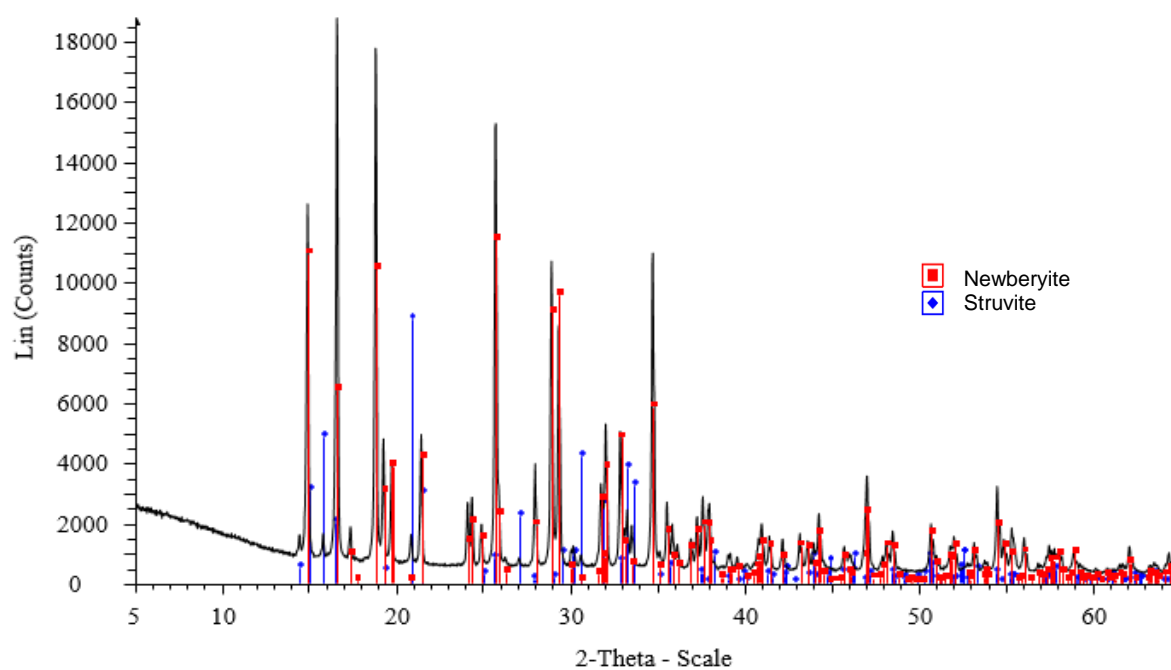
Lulu Island pellets (>1mm): T - 80°C, RH - 95%, 1 hr**Penticton B.C. pellets (<1mm): T - 80°C, RH - 95%, 1 hr**

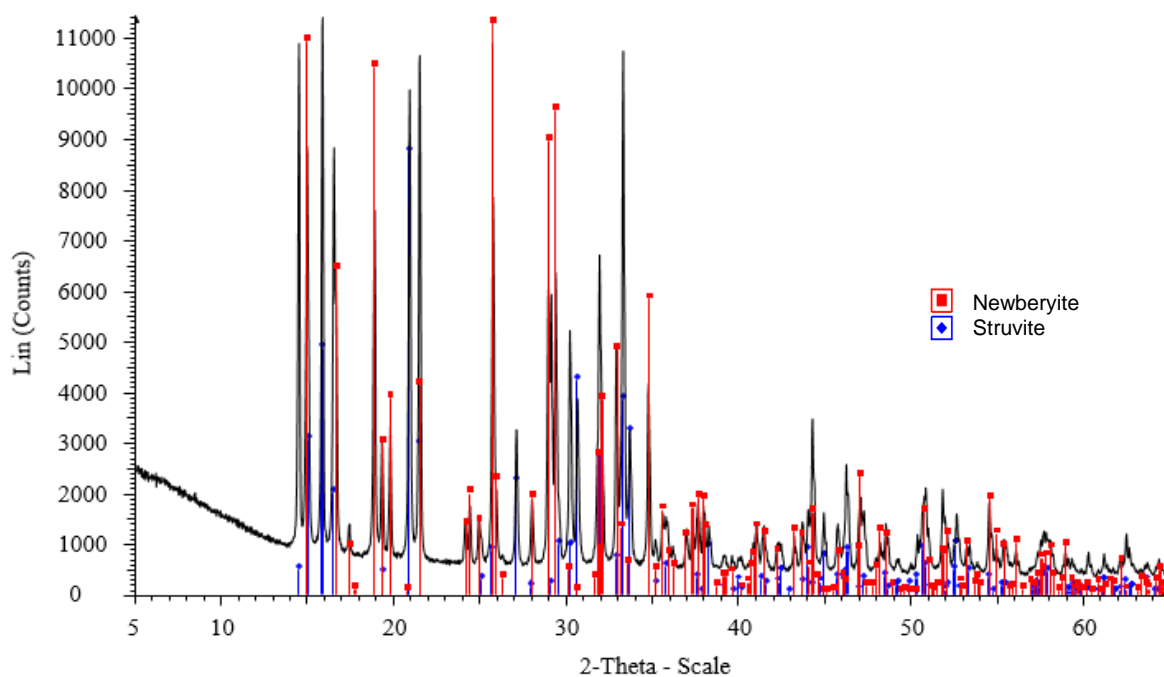
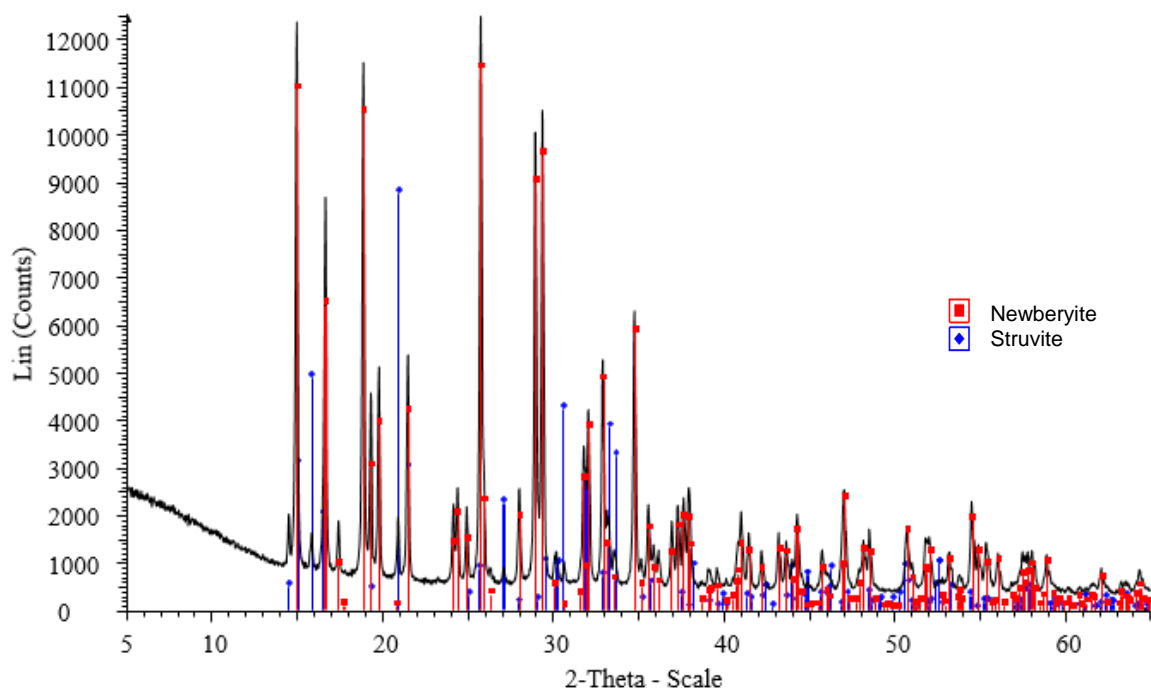
D.3 Process optimization

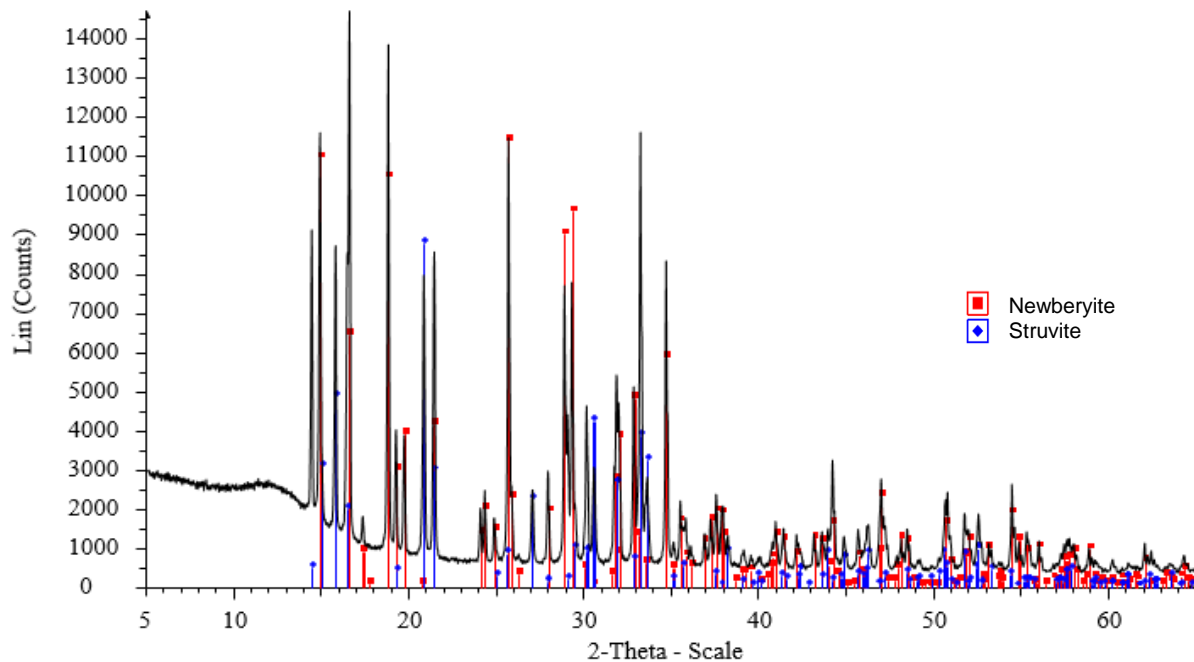
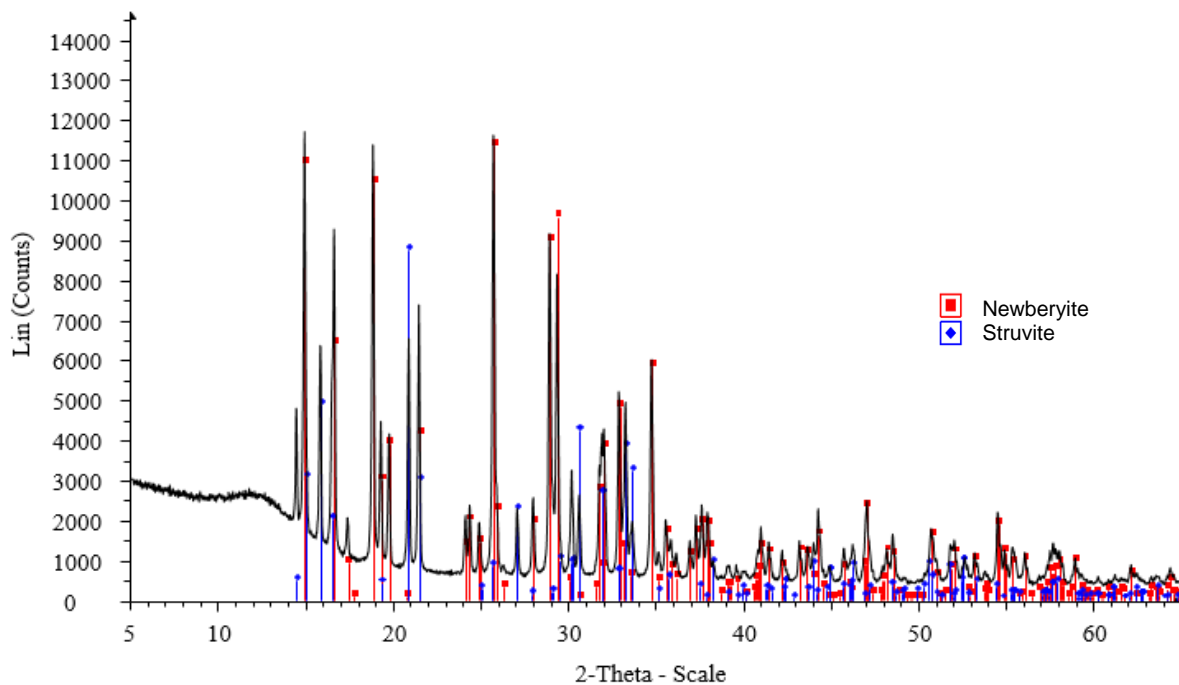
Penticton B.C. pellets (<1mm): T - 65°C, RH - 95%, 2 hr

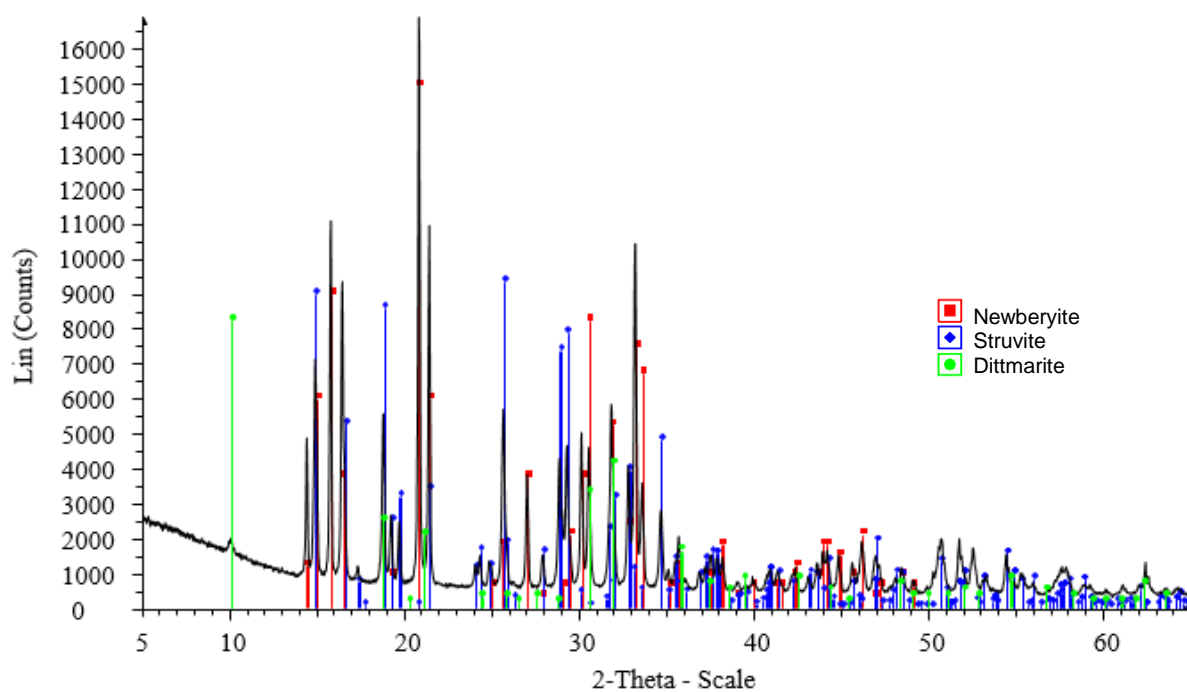
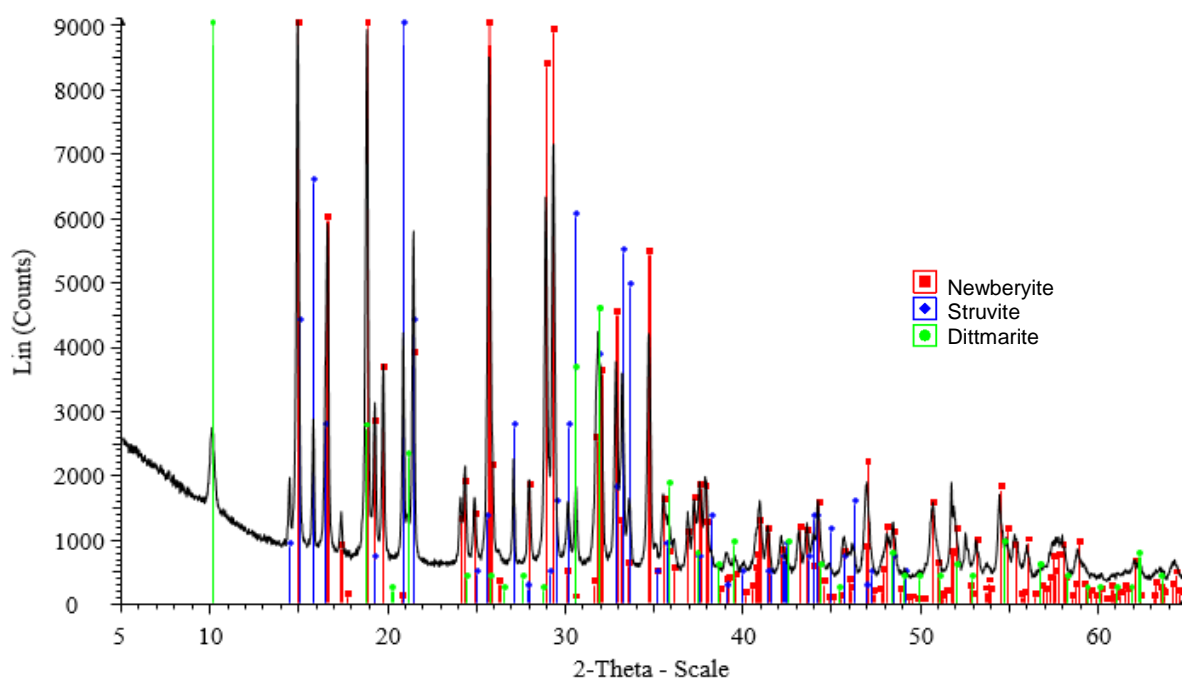


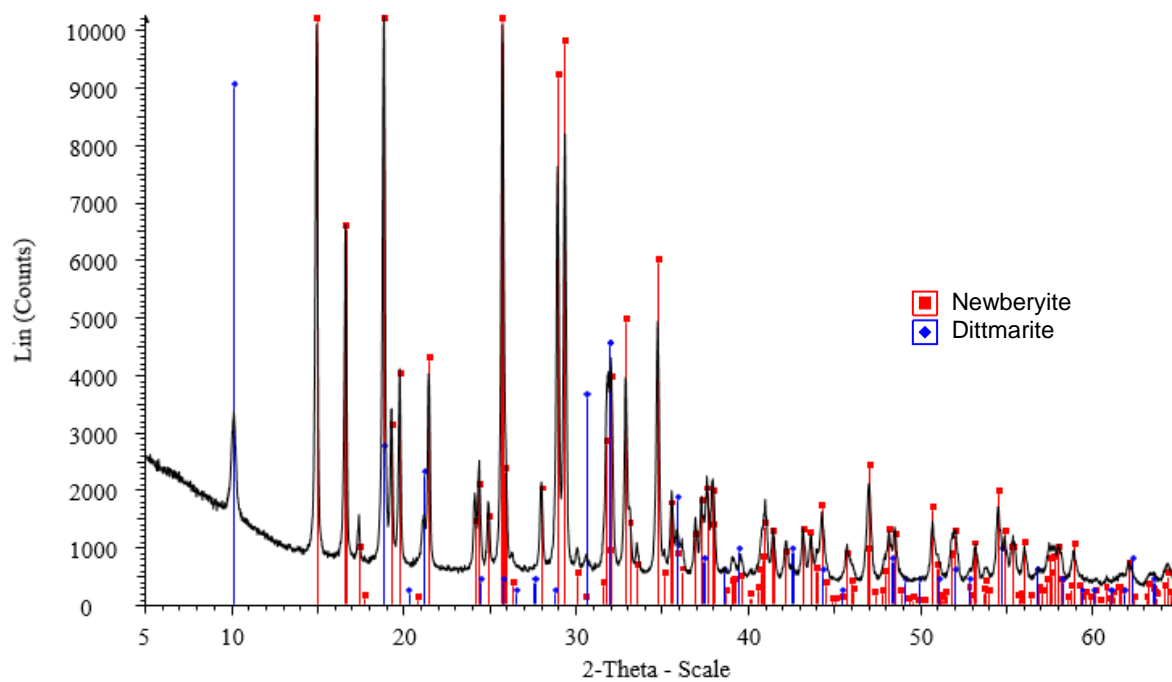
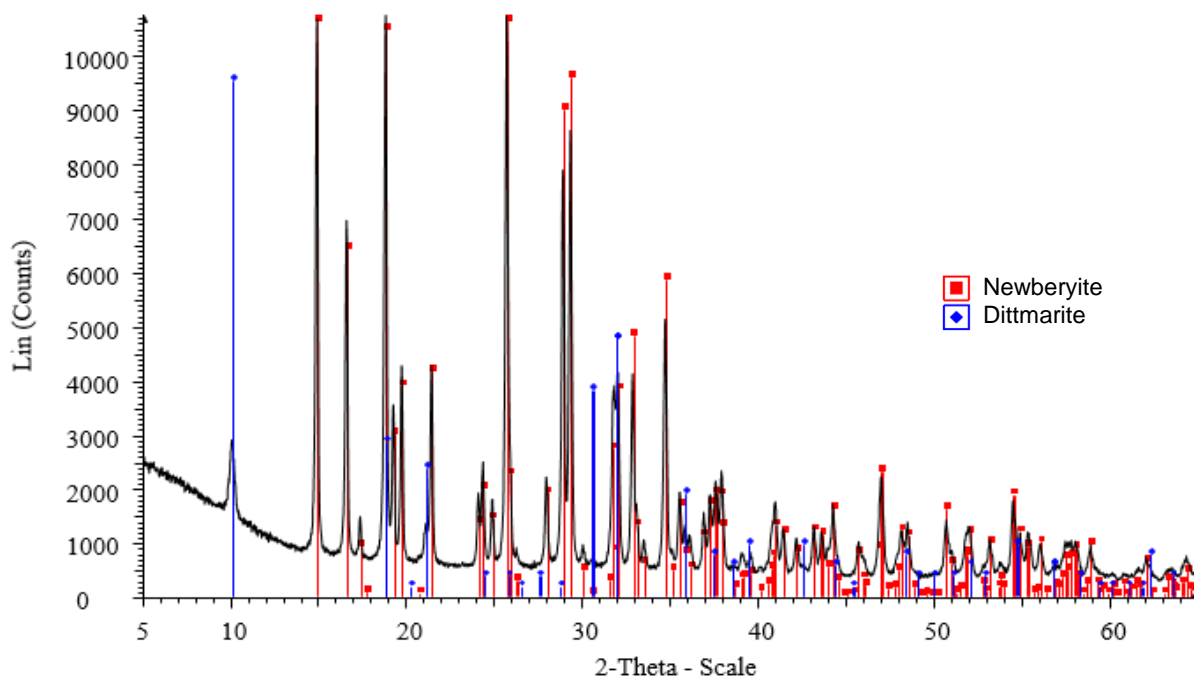
Penticton B.C. pellets (<1mm): T - 65°C, RH - 95%, 5 hr



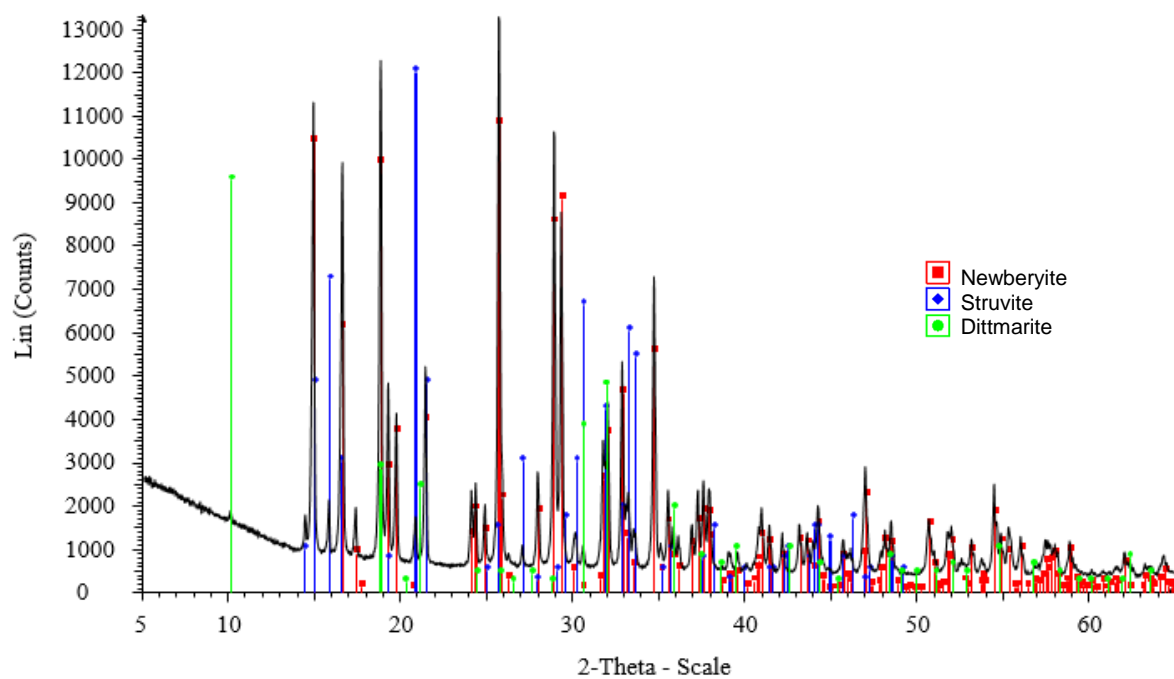
Penticton B.C. pellets (<1mm): T - 65°C, RH - 80%, 2 hr**Penticton B.C. pellets (<1mm): T - 65°C, RH - 80%, 5 hr**

Penticton B.C. pellets (<1mm): T - 75°C, RH - 95%, 1 hr**Penticton B.C. pellets (<1mm): T - 75°C, RH - 80%, 1 hr**

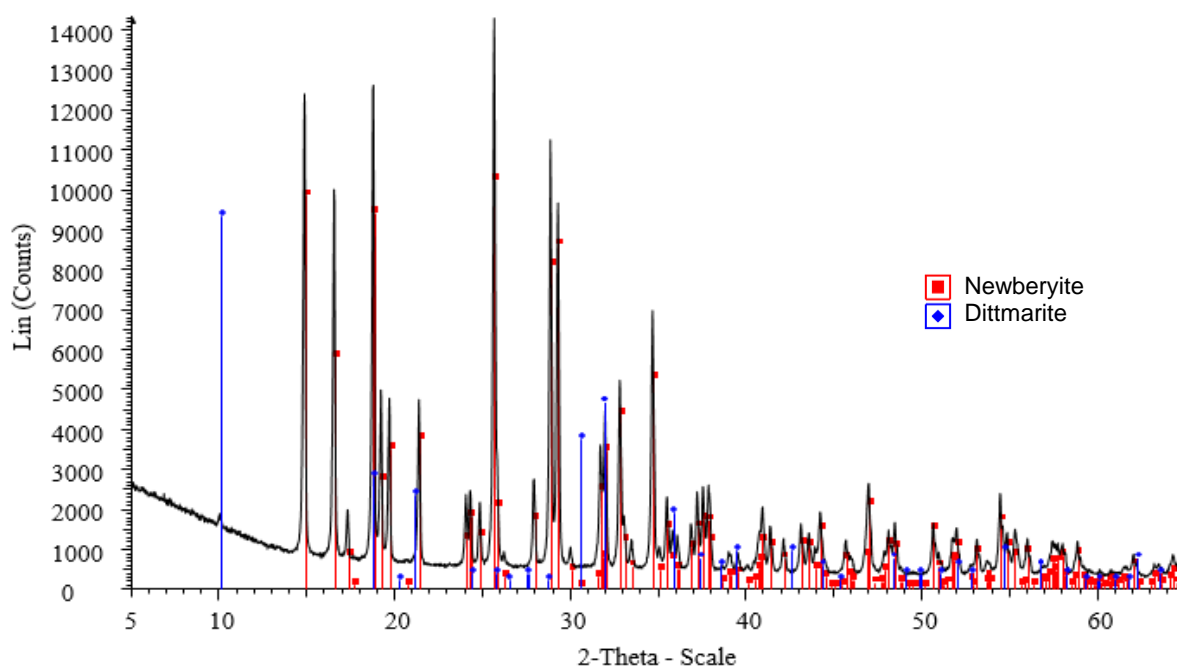
Penticton B.C. pellets (<1mm): T - 80°C, RH - 70%, 0.5 hr**Penticton B.C. pellets (<1mm): T - 80°C, RH - 70%, 1 hr**

Penticton B.C. pellets (<1mm): T - 80°C, RH - 70%, 2 hr**Penticton B.C. pellets (<1mm): T - 80°C, RH - 70%, 4 hr**

Penticton B.C. pellets (<1mm): T - 80°C, RH - 80%, 1 hr

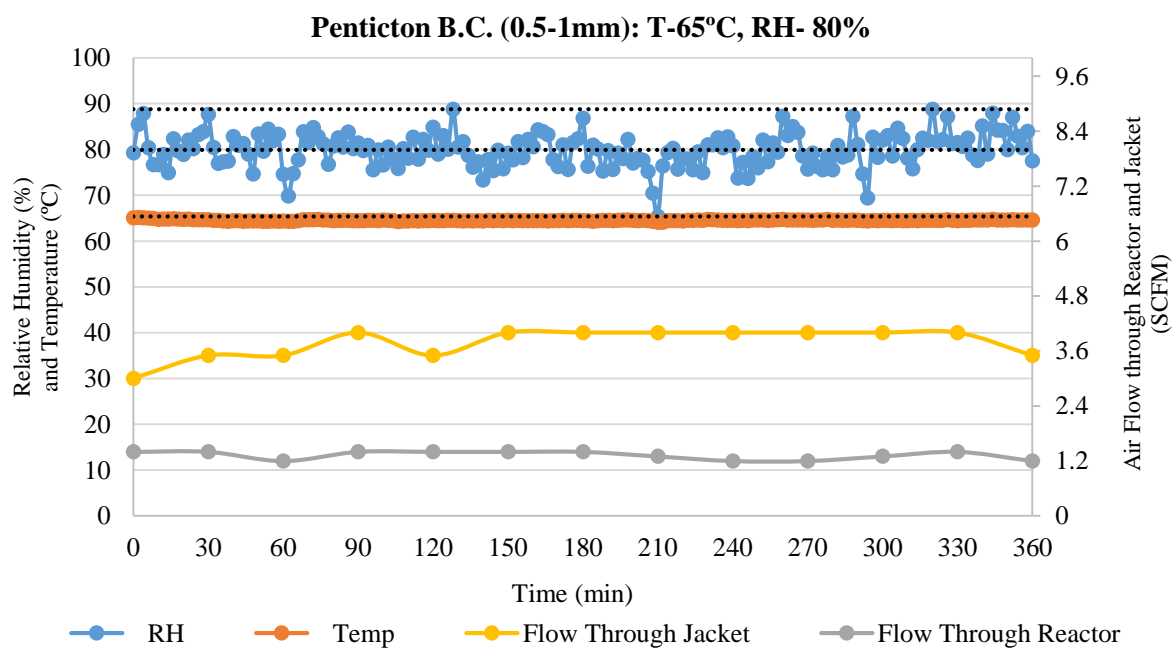
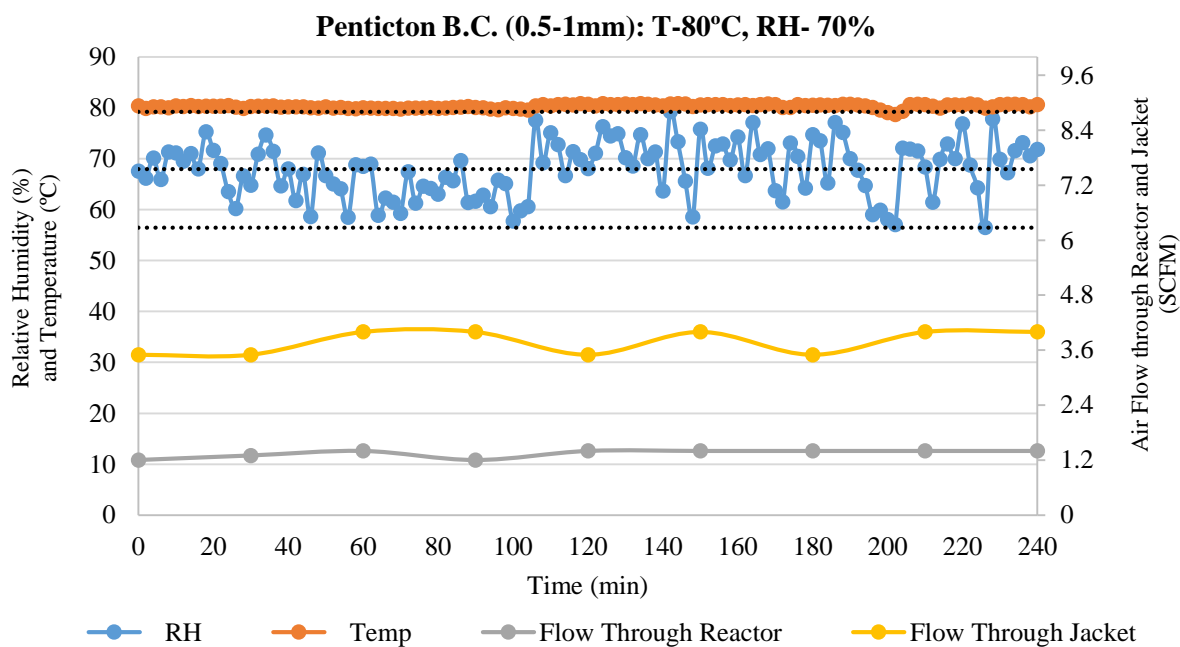


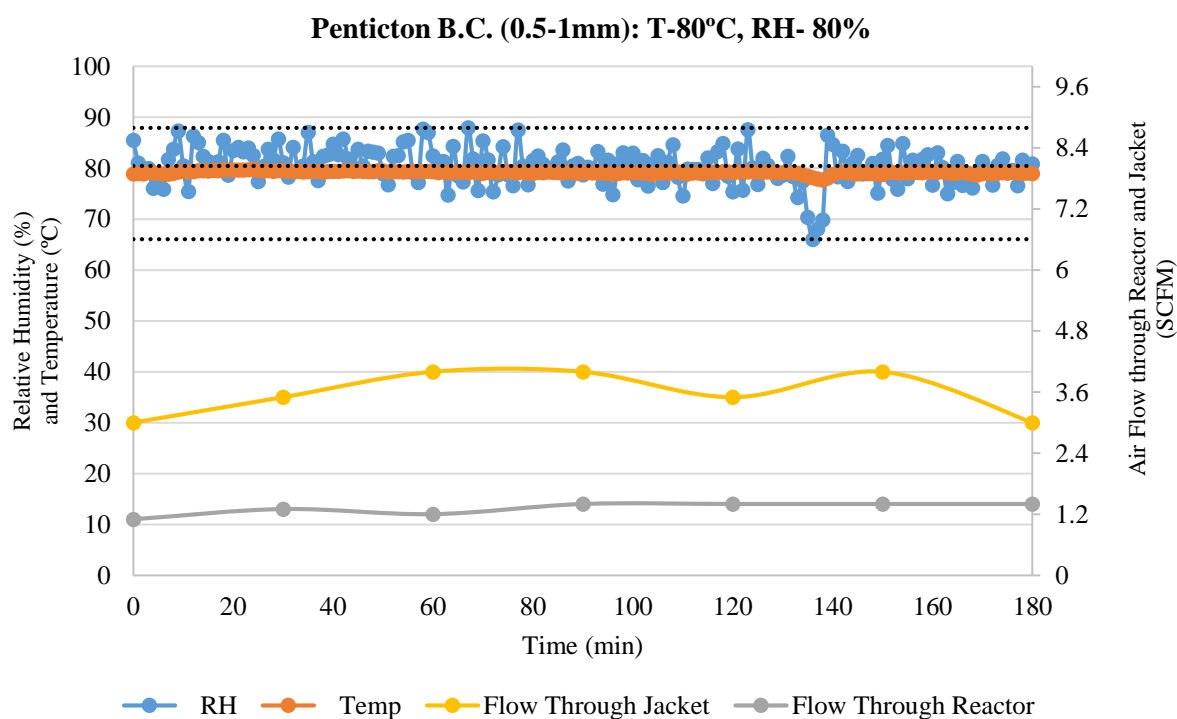
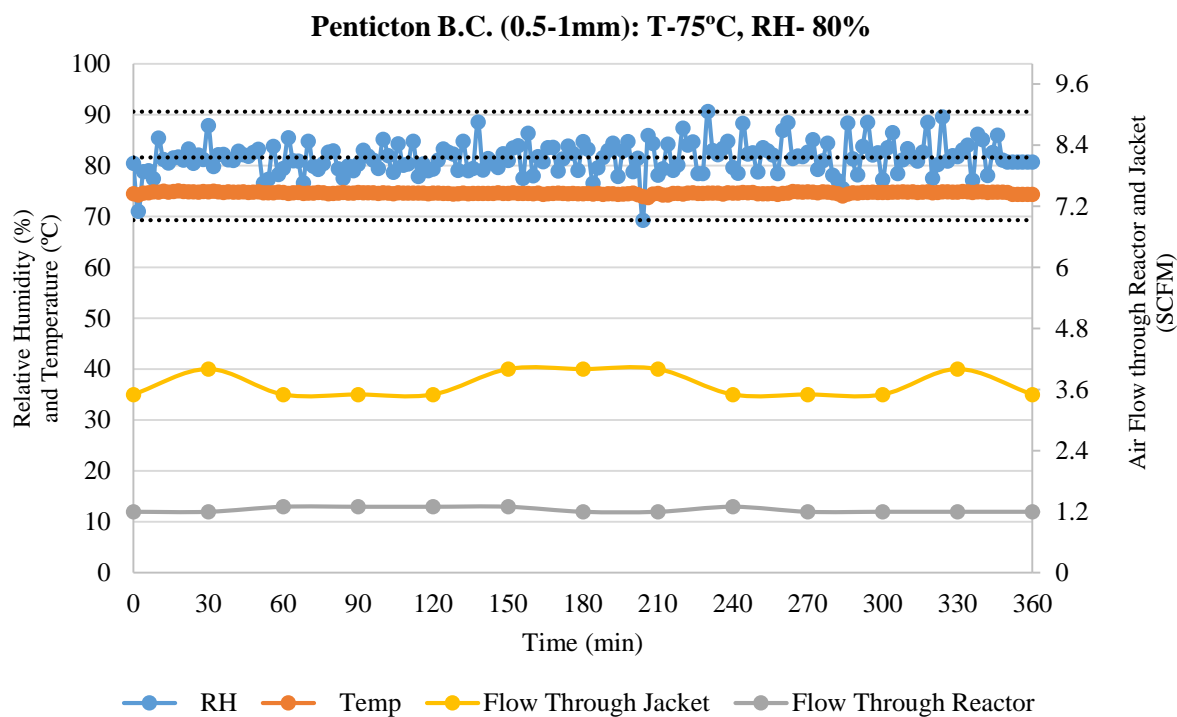
Penticton B.C. pellets (<1mm): T - 80°C, RH - 80%, 2 hr

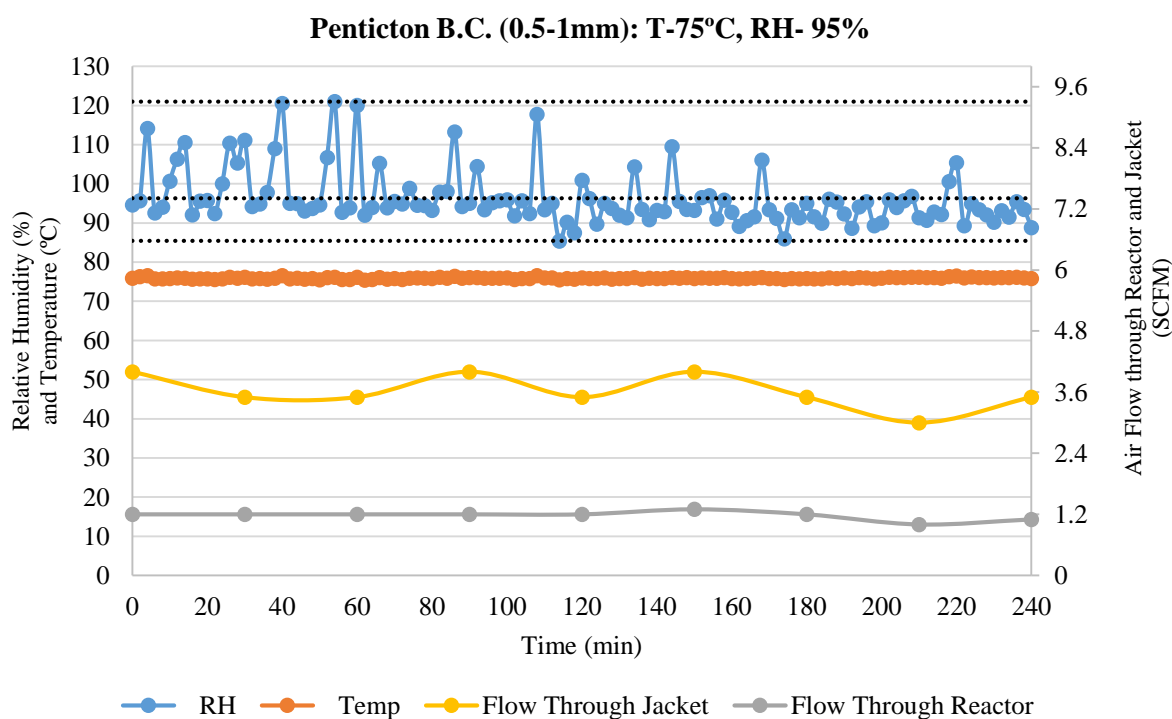
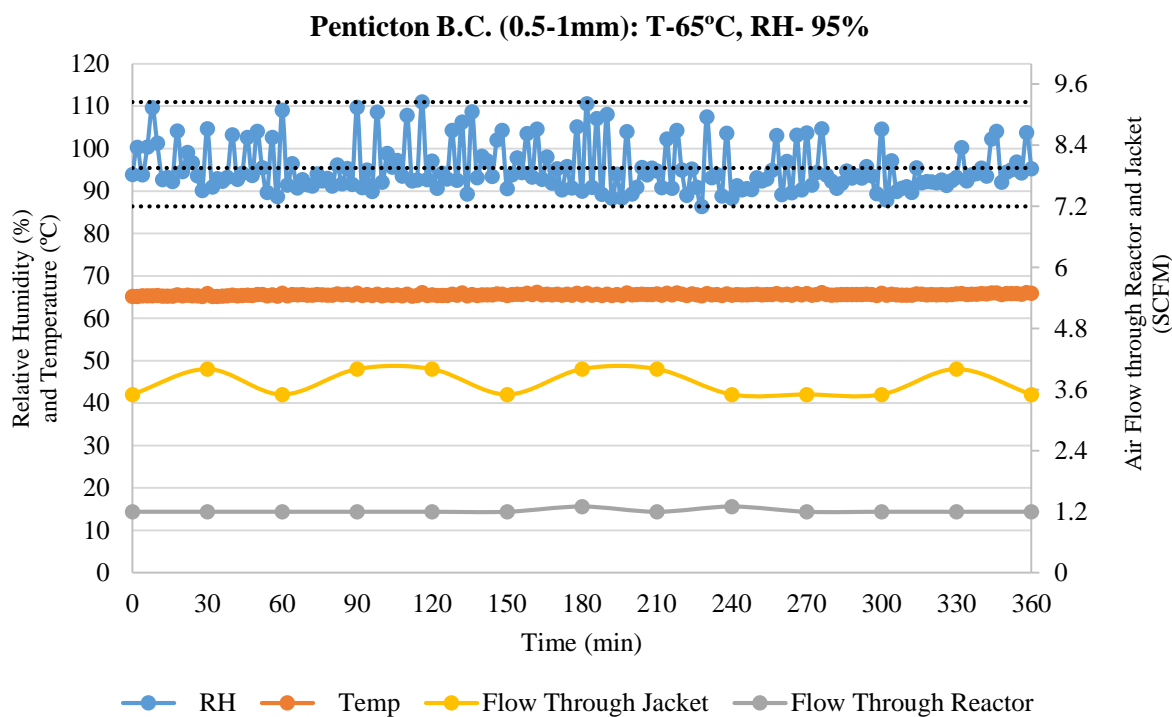


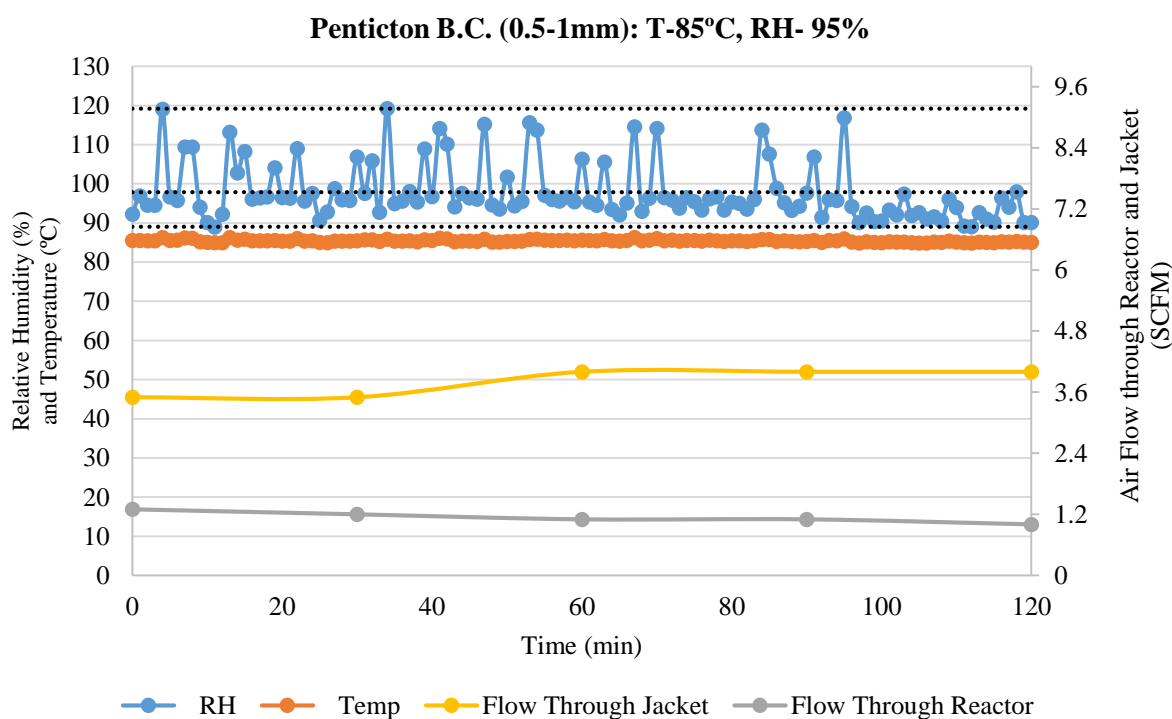
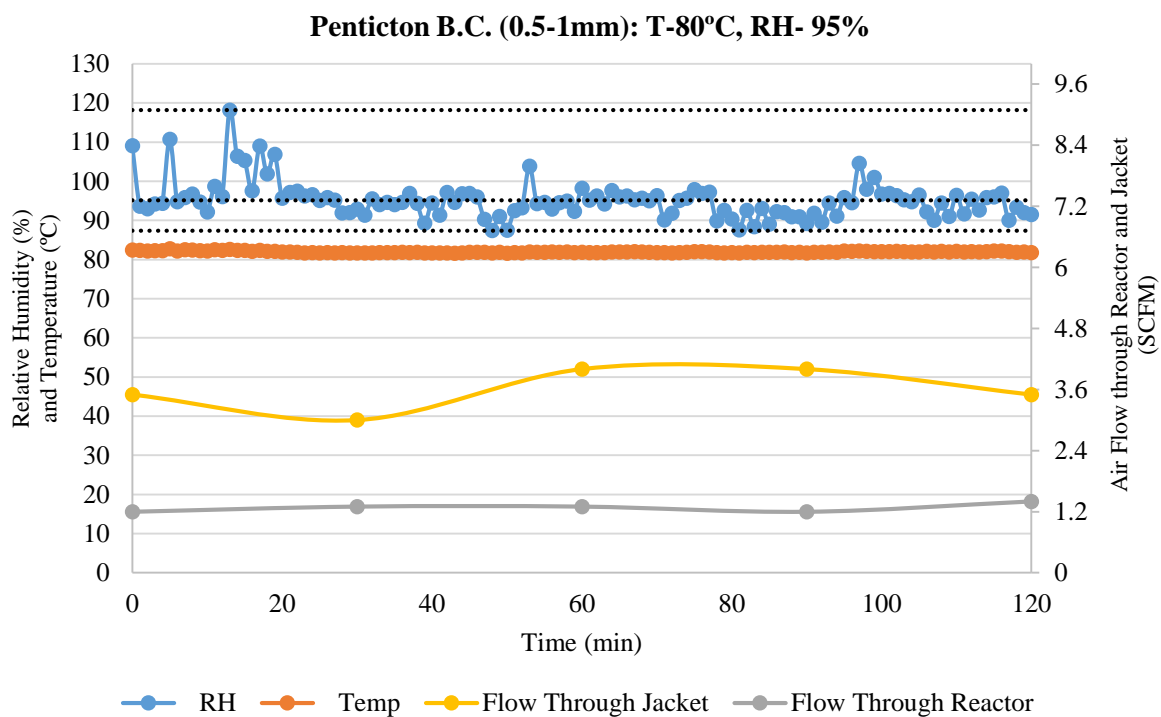
Appendix E : Log data for pilot-scale experiments

E.1 Log data for process optimization

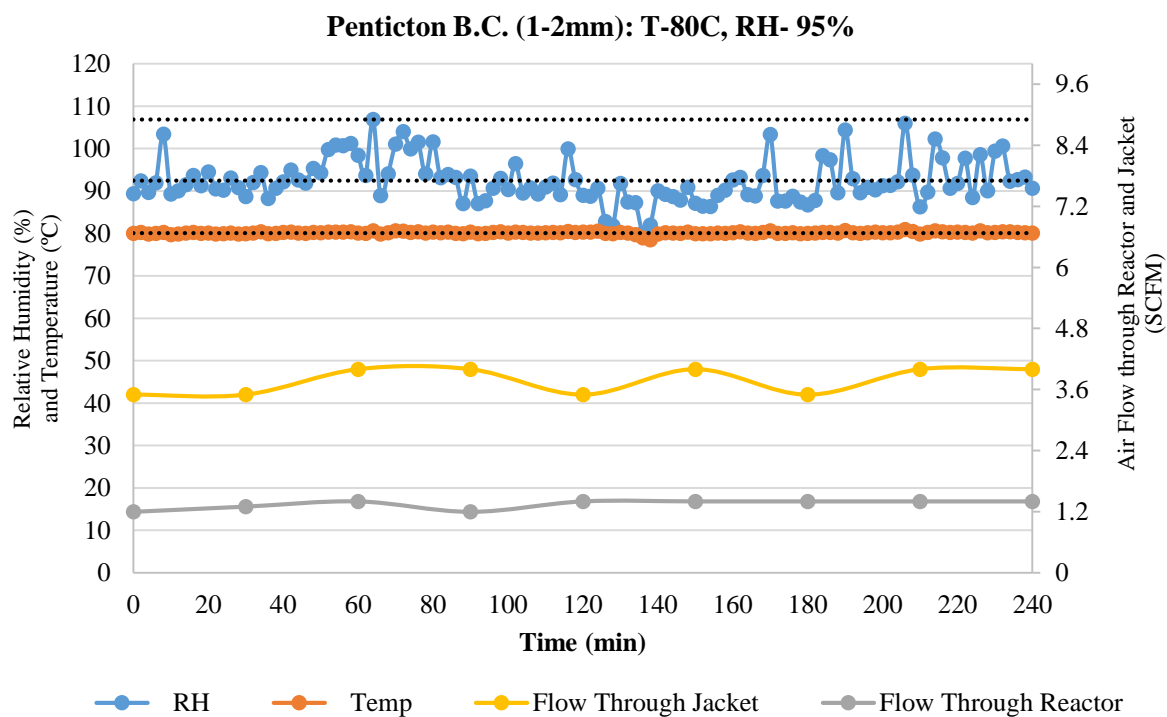
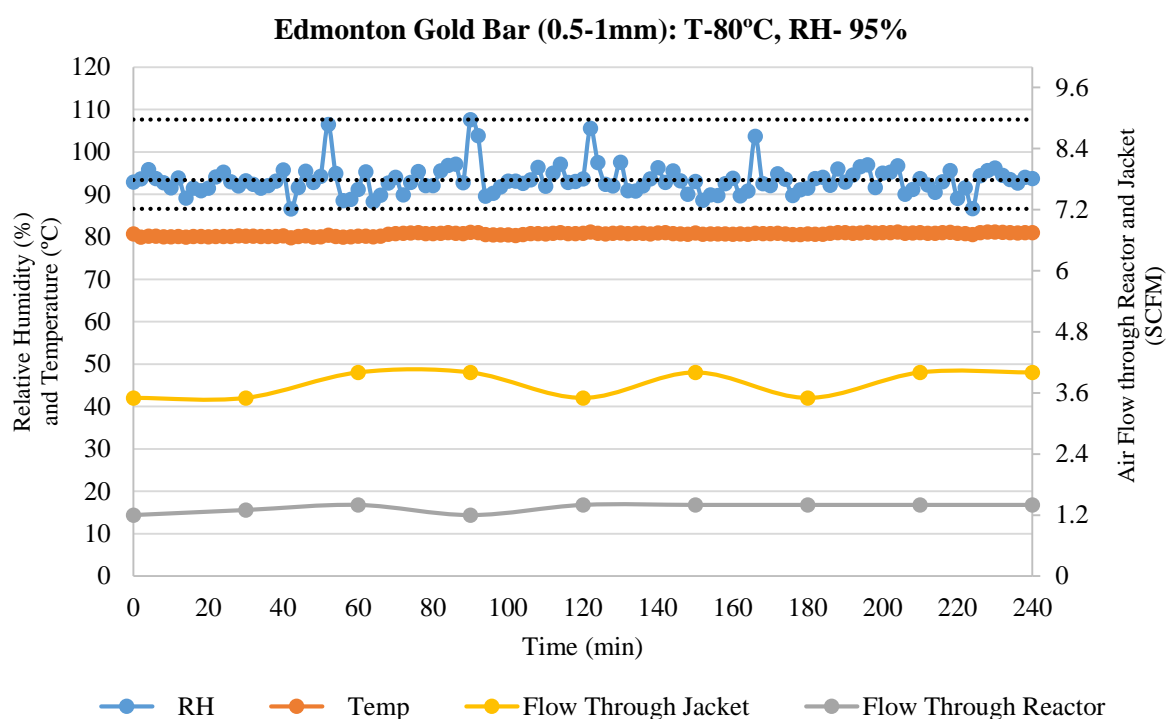


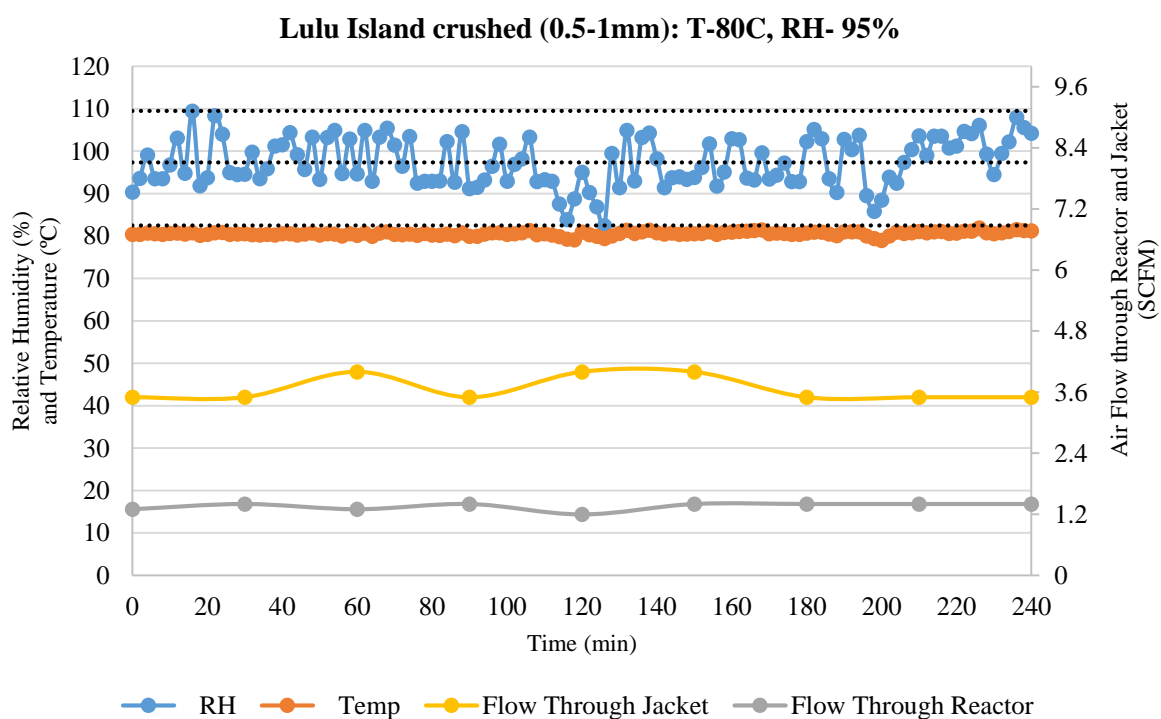
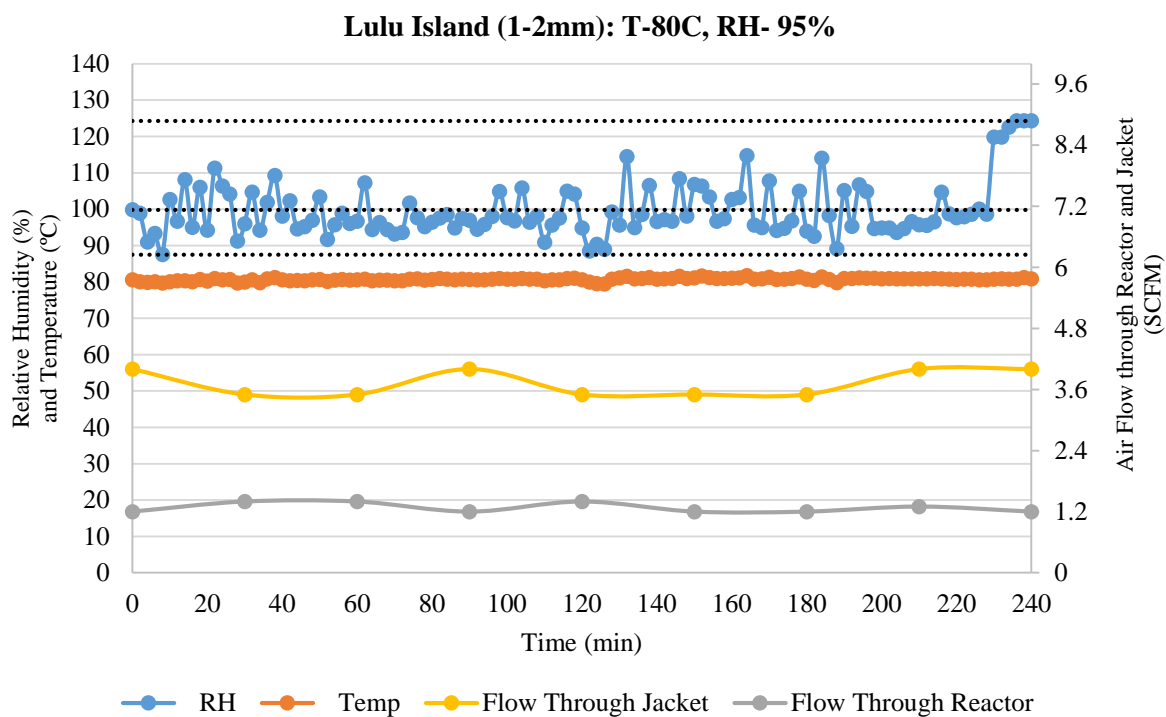


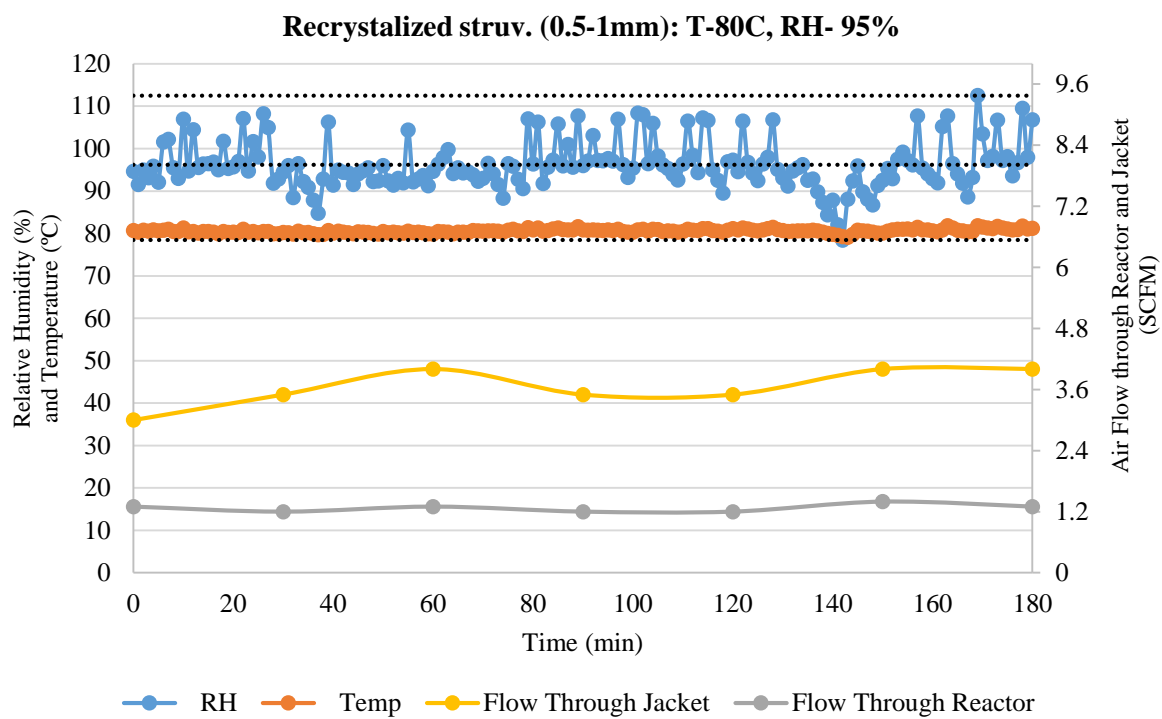




E.2 Log data for different sources and sizes of pellets







Appendix F : Cost estimation

The following calculation has been provided to treat 1 m³ wastewater containing 1000 mg/L N-NH₃

The molecular weight of struvite = 245.3 g

The amount of struvite requires to treat 1000 mg/L N-NH₃ = 14 x 245.3 = 17,521.4 g

Stage 1: Thermal decomposition of struvite

Temperature = 80°C

Relative Humidity = 80%

Based on the temperature and relative humidity, Air: Steam ratio = 1.67 (Calculated from the data presented in Kiehl and Hardt, 1933)

Average air flow through the pilot-scale reactor at 80°C and 80% = 1.3 SCFM (Appendix E)
= 0.62 L/s

Average Steam flow through the pilot-scale reactor at 80°C and 80% = 0.62/1.67 = 0.38 L/sec

Total average flow (air and steam) through the pilot-scale reactor at 80°C and 80% = 0.62+0.38
= 1 L/s

Diameter of the reactor = 13/8 inch = 4.13 cm

Area of the reactor = 13.38 cm²

Velocity through the reactor = (1 L/s) / (13.38 cm²) = 75 cm/sec

Maximum amount of struvite can be decomposed in the existing reactor per batch = 25 g

Therefore, the area of the reactor for 17,521.4 g Struvite = 9,378 cm²

The diameter of the reactor would be = 109.3 cm = 43 inch

So, flow required = 9,378 x 75 = 703,350 cm³/sec ≈ 700 L/sec

At 80C with 80% RH and Air: Steam = 1.67,

Partial pressure, P_{H2O} = 38 kPa

H₂O/air mass ratio,

$$X = \frac{0.62198 \times P_w}{(P_a - P_w)} = \frac{0.62198 \times 38 \text{ kPa}}{(101.3 - 38) \text{ kPa}} = 0.3734$$

Where,

P_w = H₂O vapor pressure

P_a = Atmospheric pressure

$$\begin{aligned}\text{Now, Density, } \rho &= \left(\frac{P}{R_a.T} \right) \cdot (1 + x) / \left(1 + \frac{xR_w}{R_a} \right) \\ &= \left(\frac{101300}{286.9 \times 353} \right) \times (1 + 0.3734) / \left(1 + \frac{0.3734 \times 461.5}{286.9} \right) \\ &= 0.858 \text{ kg/m}^3 \text{ at } 80^\circ\text{C and } 80\% \text{ RH}\end{aligned}$$

$$\text{Total mass flow} = 0.858 \text{ kg/m}^3 \times 1 \text{ L/s} = 0.858 \text{ g/s}$$

Therefore,

$$\text{Air mass flow, } m_a = 0.858 \times \frac{1}{1+0.3734} = 0.62 \text{ g/s}$$

$$\text{Water mass flow, } m_w = 0.858 \times \frac{0.3734}{1+0.3734} = 0.233 \text{ g/s}$$

Energy required for heating up moist air from 40°C up to 80°C, $Q = Q_{80^\circ\text{C}} - Q_{40^\circ\text{C}}$

Total energy required to heat up the air and water, $Q_T = Q_{Ta} + Q_{Tw}$

Energy required to heat up the air = $Q_{Ta} = m_a \cdot C_a \cdot T$

Energy required to heat up the air = $Q_{Tw} = m_w \cdot C_w \cdot T$

Table F.1 Specific heat capacity C, k J/kg. K

Type	40°C	80°C
Air (C_a)	1.005	1.009
Water Vapor (C_w)	1.868	1.881

Total energy required to heat moist air up to 40°C:

$$Q_a = 1.005 \times \frac{0.625}{1000} \cdot 313 = 0.1966 \text{ kJ}$$

$$Q_w = 1.868 \times \frac{0.233}{1000} \cdot 313 = 0.136 \text{ kJ}$$

Total energy required, $Q_{40^\circ\text{C}} = 0.1966 + 0.136 = 0.332 \text{ kJ per sec}$

Total energy required to heat moist air up to 80°C:

$$Q_a = 1.005 \times \frac{0.625}{1000} \cdot 353 = 0.223 \text{ kJ}$$

$$Q_w = 1.881 \times \frac{0.233}{1000} \cdot 353 = 0.155 \text{ kJ}$$

Total energy required, $Q_{80^\circ\text{C}} = 0.223 + 0.155 = 0.378 \text{ kJ per sec}$

Therefore,

Energy required for heating up moist air from 40°C up to 80°C, $Q = Q_{80^\circ\text{C}} - Q_{40^\circ\text{C}}$

$$= 0.378 - 0.332$$

$$= 46 \text{ J/s per 1 L/s of humid air}$$

Total time required per 1 run of reactor = 1.5h

Total flow through the reactor = 700 L/s

$$\begin{aligned} \text{So, Total energy required to run the reactor for 1.5h} &= 46 \times 700 \times 3600 \times 1.5 = 174 \text{ MJ} \\ &= 48 \text{ KW.h} \end{aligned}$$

Industrial energy rates = 5.5 cent per 1 kW.h

Therefore, the cost at the thermal decomposition stage = $48 \times 0.055 = 2.66\$$

$$\approx \$ 3 \text{ (10-15\% Losses)}$$

Stage 2: Struvite recrystallization

Chemicals:

Production of newberyite from 17, 521.4 g struvite at thermal decomposition stage = 12, 450 g

Amount of H_2SO_4 required to dissolve newberyite = 6.65 kg (from PHREEQC)

Commercial bulk price of $\text{H}_2\text{SO}_4 \approx \$300/\text{t} = 0.3\$ \text{ kg}$

Cost of adding $\text{H}_2\text{SO}_4 = 6.65 \times 0.3 = 2.0\$$

Amount of NaOH required to reform struvite back = 6. 127 kg (from PHREEQC)

Commercial bulk price of NaOH $\approx \$400/\text{t} = 0.4\$ \text{ kg}$

Cost of adding NaOH = $6. 127 \times 0.4 = 2.5\$$

Total cost from chemical addition = $2.0 + 2.5 = 4.5\$/\text{kg N removed}$

Pump energy:

Based on pilot tests for struvite recrystallization,

Pump nominal power = 0.5 hp = 373W

Operating power = 50% nominal = 186.5W

Struvite production: 1.271g from 1 L of feed (from PHREEQC)

Feed flow = 5L/min

Time to produce 17,521.4g struvite = $\frac{17,521.4}{1.271 \times 5} = 2757 \text{ min} \approx 46 \text{ hours}$

So, Total energy required = $186.5 \times 46 \times 3600 = 30.88 \text{ MJ} = 8.58 \text{ kW.h}$

Industrial energy rates = 5.5 cent per 1 kW.h

Therefore, the cost of pumping = $8.58 \times 0.055 = 0.47 \approx \$ 0.5/\text{kg N removed}$

Stage 3: Ammonia capture

Oxalic acid is used as adsorbent (dehydrate; molecular weight 126 g)

1 mole of Oxalic acid adsorbs 2 mole of N-NH₃

Therefore, amount of Oxalic acid required to adsorb 1 kg N-NH₃ = $\frac{1}{14} \times \frac{126}{2} = 4.5 \text{ kg}$

Commercial bulk price of Oxalic acid = \$650/t = 0.65\$/kg

Total cost from addition of Oxalic acid = $4.5 \times 0.65 \approx 3\$/\text{kg N removed}$

Obtained product: Oxammite (Ammonium oxalate)

Molecular weight of Oxammite ((NH₄)₂C₂O₄.H₂O) = 142 g

Market value of Oxammite = \$ 3800/t = \$3.8/kg

Amount can be produced from 4.5 kg of Oxalic acid = $\frac{4.5}{126} \times 142 = 5\text{kg Oxammite}$

Commercial value for recovered 5 kg Oxammite = $5 \times 3.8 = 19\$$ value from 1kg N recovered

Oxammite can be converted into oxamide, a valuable slow release N fertilizer, but conversion cost and value need to be determined.